Universidad de Oviedo

Departamento de Química Orgánica e Inorgánica
Programa de Doctorado: Síntesis y Reactividad Química

Furan valorization through sustainable transformations using laccases and transaminases

Thesis Doctoral

Nicoletta Cascelli

Universidad de Oviedo

Departamento de Química Orgánica e Inorgánica
Programa de Doctorado: Síntesis y Reactividad Química

Furan valorization through sustainable transformations using laccases and transaminases

Memoria presentada para optar
al grado de Doctora en Química
por Nicoletta Cascelli

RESUMEN DEL CONTENIDO DE TESIS DOCTORAL

1.- Título de la Tesis	
Español: Valorización de derivados de furano a través de transformaciones sostenibles promovidas por lacasas y transaminasas	Inglés: Furan valorization through sustainable transformations using laccases and transaminases

2.- Autor	
Nombre: Nicoletta Cascelli	
Programa de Doctorado: Síntesis y reactividad química	
Órgano responsable: Centro Internacional de Postgrado	

FOR-MAT-VOA-010 (Reg.2018)

RESUMEN (en español)

Esta Tesis Doctoral se encuadra dentro del campo de la biocatálisis, que trata acerca del uso de enzimas aplicados a procesos sintéticos. Adicionalmente, las moléculas objetivo de esta Tesis presentan una gran relevancia en el sector de la biorefinería. En los últimos años, la aplicación de enzimas como catalizadores ha sido reconocida como una solución práctica para resolver muchos problemas sintéticos en química, ya que permite el diseño y ejecución de transformaciones similares a las reacciones químicas convencionales, pero de una manera más eficiente, selectiva y sostenible. Simultáneamente, ha aparecido un interés cada vez mayor para transformar compuestos provenientes de la biomasa en derivados de alto valor añadido, debido principalmente a los problemas medioambientales relacionados con el impacto de compuesto de proveniencia fósil.

Se ha estructurado esta Tesis Doctoral en una introducción general seguida de cuatro capítulos. En ellos, se ha explorado la búsqueda y optimización de biocatalizadores, así como la investigación de nuevas rutas biocatalíticas para obtener derivados furánicos.

La introducción proporciona una visión del sector de la biorefinaría, poniendo énfasis en la valorización de la biomasa lignocelulósica (LCB). Se muestra así la ruta hacia la producción de bio-productos y compuesto químicos derivados de sacáridos y fracciones aromáticas provenientes de LCB. Adicionalmente, la introducción cubre los principios fundamentales de la Química Verde e introduce conceptos básicos en biocatálisis, con un foco especial en las enzimas usadas en este trabajo, las lacasas y las transaminasas (TAs). Se discute también la sostenibilidad de los procesos químicos, considerando el impacto medioambiental de los mismos. Además, se muestra la importancia del furfural y del 5-hidroximetilfurfural como compuestos centrales dentro de la plataforma furánica, mostrando diversos derivados que se pueden obtener a partir de ellos mediante bioprocesos. Por último, esta sección explora el diseño de reacciones multicatalíticas, mostrando ejemplos de relevancia industrial.

En el Capítulo 1, se realizó un estudio de mutagénesis para investigar como varias moléculas furánicas interaccionaban con el centro activo de la enzima. Este estudio utilizó técnicas de modelado y experimentos de evolución dirigida sobre la lacasa POXA1b de *P. ostreatus*. La investigación reveló que la barrera principal para la oxidación de los derivados furánicos era su alto potencial redox y no tanto problemas de tipo estérico. En esta aproximación, se diseñó un método colorimétrico robusto para detectar selectivamente uno de los productos de oxidación del 5-hidroximetilfurfural, el 2,5-diformilfurano. Este ensayo, hizo uso de un compuesto barato como es la 1,4-fenilendiamina, y ha demostrado un gran potencial para poder ser aplicado en cribados de gran tamaño de enzimas oxidativas, para identificar nuevas variantes más activas para la obtención de DFF. Además, se ensayó positivamente para medir las propiedades cinéticas de diferentes oxidaciones de HMF hacia DFF mediadas por lacasas.

En el Capítulo 2, el foco principal ha sido aumentar la diversidad de lacasas empleadas en este estudio. De esta manera, se usaron técnicas de recombinación para expresar una lacasa llamada Lacc12 en *P. pastoris*. Se optimizaron el medio de cultivo y las condiciones para mejorar la actividad enzimática. Puesto que esta lacasa de *P. ostreatus* se produce durante el proceso de crecimiento del cuerpo fructífero del hongo, se pensó que la inestabilidad podía estar relacionada con las altas temperaturas cuando era expresada. Para evitar esto, se disminuyó la temperatura de la fermentación y se indujo la producción enzimática con metanol. Se observó que bajo estas condiciones se obtuvieron cantidades mayores de la lacasa activa.

En el Capítulo 3, se han obtenido nuevas amino transaminasas (ATAs), y se integraron junto con otro grupo de enzimas comerciales para obtener furfuril amina a partir de furfural en medio acuoso bajo condiciones suaves, empleando un exceso molar de isopropilamina (IPA). Varias de las ATAs sobreexpresadas demostraron conversiones y selectividades excelentes. En particular, la Cv-TA dio lugar a una conversión prácticamente completa a altas concentraciones del sustrato. Posteriormente, se optimizó la oxidación del alcohol furfurílico hacia el furfural usando distintos sistemas lacasa-TEMPO. Entre ellos, las lacasas de *P. ostreatus* (POXC y POXA1b), mostraron una selectividad excelente hacia la formación del furfural, previniendo la formación del ácido 2-furoico. Debido a la gran estabilidad de la POXA1b a largos tiempos de reacción, se puedo disminuir aún más la concentración del mediador (5 mol%). Estos sistemas oxidativos pudieron tolerar además diversos disolventes orgánicos inmiscibles con el agua a concentraciones significativas. Por último, se aplicaron a un proceso en un solo recipiente en dos etapas junto con una transaminación catalizada por la Cv-TA, dando lugar a la producción de manera eficiente de la furfuril amina a partir del alcohol furfurílico.

Finalmente, en el Capítulo 4, se desarrolló la producción de BAMF y AMFC a partir de DFF y HMF, respectivamente, a través de biotransaminaciones. Estos procesos ocurrieron en paralelo con la obtención de (poli)iminas debido a la alta reactividad de los grupos aldehído y de las aminas presentes en el medio de reacción. Debido a la reversibilidad de los enlaces de tipo imina en medio acuoso, para mejorar la productividad del proceso se disminuyó el pH del medio de reacción sin comprometer la actividad enzimática. Además, se exploró la oxidación del HMF utilizando varios LMSs, investigando parámetros como la concentración de la reguladora y el mediador, así como la cantidad de la lacasa. Aunque se intentó la protección selectiva del grupo aldehído del HMF o la utilización de medios bifásicos para obtener principalmente el DFF, el producto principal fue el oxoácido FFCA. Sin embargo, nos aprovechamos de este hecho utilizándolo como sustrato de partida para estudiar su transaminación, optimizándose entre otros parámetros la concentración del sustrato y la adición de cosolventes. La BmS119G-TA convirtió de manera exitosa el FFCA en AMFC, dando muy buenas conversiones incluso a 100 mM. Posteriormente, se desarrolló el proceso secuencial combinando la oxidación del HMF con la lacasa POXA1b, seguida de la transaminación del FFCA con la BmS119G-TA, dando lugar a la formación del aminoácido final, el cual se aisló protegiendo el grupo amino con Boc.

Parte de los resultados aquí presentados, incluido el estudio de la aplicación de lacasas a nivel industrial, se han publicado o mandado para su publicación en las siguientes contribuciones científicas:

- "Versatility of microbial laccases in industrial applications.” V. Lettera, N. Cascelli, A. De Chiaro, G. Sannia, en: *Bacterial Laccases: Engineering, Immobilization, Heterologous Production, and Industrial Applications*, (Eds.: D. Yadav, T. Kudanga), Elsevier, en prensa.
- “Laccases from *Pleurotus ostreatus* applied to the oxidation of furfuryl alcohol for the synthesis of key compounds for polymer industry.” N. Cascelli, V. Lettera, G. Sannia, V. Gotor-Fernández, I. Lavandera, *ChemSusChem*, **2023**, *16*, e202300226.
- "Biotransamination of furan-based aldehydes with isopropylamine: Enzyme screening and pH influence.” A. Pintor, N. Cascelli, A. Volkov, V. Gotor-Fernández, I. Lavandera *ChemBioChem*, doi: 10.1002/cbic.202300514.
- “High-throughput spectrophotometric assay for the detection of 2,5-diformylfuran (DFF) and its validation through laccase-mediated oxidation of 5-hydroxymethylfurfural (HMF).” N. Cascelli, V. Gotor-Fernández, I. Lavandera, G. Sannia, V. Lettera, enviado para su publicación.

RESUMEN (en Inglés)

This Thesis primarily focuses on the field of Biocatalysis, which involves the use of enzymes for synthetic processes. Additionally, the compounds targeted hold significant relevance for the biorefinery sector. Over recent years, the application of enzymes as catalysts has been acknowledged as a practical solution to many challenges encountered in chemical synthesis. It enables the design and execution of transformations similar to conventional organic reactions but in a more efficient, selective, and sustainable manner. Simultaneously, there is a growing interest in developing processes that convert biomass compounds into high-value derivatives, mainly driven by environmental concerns related to the impact of fossil-based compounds.

This Doctoral Thesis is structured with a general introduction followed by four chapters. In them, the research and optimization of biocatalysts are explored alongside the investigation of biocatalytic pathways to produce furan-based derivatives.

The introductory section provides an overview of the Biorefinery sector, placing particular emphasis on the valorization of lignocellulosic biomass (LCB). It outlines a pathway towards the production of bio-products and chemicals derived from saccharides and aromatic fractions within LCB. Additionally, the introduction covers fundamental principles of Green Chemistry and introduces key concepts in Biocatalysis, with a specific focus on the biocatalysts employed in this research, namely laccases and transaminases (TAs). Sustainability within chemical processes is also discussed, considering the environmental impact of the processes. Moreover, the relevance of furfural and 5-hydroxymethylfurfural as central compounds in the furan platform is introduced, showcasing significant derivatives achievable through bioprocesses. Lastly, the section explores the design of multicatalytic reactions, highlighting industrial relevant examples.

In Chapter 1, laccase mutagenesis was employed to investigate how furan-based molecules interacted within the active site of the enzyme. This study involved molecular docking and directed evolution experiments conducted on the efficient laccase POXA1b from *P. ostreatus*. The research revealed that the primary barrier to oxidizing furan molecules was likely their redox potential rather than steric factors. In the mutagenesis approach, a robust colorimetric assay was developed to detect the oxidation products of 5-hydroxymethylfurfural, particularly 2,5-diformylfuran. This assay, utilizing the cost-effective compound 1,4-phenylenediamine, showed significant promise for high-throughput screening of redox biocatalysts to identify new or improved enzyme variants. Furthermore, it effectively assessed the kinetic properties of various laccase-mediated oxidations of HMF into DFF.

In Chapter 2, the primary focus was on expanding the diversity of laccases employed in the study. To achieve this, we used recombinant techniques to express a laccase called Lacc12 in *P. pastoris*. Growth medium and conditions were optimized to ensure the enzyme's activity. Our working hypothesis revolved around the idea that the challenge in overexpressing this particular isoform of the *P. ostreatus* laccase, which is typically produced during the fungal fruiting body growth process, was due to its instability at high temperatures when expressed constantly. To address this, we lowered the fermentation temperature and induced the enzymatic production with methanol. This approach allowed for the gradual build-up of the active enzyme form.

In Chapter 3, new amine transaminases (ATAs) were in-house produced and integrated into a group of commercial ATAs to convert furfural into valuable furfuryl amine under mild aqueous conditions, using an excess of isopropylamine (IPA). Several overexpressed ATAs exhibited high conversion rates and selectivity. Cv-TA, in particular, achieved nearly complete conversion at high substrate loadings. To establish a cascade for converting furfuryl alcohol into furfuryl amine, we optimized the initial oxidation step using different laccase-TEMPO systems. Among them, *P. ostreatus* laccases (POXC and POXA1b) displayed exceptional selectivity in producing furfural, preventing the formation of 2-furoic acid. Leveraging the high stability of POXA1b over extended reaction times, we significantly reduced mediator usage to 5 mol%. These TEMPO oxidative systems with *P. ostreatus* laccases could tolerate various water-immiscible co-solvent mixtures at significant concentrations. These laccase-mediator systems were successfully employed in a one-pot, two-step cascade in conjunction with Cv-TA, leading to the efficient production of furfuryl amine from furfuryl alcohol.

Finally, in Chapter 4, the main focus was the BAMF and AMFC production from DFF and HMF, respectively, through transamination. During these reactions, (poly)imines were formed in situ due to the presence of reactive carbonyl species and amines. We effectively took advantage of the imine bonds' reversibility by adjusting pH, primarily achieving a higher productivity without compromising the enzyme stability or activity at lower pH values. In addition, we explored HMF oxidation using LMSs, investigating factors like buffer concentration, mediator, and laccase quantity. Despite attempts to protect the aldehyde group of HMF or use biphasic systems to obtain DFF, the primary product remained FFCA. However, FFCA was then efficiently used as the starting material for transamination, and we optimized various conditions, including the substrate concentration and the addition of a co-solvent. BmS119G-TA successfully converted FFCA into AMFC, achieving high conversion rates, especially up to 100 mM. This sequential process involving POXA1b-mediated HMF oxidation, followed by transamination of FFCA using BmS119G-TA, allowed the production of the final amino acid, which was then isolated as N-Boc-protected compound.

Part of the results obtained along this PhD Thesis, along with a deep study over laccases' application in industry, have been published or submitted for publication in the following scientific contributions:

- "Versatility of microbial laccases in industrial applications." V. Lettera, N. Cascelli, A. De Chiaro, G. Sannia, in: *Bacterial Laccases: Engineering, Immobilization, Heterologous Production, and Industrial Applications*, (Eds.: D. Yadav, T. Kudanga), Elsevier, in press.
- "Laccases from *Pleurotus ostreatus* applied to the oxidation of furfuryl alcohol for the synthesis of key compounds for polymer industry." N. Cascelli, V. Lettera, G. Sannia, V. Gotor-Fernández, I. Lavandera, *ChemSusChem*, **2023**, *16*, e202300226.
- "Biotransamination of furan-based aldehydes with isopropylamine: Enzyme screening and pH influence." A. Pintor, N. Cascelli, A. Volkov, V. Gotor-Fernández, I. Lavandera *ChemBioChem*, doi: 10.1002/cbic.202300514.
- "High-throughput spectrophotometric assay for the detection of 2,5-diformylfuran (DFF) and its validation through laccase-mediated oxidation of 5-hydroxymethylfurfural (HMF)." N. Cascelli, V. Gotor-Fernández, I. Lavandera, G. Sannia, V. Lettera, submitted for publication.

SR. PRESIDENTE DE LA COMISIÓN ACADÉMICA DEL PROGRAMA DE DOCTORADO EN SÍNTESIS Y REACTIVIDAD QUÍMICA

ABBREVIATIONS AND ACRONYMS

δ	Chemical shift in parts per million downfield from tetramethylsilane
ε	Molar absorptivity
2,5-DMTHF	2,5-Dimethyltetrahydrofuran
2,6-DMP	2,6-Dimethoxyphenol
Å	Angstrom(s)
ABNO	9-Azabicyclo[3.3.1]nonane *N*-oxyl
ADH	Alcohol dehydrogenase
AFEX	Ammonia Fiber EXplosion
AMFC	5-Aminomethyl-2-furoic acid
Amp	Ampicillin
API(s)	Active Pharmaceutical Ingredient(s)
ATA	Amine transaminase
ATP	Adenosine 5’-triphosphate
AZADO	2-Azaadamantane *N*-oxyl
BAMF	2,5-Bis(aminomethyl)furan
BB	Breaking buffer
BBC	Phenoxycarbonyloxymethyl ethylene carbonate
BHMF	5-Bis(hydroxymethyl)furan
BMGY	Buffered glycerol/glucose complex medium
BMMY	Buffered methanol-complex medium
Boc	*tert*-Butoxycarbonyl
C5	5-Carbon atoms
C6	6-Carbon atoms
C-factor	Climate factor
cm^{-1}	Wavenumber(s)
COVID-19	Coronavirus disease 2019
CPME	Cyclopentyl methyl ether
d	Doublet (spectral)
DCM	Dichloromethane
DES	Deep Eutectic Solvent
DFF	Diformylfuran

DMF	*N*,*N*-Dimethylformamide
DMSO	Dimethylsulfoxide
E. coli	*Escherichia coli*
EDTA	Ethylenediaminetetraacetic acid tetrasodium salt
E-factor	Environmental factor
EG	Ethylene glycol
Et_2O	Diethyl ether
EtOAc	Ethyl acetate
EU	Europe
Fam	Furfuryl amine
FBC	Hydroxymethylfuran bis(cyclic carbonate)
FDCA	2,5-Furandicarboxylic acid
FDCC	Furan-2,5-dicarbonyl chloride
FFCA	5-Formyl-2-furoic acid
FMN	Flavin mononucleotide
g	Gram(s)
GAP	Glyceraldehyde-3-phosphate dehydrogenase promoter
GC	Gas chromatography
GHG(s)	Greenhouse gases
GOx	Glucose oxidases
h	Hour(s)
HBT	1-Hydroxybenzotriazole
HFCA	5-Hydroxymethyl-2-furancarboxylic acid
HMF	5-Hydroxymethylfurfural
HMFA	5-Hydroxymethylfurfurylamine
HPI	*N*-Hydroxyphthalimide
HPLC	Reversed Phase-High Performance Liquid Chromatography
IEA	International Energy Agency
IPA	2-Propylamine (or Isopropylamine)
IPTG	Isopropyl β-D-1-thiogalactopyranoside
KPi buffer	Potassium phosphate buffer
LB	Luria-Bertani medium

LCA	Life Cycle Assessment
LCB	Lignocellulosic biomass
LMS	Laccase-mediator system
LPMO	Lytic Polysaccharide Monooxygenases
L*Tv*	Laccase from *Trametes versicolor*
M	Molar (moles per litre)
m	Multiplet (spectral); metre(s); milli
Me	Methyl
MeCN	Acetonitrile
MES	2-(*N*-Morpholino)ethanesulfonic acid
MHz	Megahertz
min	Minute(s)
MM/MD	Minimal-methanol/dextrose medium
mol	Mol(es)
MOPS	3-(*N*-Morpholino)propanesulfonic acid
MTBE	*tert*-Butyl methyl ether
NAD(P)	Nicotinamide adenine dinucleotide (phosphate)
NGOs	Non-profit organizations
NHA	*N*-Hydroxyacetanilide
NIPUs	Nonisocyanate polyurethanes
NL	Netherlands
NMR	Nuclear magnetic resonance
ºC	Celsius degrees
Ori	Origin of Replication
P	Product
PDB	Protein Data Bank
PEF	Polyethylene furanoate
PET	Polyethylene terephthalate
PHAs	Polyhydroxyalkanoates
PHP	Phenothiazine-10-propionate
PLP	Pyridoxal 5’-phosphate
PMI	Process Mass Intensity

PMSF	Phenylmethylsulfonyl fluoride
POX-	*P. ostreatus* protein
PPD	1,4-Phenylendiamine (*p*-Phenylenediamine)
Ph_3P	Triphenylphosphine
ppm	Part(s) per million (spectral)
q	Quadruplet (spectral)
redox	Reduction-oxidation
RP	Reverse phase
rpm	Revolutions per minute
RT	Retention time
rt	Room temperature
s	Singlet (spectral)
SARS-CoV-2	Severe acute respiratory syndrome coronavirus 2
SHF	Separate Hydrolysis and Fermentation
SSCF	Simultaneous Saccharification and Co-Fermentation
SSF	Simultaneous Saccharification and Fermentation
SuBC	Succinate bis(cyclic carbonate)
SWOT	Strengths, weakness, opportunities, threats
T	Temperature
t	Triplet (spectral)
TA	Transaminase
TB	Terrific broth medium
^{t}Bu	*tert*-Butyl
t-BuOH	2-Methylpropan-2-ol
TFA	Trifluoroacetic acid
THF	Tetrahydrofuran
TLC	Thin-layer chromatography
TPA	Terephthalic acid
Tris	Trishydroxymethylaminomethane
TRL	Technology Readiness Level
U	Enzyme unit (amount of enzyme that catalyses the transformation of 1 μmol of substrate per minute)

URA	Uracil
UV-Vis	Ultraviolet-visible
v	Volume
v/v	Volume per unit volume (volume to volume ratio)
w	Weight
w/v	Weight per unit volume (weight to volume ratio)
YPDS	Yeast extract-peptone-dextrose + sorbitol medium

TABLE OF CONTENTS

INTRODUCTION **1**

I.1. The biorefinery concept 3

I.1.1 Biorefinery classification 8

I.1.2. Biorefinery in the context of circular bioeconomy 13

I.1.3. Biorefinery design and SWOT analysis of a biorefinery system 15

I.1.4. Examples of biorefineries 17

I.2. Processing lignocellulosic biomass (LBC) for the production of high-value compounds 19

I.2.1 Composition and characterization of LCBs 20

I.2.2 LCBs pretreatments and platform chemicals achieved 24

I.2.3 Challenges in scale-up and commercialization of LCBs' based biorefinery 33

I.3. Furfural and 5-hydroxymethylfurfural. Relevance in furanic biorefineries 34

I.3.1 Furfural and HMF production from LCBs 37

I.3.2 Upgrading of furfural and HMF into added-value chemicals 39

I.4. Biocatalysis 44

I.4.1. Advantages and disadvantages of Biocatalysis 46

I.4.2. Enzyme classification and catalytic efficiency 49

I.5. Strategies to achieve more efficient biocatalytic processes 51

I.5.1. Biocatalyst improvement through heterologous expression 53

I.5.2. Biocatalyst improvement through enzyme engineering 54

I.6. Biocatalysis in industrial processes 56

I.7. Tools to evaluate sustainability in chemical processes 59

I.8. Design of multicatalytic reactions 61

OBJECTIVES..65

First part. Laccases: enzyme design and application in oxidative processes

CHAPTER 1: Searching for new laccases from *Pleurotus ostreatus*.....71

1.1.1 Laccases and white biotechnology...75

1.1.1.1. General features and role in nature..76

1.1.1.2. Fungal laccases: Structure and mechanism............................77

1.1.1.3. Laccase from Trametes versicolor..78

1.1.1.4. Laccases from Pleurotus ostreatus..81

1.1.1.5. Laccase-mediator systems (LMSs)...82

1.1.1.6. Industrial application of laccases...86

1.1.2. Laccase mutagenesis...89

Results and discussion...93

1.2.1. Rational mutagenesis of POXA1b laccase: Docking studies.........95

1.2.2. Development of a high-throughput screening procedure for DFF detection...103

1.2.3. Colorimetric assay validation in the detection of DFF from real oxidation of HMF by LMSs...113

1.2.4. Directed evolution towards novel POXA1b variants..................114

Experimental Section..121

1.3.1. General information..123

1.3.2. Yasara predictions: Homology modelling and molecular docking experiments...124

1.3.3. Assay for laccase activity...125

1.3.4. High-throughput screening method.. 125

1.3.5. Determination of Z' values 126

1.3.6. Reaction progress curves for the LMSs and initial rate measurements... 126

1.3.7 Cloning vector.. 127

1.3.8. Nucleic acid manipulation 127

1.3.8.1. Digestion with restriction enzymes 128

1.3.8.2. Randomly mutated gene library construction 129

1.3.8.3. PCR 131

1.3.8.4. Saccharomyces cerevisiae: Host of mutagenesis 132

1.3.8.5. DNA gel electrophoresis 134

CHAPTER 2: Design and expression of a new laccase: Lacc12 135

2.1.1. Laccase production in yeasts: Focus on *Pichia pastoris*............. 139

2.1.2. Lacc12: a promising laccase. Gene isolation 144

Results and discussion 145

2.2.1. Recombinant Lacc12 production: inducible vs constitutive expression.. 147

Experimental Section 153

2.3.1. General information 155

2.3.2. Lacc12 constitutive expression 156

2.3.2.1. Cloning vector 156

2.3.2.2. DNA manipulation.. 157

2.3.2.3. Pichia pastoris: Recombinant laccase production................ 157

2.3.3. Lacc12 inducible expression.. 159

2.3.3.1. Cloning vector 160
2.3.3.2. DNA manipulation 160
2.3.3.3. Pichia pastoris: recombinant laccase production 162
2.3.4. *P. pastoris* cell lysis 163
2.3.5. Protein manipulation: Laccase assays and SDS-PAGE gel 163

Second part. Bienzymatic cascades to obtain valuable furan derivatives

CHAPTER 3: Valorization of furfuryl alcohol via oxidation towards furfural using laccases followed by biotransamination towards furfuryl amine **167**
3.1.1. Transferases 172
3.1.1.1. Transaminases (TAs) 173
3.1.1.2. General reaction mechanism 175
3.1.1.3. Thermodynamic aspects of the transamination reaction 178
3.1.1.4. Amine transaminases in industry 182
3.1.2. Laccases and ATAs in one-pot processes 187
Results and discussion 189
3.2.1. Study of the first reaction step: Laccase oxidation of **1a** into **1b** 191
3.2.1.1. POXA1b, POXC and LTv laccases as object of investigation: Enzymatic stability studies 191
3.2.1.2. Mediator screening 192
3.2.1.3. pH optimization 195
3.2.1.4. Influence of mediator and laccase concentrations 196

3.2.1.5. Optimization of the mediator amount 198

3.2.1.6. Co-solvent screening 199

3.2.2. Study of the second reaction step: Transamination of **1b** into **1d** 201

3.2.2.1. Broadening the panel of biocatalysts: Recombinant expression of new ATAs in E. coli 201

3.2.2.2. ATA screening for ***1d*** *biosynthesis* 202

3.2.2.3. pH influence in ***1d*** *biosynthesis* 208

3.2.3. One-pot sequential synthesis of **1d** from **1a** at preparative scale. 210

3.2.4. Environmental impact of the preparative biosynthesis of **1d** 211

Experimental Section 213

3.3.1. General information 215

3.3.2. Synthesis of reference materials 216

3.3.2.1. Synthesis of alcohol ***1a*** 216

3.3.2.2. Synthesis of carboxylic acid ***1c*** 216

3.3.3. General procedure for the LMS oxidation of **1a** into **1b** 217

3.3.4. Stability study of laccases 217

3.3.5. Mediator screening 218

3.3.6. pH influence in the LMS oxidation of **1a** 218

3.3.7. Optimization of the mediator and laccase amounts in the LMS oxidation of **1a** 219

3.3.8. Study of the solvent influence in the LMS oxidation of **1a** 219

3.3.9. New recombinant ATAs panel expression (TAs 1-8) 220

3.3.9.1. Transformation protocol 220

3.3.9.2. Protein expression and SDS-PAGE 220

3.3.9.3. Cell lysis 220

3.3.9.4. Enzymatic characterization 221

3.3.10. General protocol for in-house ATAs recombinant expression... 222

3.3.10.1. General protocol for the recombinant expression of (S)-selective (Cv-TA and ArS-TA) and (R)-selective transaminases (ArR-TA and ArRMut11-TA) 222

3.3.10.2. General protocol for the recombinant expression of Bm-TA and BmS119G 223

3.3.10.3. General protocol for the recombinant expression of Vf and Vf-mut-TA 223

3.3.10.4. General protocol for the recombinant expression of At-TA 224

3.3.11. Evaluation of the apparent activity for *E. coli*/TA whole cells .. 224

3.3.12. General procedure for the biotransamination of **1b** into **1d** 226

3.3.13. Biotransamination of furfural adding the substrate in a stepwise manner 226

3.3.14. Cascade protocol to transform **1a** into **1d** 227

3.3.15. EATOS calculations 228

3.3.16. Analytics 228

3.3.16.1. GC analyses 228

*3.3.16.2. Calibration curves of compounds **1a-d, 2a**, and **2b**.* 230

3.3.17. Compounds characterization 231

CHAPTER 4: Chemoenzymatic synthesis of HMF derivatives applying LMSs and ATAs **234**

4.1. Oxidized derivatives obtained from HMF 241

*4.1.1.1. DFF (**3b**)* 242

*4.1.1.2. FFCA (**3c**)* 245

*4.1.1.3. FDCA (**3d**)* 248

*4.1.1.4. HFCA (**3e**)* 252

4.1.2. Current challenges in the enzymatic modification of HMF (**3a**) . 254

Results and discussion 257

4.2.1. Transamination of DFF (**3b**) into BAMF (**3f**)............................ 259

4.2.1.1. ATAs screening 262

4.2.1.2. Reaction intensification 264

*4.2.1.3. pH influence on **3f** synthesis* 265

4.2.2. Study of the LMS oxidation of HMF (**3a**) 266

4.2.2.1. Influence of the buffer strength 268

4.2.2.2. Influence of the mediator amount 272

4.2.2.3. Influence of the laccase amount 275

4.2.2.4. Organic co-solvent addition 278

4.2.2.5. HMF protecting group strategy 280

4.2.3. Transamination of FFCA (**3c**) in AMFC (**3g**)............................ 283

4.2.3.1. ATAs screening 283

4.2.3.2. Study of the reaction at high substrate concentration 284

4.2.3.3. Organic co-solvent influence 286

4.2.3.4. AMFC biosynthesis from FFCA at preparative scale 288

4.2.4. One-pot sequential synthesis of AMFC from HMF at preparative scale 288

4.2.5. Environmental impact study of the preparative biosynthesis of **3g** 290

Experimental Section 293

4.3.1. General information 295

4.3.2. General procedure for the transamination of DFF into BAMF ...295

4.3.3. LMS oxidation of HMF 296

4.3.4. Biocatalytic synthesis of FFCA at preparative scale....................297

4.3.5. General procedure for the transamination of FFCA into AMFC 298

4.3.6. Preparative scale reaction for AMFC synthesis: Product isolation 298

4.3.7. General procedure for the one-pot sequential protocol from HMF into AMFC 299

4.3.8. Analytics...300

4.3.8.1. HPLC method for the separation of compounds ***3a-g***...........300

4.3.8.2. Calibration curves for compounds ***3a-g***...............................302

4.3.9. Compounds characterization 303

GENERAL CONCLUSIONS **307**

CONCLUSIONES GENERALES...**313**

INTRODUCTION

I.1. The biorefinery concept

The increase in CO_2 concentration in the atmosphere has led to environmental issues like global warming, ocean acidification, biodiversity loss, and extreme weather events. These problems are primarily caused by heavy reliance on fossil fuels for energy, materials, and chemicals. While biomass historically provided energy, the industrial and globalized world turned to fossil sources, which offered high energy density and rapid solutions. However, overconsumption depleted these resources, leading to the current crisis.[1] Rapid and extensive use of fossil fuels led to a quick release of CO_2, intensifying global warming and disrupting ecosystems: thus, biodiversity, water systems, and air quality are at risk. Population growth adds to the complexity, making solutions challenging.[2]

Since 2012, the European Union initiated the Bioeconomy Strategy, prompting global efforts to shift from fossil fuels to sustainable resources. Many countries have followed suit, investing in research and strategic plans to foster the transition towards a bio-based economy. One of the driven aspects was the sustainable development,[3] that consists in satisfying daily demands while, contemporary, preserving the capacity of future generations to provide for their own needs, through rational exploitation of natural sources.[4] Under the banner of the green revolution, global players including industry, policy makers, non-governmental organizations (NGOs), and researchers have guided countries towards a transition that preserves resources while maintaining well-being and mitigating environmental impact. Organizations like the International Energy Agency (IEA), Organization for Economic Co-Operation and Development (OECD), and the World Economic Forum are driving this change, with official reports shaping the focus of discussions. Engineering and chemical sectors, supported by industrial biotechnology, have been fundamental in providing key solutions to meet these requirements.[5] Various renewable sources like wind, solar light, and hydropower have been considered for clean energy generation,[6] while biomass is recognized as a renewable carbon source for manufacturing consumer products.[7] Regarding goods' processing, biorefineries are the real action strategy for effectively substituting the processing of fossil-based carbon with renewable carbon derived from biomass.[8]

---

[1] S. V. Mohan, G. N. Nikhil, P. Chiranjeevi, C. N. Reddy, M. V. Rohit, A. N. Kumar, O. Sarkar, *Bioresour. Technol.* **2016**, *215*, 2–12.

[2] a) D. Hernández, *Soc. Sci. Med.* **2016**, *167*, 1–10; b) B. H. Kreps, *Am. J. Econ. Sociol.* **2020**, *79*, 695–717.

[3] S. Stark, L. Biber-Freudenberger, T. Dietz, N. Escobar, J. J. Förster, J. Henderson, N. Laibach, J. Börner, *Sustain. Prod. Consum.* **2022**, *29*, 215–227.

[4] C. A. Ruggerio, *Sci. Total Environ.* **2021**, *786*, 147481.

The biorefinery concept, originated on the late 1990s, has evolved through diverse definitions, shaped by context and interpretation.[9] The IEA Bioenergy Task 42 offers a clear biorefinery definition: "*the sustainable processing of biomass into marketable products (food, feed, materials, chemicals) and energy (fuels, power, heat)*".[10] This concept extends to diverse forms, encompassing both individual facilities units and long-term clusters of facilities. Biorefineries use integrated conversion methods, including biochemical, thermochemical, and microorganism-based processes, to sustainably transform non-fossil resources into a variety of valuable products, such as energy, materials, and chemicals (Figure I.1).[11]

---

[5] F.-D. Vivien, M. Nieddu, N. Befort, R. Debref, M. Giampietro, *Ecol. Econ.* **2019**, *159*, 189–197.

[6] a) A. M. Omer, *Renew. Sustain. Energy Rev.* **2008**, *12*, 1789–1821; b) A. Gasparatos, C. N. H. Doll, M. Esteban, A. Ahmed, T. A. Olang, *Renew. Sustain. Energy Rev.* **2017**, *70*, 161–184.

[7] a) M. Antar, D. Lyu, M. Nazari, A. Shah, X. Zhou, D. L. Smith, *Renew. Sustain. Energy Rev.* **2021**, *139*, 110691; b) P. Duarah, D. Haldar, A. K. Patel, C.-D. Dong, R. R. Singhania, M. K. Purkait, *Bioresour. Technol.* **2022**, *348*, 126791.

[8] A. T. Ubando, C. B. Felix, W.-H. Chen, *Bioresour. Technol.* **2020**, *299*, 122585.

[9] C. Conteratto, F. D. Artuzo, O. I. B. Santos, E. Talamini, *Renew. Sustain. Energy Rev.* **2021**, *151*, 111527.

[10] E. de Jong, H. Langeveld, R. van Ree, IEA Bioenergy Task 42 Biorefinery, IEA Bioenergy, **2011**. https://edepot.wur.nl/164503.

[11] A. F. Ferreira, in *Lecture Notes in Energy*, vol. 57, (Eds.: M. Rabaçal, A. Ferreira, C. Silva, M. Costa), Springer, Cham (Switzerland), **2017**, pp. 1–20.

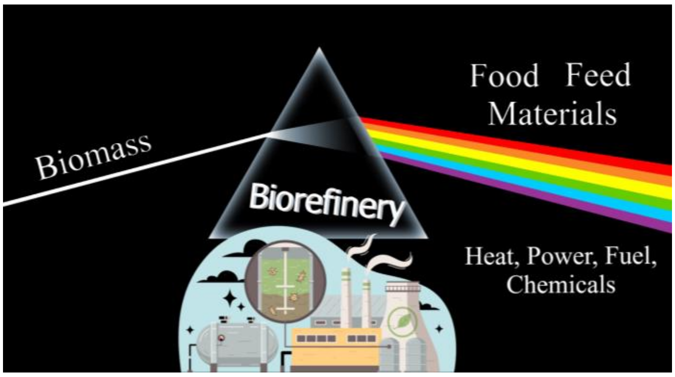

Figure I.1. Biorefinery concept representation: from biomass to high-value compounds (revised from reference 10).

Unlike fossil fuel-dependent petroleum refineries, biorefineries employ biomass as feedstock to produce energy and chemicals. Significant distinctions encompass feedstocks, building blocks, processes, and chemical intermediates between both approaches.[12] A brief summary is reported in Table I.1.

The primary distinction lies in the inherent nature of the systems. Crude oil refineries possess minimal uncertainties regarding plant location, size, raw materials, technologies, and products, which are well-defined. In contrast, biorefineries exhibit uncertainties in these aspects. Factors like location, scale, and products are not predetermined and require holistic analyses of feedstock, market, and process design for their determination.

---

[12] a) E. de Jong, G. Jungmeier, in *Industrial Biorefineries & White Biotechnology*, (Eds.: A. Pandey, R. Höfer, M. Taherzadeh, K. M. Nampoothiri, C. Larroche), Elsevier, Amsterdam (The Netherlands), **2015**, pp. 3–33; b) R. V. Kumar, K. Pakshirajan, G. Pugazhenthi, in *Platform Chemical Biorefinery. Future Green Chemistry*, (Eds.: S. K. Brar, K. Pakshirajan), Elsevier, Amsterdam (The Netherlands), **2016**, pp. 33–53.

Table I.1. Comparison between refineries and biorefineries in terms of feedstock, products, processes and facilities.

Aspect	Refinery	Biorefinery
Feedstocks	Homogeneous	Heterogeneous
	Low oxygen content	High oxygen content
	Rich in hydrocarbons	Less amount of carbon and hydrogen
	No storage is required	Long-term storage, delicate for water-rich biomasses
Transformation processes to obtain building blocks	Homogeneous chemical processes (e.g., steam cracking and catalytic reforming)	Combination of heterogeneous chemical and biotechnological processes (e.g., hydrogenation, fermentation)
	Narrow and traditional range of processing technologies	Large array of processing technologies
Product spectrum	One or few products, well-established production chain	Wide range of products, due to seasonal feedstocks
Chemicals commercialized	Many	Still few, but increasing
Facilities	Close to feedstock: reduced transportation costs	Far away from oil resources: increased transportation costs
	Single large industries in urban areas	Different industrial complexes, possibly in rural areas

Seasonal variability and feedstock composition pose challenges for biorefineries, unlike oil refineries with consistent supply.[13] The solution is to integrate biorefineries operating at multiple levels, utilizing diverse feedstocks like crops and food wastes. This flexibility allows adaptation to changing patterns without compromising cost-efficiency or effectiveness. Additionally, selecting easily accessible biomass simplifies supply logistics and reduces associated costs.[14]

---

[13] S. Fernando, S. Adhikari, C. Chandrapal, N. Murali, *Energy Fuels* **2006**, *20*, 1727–1737.

Integration in a biorefinery involves designing processes for self-sufficiency and long-term viability. The costliness of biorefinery investment is mitigated by producing a diverse range of compounds rather than a single product. Biomass serves as a source for primary goods like biofuels and energy. Process residues are repurposed for heat, electricity, or further upgraded for coproducing value-added chemicals, materials, food, and feed. This sustains the supply chain, lowering production costs and sale prices.[15] Integration extends to the biorefinery's location, intertwining with the local area for progressive development. A biorefinery, comprising multiple plants, fosters coordinated relationships with various local stakeholders across different value chains-cooperatives, farmers, institutions, universities, and others. Traditional facilities can contribute by supplying pretreated biomass and energy. This collaborative framework involves compound and energy exchanges with local entities, bolstering plant acceptance, competitive edge, and regional growth.[16]

Under these perspectives, an integrated biorefinery envisions a solid production chain with zero (or minimal) wastes by reusing residues within the same facility cluster. This creates a closed-loop system where primary and secondary products, energy generation, raw material supply, and wastewater treatment ensure self-sufficiency and competitiveness in the market, while fostering local development (Figure I.2).[17]

---

[14] W. M. Budzianowski, K. Postawa, *Appl. Energy* **2016**, *184*, 1432–1446.

[15] J. Clark, F. Deswarte, in *Introduction to Chemicals from Biomass*,John Wiley Sons, Ltd (Eds.: J. Clark, F. Deswarte), John Wiley & Sons, Ltd, **2015**, 1–29.

[16] I. L. Ceapraz, G. Kotbi, L. Sauvée, *Bio-based Appl. Econ.* **2016**, *5*, 47–62.

[17] a) S. Venkata Mohan, S. Dahiya, K. Amulya, R. Katakojwala, T. K. Vanitha, *Bioresour. Technol. Reports* **2019**, *7*, 100277; b) S. Sachdeva, V. K. Garg, N. K. Labhsetwar, A. Singh, K. N. Yogalakshmi, in *Energy, Environ. Sustain.* (Eds.: Y.K. Nandabalan, V.K. Garg, N.K. Labhsetwar, A. Singh), Springer Singapore, **2022**, pp. 3–22.

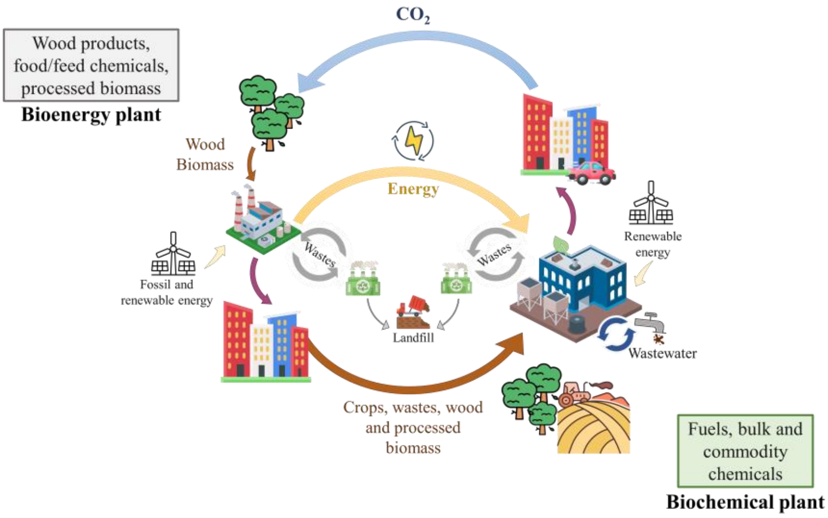
CO$_2$
Wood products, food/feed chemicals, processed biomass
Bioenergy plant
Wood Biomass
Energy
Renewable energy
Fossil and renewable energy
Wastes
Wastes
Landfill
Wastewater
Crops, wastes, wood and processed biomass
Fuels, bulk and commodity chemicals
Biochemical plant

Figure I.2. Example of a real integrated biorefinery, consisting of two main productive sites: the energy producing plant (left side) and the main chemical producing plant (right side). Pictures were taken from https://pngtree.com/ and https://it.freepik.com/.

I.1.1. Biorefineries classification

A systematic classification for biorefineries remains absent. Drawing from literature and official reports, four classification methods have been identified categorizing based on: (i) feedstocks, platforms, processes, and products; (ii) systems or models; (iii) size; and (iv) technological implementation status. The initial classification method was introduced by the IEA Bioenergy Task 42 committee. Although the latest report on 2022 features more detailed sub-categories reflecting recent techniques, the original graph on 2008 is herein reported, as the fundamental classification basis. Notably, this method encompasses feedstocks, processes, and products, offering a comprehensive framework for understanding biorefinery types. It unambiguously categorizes biorefineries according to four main features:[18]

---

[18] a) F. Cherubini, G. Jungmeier, M. Wellisch, T. Willke, I. Skiadas, R. Van Ree, E. de Jong, *Biofuels, Bioprod. Biorefining* **2009**, *3*, 534–546; b) V. Aristizábal-Marulanda, C. A. Cardona Alzate, *Biofuels, Bioprod. Biorefining* **2019**, *13*, 789–808.

feedstock, conversion processes, platforms, and products. All categories are, then, further divided into subgroups (Figure I.3).

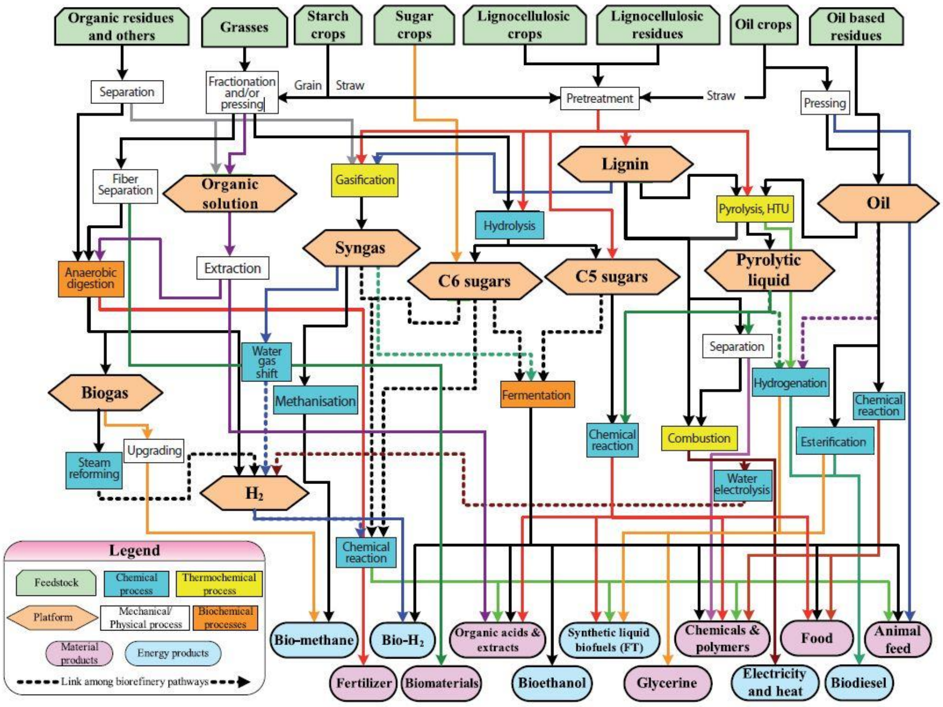
Organic residues and others
Grasses
Starch crops
Sugar crops
Lignocellulosic crops
Lignocellulosic residues
Oil crops
Oil based residues
Separation
Fractionation and/or pressing
Grain
Straw
Pretreatment
Straw
Pressing
Fiber Separation
Organic solution
Gasification
Lignin
Pyrolysis, HTU
Oil
Hydrolysis
Syngas
C6 sugars
C5 sugars
Pyrolytic liquid
Anaerobic digestion
Extraction
Separation
Water gas shift
Biogas
Methanisation
Fermentation
Hydrogenation
Chemical reaction
Chemical reaction
Combustion
Esterification
Steam reforming
Upgrading
Water electrolysis
H₂
Chemical reaction
Legend
Feedstock
Chemical process
Thermochemical process
Platform
Mechanical/ Physical process
Biochemical processes
Material products
Energy products
Link among biorefinery pathways
Bio-methane
Bio-H₂
Organic acids & extracts
Synthetic liquid biofuels (FT)
Chemicals & polymers
Food
Animal feed
Fertilizer
Biomaterials
Bioethanol
Glycerine
Electricity and heat
Biodiesel

Figure I.3. Sum-up of the network used for the classification of biorefineries, taken from reference 19, drafted by the authors according to IEA Bioenergy Task 42 Report,[20] highlighting four features and its subgroups: feedstock (green), conversion processes (dark blue, yellow, white, and dark orange), platforms (light orange) and products (purple and light blue).

The term "feedstock" refers to materials entering a process, divided into "crops" (e.g., starch crops) and "residues" (e.g., bark, straw, waste cooking oils). Conversion processes fall into chemical (acid hydrolysis, esterification), thermochemical (gasification, pyrolysis), biochemical

---

[19] F. Cherubini, *Energy Convers. Manag.* **2010**, *51*, 1412–1421.

[20] IEA Bioenergy Task 42, *Biorefineries: adding value to the sustainable utilisation of biomass* **2008**. Available: https://www.ieabioenergy.com/wp-content/uploads/2013/10/IEA-Bioenergy-2008-Annual-Report_6127.pdf.

(fermentation, enzymatic conversion), and mechanical (fractionation, pressing, size reduction) categories. The 2022 update has introduced blending processes, mechanical pulping, and a new thermochemical sub-type: “torrefaction and carbonization processes”.[21] Platforms in biorefineries are like intermediate compounds in petrochemical refineries, bridging feedstock and final products. They include crucial chemicals like C5-C6 sugars, syngas, biogas, lignin, and pyrolysis liquid, also termed pillars or building-blocks. Platforms may serve as both intermediates and final products, reflecting the system complexity. The 2022 report introduced innovative platforms such as biochar, bio-naphtha, and CO_2, leading to a total number of 17. Biorefinery outputs are divided into two main categories: energy products (e.g., biofuels, biomethane) and material goods (e.g., food, chemicals). A comprehensive biorefinery features both types of products, energy-driven biorefineries produce valuable compounds alongside primary products, while product-focused biorefineries utilize by-products to generate secondary energy carriers like power and heat for market distribution or internal use.[22]

Status Report Biorefinery 847 classified biorefineries considering the systems or models of the producing lines related to the raw material utilized,[23] as shown in Table I.2. The six biorefinery types are briefly introduced with a mention to the different stages of development, based on the Technology Readiness Level (TRL).[24]

---

[21] B. Annevelink, L. Garcia Chavez, R. van Ree, I. V. Gursel, IEA Bioenergy Task 42, *Biorefining in a Circular Economy*, **2022**. Available: https://www.ieabioenergy.com/wp-content/uploads/2022/09/IEA-Bioenergy-Task-42-Global-biorefinery-status-report-2022-220712.pdf.

[22] R. Reshmy, T. A. P. Paulose, E. Philip, D. Thomas, A. Madhavan, R. Sirohi, P. Binod, M. K. Awasthi, A. Pandey, R. Sindhu, *Fuel* **2022**, *308*, 122056.

[23] R. van Ree, B. Annevelink, Status Report Biorefinery 847, **2007**. https://edepot.wur.nl/42141.

[24] G. Jungmeier, R. Van Ree, H. Jorgensen, E. de Jong, H. Stichnote, M. Wellisch, *The Biorefinery Complexity Index*, **2014**. Available at: https://task42.ieabioenergy.com/wp-content/uploads/sites/10/2017/06/BCI-working-document-20140709.pdf.

Table I.2. Biorefinery types according to the producing lines.

Biorefinery (BR) type	Feedstock	TRL[a]
Conventional	Existing industries (sugar, starch, vegetable oils)	9
Whole Crop	Crops (straw, biomasses) and cereals (corn, wheat, maize)	7-8
Ligno-Cellulosic Feedstock	Lignocellulosic biomass (reed, wood)	6-8
Green	Wet biomass (grass and crops as clover)	5-7
Two Platform	Sugar and syngas platforms combined	Pilot Plant
Marine	Seaweed and marine biomass (Micro and Macroalgae)	5-6
Thermo-Chemical	Thermochemical conversion of wide range of biomasses	7-9

[a] Technology Readiness Level (TRL): between 1 ("basic research") to 9 ("system proven and ready for full commercial deployment"). TRL values were obtained from reference 25.

Apart from the size of the plant and number of outputs, a useful method of sorting biorefineries is taking into account the status of the technological implementation, classified as: first, second and third generation of biorefinery.[26] In Table I.3, the main biorefinery types according to this method are described.

---

[25] J. Lindorfer, M. Lettner, F. Hesser, K. Fazeni, D. Rosenfeld, B. Annevelink, M. Mandl, *Technical, Economic and Environmental Assessment of Biorefinery Concepts*, **2019**. Available: https://task42.ieabioenergy.com/wp-content/uploads/2019/07/TEE_assessment_report_final_20190704-1.pdf.

[26] a) B. Kamm, M. Kamm, *Appl. Microbiol. Biotechnol.* **2004**, *64*, 137–145; b) J. Moncada, J. A. Tamayo, C. A. Cardona, *Chem. Eng. Sci.* **2014**, *118*, 126–140; c) A. T. Ubando, A. J. R. Del Rosario, W.-H. Chen, A. B. Culaba, *Environ. Pollut.* **2021**, *269*, 116149; d) F. G. Calvo-Flores, F. J. Martin-Martinez, *Front. Chem.* **2022**, *10*, 1–23.

Table I.3. Distinctive features of first, second, and third generation of biorefineries in terms of raw material, key characteristics and real applications in advanced TRL.

Generation	Feedstock	Characteristics	Real examples
First[27] (Conventional)	Agricultural and forestry biomass (starch, vegetables, sugar)	Low flexibility and integration. Competition with food industry. Intensive cultures	Pomacle-Bazancourt Biorefinery, FR; BioWanze, Wanze Bioethanol Plant, BE
Second[28] (Advanced)	Lignocellulosic biomass (residues from crops, forestry, agriculture)	Medium flexibility and integration. Less dependence from seasonal availability of feedstock. Land-use efficiency	Beta Renewables, IT; Fortum, FI
Third[29] (Advanced)	Organic waste streams and algae to obtain, e.g., biofuels	High flexibility and integration. Wide range of products. Mainly wastes as raw materials. No competition with food-feed industry	Sapphire Energy Inc., USA; Gas Technology Institute – GTI, USA

First-generation biorefineries initially used food crops for liquid biofuels, raising concerns about food competition and environmental impact.[30] Second-generation biorefineries addressed these issues by utilizing non-edible and waste materials. These alternatives, such as glycerol (as by-product of diesel production), and industrial and domestic wastes, have reduced bio-waste accumulation, do not compete with food production, and remain available year-round.[31] However, dedicated crop use could still compete with food crops requiring the forest to be cleared for new land. Third-generation biorefineries employ microalgae, growing year-round in basic photo-bioreactors without land or resource conflicts.[32] Fourth-generation biorefineries, recently developed, employ genetically modified microorganisms for CO_2 capture, enhancing biofuel production as artificial "carbon sinks".[33]

---

[27] Ó. J. Sánchez, C. A. Cardona, *Bioresour. Technol.* **2008**, *99*, 5270–5295.

[28] N. Qureshi, B. C. Saha, R. E. Hector, B. Dien, S. Hughes, S. Liu, L. Iten, M. J. Bowman, G. Sarath, M. A. Cotta, *Biomass and Bioenergy* **2010**, *34*, 566–571.

[29] a) L. Goswami, R. Kayalvizhi, P. K. Dikshit, K. C. Sherpa, S. Roy, A. Kushwaha, B. S. Kim, R. Banerjee, S. Jacob, R. C. Rajak, *Chem. Eng. J.* **2022**, *448*, 137677; c) A. Saravanan, P. Senthil Kumar, M. Badawi, G. Mohanakrishna, T. M. Aminabhavi, *Chem. Eng. J.* **2023**, *453*, 139754.

[30] J. Jeevahan, A. Anderson, V. Sriram, R. B. Durairaj, G. Britto Joseph, G. Mageshwaran, *Int. J. Ambient Energy* **2021**, *42*, 1083–1101.

I.1.2. Biorefinery in the context of circular bioeconomy

Biorefineries embody the transition to sustainable products from renewable resources, aligning with the global shift towards a circular bioeconomy.[34] Circular bioeconomy idea reflects the principles of bioeconomy, but integrated with the concept of circularity.[35] The bioeconomy principles, indeed, deal with a more general transition from a fossil-based to a biomass-based economy, promoting the sustainable use of renewable resources for economic, environmental, and social benefits.[36] Conversely, circular economy concept takes into account more the economic prosperity than the environment quality and the social aspect of sustainability (i.e., human well-being).[37] It remodels the life-cycle of a product, in the "4R" framework: Reduce, Reuse, Recycle (of resources for preservation of natural capital), and Recovery (of the resource in the form of energy).[38]

---

[31] F. H. Isikgor, C. R. Becer, *Polym. Chem.* **2015**, *6*, 4497–4559.

[32] L. Bhatia, R. K. Bachheti, V. K. Garlapati, A. K. Chandel, *Biomass Convers. Biorefinery* **2022**, *12*, 4215–4230.

[33] S. Y. A. Siddiki, M. Mofijur, P. S. Kumar, S. F. Ahmed, A. Inayat, F. Kusumo, I. A. Badruddin, T. M. Y. Khan, L. D. Nghiem, H. C. Ong, T. M. I. Mahlia, *Fuel* **2022**, *307*, 121782.

[34] S. Dahiya, R. Katakojwala, S. Ramakrishna, S. V. Mohan, *Mater. Circ. Econ.* **2020**, *2*, 7

[35] D. D'Amato, S. Veijonaho, A. Toppinen, *For. Policy Econ.* **2020**, *110*, 101848.

[36] a) A. Aguilar, T. Twardowski, R. Wohlgemuth, *Biotechnol. J.* **2019**, *14*, 1800638; b) E. Gawel, N. Pannicke, N. Hagemann, *Sustainability* **2019**, *11*, 3005; c) T. A. Swetha, K. Mohanrasu, M. Sudhakar, R. Raja, K. Ponnuchamy, G. Muthusamy, A. Arun, *Sustain. Energy Technol. Assess.* **2022**, *53*, 102682.

[37] a) P. Ghisellini, C. Cialani, S. Ulgiati, *J. Clean. Prod.* **2016**, *114*, 11–32; b) A. Murray, K. Skene, K. Haynes, *J. Bus. Ethics* **2017**, *140*, 369–380.

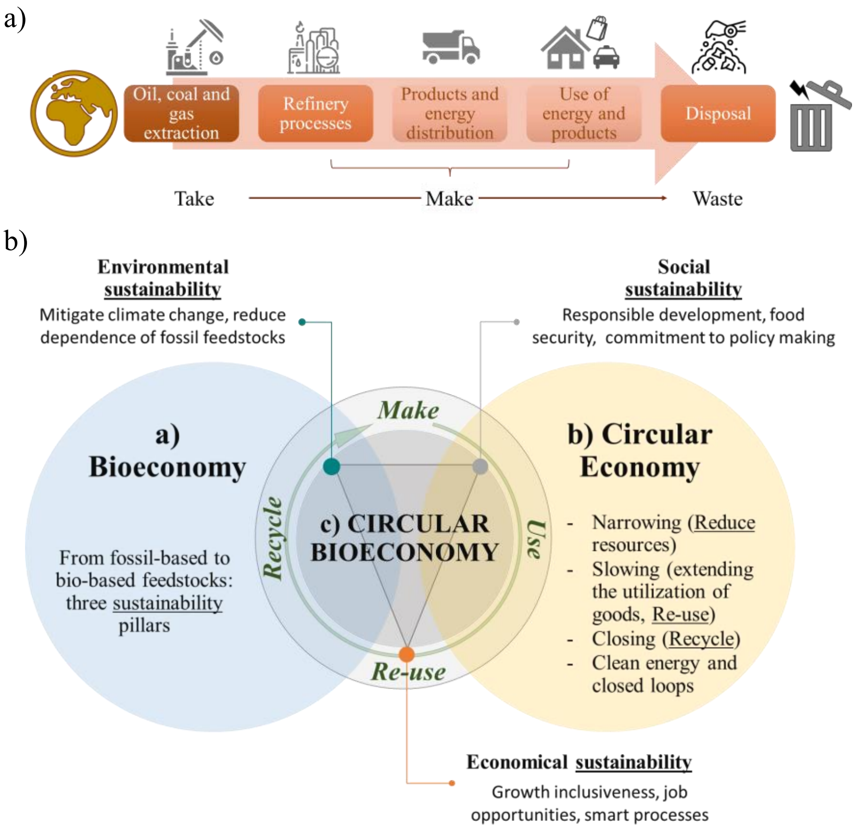
a)
Oil, coal and gas extraction
Refinery processes
Products and energy distribution
Use of energy and products
Disposal
Take
Make
Waste
b)
Environmental sustainability
Mitigate climate change, reduce dependence of fossil feedstocks
Social sustainability
Responsible development, food security, commitment to policy making
a) Bioeconomy
From fossil-based to bio-based feedstocks: three sustainability pillars
Make
Recycle
Use
Re-use
c) CIRCULAR BIOECONOMY
b) Circular Economy
- Narrowing (Reduce resources)
- Slowing (extending the utilization of goods, Re-use)
- Closing (Recycle)
- Clean energy and closed loops
Economical sustainability
Growth inclusiveness, job opportunities, smart processes

Figure I.4. a) Schematic representation of a linear economy for fossil energy; b) representation of circular bioeconomy in sections, resulting from the intersection between bioeconomy and circular economy concepts. Pictures were taken from https://pngtree.com/.

While traditional economy in the past has considered manufacturing processes (and also economy development) as a straight arrow (Figure I.4a), the circular economy introduced the circularity of resources as part of a slow, narrow, and close loop, to minimize the whole process' environmental footprint (Figure I.4b).[39] The crossroad of the circular economy and the bioeconomy emerged as circular bioeconomy, where both concepts are complemented to resolve sustainability challenges.[40]

---

[38] M. Lieder, A. Rashid, *J. Clean. Prod.* **2016**, *115*, 36–51.

Biorefinery and circular bioeconomy align to enhance sustainability and biomass utilization. Biorefineries exemplify cradle-to-cradle of wastes, use of renewable feedstocks, and favour closed-loops of energy cycles, supporting the bioeconomy's pillars. The synergy between biorefineries and circular bioeconomy optimizes the resource use, minimizes waste, and advances sustainable biomass practices. Second, third, and waste biorefineries (based on urban, and other waste processes, as solid and liquid residues),[41] represent the core of a circular bioeconomy paradigm.[42]

I.1.3. Biorefinery design and SWOT analysis of a biorefinery system

For economic viability, a biorefinery must yield valuable products, high-volume low-grade goods, and energy outputs. Sustainability is vital, minimizing solid, liquid, and gaseous waste, potentially reusing them. Biorefinery design must maintain continuous, centralized, capital-intensive operations while distributing collection, separation, and storage to decentralized sites. This addresses limitations like long-distance feedstock transport and costly storage, enhancing cost-effectiveness.[43] Moreover, decentralized pretreatment units prepare biomass by handling collection, drying, and densification prior to transportation to the central biorefinery or storage place.[44] In light of all these evidences, biorefineries address sustainability and environmental concerns by supplying diverse bio-based products and energy sustainably, benefiting both developed and developing countries through novel skills, jobs, and markets.

---

[39] a) F. Sariatli, *Visegr. J. Bioecon. Sustain. Dev.* **2017**, *6*, 31–34; b) J. Korhonen, C. Nuur, A. Feldmann, S. E. Birkie, *J. Clean. Prod.* **2018**, *175*, 544–552.

[40] E. C. D. Tan, P. Lamers, *Front. Sustain.* **2021**, *2*, 701509.

[41] H. Y. Leong, C.-K. Chang, K. S. Khoo, K. W. Chew, S. R. Chia, J. W. Lim, J.-S. Chang, P. L. Show, *Biotechnol. Biofuels* **2021**, *14*, 87.

[42] R. Katakojwala, S. V. Mohan, *Curr. Opin. Green Sustain. Chem.* **2021**, *27*, 100392.

[43] S. S. Hassan, G. A. Williams, A. K. Jaiswal, *Trends Biotechnol.* **2019**, *37*, 231–234.

[44] a) R. J. Stoklosa, A. del Pilar Orjuela, L. da Costa Sousa, N. Uppugundla, D. L. Williams, B. E. Dale, D. B. Hodge, V. Balan, *Bioresour. Technol.* **2017**, *226*, 9–17; b) J. Venus, S. Fiore, F. Demichelis, D. Pleissner, *J. Clean. Prod.* **2018**, *172*, 778–785.

Table I.4. Strengths, weaknesses, opportunities, and threats (SWOT) analysis on biorefineries.

Strengths	Weaknesses
♦ Sustainable utilization of biomass ♦ Efficiency of biomass conversion: circular bioeconomy principles ♦ Well-established practice in certain market sectors ♦ Self-sufficiency of local realities ♦ Diverse range of bio-based products and bioenergy ♦ Reduced dependence of fossil biomasses – climate impact reduced	♦ Immaturity of producing plants ♦ High investments due to new process developments ♦ Biomass variability ♦ Uncertainty about processes set-up ♦ Lack of infrastructures to support the collaboration between stakeholders ♦ Emphasis on developing new concepts rather than implementing them in the actual market
Opportunities	**Threats**
♦ Addresses the global policy objectives and GHG emissions brought down ♦ International interest ♦ Enhancement of an economic position of various market sectors ♦ Independence of economies - improved conditions for developing economies ♦ Reducing overall waste generation	♦ Competitiveness with fossil fuels which more easily decrease in prices ♦ Availability of raw materials, affected by climate change, policies, and logistics ♦ Difficulty in securing high investment capital ♦ Fluctuating long-term governmental policies

The SWOT analysis encompasses strengths, weaknesses, opportunities, and threats for various biorefinery types (first,[45] second,[46] third,[47] and new generation[48] ones), illustrating their advantages and challenges in establishing competitiveness against conventional fuel and chemical ones.[49] A summary can be found in Table I.4.

I.1.4. Examples of biorefineries

Governments encourage multidisciplinary partnerships and research to decouple from oil and gas inputs. This includes repurposing old refineries and fostering new biorefineries, ranging from start-ups to competitive ventures. Notably, first and second generation biorefineries, as well as waste ones, have gained traction, while third and fourth generation biorefineries (e.g., algae and modified organisms) are still evolving due to technological readiness. The 2022 IEA Global Biorefinery report highlights examples of such biorefineries in EU (partner) countries.[19] Amongst them, Lenzing AG in Austria,[50] a second-generation biorefinery, uses sustainable spruce, birch, and beech wood. It produces pulp, high-quality fibers, acetic acid, xylose, and furfural. Moreover, wood energy powers the facilities, ensuring self-sufficiency.

In Italy, Crescentino, the Versalis biorefinery (Figure I.5a),[51] funded by Beta Renewable, is a TRL8 second-generation plant producing bioethanol, disinfectants, and biogas. It integrates wastewater treatment for energy generation. Three platforms (sugars, lignin, and power/heat) use hardwood and agricultural residuals. Generated energy supports operations and excess is fed to the grid. The plant shifted the focus on 2017 to chemical intermediates, polyethylene, styrene, and elastomer production. Still in Italy, a waste-biorefinery located in Venice funded by the national energy company Eni, utilizes diverse feedstocks including vegetable oil, animal fats, algae, and local waste by-products. It is the world's first converted conventional refinery, aiming to produce high-quality biofuels like bio-naphtha and bio-jet fuel from wastes (Figure I.5b).

---

[45] A. Peeters, *Grassl. Sci.* **2009**, *55*, 113–125.

[46] N. Singh, R. R. Singhania, P. S. Nigam, C.-D. Dong, A. K. Patel, M. Puri, *Bioresour. Technol.* **2022**, *344*, 126415.

[47] X. Zhang, M. Thomsen, *Algal Res.* **2021**, *60*, 102499.

[48] R. B. Sartori, R. R. Dias, L. Q. Zepka, E. Jacob-Lopes, in *Handb. Waste Biorefinery* (Eds.: E. Jacob-Lopes, L. Q. Zepka, M. Costa Deprá), Springer International Publishing, Cham, **2022**, 119–136.

[49] a) Z. Usmani, M. Sharma, A. K. Awasthi, T. Lukk, M. G. Tuohy, L. Gong, P. Nguyen-Tri, A. D. Goddard, R. M. Bill, S. C. Nayak, V. K. Gupta, *Renew. Sustain. Energy Rev.* **2021**, *148*, 111258; b) D. Pérez Almada, Á. Galán-Martín, M. del M. Contreras Gámez, E. Castro Galiano, *Sustain. Energy Fuels* **2023**

[50] https://www.lenzing.com/.

[51] https://www.versalis.eni.com/en-IT/home.html.

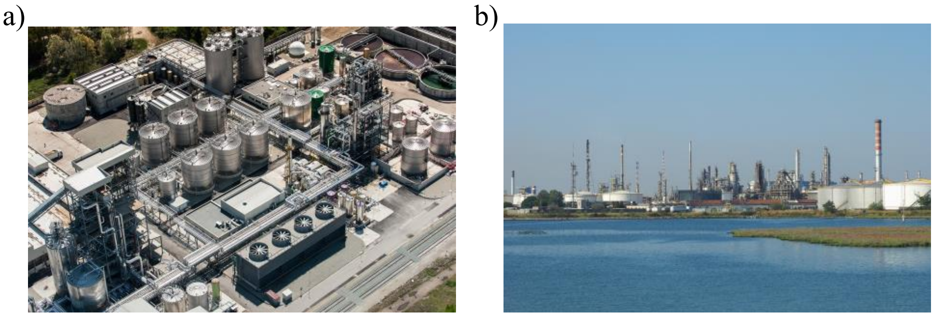

Figure I.5. a) Versalis Biorefinery; and b) Eni Biorefinery plant, both in Italy. Pictures taken from reference 52.

In the Netherlands, Avantium YXY® Technology[53] operates a non-energy producing pilot biorefinery. It utilizes furan derivatives from starch and sucrose in waste lignocellulosic biomasses to create furan-based monomer (FDCA) for biopolymer synthesis, fuels, resins, solvents, flavors, and fragrances. The integrated approach includes a local gasification facility for efficient residue utilization. Collaborative efforts aim to introduce

---

[52] a) https://www.eni.com/en-IT/operations/italy-crescentino-renewables-chemicals-integrated-plant.html; b) https://www.venetoeconomia.it/2019/02/eni-porto-marghera-manutenzione/.

[53] https://www.avantium.com/technologies/yxy/.

polyethylene furan-2,5-dicarboxylate (PEF) and polyethylene terephthalate (PET)/PEF bottles to the market.

Other noteworthy biorefineries include Cellulac (Ireland), which produces lactic acid, ethyl lactate, and polylactic acid from lactose whey permeate and biomass; Lantmännen Agroethanol (Sweden), which processes lignocellulosic biomass for bioethanol, animal feed, and CO_2; BIOWERT GmbH (Germany), that uses grass for insulation, plastic, and fertilizer; and Billund Biorefinery (Denmark), which utilizes household wastes for biogas, bioplastics, and organic fertilizers. These European facilities, along with DuPont (USA), Shandong Longlive (China), and Sarina Biorefinery MacKay (Australia), demonstrate the global interest for sustainable biorefineries.

I.2. Processing lignocellulosic biomass for the production of high-value compounds

Nations are driven by global environmental concerns to establish a new bioeconomy. For instance, EU countries aim for a 40% GHG reduction and 27% renewable energy share by 2030,[54] with a 2050 goal of climate neutrality, pursued by the US.[55] Yet, the path to "net 0 CO_2" by 2050 appears distant, with 30.6 Gt of CO_2 emissions still present. Mismanaged solid waste contributes with 1.6 billion tonnes of CO_2 equivalents. Globally, municipal solid waste production of 2.01 billion tonnes annually is predicted to increase by 2050.[56] Around 33% of this waste is unsustainably handled, offering a valuable resource for biorefineries, especially lignocellulose-rich biomasses (LCBs), which are highly abundant but underutilized. This vast potential could power the renewable biorefinery sector. Natural lignocellulose-rich biomasses, offer significant potential as renewable biorefineries feedstock for a wide array of bio-products: their annual production is estimated to be nearly 200 billion tons,[57] and only 8.2 billion tons are currently utilized by different application areas, being the rest disposed as fodder for animals or burnt in open lands.[58] Hence, both municipal and agro-food lignocellulose-rich biomasses (LCBs) hold vast untapped potential as feedstock for diverse bio-products in renewable biorefineries.[59]

---

[54] A European Green Deal (europa.eu).

[55] a) EUR-Lex - 52016PC0767 - EN - EUR-Lex (europa.eu) b) United Nations. Climate action. 2020; b) https://www.un.org/en/climatechange/science/key-findings.

[56] World Bank. What a waste 2.0: trends in solid waste management. 2020. https://datatopics.worldbank.org/what-a-waste/trends_in_solid_waste_management.html.

I.2.1. Composition and characterization of LCBs

Lignocellulosic biomass is a complex mixture of carbohydrates and aromatic polymers within plant cell walls, varying by biomass type. This affects its suitability for biorefinery processes. The primary cell wall contains cellulose non-oriented microfibrils, connected by hemicellulose, pectins, and proteins. The highly hydrated structure contributes to the elasticity and sustainment of cell pressure, providing support to cell expansion. The secondary cell wall, more relevant for biomass processes, offers wood cells strength and rigidity, being a support to compressive and tensile strength due to cell expansion.[60] Secondary cell walls exhibit a differentiated structure in lamellae with a higher quantity of oriented cellulose microfibrils contained in a matrix of hemicelluloses and lignin.[61] Extractives, pectin, proteins, and metals or ashes in fractions are also present (Figure I.6).[62]

---

[57] J. Sharma, V. Kumar, R. Prasad, N. A. Gaur, *Biotechnol. Adv.* **2022**, *56*, 107925.

[58] V. Ashokkumar, R. Venkatkarthick, S. Jayashree, S. Chuetor, S. Dharmaraj, G. Kumar, W.-H. Chen, C. Ngamcharussrivichai, *Bioresour. Technol.* **2022**, *344*, 126195.

[59] a) J. A. Okolie, S. Nanda, A. K. Dalai, J. A. Kozinski, *Waste and Biomass Valorization* **2021**, *12*, 2145–2169; b) M. V. Rodionova, A. M. Bozieva, S. K. Zharmukhamedov, Y. K. Leong, J. Chi-W. Lan, A. Veziroglu, T. N. Veziroglu, T. Tomo, J.-S. Chang, S. I. Allakhverdiev, *Int. J. Hydrogen Energy* **2022**, *47*, 1481–1498.

[60] D. J. Cosgrove, M. C. Jarvis, *Front. Plant Sci.* **2012**, *3*, 204.

[61] N. N. Deshavath, V. D. Veeranki, V. V. Goud, in *Sustainable Bioenergy*, (Eds.: M. Rai, A. P. Ingle), Elsevier, Amsterdam (The Netherlands), **2019**, pp. 1–19.

[62] P. E. Marriott, L. D. Gómez, S. J. McQueen-Mason, *New Phytol.* **2016**, *209*, 1366–1381.

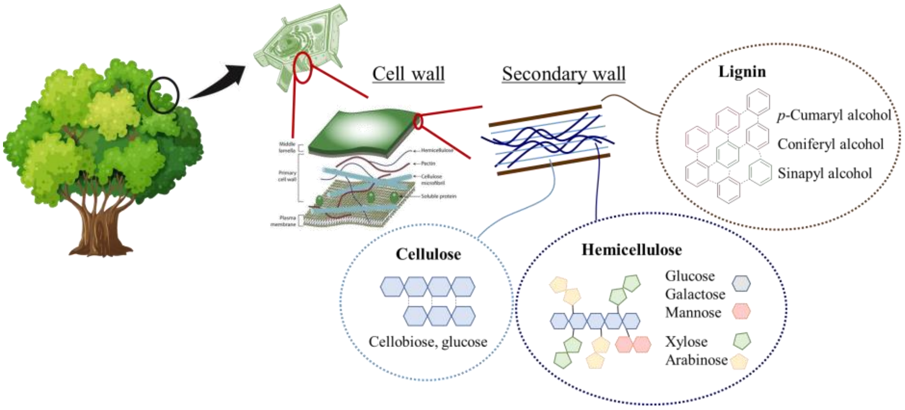
Cell wall
Secondary wall
Lignin
p-Cumaryl alcohol
Coniferyl alcohol
Sinapyl alcohol
Middle lamella
Primary cell wall
Plasma membrane
Hemicellulose
Pectin
Cellulose microfibril
Soluble protein
Cellulose
Cellobiose, glucose
Hemicellulose
Glucose
Galactose
Mannose
Xylose
Arabinose

Figure I.6. Structural composition of plant cell walls and main LCB components. Pictures were taken from https://pngtree.com/ and https://bioicons.com/.

Cellulose, Earth's most abundant polysaccharide, is a glucose-based homopolymer (β-1,4-glycosidic bonds between monomers). Its natural role consists of providing strength and rigidity to the plant cell wall. Variations in lignocellulosic biomass affect the degree of polymerization and the length of the cellulose chain,[63] as well as hydrogen bonds,[64] influencing the water solubility of the chains. Most cellulose is crystalline, with a small amorphous fraction, their proportions depending on the polymer source.[65]

Hemicellulose is the nature's second-most abundant carbohydrate, forming a diverse, branched matrix in lignocellulosic biomass. It is the cross-linker between cellulose polymers and lignin in the plant cell walls, providing support and flexibility. Unlike the uniform cellulose, hemicellulose is heteropolymeric and shorter. The main backbone is made up of homopolymers (xylan, glucan, and galactan) or heteropolymers (glucomannan). Substituents of the polymeric basis are pentoses (xylose, rhamnose, and arabinose), hexoses (glucose, mannose, and galactose), and organic acids.[66] Composition, structure, and amount of hemicellulose depends again from its natural source:[67] in general, xylose is the most abundant monomer in hardwood and herbaceous plants, while mannose-type monomers in softwoods.[68]

---

[63] H. Seddiqi, E. Oliaei, H. Honarkar, J. Jin, L. C. Geonzon, R. G. Bacabac, J. Klein-Nulend, *Cellulose* **2021**, *28*, 1893–1931.

[64] L. Alves, B. Medronho, F. E. Antunes, D. Topgaard, B. Lindman, *Carbohydr. Polym.* **2016**, *151*, 707–715.

[65] A. Khenblouche, D. Bechki, M. Gouamid, K. Charradi, L. Segni, M. Hadjadj, S. Boughali, *Polímeros* **2019**, *29*, e2019011.

Lignin, a complex and rigid polymer, offers structural support and protection to plant tissues. It consists mainly of 4-hydroxyphenylpropanoids (*p*-coumaryl, coniferyl, and sinapyl alcohols), varying in methoxylation and bonded by ether or carbon–carbon linkages.[69] The three-dimensional structure fills spaces between cellulose and hemicellulose, forming a strong and resistant material that avoids microbial degradation.[70] Moreover, it gives rigidity and hydrophobicity, avoiding secondary wall swelling in water, which is essential for water conductivity in vascular tissues.[71]

Lignocellulosic biomass sources include forest woody residues, agriculture and herbaceous wastes, food and municipal residues, and pulp and paper mill industry residues.[72] These categories encompass forestry residues,[73] dedicated crops like perennial herbaceous plants, hardwood sources, grassy and woody inedible crops,[74] agricultural straw, food peels, and pulp and paper industry sludge (Table I.5).[75]

---

[66] J. Rao, Z. Lv, G. Chen, F. Peng, *Prog. Polym. Sci.* **2023**, *140*, 101675.

[67] C. Schädel, A. Blöchl, A. Richter, G. Hoch, *Plant Physiol. Biochem.* **2010**, *48*, 1–8.

[68] F. Peng, P. Peng, F. Xu, R.-C. Sun, *Biotechnol. Adv.* **2012**, *30*, 879–903.

[69] a) A. N. M. A. Haque, R. Remadevi, M. Naebe, *Cellulose* **2018**, *25*, 5455–5477; b) R.-C. Sun, *ChemSusChem* **2020**, *13*, 4385–4393.

[70] N. Ithal, J. Recknor, D. Nettleton, T. Maier, T. J. Baum, M. G. Mitchum, *Mol. Plant-Microbe Interact.* **2007**, *20*, 510–525.

[71] M. Schuetz, A. Benske, R. A. Smith, Y. Watanabe, Y. Tobimatsu, J. Ralph, T. Demura, B. Ellis, A. L. Samuels, *Plant Physiol.* **2014**, *166*, 798–807.

[72] Y. Hadar, in *Lignocellulose Conversion*, (Ed.: V. Faraco), Springer-Verlag, Berlin (Germany), **2013**, pp. 21–38.

[73] M. Hoogwijk, A. Faaij, R. van den Broek, G. Berndes, D. Gielen, W. Turkenburg, *Biomass Bioenerg.* **2003**, *25*, 119–133.

[74] D. K. Lee, E. Aberle, E. K. Anderson, W. Anderson, B. S. Baldwin, D. Baltensperger, M. Barrett, J. Blumenthal, S. Bonos, J. Bouton, *et al.*, *GCB Bioenergy* **2018**, *10*, 698–716.

[75] Mandeep, G. K. Gupta, P. Shukla, *Bioresour. Technol.* **2020**, *297*, 122496.

Table I.5. Types of lignocellulose sources and their alternative use.[72]

Lignocellulosic material	Residue	Other uses
Trees' logs residues	Wood, barks, leaves	Burnt
Saw and lumber wastes	Woodchips, saw dust	Fibre Boards
Pulp and paper mills	Fibre wastes and liquors	Reused as fuels
Community's wastes	Newspapers, furniture	Recycled or burnt
Grass	Marginal lands' grass	Burnt
Cereal's processing residues	Corn, rice waste water	Animal feed
Fruit and vegetable harvesting	Peels, husks, shell, stones, rejected fruits, seeds' residues	Animal feed
Sugar products	Bagasse	Burnt
Oilseed plants (nuts, cotton seeds, soybean…)	Sludge, fibre, husks, press-cake	Animal feed, fertiliser or burnt
Animal wastes	Manure	Soil amendment

Generally, lignocellulosic biomass consists of 35–60% cellulose, 20–40% hemicellulose, and 10–25% lignin.[76] The knowledge of their exact amounts is essential when setting up producing lines of a lignocellulosic-based biorefinery, since it significantly affects biorefinery processes and final products. Forest woody biomass and agricultural crops are rich in cellulose and lignin, with softwood having 30–35% lignin and hardwood up to 25%. Grasses and agricultural residues have lower lignin content (10–30% and 3–15%). Cotton and flax are abundant cellulose sources (80–95% and 60–70%, respectively). Non-woody agri-food crop residues like grasses, corn stover, rice, and wheat straws contain hemicellulose. Table I.6 provides an overview of average lignocellulosic biomass composition. Actual amounts of the main elements vary based on LCB type, while woody residues are influenced by factors like age, growth stage, climate, and soil conditions.

---

[76] J. N. Putro, F. E. Soetaredjo, S.-Y. Lin, Y.-H. Ju, S. Ismadji, *RSC Adv.* **2016**, *6*, 46834–46852.

Table I.6. Average content of cellulose, hemicellulose, and lignin in the chemical composition of main categories of LCBs feedstock used in second generation biorefineries. Values were taken from the reported references.

Type	Source	Cellulose (wt%)	Hemicellulose (wt%)	Lignin (wt%)
Plant fibers (except cotton)[77]		63-76	10-15	2-6
Softwood[78]	Wood fibers	33-42	22-40	27-35
Hardwood[79]	Mainly stems	40-51	17-38	18-25
Grasses[79]		25-40	25-50	10-30
Agricultural wastes[79]	Straw, husk, bagasse	23-45	12-36	6-25
Food industry's wastes[80]	Peel, leaves, pomaces (excluded stones and shells)	13-53	10-22	11-22
Pulp and paper industry wastes[81]		60-70	10-20	5-10

I.2.2. LCBs pretreatments and platform chemicals obtained

In an LCB-based biorefinery, biomass can be converted into biofuels and bio-products through two pathways: thermochemical and biological conversion.[82] An overview of LCB pretreatments is depicted in Figure I.7.

---

[77] B. Madsen, E. K. Gamstedt, *Adv. Mater. Sci. Eng.* **2013**, *2013*, 564346.

[78] D. R. Nhuchhen, P. Basu, B. Acharya, *Int. J. Renew. Energy Biofuels* **2014**, *2014*, 506376.

[79] V. Menon, M. Rao, *Prog. Energy Combust. Sci.* **2012**, *38*, 522–550.

[80] P. Ning, G. Yang, L. Hu, J. Sun, L. Shi, Y. Zhou, Z. Wang, J. Yang, *Biotechnol. Biofuels* **2021**, *14*, 102.

[81] R. L. Howard, E. Abotsi, E. L. J. van Rensburg, S. Howard, *Afr. J. Biotechnol.* **2003**, *2*, 602–619.

[82] M. Mujtaba, L. Fernandes Fraceto, M. Fazeli, S. Mukherjee, S. M. Savassa, G. A. de Medeiros, A. do Espírito Santo Pereira, S. D. Mancini, J. Lipponen, F. Vilaplana, *J. Clean. Prod.* **2023**, *402*, 136815.

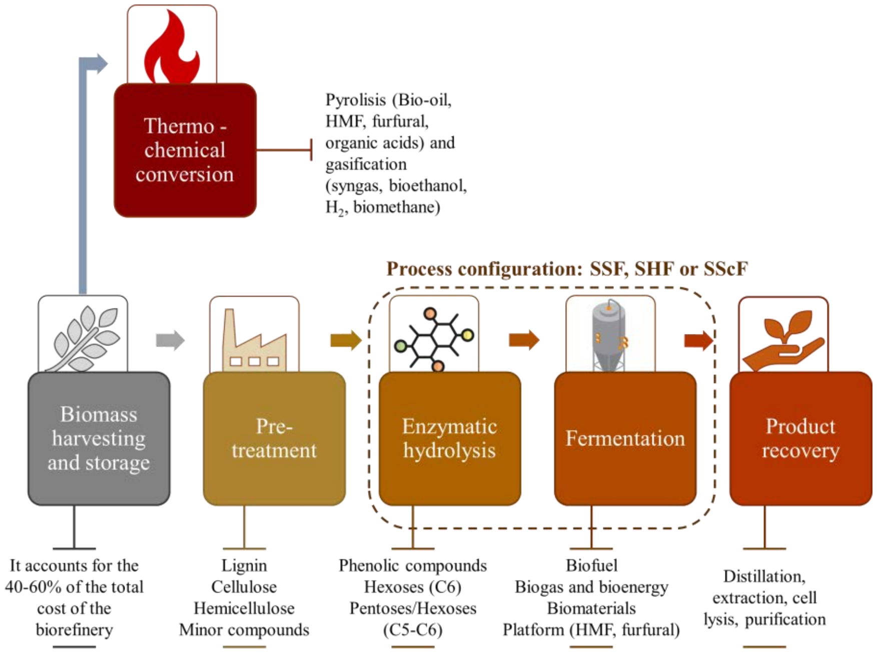
Thermo - chemical conversion
Pyrolisis (Bio-oil, HMF, furfural, organic acids) and gasification (syngas, bioethanol, H_2, biomethane)
Process configuration: SSF, SHF or SScF
Biomass harvesting and storage
Pre- treatment
Enzymatic hydrolysis
Fermentation
Product recovery
It accounts for the 40-60% of the total cost of the biorefinery
Lignin
Cellulose
Hemicellulose
Minor compounds
Phenolic compounds
Hexoses (C6)
Pentoses/Hexoses (C5-C6)
Biofuel
Biogas and bioenergy
Biomaterials
Platform (HMF, furfural)
Distillation, extraction, cell lysis, purification

Figure I.7. Schematic representation of LCBs conversion steps into added-value products, showing the main steps of the process.

Thermochemical conversion involves controlled heating or oxidation of raw materials, producing energy and valuable products.[83] Common techniques include pyrolysis and gasification. Biomass pyrolysis results in the production of solid biochar, bio-oil and gaseous compounds, while gasification leads to syngas, a mixture of CO_2, CO, CH_4, and H_2.[59b,84] Further processing of the bio-oils allows the production of valuable products (like 5-hydroxymethylfurfural (HMF) and furfural); if fermentation of gases via acetogenic bacteria occurs, methanol, ethanol (biofuels) and biohydrogen may be achieved.[85] Nevertheless, the preferred conversion method of biomass is the biological, consisting of saccharification and fermentation.[86] LCB components first need extraction and fractionation.[87] The challenge lies in breaking down lignin's strong linkage to polysaccharides. This resistance reduces cellulose and hemicellulose bioavailability, necessitating hydrolysis into fermentable sugars.[88] Effective and economically viable processes, known as pretreatment steps, are essential to overcome recalcitrance.[89]

---

[83] J. U. Hernández-Beltrán, I. O. Hernández-De Lira, M. M. Cruz-Santos, A. Saucedo-Luevanos, F. Hernández-Terán, N. Balagurusamy, *Appl. Sci.* **2019**, *9*, 3721.

[84] A. Devi, S. Bajar, H. Kour, R. Kothari, D. Pant, A. Singh, *BioEnergy Res.* **2022**, *15*, 1820–1841.

[85] a) C. Ciliberti, A. Biundo, R. Albergo, G. Agrimi, G. Braccio, I. de Bari, I. Pisano, *Processes* **2020**, *8*, 1567; b) M. K. Awasthi, T. Sar, S. C. Gowd, K. Rajendran, V. Kumar, S. Sarsaiya, Y. Li, R. Sindhu, P. Binod, Z. Zhang, *et al.*, *Fuel* **2023**, *342*, 127790.

Pretreatment is an essential upstream process to remove lignin and improve lignocellulosic material's permeability for enzymatic hydrolysis. An ideal pretreatment should be affordable, efficient, minimize sugar loss, and reduce inhibitor generation. The choice of pretreatment varies based on the feedstock and is typically energy- and cost-intensive, impacting about 40% of the total biomass processing cost.[90] For tougher biomasses, pretreatments can be combined with other physical, chemical, biological, and thermochemical methods. Traditional techniques include extrusion, milling, use of ionic liquids, alkali, concentrated acid hydrolysis, fungi, bacteria, enzymes, pyrolysis, and gasification.[91] More recent methods include physicochemical approaches like ammonia fiber expansion, CO_2 and steam explosion.[85b,92]

In Figure I.8, a sum-up of the principal techniques applied to LCBs are summarized.

---

[86] M. K. Awasthi, S. Sarsaiya, S. Wainaina, K. Rajendran, S. K. Awasthi, T. Liu, Y. Duan, A. Jain, R. Sindhu, P. Binod, *et al.*, *Renew. Sustain. Energy Rev.* **2021**, *144*, 110837.

[87] D. R. Lobato-Peralta, E. Duque-Brito, H. I. Villafán-Vidales, A. Longoria, P. J. Sebastian, A. K. Cuentas-Gallegos, C. A. Arancibia-Bulnes, P. U. Okoye, *J. Clean. Prod.* **2021**, *293*, 126123.

[88] E. C. Achinivu, M. Mohan, H. Choudhary, L. Das, K. Huang, H. D. Magurudeniya, V. R. Pidatala, A. George, B. A. Simmons, J. M. Gladden, *Green Chem.* **2021**, *23*, 7269–7289.

[89] D. Weidener, H. Klose, W. Graf von Westarp, A. Jupke, W. Leitner, P. Domínguez de María, P. M. Grande, *Green Chem.* **2021**, *23*, 6330–6336.

[90] D. Haldar, M. K. Purkait, *Chemosphere* **2021**, *264*, 128523.

[91] S. Periyasamy, V. Karthik, P. S. Kumar, J. B. Isabel, T. Temesgen, B. M. Hunegnaw, B. B. Melese, B. A. Mohamed, D.-V. N. Vo, *Environ. Chem. Lett.* **2022**, *20*, 1129–1152.

[92] B. Basak, R. Kumar, A. V. S. L. S. Bharadwaj, T. H. Kim, J. R. Kim, M. Jang, S.-E. Oh, H.-S. Roh, B.-H. Jeon, *Bioresour. Technol.* **2023**, *369*, 128413.

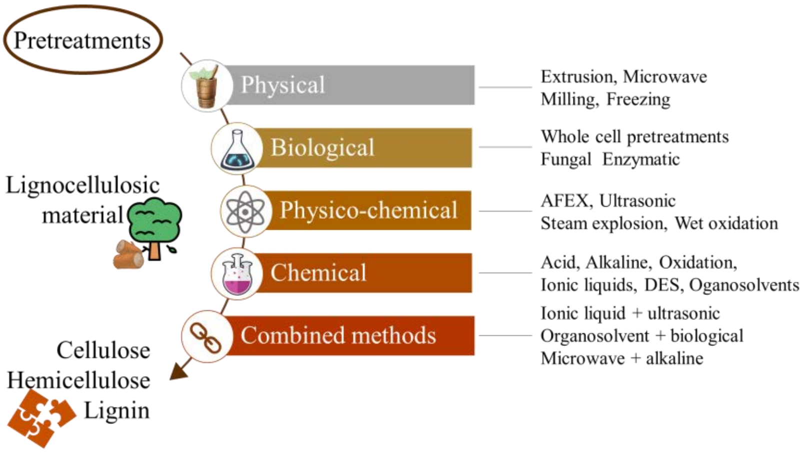
Pretreatments
Physical
Extrusion, Microwave
Milling, Freezing
Biological
Whole cell pretreatments
Fungal Enzymatic
Lignocellulosic material
Physico-chemical
AFEX, Ultrasonic
Steam explosion, Wet oxidation
Chemical
Acid, Alkaline, Oxidation,
Ionic liquids, DES, Oganosolvents
Combined methods
Ionic liquid + ultrasonic
Organosolvent + biological
Microwave + alkaline
Cellulose
Hemicellulose
Lignin

Figure I.8. Main pretreatment processes for fractionating LCBs into cellulose, hemicellulose and lignin. Pictures were taken from https://bioicons.com/.

Developing a universal pretreatment methodology for lignocellulosic biomass is challenging due to varying biomass properties. Each method has its advantages and disadvantages, impacting biorefinery sustainability and economics. Standard methods are costly, produce inhibitory intermediates and by-products, diminishing biomass appeal.[93] Physical pretreatment methods, for instance, require energy and machinery, hindering scalability and increasing costs.[94] Chemical methods involve hazardous reagents and digesters, impacting costs and the environment.[95] Produced hydrolysate often contains inhibitors, hindering enzymatic saccharification. These derivatives are toxic and must be treated before disposal, adding to the costs.[96] Continuous inhibitor removal, using membranes or via evaporation, offers a potential solution.[97] Conversely, biological pretreatment is environmentally friendly, energy-efficient, and cost-effective, without generating many by-products. Microorganisms used in the process can also produce enzymes necessary for fermentation, reducing enzyme production costs. However, large reactors are needed for scalability, and harsh biomasses are less suitable.[98] Finally, combining pretreatments offers synergistic benefits, especially for challenging biomass.[99]

---

[93] S. S. Hassan, G. A. Williams, A. K. Jaiswal, *Bioresour. Technol.* **2018**, *262*, 310–318.
[94] T. M. Thompson, B. R. Young, S. Baroutian, *Fuel Process. Technol.* **2019**, *195*, 106151.
[95] F. Passos, V. Ortega, A. Donoso-Bravo, *Bioresour. Technol.* **2017**, *227*, 239–246.
[96] B. Yang, L. Tao, C. E. Wyman, *Biofuels Bioprod. Biorefining* **2018**, *12*, 125–138.
[97] S. K. Bhatia, S. S. Jagtap, A. A. Bedekar, R. K. Bhatia, A. K. Patel, D. Pant, J. R. Banu, C. V. Rao, Y.-G. Kim, Y.-H. Yang, *Bioresour. Technol.* **2020**, *300*, 122724.

After pretreatment, the recovered cellulose, hemicellulose, and lignin fractions can be further fractionated.[100] Cellulose and hemicellulose find applications in industries like pulp, paper, textile, and coating ones.[101] In second-generation biorefineries, these carbohydrate fractions are typically hydrolyzed into sugar monomers through saccharification. This step greatly impacts the final product yield, with enzymatic hydrolysis being the most efficient method, converting over 90% of cellulose and hemicellulose into fermentable sugars. Efficient saccharification is crucial for high-value product formation via fermentation and accounts for around 35% of biomass processing costs in lignocellulosic biorefineries.[102]

Cellulose is converted into glucose, while hemicellulose yields pentose and hexose compounds. Cellulases and hemicellulases are responsible for their hydrolysis. The challenge lies in the interconnectedness of lignin and hemicellulose with cellulose, impeding proper enzyme action.[103] Undesirable cellulase-lignin bonding during fermentation can also deactivate hydrolytic enzymes.[104] Hemicellulose hydrolysis, particularly into pentose sugars, enhances cellulose accessibility by removing the xylan layer.[105] Thus, a mix of enzymes, including xylosidases, mannanases, and xylanases, is needed due to hemicellulose's complexity. Their combined action improves saccharification efficiency.[106] To enhance saccharification, ligninolytic enzymes like lytic polysaccharide monooxygenases (LPMOs) and laccases have been successfully used. LPMOs cleave glycosidic bonds of cellulose and hemicellulose with oxidizing agents,[107] while laccases act on lignin, creating micropores that expose glycosidic polymers.[108]

---

[98] N. R. Baral, A. Shah, *Bioresour. Technol.* **2017**, *232*, 331–343.

[99] a) X. Yan, Z. Wang, K. Zhang, M. Si, M. Liu, L. Chai, X. Liu, Y. Shi, *Bioresour. Technol.* **2017**, *245*, 419–425; b) R. Guan, X. Li, A. C. Wachemo, H. Yuan, Y. Liu, D. Zou, X. Zuo, J. Gu, *Sci. Total Environ.* **2018**, *637–638*, 9–17.

[100] C. Liu, K. Wang, X. Zhao, Z. Chen, X. Yin, T. Cai, X. Zhang, J. Xu, J. Hu, X. Meng, *et al.*, *Chem. Eng. J.* **2023**, *453*, 139688.

[101] a) L. Hu, X. Fang, M. Du, F. Luo, S. Guo, *Am. J. Plant Sci.* **2020**, *11*, 2066–2079; b) T. Aziz, F. Haq, A. Farid, M. Kiran, S. Faisal, A. Ullah, N. Ullah, A. Bokhari, M. Mubashir, L. F. Chuah, P. L. Show, *Environ. Res.* **2023**, *223*, 115429.

[102] M. Valdivia, J. L. Galan, J. Laffarga, J.-L. Ramos, *Microb. Biotechnol.* **2016**, *9*, 585–594.

[103] R. Agrawal, A. Satlewal, M. Kapoor, S. Mondal, B. Basu, *Bioresour. Technol.* **2017**, *224*, 411–418.

[104] a) A. S. da Silva, R. P. Espinheira, R. S. S. Teixeira, M. F. de Souza, V. Ferreira-Leitão, E. P. S. Bon, *Biotechnol. Biofuels* **2020**, *13*, 58; b) C. Huang, X. Jiang, X. Shen, J. Hu, W. Tang, X. Wu, A. Ragauskas, H. Jameel, X. Meng, Q. Yong, *Renew. Sustain. Energy Rev.* **2022**, *154*, 111822.

Finally, the cellulose hydrolysis is carried out mainly by fungal cellulase cocktails, as the combination of exo-β-(1,4)-glucanases, endo-β-(1,4)-glucanases, and β-D-glucosidases, which release D-glucose and D-cellobiose from the substrate.[109] These enzymes work synergistically, but efficient mixtures for complete hydrolysis remain as a challenge.[110] Commercial enzymes are costly, driving research into cost-effective enzymatic cocktails for large-scale implementation.[111]

The pretreated biomass can undergo saccharification and fermentation through separate hydrolysis and fermentation (SHF), simultaneous saccharification and fermentation (SSF), or simultaneous saccharification and co-fermentation (SSCF) configurations.[112] Aerobic fermentative processes of cellulose and hemicellulose C6 fractions yield biofuels like ethanol[113] and butanol.[114] Anaerobic fermentation produces methane,[115] while transesterification generates biodiesel along with glycerol.[116] Acid-catalyzed dehydration of LCB and fructose leads to HMF.[117] Lactic acid,[118] succinic acid,[119] and sorbitol[120] are platform chemicals from C6 monomers and furan intermediates. Xylose from C5 sugars yields furfural and isoprene as main products.[121]

---

[105] W. Gao, Z. Li, T. Liu, Y. Wang, *Biochem. Eng. J.* **2021**, *176*, 108186.

[106] M. R. Mukasekuru, P. Kaneza, H. Sun, F. F. Sun, J. He, P. Zheng, *Ind. Crops Prod.* **2020**, *146*, 112156.

[107] A. A. Stepnov, V. G. H. Eijsink, Z. Forsberg, *Sci. Rep.* **2022**, *12*, 6129.

[108] U. Moilanen, M. Kellock, S. Galkin, L. Viikari, *Enzyme Microb. Technol.* **2011**, *49*, 492–498.

[109] M. E. Himmel, Q. Xu, Y. Luo, S.-Y. Ding, R. Lamed, E. A. Bayer, *Biofuels* **2010**, *1*, 323–341.

[110] A. M. Lopes, E. X. Ferreira Filho, L. R. S. Moreira, *J. Appl. Microbiol.* **2018**, *125*, 632–645.

[111] a) R. Agrawal, S. Semwal, R. Kumar, A. Mathur, R. P. Gupta, D. K. Tuli, A. Satlewal, *Front. Energy Res.* **2018**, *6*, 122; b) I. Corrado, N. Cascelli, G. Ntasi, L. Birolo, G. Sannia, C. Pezzella, *Front. Bioeng. Biotechnol.* **2021**, *9*, 616908.

[112] J. A. da Costa Correia, J. de Sousa Silva, L. R. B. Gonçalves, M. V. P. Rocha, *Biomass Convers. Biorefinery* **2022**, *12*, 2767–2780.

[113] P. Unrean, N. Ketsub, *Ind. Crops Prod.* **2018**, *123*, 238–246.

Lignin has historically been treated as a by-product used for power generation in traditional biorefineries.[122] However, its unique structure and circularity potential has prompted research into its upgrading.[123] Research on lignin extraction from pretreated LCBs has led to efficient methods like kraft, soda, and sulphite pulping.[124] Lignin sulphonated polymers have versatile applications as adhesives and emulsifiers. For instance, depolymerization of sulphonate chains yields high-value aromatic compounds.[125] Lignin depolymerization methods include pyrolysis, solvolysis, acid-base catalysis, and enzymatic processes.[126] The utilization of ligninolytic enzymes obtained from white rot fungi in this step is remarkable, including laccases.[127] Phenolic monomers like guaiacol, vanillin, and catechol are obtained, finding uses as chemicals, fuels, and flavors.[128] These compounds can also be transformed into other valuable products via enzymatic cascades, applying e.g. decarboxylases, alcohol and aldehyde dehydrogenases, and demethylases.[129]

---

[114] T.-Y. Tsai, Y.-C. Lo, C.-D. Dong, D. Nagarajan, J.-S. Chang, D.-J. Lee, *Appl. Energy* **2020**, *277*, 115531.

[115] M. Yadav, V. Balan, S. Varjani, V. K. Tyagi, G. Chaudhary, N. Pareek, V. Vivekanand, *BioEnergy Res.* **2023**, *16*, 228–247.

[116] S. Uthandi, A. Kaliyaperumal, N. Srinivasan, K. Thangavelu, I. K. Muniraj, X. Zhan, N. Gathergood, V. K. Gupta, *Crit. Rev. Environ. Sci. Technol.* **2022**, *52*, 2197–2225.

[117] A. Kumar, A. S. Chauhan, Shaifali, P. Das, *Cellulose* **2021**, *28*, 3967–3980.

[118] E. Cubas-Cano, J. P. López-Gómez, C. González-Fernández, I. Ballesteros, E. Tomás-Pejó, *Renew. Energy* **2020**, *153*, 759–765.

[119] M. Alexandri, R. Schneider, H. Papapostolou, D. Ladakis, A. Koutinas, J. Venus, *ACS Sustain. Chem. Eng.* **2019**, *7*, 6569–6579.

[120] N. Chamnipa, P. Klanrit, S. Thanonkeo, P. Thanonkeo, *Ind. Crops Prod.* **2022**, *188*, 115741.

[121] E. Cousin, K. Namhaed, Y. Pérès, P. Cognet, M. Delmas, H. Hermansyah, M. Gozan, P. A. Alaba, M. K. Aroua, *Sci. Total Environ.* **2022**, *847*, 157599.

[122] S. Van den Bosch, S.-F. Koelewijn, T. Renders, G. Van den Bossche, T. Vangeel, W. Schutyser, B. F. Sels, *Top. Curr. Chem.* **2018**, *376*, 36.

[123] V. Sharma, M.-L. Tsai, P. Nargotra, C.-W. Chen, P.-P. Sun, R. R. Singhania, A. K. Patel, C.-D. Dong, *Sci. Total Environ.* **2023**, *861*, 160560.

[124] W. Schutyser, T. Renders, S. Van den Bosch, S.-F. Koelewijn, G. T. Beckham, B. F. Sels, *Chem. Soc. Rev.* **2018**, *47*, 852–908.

[125] V. K. Garlapati, A. K. Chandel, S. P. J. Kumar, S. Sharma, S. Sevda, A. P. Ingle, D. Pant, *Renew. Sustain. Energy Rev.* **2020**, *130*, 109977.

[126] P. Kaur, G. Singh, S. K. Arya, *Biomass Convers. Biorefinery* **2022**, DOI: 10.1007/s13399-

Two of the commercialized products are *cis*,*cis*-muconic acid[130] used for nylon synthesis[131] and terephthalic acid applied in synthetic fibers and bottles.[132] Additional platform chemicals like pyruvic acid[133] and lactic acid[134] can be derived. Polyhydroxyalkanoates (PHAs) have been directly synthesized from lignin or sugar fractions for packaging, bottles, and medical devices, showcasing biotechnology's potential in LCBs' biorefineries.[135] A general overview of the platform chemicals and products obtained by the whole treatments of LCBs in second generation biorefineries is reported in Figure I.9.

022-02980-6.

[127] P. Bhatt, M. Tiwari, P. Parmarick, K. Bhatt, S. Gangola, M. Adnan, Y. Singh, M. Bilal, S. Ahmed, S. Chen, *Bioremediat. J.* **2022**, *26*, 281–291.

[128] a) V. K. Ponnusamy, D. D. Nguyen, J. Dharmaraja, S. Shobana, J. R. Banu, R. G. Saratale, S. W. Chang, G. Kumar, *Bioresour. Technol.* **2019**, *271*, 462–472; b) L. A. Zevallos Torres, A. L. Woiciechowski, V. O. de Andrade Tanobe, S. G. Karp, L. C. Guimarães Lorenci, C. Faulds, C. R. Soccol, *J. Clean. Prod.* **2020**, *263*, 121499.

[129] E. Erickson, A. Bleem, E. Kuatsjah, A. Z. Werner, J. L. DuBois, J. E. McGeehan, L. D. Eltis, G. T. Beckham, *Nat. Catal.* **2022**, *5*, 86–98.

[130] N. Barton, L. Horbal, S. Starck, M. Kohlstedt, A. Luzhetskyy, C. Wittmann, *Metab. Eng.* **2018**, *45*, 200–210.

[131] D. R. Vardon, N. A. Rorrer, D. Salvachúa, A. E. Settle, C. W. Johnson, M. J. Menart, N. S. Cleveland, P. N. Ciesielski, K. X. Steirer, J. R. Dorgan, G. T. Beckham, *Green Chem.* **2016**, *18*, 3397–3413.

[132] S. Song, J. Zhang, G. Gözaydın, N. Yan, *Angew. Chemie Int. Ed.* **2019**, *58*, 4934–4937.

[133] C. W. Johnson, G. T. Beckham, *Metab. Eng.* **2015**, *28*, 240–247.

[134] C.-Y. Hong, S.-H. Ryu, H. Jeong, S.-S. Lee, M. Kim, I.-G. Choi, *ACS Chem. Biol.* **2017**, *12*, 1749–1759.

[135] S. G. Arhin, A. Cesaro, F. Di Capua, G. Esposito, *Sci. Total Environ.* **2023**, *857*, 159333.

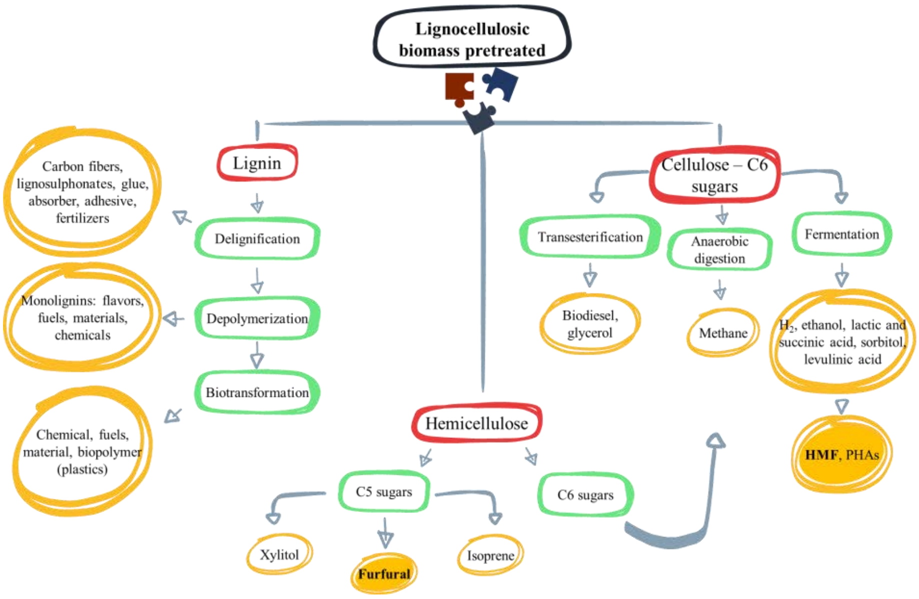
Lignocellulosic biomass pretreated
Lignin
Cellulose – C6 sugars
Hemicellulose
Carbon fibers, lignosulphonates, glue, absorber, adhesive, fertilizers
Delignification
Monolignins: flavors, fuels, materials, chemicals
Depolymerization
Biotransformation
Chemical, fuels, material, biopolymer (plastics)
Transesterification
Anaerobic digestion
Fermentation
Biodiesel, glycerol
Methane
H2, ethanol, lactic and succinic acid, sorbitol, levulinic acid
HMF, PHAs
C5 sugars
C6 sugars
Xylitol
Furfural
Isoprene

Figure I.9. Valorisation of saccharides and aromatic fractions from LCB into bio-products and chemicals.

Downstream processing, the final biorefinery step, incurs costs ranging from 15% to 90%, depending on the product type. High-purity products like chemicals and biopharmaceuticals have higher downstream costs, while bulk chemicals and fuels, with lower purity requirements, present lower downstream costs.[136] Selecting the optimal downstream process depends on factors like product concentration, solubility, and, if whole cells are employed, localization of the molecule.[137] The aim is cost-effective, high-purity product recovery. Techniques encompass separation, extraction, concentration, purification, and drying. For instance, distillation suits for bioethanol, but other methods are required for food and pharma applications. Energy-intensive downstream processes can be alleviated by in-situ removal during fermentation, enhancing productivity and reducing costs.[138]

---

[136] A. J. J. Straathof, in *Comprehensive Biotechnology*, 2nd Ed., (Ed.: M. Moo-Young), Elsevier, Amsterdam (The Netherlands), Vol. 2, **2011**, pp. 811–814.

[137] K. M. Yenkie, W. Wu, C. T. Maravelias, *Biotechnol. Biofuels* **2017**, *10*, 119.

[138] A. A. Kiss, J.-P. Lange, B. Schuur, D. W. F. Brilman, A. G. J. van der Ham, S. R. A. Kersten, *Biomass Bioenerg.* **2016**, *95*, 296–309.

Intensification through integrated unit operations is vital for large-scale biorefineries producing valuable products.[139]

I.2.3. Challenges in scale-up and commercialization of LCBs' based biorefineries

The commercial success of biorefineries is tied to the availability and cost-effectiveness of lignocellulosic biomass feedstock. Initially, first-generation biorefineries used food-grade feedstock, easy to supply for each country. However, sustainability and economical concerns led to the rise of second-generation and waste-based biorefineries.[140] They utilize non-edible components from the food production value chain, often blending different feedstocks for consistent operation.[141] Nevertheless, challenges persist in biomass storage, transportation, and processing, especially for hydrated biomasses, which account for a significant portion of process costs.[142] Technological maturity remains a hurdle, especially in achieving efficient and cost-effective pretreatment methods tailored to diverse biomass.[143] For instance, the lack of universally effective enzymatic cocktails for biomass saccharification and scaling-up further complicates these processes.[144] Commercially available enzyme prices also hinder biorefinery viability; nowadays big companies are key players in supplying existing LCB biorefineries the cellulase/xylanase cocktail for lignocellulosic biomass hydrolysis. Nevertheless, the selling prices of these preparation are not compatible with scaling-up of the processes.[145]

---

[139] R. Liguori, V. Faraco, *Bioresour. Technol.* **2016**, *215*, 13–20.

[140] H. Kargbo, J. S. Harris, A. N. Phan, *Renew. Sustain. Energy Rev.* **2021**, *135*, 110168.

[141] S. Amaducci, G. Facciotto, S. Bergante, A. Perego, P. Serra, A. Ferrarini, C. Chimento, *GCB Bioenergy* **2017**, *9*, 31–45.

[142] a) A. Patel, A. R. Shah, *J. Bioresour. Bioprod.* **2021**, *6*, 108–128; b) N. T. Albashabsheh, J. L. H. Stamm, *Biomass Bioenerg.* **2021**, *144*, 105888.

[143] A. R. Mankar, A. Pandey, A. Modak, K. K. Pant, *Bioresour. Technol.* **2021**, *334*, 125235.

[144] M. Adsul, S. K. Sandhu, R. R. Singhania, R. Gupta, S. K. Puri, A. Mathur, *Enzyme Microb. Technol.* **2020**, *133*, 109442.

[145] J. G. W. Siqueira, C. Rodrigues, L. P. de Souza Vandenberghe, A. L. Woiciechowski, C. R. Soccol, *Biomass Bioenerg.* **2020**, *132*, 105419.

Moving from laboratory to industrial operations shows substantial challenges due to complexities and variations in heat and mass balances. Successful scaling requires careful process optimization, techno-economic modeling, and automation.[146] Economic instability has led to the closure of some biorefineries, emphasizing the need for continuous innovation and improved production technology. As representative examples, Versalis, the world's largest commercial bioethanol refinery, from Italy, in 2017 announced the closure of the ethanol plant due to their financial restructuring, with the change of the producing lines towards building blocks for bioplastics. The integration of biomass-based refineries with existing petroleum refineries shows promise in maximizing infrastructure and technology utilization.[147]

I.3. Furfural and 5-hydroxymethylfurfural. Relevance in furanic biorefineries

The carbohydrate fraction of lignocellulosic biomass has high oxygen content, acidity, and reactivity.[148] To modify it, reducing oxygen content is crucial. This can be achieved through approaches like fermentative conversion of carbohydrates to ethanol, butanol, and CO_2,[149] hydrogenolysis,[150] or dehydration of carbohydrates to create valuable compounds.[151]

Amongst the possible products of these processes, HMF and furfural (Figure I.10) have emerged as crucial intermediates between biomass and desired chemicals and fuels, gaining significance in biorefineries. The U.S. Department of Energy acknowledges their importance in bio-based chemicals, featuring them in their top “10+4” list.[152] Furfural is also highlighted in the top 30 biomass-derived platforms.[153]

---

[146] M. Tschulkow, T. Compernolle, S. Van den Bosch, J. Van Aelst, I. Storms, M. Van Dael, G. Van den Bossche, B. Sels, S. Van Passel, *J. Clean. Prod.* **2020**, *266*, 122022.

[147] a) E. Ketabchi, L. Pastor-Perez, T. R. Reina, H. Arellano-Garcia, *IFAC-PapersOnLine* **2019**, *52*, 616–621; b) W. Deng, Y. Feng, J. Fu, H. Guo, Y. Guo, B. Han, Z. Jiang, L. Kong, C. Li, H. Liu, *et al.*, *Green Energy Environ.* **2023**, *8*, 10–114.

[148] H. Wang, J. Male, Y. Wang, *ACS Catal.* **2013**, *3*, 1047–1070.

[149] L. Petrus, M. A. Noordermeer, *Green Chem.* **2006**, *8*, 861–867.

[150] M. J. Gilkey, B. Xu, *ACS Catal.* **2016**, *6*, 1420–1436.

[151] M. A. Mellmer, C. Sanpitakseree, B. Demir, P. Bai, K. Ma, M. Neurock, J. A. Dumesic, *Nat. Catal.* **2018**, *1*, 199–207.

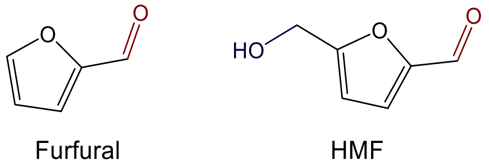

Figure I.10. Chemical structures of furfural and HMF.

While investigations into sugar dehydration and its derivatives date back to the mid-19th century, the first lab-scale publication on furfural isolation was in 1951.[154] Commercially, furfural gained importance in 1921 with the Quaker Oats Company establishing the first large-scale production facility utilizing surplus oat hulls.[155] Since then, furfural production from biomass and transformation processes has been extensively optimized. Today, the Central Romana Corporation in the Dominican Republic is the largest producer, mainly using sugar cane bagasse, while China contributes with 80% of the total production capacity.

HMF holds greater appeal over furfural for various reasons. It benefits from abundant cellulose feedstock and displays versatility. Initial HMF synthesis date back to 1895, setting the groundwork for exploration.[156] Since then, research has progressed, making HMF a vital biorefinery platform chemical. While both compounds see growing interest, furfural applications have been more extensively reported, evident from the 2.5-times higher number of publications compared to HMF in 2022, as shown in Figure I.11.

---

[152] J. J. Bozell, G. R. Petersen, *Green Chem.* **2010**, *12*, 539–554.

[153] T. Werpy, G. Petersen, *Top Value Added Chemicals from Biomass*, US Department of Energy, Washington, USA, **2004**.

[154] F. H. Newth, *Adv. Carbohydr. Chem.* **1951**, *6*, 83–106.

[155] a) F. Delbecq, Y. Wang, A. Muralidhara, K. El Ouardi, G. Marlair, C. Len, *Front. Chem.* **2018**, *6*, 146; b) C. Xu, E. Paone, D. Rodríguez-Padrón, R. Luque, F. Mauriello, *Chem. Soc. Rev.* **2020**, *49*, 4273–4306.

[156] a) G. Düll, *Chem. Ztg.* **1895**, *19*, 166–216; b) J. Kiermayer, *Chem. Ztg.* **1895**, *19*, 1003–1006.

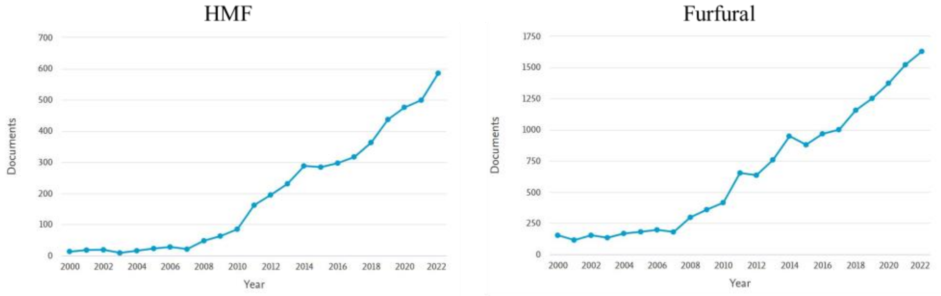

Figure I.11. Number of publications on HMF and furfural per year (January 2000–December 2022). Source: Scopus. Keywords for HMF: 5-hydroxymethylfurfural, 5-hydroxymethyl 2-furfuraldehyde, 5-hydroxymethyl furfural, 5-HMF, and HMF. Keywords for furfural: furfural, 2-furancarboxaldehyde, furfuraldehyde, and 2-furfuraldehyde.

Furfural's higher research attention could be attributed to its longer industrial history and established uses. Commercially, furfural is ahead with a number of operating plants, unlike HMF.[157] The first commercial producing plant for HMF production was established in Switzerland in 2014. Its commercialization is still in progress, exemplified by AVA Biochem', as they have recently scaled-up HMF production to a range of 5,000-10,000 tons per year. This trend underscores the need for continued exploration and development of HMF as a promising chemical biorefinery platform.

---

[157] C. Rosenfeld, J. Konnerth, W. Sailer-Kronlachner, P. Solt, T. Rosenau, H. W. G. van Herwijnen, *ChemSusChem* **2020**, *13*, 3544–3564.

I.3.1. Furfural and HMF production from LCBs

Furfural and HMF are obtained from biomasses through hydrolysis and dehydration of hexose and pentose sugars, respectively (Scheme I.1).[158]

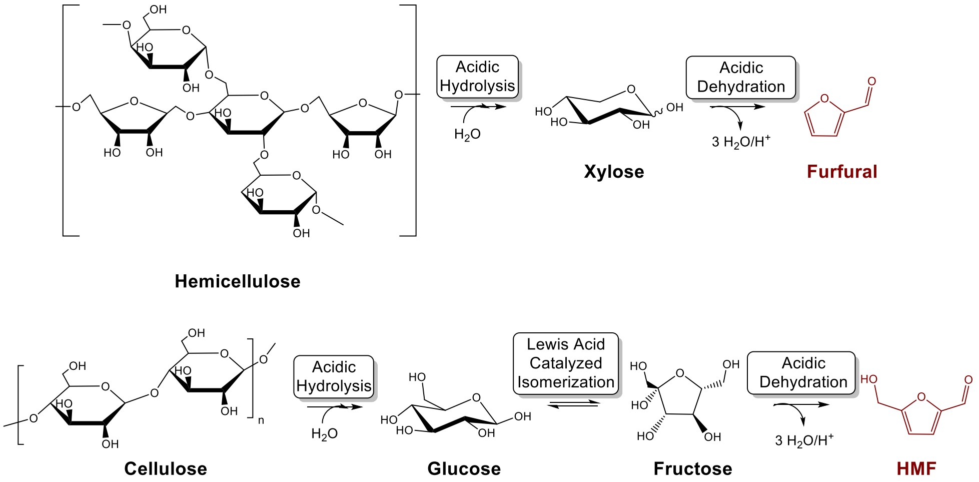
Acidic Hydrolysis
H_2O
Acidic Dehydration
3 H_2O/H^+
Xylose
Furfural
Hemicellulose
Cellulose
Acidic Hydrolysis
H_2O
Glucose
Lewis Acid Catalyzed Isomerization
Fructose
Acidic Dehydration
3 H_2O/H^+
HMF

Scheme I.1. Biomass hydrolysis and dehydration of hexoses and pentoses obtained from lignocellulosic biomass for achieving furfural and HMF, respectively.

The production of furans involves pretreating and hydrolyzing lignocellulosic biomasses through chemical or physical methods.[159] Among the first ones, Lewis acids, like $AlCl_3$ or $CrCl_3$, either alone or in conjunction with heat and Brønsted acid catalysts, such as sulfuric and hydrochloric acids, form xylose from hemicellulose and glucose from cellulose.[160] Dehydration with conventional acids and steam yields furfural from xylose and HMF from glucose. HMF synthesis includes glucose isomerization to fructose, requiring selective catalysts due to HMF sensitivity to temperature and acidity.[161] Isomerization is carried out by solid bases, like borates, boronates, aluminates or amines, as well as Lewis acids under anhydrous conditions, including metal halides and solid acids.[162] HMF instability together with the low volatility, creates challenges for its purification through the most commonly applied distillation methods, complicating the process integration in furan biorefineries. Current dehydration and isolation of carbohydrates have limitations: low yields, acidic wastes, side reactions as condensation and polymerization, ring-opening, hydrolysis, and nucleophilic additions with formation of unwanted low-value humins.[163]

---

[158] T. Wang, M. W. Nolte, B. H. Shanks, *Green Chem.* **2014**, *16*, 548–572.

[159] a) I. K. M. Yu, D. C. W. Tsang, *Bioresour. Technol.* **2017**, *238*, 716–732; b) H. Wang, C. Zhu, D. Li, Q. Liu, J. Tan, C. Wang, C. Cai, L. Ma, *Renew. Sustain. Energy Rev.* **2019**, *103*, 227–247; c) Y. Zhao, K. Lu, H. Xu, L. Zhu, S. Wang, *Renew. Sustain. Energy Rev.* **2021**, *139*, 110706.

[160] a) V. Choudhary, S. H. Mushrif, C. Ho, A. Anderko, V. Nikolakis, N. S. Marinkovic, A. I. Frenkel, S. I. Sandler, D. G. Vlachos, *J. Am. Chem. Soc.* **2013**, *135*, 3997–4006; b) K. J. Yong, T. Y. Wu, C. B. T. L. Lee, Z. J. Lee, Q. Liu, J. M. Jahim, Q. Zhou, L. Zhang, *Biomass Bioenerg.* **2022**, *161*, 106458.

Therefore, different techniques have been designed to overcome these issues. Hence, one-pot processes directly producing furfural and HMF from raw biomass show economic and environmental promise.[164] Amongst the strategies, heterogeneous catalysts offer recyclability and control of reaction conditions,[165] while biphasic systems minimize side reactions and improve separation.[166] In particular, mixtures of water and methyl isobutyl ketone (MIBK)[167] or tetrahydrofuran (THF)[168] have emerged as the most performing systems, especially when combined with solid-acid catalysts. Ionic liquids

---

[161] a) L. T. Mika, E. Cséfalvay, Á. Németh, *Chem. Rev.* **2018**, *118*, 505–613; b) G. Portillo Perez, A. Mukherjee, M.-J. Dumont, *J. Ind. Eng. Chem.* **2019**, *70*, 1–34.

[162] I. Delidovich, R. Palkovits, *ChemSusChem* **2016**, *9*, 547–561.

[163] Z. Cheng, J. L. Everhart, G. Tsilomelekis, V. Nikolakis, B. Saha, D. G. Vlachos, *Green Chem.* **2018**, *20*, 997–1006.

[164] a) T. Zhang, W. Li, H. Xiao, Y. Jin, S. Wu, *Bioresour. Technol.* **2022**, *354*, 127126; b) W. Adhami, A. Richel, C. Len, *Mol. Catal.* **2023**, *545*, 113178; c) A. Kumar, A. S. Chauhan, R. Bains, P. Das, *Green Chem.* **2023**, *25*, 849–870; d) K. Wiranarongkorn, K. Im-orb, Y. Patcharavorachot, F. Maréchal, A. Arpornwichanop, *Renew. Sustain. Energy Rev.* **2023**, *175*, 113146.

[165] a) J. E. Romo, N. V. Bollar, C. J. Zimmermann, S. G. Wettstein, *ChemCatChem* **2018**, *10*, 4805–4816; b) C. Sonsiam, A. Kaewchada, S. Pumrod, A. Jaree, *Chem. Eng. Process.* **2019**, *138*, 65–72.

[166] Q. Lin, S. Liao, L. Li, W. Li, F. Yue, F. Peng, J. Ren, *Green Chem.* **2020**, *22*, 532–539.

[167] Y. Muranaka, K. Matsubara, T. Maki, S. Asano, H. Nakagawa, K. Mae, *ACS Omega* **2020**, *5*, 9384–9390.

[168] J.-H. Kim, S.-M. Cho, J.-H. Choi, H. Jeong, S. M. Lee, B. Koo, I.-G. Choi, *Appl. Sci.* **2021**, *11*, 163.

(ILs)[169] and deep eutectic solvents (DES)[170] can enhance furan aldehydes production and isolation, even with the aid of supercritical CO_2.[171] Moreover, pervaporation-assisted continuous membrane reactors offer pure furfural isolation,[172] while reactive adsorption onto active carbon has shown to be technically viable for large scale furans production.[173] Finally, zeolites have been explored as efficient solid acid catalysts for sugar dehydration reactions.[174] Although effective, zeolites are prone to instability issues caused by water at high temperatures and catalyst deactivation due to strong adsorption of humins.[175]

The existing extensive literature on furan production and innovative methods for isolation highlight the potential of efficient systems that could combine green, selective, and cost-effective technologies. As a summary, this ideal system should enable solvent(s) and catalyst(s) recovery, minimizing waste, following efficient separation and purification steps, and being compatible with large-scale production.

I.3.2. Upgrading of furfural and HMF into added-value chemicals

Furfural and HMF chemical structures make them versatile for diverse transformations, yielding valuable novel products.[176] These processes involve chemical reactions that modify the heteroaromatic ring and/or the pending aldehyde group in both cases, as well as the hydroxymethyl group at C_5-position in the case of HMF.[177]

---

[169] S. Zhang, J. Sun, X. Zhang, J. Xin, Q. Miao, J. Wang, *Chem. Soc. Rev.* **2014**, *43*, 7838–7869; b) Z. Zhang, J. Song, B. Han, *Chem. Rev.* **2017**, *117*, 6834–6880.

[170] P. H. Tran, P. V. Tran, *Fuel* **2019**, *246*, 18–23.

[171] a) C. Shi, J. Xin, X. Liu, X. Lu, S. Zhang, *ACS Sustain. Chem. Eng.* **2016**, *4*, 557–563; b) X. Fu, J. Dai, X. Guo, J. Tang, L. Zhu, C. Hu, *Green Chem.* **2017**, *19*, 3334–3343.

[172] a) A. Wang, N. P. Balsara, A. T. Bell, *Green Chem.* **2018**, *20*, 2903–2912; b) Y. Zhuang, Z. Si, S. Pang, H. Wu, X. Zhang, P. Qin, *J. Clean. Prod.* **2023**, *396*, 136481.

[173] K. Schute, Y. Louven, C. Detoni, M. Rose, *Chemie Ing. Tech.* **2016**, *88*, 355–362.

[174] a) N. Candu, M. El Fergani, M. Verziu, B. Cojocaru, B. Jurca, N. Apostol, C. Teodorescu, V. I. Parvulescu, S. M. Coman, *Catal. Today* **2019**, *325*, 109–116; b) S. Xu, D. Pan, G. Xiao, *J. Cent. South Univ.* **2019**, *26*, 2974–2986.

[175] a) C. J. Heard, L. Grajciar, F. Uhlík, M. Shamzhy, M. Opanasenko, J. Čejka, P. Nachtigall, *Adv. Mater.* **2020**, *32*, 2003264; b) E. Grifoni, G. Piccini, J. A. Lercher, V.-A. Glezakou, R. Rousseau, M. Parrinello, *Nat. Commun.* **2021**, *12*, 2630.

[176] K. Kohli, R. Prajapati, B. K. Sharma, *Energies* **2019**, *12*, 233.

Furfural's intermediate polarity enables it to act as a solvent and achieve various compounds.[178] Over 80 chemicals can be derived from furfural via chemical transformations.[179] Despite these possibilities, industrial-scale use for fine/commodity chemicals and fuels remains limited. Noteworthy derivatives can be categorized as shown in Figure I.12, encompassing biofuels, fuel additives, industrial chemicals, polymers, and resins.[180]

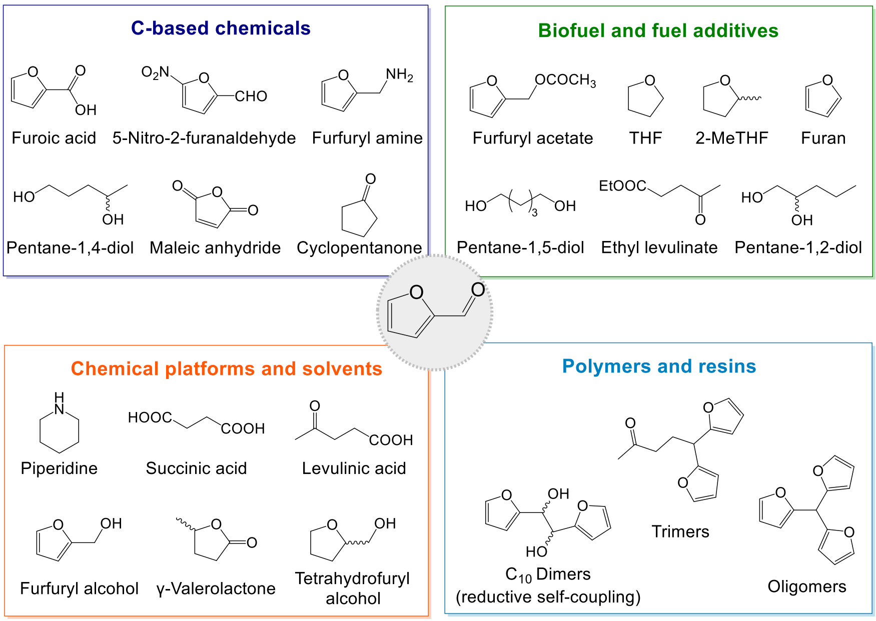
C-based chemicals
Furoic acid
5-Nitro-2-furanaldehyde
Furfuryl amine
Pentane-1,4-diol
Maleic anhydride
Cyclopentanone
Biofuel and fuel additives
Furfuryl acetate
THF
2-MeTHF
Furan
Pentane-1,5-diol
Ethyl levulinate
Pentane-1,2-diol
Chemical platforms and solvents
Piperidine
Succinic acid
Levulinic acid
Furfuryl alcohol
γ-Valerolactone
Tetrahydrofuryl alcohol
Polymers and resins
Trimers
C10 Dimers (reductive self-coupling)
Oligomers

Figure I.12. Representative value-added products derived from furfural.

---

[177] a) F. A. Kucherov, L. V. Romashov, K. I. Galkin, V. P. Ananikov, *ACS Sustain. Chem. Eng.* **2018**, *6*, 8064–8092; b) K. Gupta, R. K. Rai, S. K. Singh, *ChemCatChem* **2018**, *10*, 2326–2349.

[178] M. Kabbour, R. Luque, in *Biomass, Biofuels, Biochemicals*, (Eds.: S. Saravanamurugan, A. Pandey, H. Li, A. Riisager), Elsevier, Amsterdam (The Netherlands), **2020**, pp. 283–297.

[179] A. Jaswal, P. P. Singh, T. Mondal, *Green Chem.* **2022**, *24*, 510–551.

[180] N. Vinod, S. Dutta, *Sustain. Chem.* **2021**, *2*, 521–549.

Notable derivatives of furfural include: *furfuryl alcohol*, used in the foundry, forestry (it enhances the durability and resistance of wood against decay and pests), and manufacturing industries, in corrosion-resistant fibers and reinforced plastics. Also applied as solvent, additive in phenolic resins, lubricant, dispersing agent, and as viscosity reducer for epoxy resins. It is also a building block in pharma (for the synthesis of lysine and vitamin C) and in material industry (synthetic fibers and rubbers).[181] Due to the tested reinforced thermo-mechanical properties of carbon-carbon composite materials impregnated with furfuryl alcohol, it has been used as a protective coating to safeguard Space Shuttles against the intense thermal effects during the journeys into space and returns to Earth.[182]

Furfuryl amine is a platform for diuretics, herbicides, and pharmaceuticals.[183] *Furoic acid* is a precursor for drugs, insecticides, and perfumes.[184] *γ-Valerolactone* is used as renewable solvent, biofuel, and chemical platform.[185] *Succinic acid* is used in pharmaceutical chemistry, food, and agrochemicals,[186]while *levulinic acid* is a key substrate for polymer and pharma applications.[187] *Maleic anhydride* is a petrochemical with a market volume of 1,600 kTon per year, and a commodity compound used for pharmaceuticals, agrochemicals, resins, and vinyl copolymers.[188]

---

[181] D. K. Mishra, S. Kumar, R. S. Shukla, in *Biomass, Biofuels, Biochemicals*, (Eds.: S. Saravanamurugan, A. Pandey, H. Li, A. Riisager), Elsevier, Amsterdam (The Netherlands), **2020**, pp. 323–353.

[182] A. Pirolini, *Materials Used in Space Shuttle Thermal Protection Systems*, **2014**. https://www.azom.com/article.aspx?ArticleID=11443.

[183] M. Pelckmans, T. Renders, S. Van de Vyver, B. F. Sels, *Green Chem.* **2017**, *19*, 5303–5331.

[184] R. Mariscal, P. Maireles-Torres, M. Ojeda, I. Sádaba, M. López Granados, *Energy Environ. Sci.* **2016**, *9*, 1144–1189.

[185] K. Yan, Y. Yang, J. Chai, Y. Lu, *Appl. Catal. B-Environ.* **2015**, *179*, 292–304.

[186] R. K. Saxena, S. Saran, J. Isar, R. Kaushik, in *Current Developments in Biotechnology and Bioengineering*, (Eds.: A. Pandey, S. Negi, C. R. Soccol), Elsevier, Amsterdam (The Netherlands), **2017**, pp. 601–630.

[187] A. Kumar, D. Z. Shende, K. L. Wasewar, *Mater. Today Proc.* **2020**, *29*, 790–793.

[188] N. G. Savani, T. Naveen, B. Z. Dholakiya, *J. Polym. Res.* **2023**, *30*, 175.

HMF is often termed the "sleeping giant" of sustainable chemistry due to its vast untapped potential.[189] Chemical modifications involving its reactive groups and furan ring yield diverse derivatives.[190] These include oxidations, reductions, alkylations, esterifications, condensations, hydrogenations, and more. These reactions have been extensively studied, continuously expanding the range of valuable HMF-derived compounds. They find applications in polymer, fine chemical, and fuel industries (Figure I.13).[191]

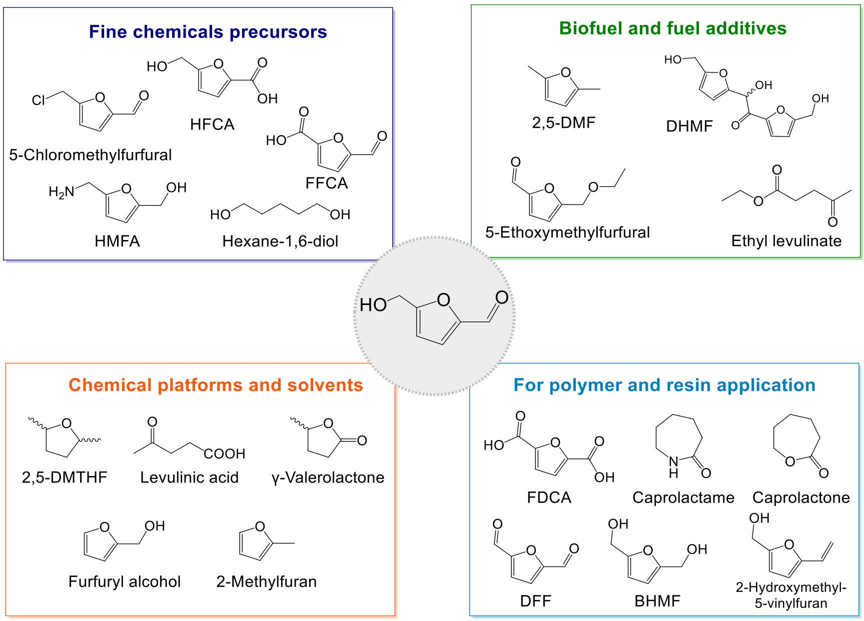
Fine chemicals precursors
5-Chloromethylfurfural
HFCA
FFCA
HMFA
Hexane-1,6-diol
Biofuel and fuel additives
2,5-DMF
DHMF
5-Ethoxymethylfurfural
Ethyl levulinate
Chemical platforms and solvents
2,5-DMTHF
Levulinic acid
γ-Valerolactone
Furfuryl alcohol
2-Methylfuran
For polymer and resin application
FDCA
Caprolactame
Caprolactone
DFF
BHMF
2-Hydroxymethyl-5-vinylfuran

Figure I.13. Representative value-added products derived from HMF.

Key intermediates derived from HMF include *2,5-furandicarboxylic acid* (FDCA), which is a renewable substitute for terephthalic acid, used in polyesters, polyamides, and coordination compounds.[192] A practical industrial application of FDCA has been shown by Avantium (The Netherlands), already described in Section I.1.4, which produces polyethylene furanoate (PEF) packaging films, bottles and textile fibers by co-polymerization of FDCA and ethylene glycol. *5-Hydroxymethyl-2-furoic acid* (HFCA) is used for pharmaceuticals and polyester production.[193] *2,5-Diformylfuran* (DFF) is a crucial precursor for pharmaceuticals, polymers, and other chemicals.[194] Challenging to be synthesized from HMF, due to the highly (but not the highest) oxidized state, *5-formyl-2-furancarboxylic acid* (FFCA) is a valuable derivative for surfactants and resins.[195] *2,5-Dimethyltetrahydrofuran* (2,5-DMTHF) is a green aprotic solvent used in organic synthesis,[196] while *5-bis(hydroxymethyl)furan* (BHMF) is a multifunctional compound used as an additive for fuels and long-chain alkane diesels, and as monomer for linear or branched polyesters and polyurethanes.[197] *5-Hydroxymethylfurfurylamine* (HMFA) is applied to the synthesis of diuretics, antihypertensives, and antiseptics. It is usually obtained from HMF via direct reductive amination, although due to the sensitivity of the furan ring and undesired formation of secondary and tertiary amines, biocatalytic routes are preferred.[198]

---

[189] K. I. Galkin, V. P. Ananikov, *ChemSusChem* **2019**, *12*, 2976–2982.

[190] A. Messori, A. Fasolini, R. Mazzoni, *ChemSusChem* **2022**, *15*, e202200228.

[191] a) V. K. Vaidyanathan, K. Saikia, P. S. Kumar, A. K. Rathankumar, G. Rangasamy, G. D. Saratale, *Bioresour. Technol.* **2023**, *378*, 128975; b) Z. Jiang, Y. Zeng, D. Hu, R. Guo, K. Yan, R. Luque, *Green Chem.* **2023**, *25*, 871–892.

Oher significant non-furanic compounds derived from HMF and its intermediates are *levulinic* and *adipic acids*, *γ-valerolactone*, *hexane-1,6-diol*, and monomers used in bio-based polymer synthesis such as *caprolactam* and *caprolactone*.[199] HMF derivatives create dynamic materials and various furan polymers, including with furfural.[200] However, challenges stem from HMF's reactivity, instability, and costs in production from biomasses. These obstacles have restricted its potential as a platform chemical biorefinery.

---

[192] a) S. Pandey, M.-J. Dumont, V. Orsat, D. Rodrigue, *Eur. Polym. J.* **2021**, *160*, 110778; b) R. Gao, J. Wang, F. Liu, H. Dai, X. Zhang, X. Wang, Y. Li, J. Zhu, *Polym. Degrad. Stab.* **2023**, *210*, 110292.

[193] A. Todea, I. Bîtcan, D. Aparaschivei, I. Păuşescu, V. Badea, F. Péter, V. D. Gherman, G. Rusu, L. Nagy, S. Kéki, *Polymers* **2019**, *11*, 1402.

[194] J. Dai, *Green Energy Environ.* **2021**, *6*, 22–32.

[195] a) C. Moreau, M. N. Belgacem, A. Gandini, *Top. Catal.* **2004**, *27*, 11–30; b) M. Ventura, M. Aresta, A. Dibenedetto, *ChemSusChem* **2016**, *9*, 1096–1100.

[196] C. Zhang, Y. Wang, W. Yang, J. Zheng, *Org. Process Res. Dev.* **2022**, *26*, 2685–2693.

[197] F. Aricò, *Pure Appl. Chem.* **2021**, *93*, 551–560.

[198] a) Z. Wang, H. Chai, J. Ren, Y. Tao, Q. Li, C. Ma, Y. Ai, Y. He, *ACS Sustain. Chem. Eng.* **2022**, *10*, 8452–8463; b) T. Heinks, L. M. Merz, J. Liedtke, M. Höhne, L. M. van Langen, U. T. Bornscheuer, G. F. von Mollard, P. Berglund, *Catalysts* **2023**, *13*, 875.

I.4. Biocatalysis

Biocatalysis involves the application of biological systems, such as enzymes, whole-cells, or cell-free extracts, to drive a selective chemical transformation.[201] By harnessing the power of nature's catalysts, biocatalysis offers a sustainable and efficient approach to chemical synthesis: enzymes, indeed, allow to catalyze a reaction by reducing the energy required for the conversion of a substrate into a product, called activation energy. By stabilizing the transition state of the reaction, they lead to an increase in the rate, that would otherwise be impractical or time-consuming.[202] For centuries, enzymes in biological systems have been utilized in processes like fermentation (cheese, beer, vinegar) and biotransformations (indigo, linen, leather). However, these processes used naturally occurring enzymes from microorganisms without formal isolation or characterization of the catalysts.[203]

Louis Pasteur is credited by providing the earliest example of modern biocatalysis in 1848. He conducted experiments on the resolution of racemic tartaric acid using various microorganisms, including *Penicillium*

---

[199] a) R. Gérardy, D. P. Debecker, J. Estager, P. Luis, J.-C. M. Monbaliu, *Chem. Rev.* **2020**, *120*, 7219–7347; b) Q.-S. Kong, X.-L. Li, H.-J. Xu, Y. Fu, *Fuel Process. Technol.* **2020**, *209*, 106528.

[200] a) A. Gandini, T. M. Lacerda, *Macromol. Mater. Eng.* **2022**, *307*, 2100902; b) F. Chacón-Huete, C. Messina, B. Cigana, P. Forgione, *ChemSusChem* **2022**, *15*, e202200328; c) K. I. Galkin, *Mendeleev Commun.* **2023**, *33*, 1–8.

[201] a) J. B. Pyser, S. Chakrabarty, E. O. Romero, A. R. H. Narayan, *ACS Cent. Sci.* **2021**, *7*, 1105–1116; b) *Biocatalysis for Practitioners. Techniques, Reactions and Applications*, (Eds.: G. de Gonzalo, I. Lavandera), Wiley-VCH, Weinheim (Germany), **2021**.

[202] D. Ringe, G. A. Petsko, *Science* **2008**, *320*, 1428–1429.

[203] O. May, in *Industrial Enzyme Applications*, (Eds.: A. Vogel, O. May), John Wiley & Sons Ltd, Chichester (UK), **2019**, pp. 1–24.

glaucum.[204] Later, in the late 19th century, Emil Fischer proposed the "lock and key" model for enzyme catalysis, that described the hypothetic fitting between a substrate and an enzyme, involving the so-called active site. Although not quite accurate and replaced with the "induced fit" theory developed by Koshland Jr in the 1950s, this conceptual representation was crucial in the comprehension of the mechanisms underlying enzymatic reactions.[205] On the other hand, Buchner demonstrated that also cell-free extracts could catalyze fermentation processes.[206] These milestones played pivotal roles in shaping our understanding of biocatalysis and paved the way for further advancements in the field.

From then, biocatalysis gained traction as an eco-friendly alternative to traditional chemical synthesis. It is a key component of the "green" chemistry shift, vital for environmentally conscious industrial processes, optimizing resources use and minimizing waste.[207] Enzymes' ability to work under mild reaction conditions, their biodegradability, and reusability when immobilized make these processes to fit with the 12 principles of Green Chemistry, established by the US Environmental Protection Agency (Figure I.14).[208] These breakthroughs have allowed to integrate enzymes in catalytic processes for both academia and industrial research, pointed also as valuable tool for the development of chemical processes in biorefineries.

---

[204] L. Pasteur, *Ann. Chim. Phys.* **1848**, *24*, 442–459.

[205] D. E. Koshland Jr, *Proc. Natl. Acad. Sci. USA* **1958**, *44*, 98–104.

[206] E. Buchner, *Ber. Dtsch. Chem. Ges.* **1897**, *30*, 117–124.

[207] R. A. Sheldon, in *Green Biocatalysis*, (Ed.: R. N. Patel), John Wiley & Sons Inc., Hoboken (USA), **2016**, pp. 1–15.

[208] a) P. Anastas, N. Eghbali, *Chem. Soc. Rev.* **2010**, *39*, 301–312; b) H. C. Erythropel, J. B. Zimmerman, T. M. de Winter, L. Petitjean, F. Melnikov, C. H. Lam, A. W. Lounsbury, K. E. Mellor, N. Z. Janković, Q. Tu, *et al.*, *Green Chem.* **2018**, *20*, 1929–1961.

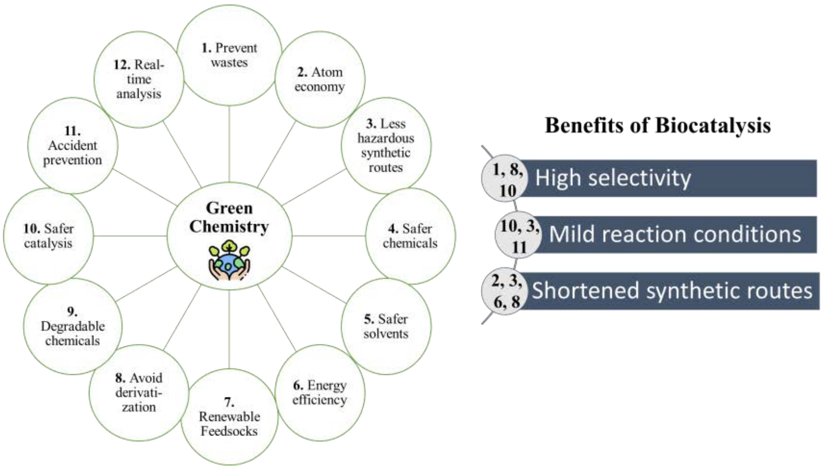
Green Chemistry
1. Prevent wastes
2. Atom economy
3. Less hazardous synthetic routes
4. Safer chemicals
5. Safer solvents
6. Energy efficiency
7. Renewable Feedsocks
8. Avoid derivati-zation
9. Degradable chemicals
10. Safer catalysis
11. Accident prevention
12. Real-time analysis
Benefits of Biocatalysis
1, 8, 10
High selectivity
10, 3, 11
Mild reaction conditions
2, 3, 6, 8
Shortened synthetic routes

Figure I.14. Biocatalysis in the frame of Green Chemistry.

The present biocatalysis era, framed in the so-called third wave, is driven by advances in Industrial Biotechnology. These encompass improved fermentation, protein engineering, crystallography, and molecular biology tools.[209] Enzymes can now be tuned for improved selectivity and stability, and optimized to efficiently work under diverse reaction conditions, expanding their use in unconventional applications.

I.4.1. Advantages and disadvantages of Biocatalysis

Besides their benign and renewable origins, which make biocatalyzed processes as environmentally acceptable, enzymes are also very efficient catalysts and in many cases more effective than their chemical counterparts: the latter are generally employed in concentrations of at least 0.1–1%, while enzymatic reactions can be performed at reasonable rates with 10^{-3}–10^{-4}% in mole ratio with respect to the substrate.[210] Biocatalysts, whether pure or crude, function under mild pH and temperature conditions. Enzymes are versatile, may be combined with each other to simplify reaction processes, catalyzing a wide range of reactions, including with non-natural substrates. Advances in enzyme discovery and molecular biology also enable more efficient biocatalysis in organic solvent media. Some enzymes even exhibit catalytic promiscuity, performing multiple reactions beyond their primary function, which aids in transforming diverse substrates with the same catalyst.[211] An overview of the advantages of using biocatalysts compared to chemocatalysts is provided in Figure I.15.[212]

---

[209] a) U. T. Bornscheuer, G. W. Huisman, R. J. Kazlauskas, S. Lutz, J. C. Moore, K. Robins, *Nature* **2012**, *485*, 185–194; b) U. Hanefeld, F. Hollmann, C. E. Paul, *Chem. Soc. Rev.* **2022**, *51*, 594–627.

[210] K. Faber, *Biotransformations in Organic Chemistry*, 7th Ed., Springer, Berlin (Germany), **2018**, pp. 1–30.

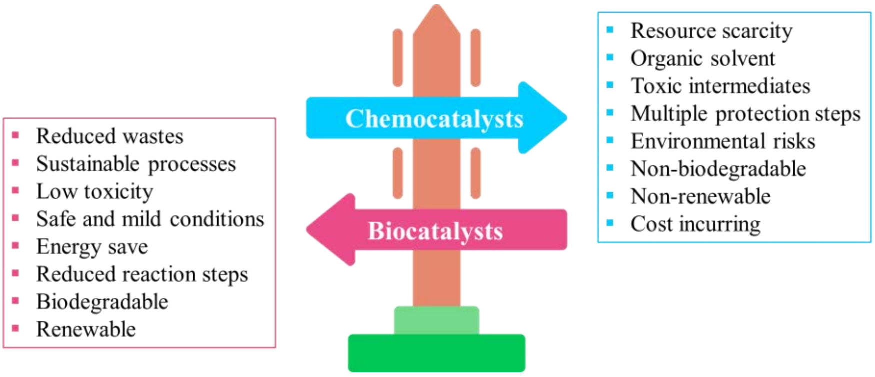
Chemocatalysts
Biocatalysts
Resource scarcity
Organic solvent
Toxic intermediates
Multiple protection steps
Environmental risks
Non-biodegradable
Non-renewable
Cost incurring
Reduced wastes
Sustainable processes
Low toxicity
Safe and mild conditions
Energy save
Reduced reaction steps
Biodegradable
Renewable

Figure I.15. Main advantages of using biocatalysts over chemocatalysts in synthetic processes.

The most relevant advantage of employing enzymes in conversion processes is the exceptional selectivity that they usually provide. Biocatalysts have the remarkable ability to exhibit high levels of specificity, allowing them to selectively catalyze the desired reaction while minimizing unwanted side transformations. Moreover, thanks to their complex tridimensional structures and intrinsic chirality, enzymes can display three types of selectivities: chemoselectivity (specific functional groups of a molecule are modified by enzymes, while others that have similar reactivity are left unchanged, thus avoiding the need for protecting groups); regioselectivity (two identical functional groups within the same compound may be distinguished by enzymes depending on their position, only transforming one of them); enantioselectivity and diastereoselectivity (a prochiral substrate is transformed into an optically active product selectively - desymmetrization process - as well as only one stereoisomer from others, e.g., one enantiomer of a racemic substrate can be converted into a product through a kinetic resolution). This last selectivity is of pivotal importance for the synthesis of enantiopure compounds, which finds relevant applications in pharmaceutical or agrochemical sectors.[213] Two enantiomers of the same molecule present different biological properties linked to their chirality; as in many cases only one may possess the desired scent, flavor, or medicinal effect, whilst the other one can be less or completely inactive, or in the worst case, toxic. The production of one enantiomer over another instead of the cheaper racemic mixture has become a main concern in the pharmaceutical and agrochemical industry in the last decades.[214]

---

[211] U. T. Bornscheuer, R. J. Kazlauskas, *Angew. Chem. Int. Ed.* **2004**, *43*, 6032–6040.

[212] R. A. Sheldon, in *Biomass Valorization*, (Eds.: D. Ravelli, C. Samorì), Wiley-VCH, Weinheim (Germany), **2021**, pp. 113–146.

Probably the most known example is thalidomide, a drug that gained popularity in the 1960s for its ability to alleviate morning sickness during pregnancy. Sold as racemic mixture for many years, only later the (*S*)-enantiomer was shown to be highly teratogenic, causing limbs malformation in the fetus, while the (*R*)-counterpart possessed the therapeutic characteristics. The drug was withdrawn from the market, and pure (*R*)-thalidomide successively produced.[215] In Figure I.16, other representative examples of different behavior of enantiomers are shown.

---

[213] S. P. France, R. D. Lewis, C. A. Martinez, *JACS Au* **2023**, *3*, 715–735.

[214] D. Muñoz Solano, P. Hoyos, M. J. Hernáiz, A. R. Alcántara, J. M. Sánchez-Montero, *Bioresour. Technol.* **2012**, *115*, 196–207.

[215] J. H. Kim, A. R. Scialli, *Toxicol. Sci.* **2011**, *122*, 1–6.

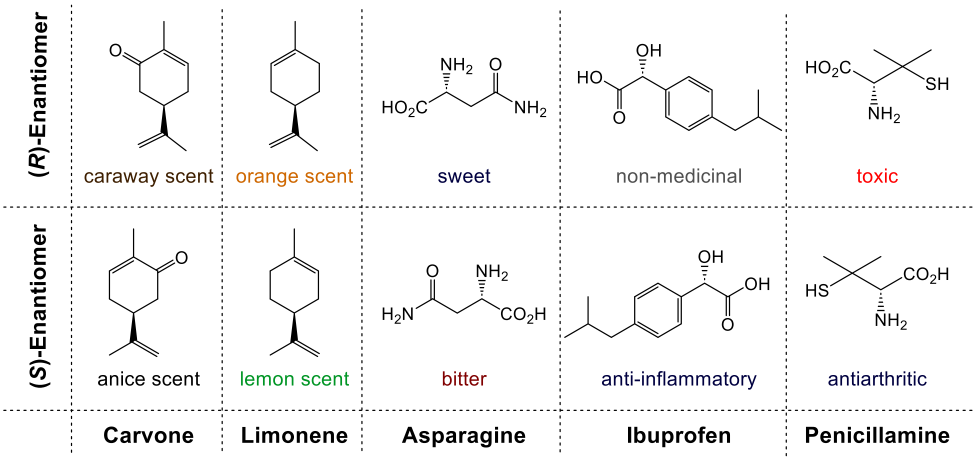
(R)-Enantiomer
(S)-Enantiomer
caraway scent
orange scent
sweet
non-medicinal
toxic
anice scent
lemon scent
bitter
anti-inflammatory
antiarthritic
Carvone
Limonene
Asparagine
Ibuprofen
Penicillamine

Figure I.16. Biological effect of enantiomers applied in pharmaceutical, flavour and agrochemical industries.

Despite their benefits, biocatalysts have limitations. Enzymes can be too specific to certain reactions or narrow operation parameters, needing optimal conditions and costly cofactors. Furthermore, enzymes are composed of L-amino acids and exist in nature in only one enantiomeric form. Consequently, enantiomerically pure compounds often require different biocatalysts. Enzymes are sensitive to substrate or product inhibition, solvents, temperature, and pH changes. Limited availability and high purification costs may also hinder their use. Moreover, regulatory barriers exist in the production of pharmaceutical ingredients with the aid of enzymes.[216] These challenges are being tackled via enzyme engineering, immobilization, and robust biocatalytic (flow) processes.

I.4.2. Enzyme classification and catalytic efficiency

A wide range of enzymes is nowadays available thanks to the huge reservoir of biocatalysts in nature as well as through innovative protein engineering strategies. Enzymes were divided into six categories based on the specific reactions they could catalyze, according to the criterion proposed by Dixon and Webb in 1958.[217] Additionally, in 2018, a seventh class, namely translocases, was added to this list; nevertheless, the latter do not possess catalytic activity, being their role limited to the transport of molecules across cellular membranes.[218] Each biocatalyst is named with a unique four-digit number (EC a.b.c.d) that denotes: (a) the main type of reaction, (b) the substrate class or the type of transferred molecule, (c) the nature of the co-substrate, and (d) the individual enzyme number (Table I.7).[219]

---

[216] S. Wenda, S. Illner, A. Mell, U. Kragl, *Green Chem.* **2011**, *13*, 3007–3047.

Table I.7. Enzyme classification according to the catalyzed reaction.

EC[a] number	Enzyme class	Reaction type (examples)
1	Oxidoreductases	Oxidation of C–H, C=C, C–N and C–O; reduction of C=O and C=C, reductive amination of C=O
2	Transferases	Transfer of acyl, amino, glycosyl, methyl, phosphoryl, sulfur-containing groups
3	Hydrolases	Hydrolysis or formation of esters, amides, lactones, lactams, epoxides, nitriles, anhydrides, glycosides
4	Lyases	Addition or elimination of small molecules to double bonds such as C=C, C=N and C=O
5	Isomerases	Isomerization: racemization, epimerization and intramolecular rearrangement
6	Ligases	Formation or cleavage of C–O, C–S, C–N and C–C bonds
7	Translocases	Transfer of molecules across cell membranes

[a] EC = Enzyme Commission.

The catalytic activity of different enzymes towards their substrates is measured in Units, defined by the International System as μmol of substrate converted into the product per unit of time. The catalytic power of a biocatalyst is called turnover frequency (TOF) and is defined as the number of substrate molecules (mol) converted by a single molecule (mol) of catalyst per unit of time. Being mass-independent, this value is used for comparing enzymatic performances in different biotransformations. The productivity of the enzymes is the dimensionless TON, "turnover number", denoting the number of substrate molecules (mol) converted per molecule (mol) of catalyst, within a given time range. Conversely, the total turnover number (TTN) is the TON intended for the whole lifetime of the catalyst.[220] Finally, if the specific enzymatic activity cannot be measured (because whole cells are used), the utile parameter is the productivity number (PN), which is the amount of product formed by a given quantity of the catalyst (dry weight) within a certain period of time.[221]

---

[217] M. Dixon, E. C. Webb, *Enzymes*, Longsman Green, London (UK), **1958**, pp. 183–227.
[218] A. G. McDonald, K. F. Tipton, *FEBS J.* **2023**, *290*, 2214–2231.
[219] https://iubmb.qmul.ac.uk/enzyme/.

I.5. Strategies to achieve more efficient biocatalytic processes

To enhance productivity and sustainability, effective biocatalysis employs strategies targeting process parameters, reaction products, and the biocatalyst itself. Some of them include:

1. *Process engineering*: careful biocatalyst(s) choose, optimization of reaction conditions, such as temperature, pH, and substrate and enzyme concentrations, can significantly enhance biocatalytic efficiency and yield.[222]
2. *Product removal*: continuous product extraction from the reaction mixture may help in shifting the reaction equilibrium towards the product side, leading to increased conversion rates and driving it to

---

[220] S. Kozuch, J. M. L. Martin, *ACS Catal.* **2012**, *2*, 2787–2794.

[221] A. S. Bommarius, M. F. Paye, *Chem. Soc. Rev.* **2013**, *42*, 6534–6565.

[222] Y. Bai, X. Yang, H. Yu, X. Chen, *ChemSusChem* **2022**, *15*, e202102539.

completion without formation of secondary product(s) or biocatalyst inhibition phenomena.[223]

3. *Process integration*: Integrating biocatalysis with other chemical catalysts (commonly metals and photocatalysts) or technologies such as flow chemistry, can lead to more efficient and streamlined processes.[224]
4. *Use of whole cell biocatalysts*: enzymatic preparations can be whole-cells, crude extracts, or isolated enzymes. Pure enzymes enhance activity but require cofactor systems and face scalability challenges. Using microbial cells with overexpressed enzymes and cofactors is an alternative, but secondary reactions and lower productivity can result, also due to inefficient transport across cell membranes.[225]
5. *Enzyme immobilization and recycling*: immobilizing pure biocatalysts improve their stability, reusability, and facilitate their separation from the reaction mixture and therefore scaling-up, leading to more efficient and sustainable processes.[226] Enzymes can be immobilized under the form of covalently linked or cross-linked enzyme aggregates, physically adsorbed onto resins, beads or as well as new nanomaterials such as organic–inorganic nanocrystals, metal–organic frameworks, graphene-

---

[223] a) M. Wierschem, S. Schlimper, R. Heils, I. Smirnova, A. A. Kiss, M. Skiborowski, P. Lutze, *Chem. Eng. J.* **2017**, *312*, 106–117; b) D. Hülsewede, L.-E. Meyer, J. von Langermann, *Chem. Eur. J.* **2019**, *25*, 4871–4884.

[224] a) L. Schmermund, V. Jurkaš, F. F. Özgen, G. D. Barone, H. C. Büchsenschütz, C. K. Winkler, S. Schmidt, R. Kourist, W. Kroutil, *ACS Catal.* **2019**, *9*, 4115−4144; b) L. Rodríguez-Fernández, J. Albarrán-Velo, I. Lavandera, V. Gotor-Fernández, *Adv. Synth. Catal.* **2023**, *365*, 1883–1892; c) S. González-Granda, L. Escot, I. Lavandera, V. Gotor-Fernández, *Angew. Chem. Int. Ed.* **2023**, *62*, e202217713.

[225] P. Jeandet, E. Sobarzo-Sánchez, A. S. Silva, C. Clément, S. F. Nabavi, M. Battino, M. Rasekhian, T. Belwal, S. Habtemariam, M. Koffas, S. M. Nabavi, *Biotechnol. Adv.* **2020**, *39*, 107461.

[226] a) M. Ripoll, S. Velasco-Lozano, E. Jackson, E. Diamanti, L. Betancor, F. López-Gallego, *Green Chem.* **2021**, *23*, 1140–1146; b) Y. R. Maghraby, R. M. El-Shabasy, A. H. Ibrahim, H. M. E.-S. Azzazy, *ACS Omega* **2023**, *8*, 5184–5196.

based nanomaterials, and functionalized solid surfaces.[227] This strategy allows its use in flow, which favors process intensification.[228]

6. *Cofactor recycling*: a cofactor is a non-protein molecule or ion that is covalently (so called prosthetic group) or non-covalently (so called coenzyme) bound to the enzymatic active site. It is essential for the activity of the enzyme and usually quite expensive when purchased. Enabling its regeneration in a transformation through a coupled reaction or immobilization, enhances the overall efficiency of the biocatalytic process, reducing as well costs and waste generation.[229]
7. *Biocatalyst engineering*: with the aid of protein engineering techniques, enzymes can be modified and optimized to improve their efficiency, specificity, and stability, thereby facilitating more effective and sustainable production of desired compounds.

Due to the relevance of some of these techniques in the present Thesis, they are explained in more detail in the ongoing sections.

I.5.1. Biocatalyst improvement through heterologous expression

Amongst all the potential strategies, enhancing biocatalyst performance is crucial for increasing process efficiency. Particularly, optimizing its recombinant expression and engineering is the first key step for achieving a suitable enzyme for (large-scale) synthetic applications.

The heterologous expression of an enzyme consists of expressing the gene encoding the enzyme in a host organism. This approach yields large biocatalyst quantities with improved features, sidestepping wild type limitations and reducing reliance on costly commercial preparations. Genetic manipulation enhances customization, rendering enzymes more robust and adaptable to diverse conditions, especially advantageous in industrial applications.[230]

---

[227] K. T.sriwong, T. Matsuda, *Org. Process Res. Dev.* **2022**, *26*, 1857–1877.

[228] J. Coloma, Y. Guiavarc'h, P.-L. Hagedoorn, U. Hanefeld, *Chem. Commun.* **2021**, *57*, 11416–11428.

[229] S. Mordhorst, J. N. Andexer, *Nat. Prod. Rep.* **2020**, *37*, 1316–1333.

The main challenges in heterologous enzyme expression include choosing the right host and system, driven by protein folding and modifications. Toxicity to the host due to enzyme overexpression can lead to failed expression or mislocalization, affecting its function and effectiveness. Inclusion bodies form due to enzyme instability, causing inactivation. Other issues are related to low expression levels and difficulties in scaling-up the fermentation process for the recombinant expression at large-scale.[231]

I.5.2. Biocatalyst improvement through enzyme engineering

In order to apply enzymes in industrial processes, endurance and performance under the target operational conditions are often challenging. Wild-type enzymes might not meet industrial needs due to instability in non-conventional media or activity inhibition. Progress is being made to expand enzyme options for synthetic chemists engineering enzymes with enhanced activity, broad substrate scope, and improved selectivity and stability.[232] One remarkable milestone is the acknowledgment of biocatalysis with the 2018 Nobel Prize in Chemistry, awarded to Prof. Frances Arnold for her pioneering work in advancing directed evolution techniques for enzyme engineering.[233]

There are three fundamentally different strategies that can be employed to modify enzymatic properties as desired (Figure I.17).

---

[230] A. M. Mendes Lopes, M. Martins, R. Goldbeck, *Mol. Biotechnol.* **2021**, *63*, 184–199.

[231] C. Lambertz, M. Garvey, J. Klinger, D. Heesel, H. Klose, R. Fischer, U. Commandeur, *Biotechnol. Biofuels* **2014**, *7*, 135.

[232] a) D. L. Trudeau, D. S. Tawfik, *Curr. Opin. Biotechnol.* **2019**, *60*, 46–52; b) K. Chen, F. H. Arnold, *Nat. Catal.* **2020**, *3*, 203–213; c) D. C. Miller, S. V. Athavale, F. H. Arnold, *Nat. Synth.* **2022**, *1*, 18–23.

[233] F. H. Arnold, *Angew. Chem. Int. Ed.* **2019**, *58*, 14420–14426.

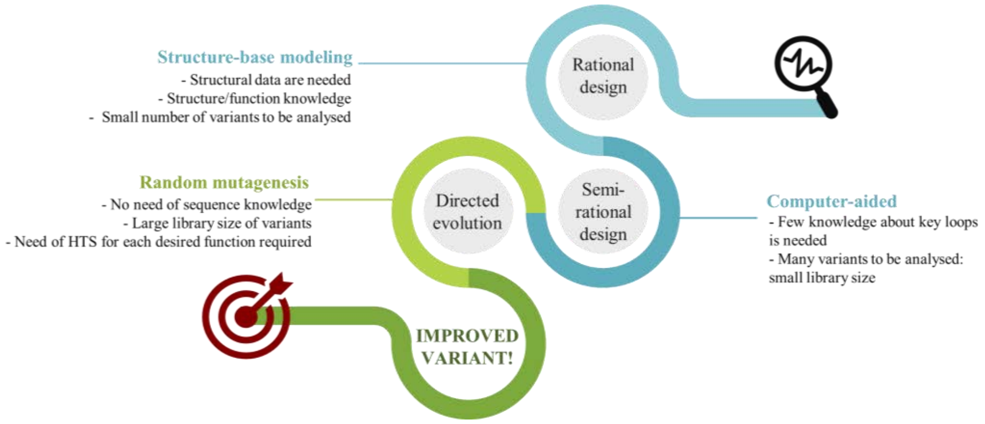
Structure-base modeling
- Structural data are needed
- Structure/function knowledge
- Small number of variants to be analysed
Rational design
Random mutagenesis
- No need of sequence knowledge
- Large library size of variants
- Need of HTS for each desired function required
Directed evolution
Semi-rational design
Computer-aided
- Few knowledge about key loops is needed
- Many variants to be analysed: small library size
IMPROVED VARIANT!

Figure I.17. Overview of approaches for protein engineering by rational design, semi-rational design, and directed evolution.

One of these strategies is the *rational design*, which involves redesigning the protein sequence through site-directed mutagenesis. Modified enzymes are assessed and further rounds of mutagenesis can improve its characteristics. This iterative approach systematically optimizes enzyme properties through planned modifications.[234] In addition, molecular docking supports site-directed mutagenesis, evaluating interactions in static or dynamic environment between proteins and target molecules. This aids in selecting key residues to be changed based on binding energies and electrostatic interactions at the active site.[235] The second strategy is *directed evolution*, which differs from rational design as it does not rely on detailed knowledge of the enzyme's structure or function. Directed evolution requires the gene (or genes) of interest, and diversity is introduced using methods of random mutagenesis. Through this approach, a variety of enzyme variants are expressed. They are subsequently screened or selected to identify those with the desired property, or subjected to iterative rounds of mutagenesis until the desired function is achieved.[236] A third option is represented by the *in silico*

---

[234] M. Ali, H. M. Ishqi, Q. Husain, *Biotechnol. Bioeng.* **2020**, *117*, 1877–1894.
[235] Z. Song, Q. Zhang, W. Wu, Z. Pu, H. Yu, *Front. Bioeng. Biotechnol.* **2023**, *11*, 1129149.
[236] M. S. Packer, D. R. Liu, *Nat. Rev. Genet.* **2015**, *16*, 379–394.

saturated mutagenesis (or semi-rational design), that is a widely used approach in computational biology. Being a compromise between the two previous techniques, it is employed to successfully assess the impact of each nucleotide or amino acid in a specific sequence, combining directed evolution with rational tools. This method systematically analyzes all potential mutations in a chosen enzyme region. It predicts how sequence alterations can impact the final function of the biological entity being studied.[237]

Rational redesign faces challenges due to the extensive amount of data required, like structure/function insights. Saturation mutagenesis can partially address this drawback. In contrast, directed evolution does not rely on detailed enzyme understanding. It can produce improved variants without requiring comprehensive structure-function knowledge.[238] Yet, it struggles to identify efficient hits from large variant libraries. Traditional methods like GC, HPLC, or MS are slow and labor-intensive. Novel high throughput screening (HTS) methods are being developed to speed up protein optimization and identification, saving time and resources.[239]

I.6. Biocatalysis in industrial processes

The industrial interest in biocatalysis experienced a significant growth in the 20th century. From these years onward, notable efforts have been made to carry out scalable reactions with high productivity, encompassing the production of bulk and fine chemicals.[240] From an historical point of view, in 1924, Kluyver and de Leeuw proved that *Acetobacter suboxydans* could oxidize D-sorbitol to L-sorbose, an important intermediate in the synthesis of

---

[237] K. Gupta, R. Varadarajan, *Curr. Opin. Struct. Biol.* **2018**, *50*, 117–125.

[238] I. V. da Silva Amatto, N. G. da Rosa-Garzon, F. A. de Oliveira Simões, F. Santiago, N. P. da Silva Leite, J. R. Martins, H. Cabral, *Biotechnol. Appl. Biochem.* **2022**, *69*, 389–409.

[239] a) L. Ye, C. Yang, H. Yu, *Appl. Microbiol. Biotechnol.* **2018**, *102*, 559–567; b) S. Hecko, A. Schiefer, C. P. S. Badenhorst, M. J. Fink, M. D. Mihovilovic, U. T. Bornscheuer, F. Rudroff, *Chem. Rev.* **2023**, *123*, 2832–2901.

[240] *Biocatalysis: An Industrial Perspective*, (Eds.: G. de Gonzalo, P. Domínguez de María), Royal Society of Chemistry, Cambridge (UK), **2017**.

L-ascorbic acid (vitamin C). In the 1930s, indeed, this synthesis was turned into an industrial process by Roche (now part of DSM).[241]

The first example of biocatalysis replacing a conventional industrial chemical process dates back to the mid-20th century, when Peterson reported a simplified method for the conversion of progesterone by means of *Rhizopus arrhius* into an intermediate used for the synthesis of corticosteroid hormones.[242] At that moment, the original chemical synthesis developed at Merck required 31 steps to obtain 1 kg of cortisone acetate from 615 kg of the starting precursor, rendering the process expensive. The introduction of biocatalysis reduced cortisol's price from \$200 to \$6 per gram and further improvements brought it down to \$1 per gram.[243] On the other side, a prominent large-scale biocatalysis application is Mitsubishi Rayon's production (Nitto Chemicals) of acrylamide from acrylonitrile, generating 50,000 tons annually using nitrile hydratase from *Rhodococcus rhodochrous*. Again, the enzymatic process excels over the chemical alternative due to the greater selectivity, minimizing complex downstream procedures.[244]

The fruitful collaboration of Merck and Codexis® during the recent COVID-19 pandemic led to the development of an elegant multicatalytic route for the production of *Molnupiravil*, an antiviral drug used in moderate cases of illness due to SARS-CoV-2 infection. Thanks to the combination of an improved variant of a ribosyl-1-kinase and a uridine phosphorylase, with reaction optimization, the drug was produced from low-cost raw material replacing the original 10-step chemical synthesis process (<10% overall yield) by a 3-step procedure (70% overall yield). The biocatalytic process was set-up and rapidly implemented on a large-scale within only 6 months, thus facing the need of urgent supply of therapies against coronavirus disease.[245]

---

[241] G. Pappenberger, H.-P. Hohmann, in *Biotechnology of Food and Feed Additives*, (Eds.: H. Zorn, P. Czermak), Springer, Berlin (Germany), **2013**, pp. 143–188.

[242] a) D. H. Peterson, H. C. Murray, S. H. Eppstein, L. M. Reineke, A. Weintraub, P. D. Meister, H. M. Leigh, *J. Am. Chem. Soc.* **1952**, *74*, 5933–5936; b) J. A. Hogg, *Steroids* **1992**, *57*, 593–616.

[243] S. H. Pines, *Org. Process Res. Dev.* **2004**, *8*, 708–724.

[244] H. Yamada, M. Kobayashi, *Biosci. Biotechnol. Biochem.* **1996**, *60*, 1391–1400.

Biocatalysis holds immense potential within the lignocellulosic biorefinery industry by driving the processes towards a sustainable circular economy.[246] Biocatalytic strategies are applied for the lignin pretreatment,[247] initial conversion of polysaccharide feedstocks into fermentable sugars, as well as in downstream processing of carbohydrate intermediates and their conversion into high-added value compounds, such as bioplastics.[248] Other applications for industrial enzymes include dairy processing, cleaning agents manufacturing, animal feed, bio-fuel production, textiles, leather, and paper processing (Figure I.18).[249]

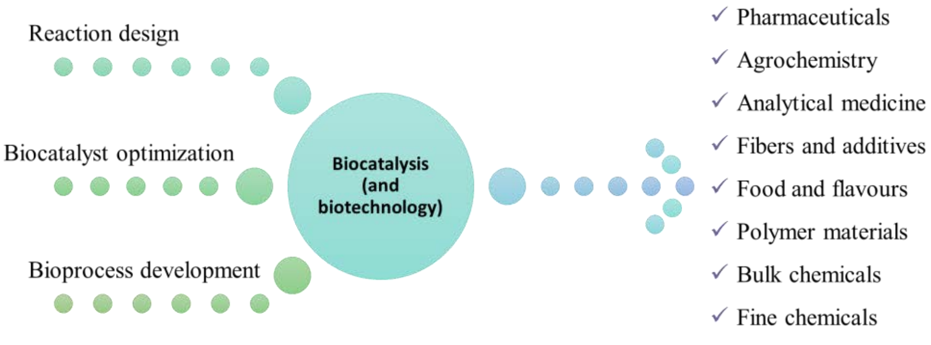
Reaction design
Biocatalyst optimization
Bioprocess development
Biocatalysis (and biotechnology)
✓ Pharmaceuticals
✓ Agrochemistry
✓ Analytical medicine
✓ Fibers and additives
✓ Food and flavours
✓ Polymer materials
✓ Bulk chemicals
✓ Fine chemicals

Figure I.18. Role of biocatalysis in different industrial sectors.

---

[245] J. A. McIntosh, T. Benkovics, S. M. Silverman, M. A. Huffman, J. Kong, P. E. Maligres, T. Itoh, H. Yang, D. Verma, W. Pan, *et al.*, *ACS Cent. Sci.* **2021**, *7*, 1980–1985.

[246] a) R. A. Sheldon, D. Brady, *ChemSusChem* **2022**, *15*, e202102628; b) A. Yadav, V. Sharma, M.-L. Tsai, C.-W. Chen, P.-P. Sun, P. Nargotra, J.-X. Wang, C.-D. Dong, *Bioresour. Technol.* **2023**, *381*, 129145.

[247] D. Silva, C. F. Rodrigues, C. Lorena, P. T. Borges, L. O. Martins, *Biotechnol. Adv.* **2023**, *65*, 108153.

[248] R. Wei, T. Tiso, J. Bertling, K. O'Connor, L. M. Blank, U. T. Bornscheuer, *Nat. Catal.* **2020**, *3*, 867–871.

[249] a) J. Nazor, J. Liu, G. Huisman, *Curr. Opin. Biotechnol.* **2021**, *69*, 182–190; b) S. Wu, R. Snajdrova, J. C. Moore, K. Baldenius, U. T. Bornscheuer, *Angew. Chem. Int. Ed.* **2021**, *60*, 88–119.

I.7. Tools to evaluate sustainability in chemical processes

The utilization of a biocatalyst in a chemical reaction does not automatically ensure the inherent sustainability of the reaction.[250] Thus, different chemometric parameters have been proposed as evaluating tools of the sustainability of a (bio)catalytic process, reflecting its environmental impact and eco-compatibility by considering resource efficiency and waste generation.[251]

The first metric, atom economy, also known as the "*atom efficiency*" or "atom utilization", proposed by Trost in 1991 evaluates reaction efficiency by measuring the proportion of reactant atoms in the desired product.[252] The *environmental factor* or *E*-factor, introduced by Sheldon in 1992, quantifies waste generated during a process, expressed as the ratio of the mass of waste produced to produce 1 kg of the desired product, aiming for zero waste in alignment with Green Chemistry's principles.[253] However, zero *E*-factor is an ideal goal, because of the impact of water and solvents on the metric calculations, particularly in biocatalysis. The *E*-factor concept has been expanded upon with other alternatives like the *E^+-factor* for bulk chemicals. This extended version considers not only the mass of waste produced but also the energy contribution to the waste, reflected in the form of CO_2 emissions.[254] Similarly, Christensen proposed a *Climate Factor* (*C*-factor), as the amount of CO_2 emitted per amount of product formed, to quantify carbon footprints of the processes.[255] As well, *Process Mass Intensity* (PMI, the total mass of chemicals used in a process per mass of desired product) is also reported, and nowadays adopted by the Institute Pharmaceutical Round Table to benchmark the environmental footprints of processes for APIs, and guide the pharma industry towards the green catalysis.[256]

---

[250] Y. Ni, D. Holtmann, F. Hollmann, *ChemCatChem* **2014**, *6*, 930–943.

[251] P. Domínguez de María, *Curr. Opin. Green Sustain. Chem.* **2021**, *31*, 100514.

[252] B. M. Trost, *Science* **1991**, *254*, 1471–1477.

[253] a) R. A. Sheldon, *Chem. Ind. (London)* **1992**, 903–906; b) R. A. Sheldon, *Green Chem.* **2007**, *9*, 1273–1283.

[254] F. Tieves, F. Tonin, E. Fernández-Fueyo, J. M. Robbins, B. Bommarius, A. S. Bommarius, M. Alcalde, F. Hollmann, *Tetrahedron* **2019**, *75*, 1311–1314.

[255] C. H. Christensen, J. Rass-Hansen, C. C. Marsden, E. Taarning, K. Egeblad, *ChemSusChem* **2008**, *1*, 283–289.

However, to comprehensively assess impact, metrics like *Life Cycle Assessment* (LCA) consider the environmental effects of a product or a process throughout its entire life cycle. With this approach, the whole environmental impact of a product or process is evaluated, from raw material extraction to manufacturing, use, and disposal, in a circularity mean.[257] Economic factors (productivity, conversions, yields) guide biocatalyst development, while Green Chemistry metrics promote eco-friendly processes. These factors aid in evaluating raw materials, biocatalyst efficiency, reactor size, downstream expenses, and overall process sustainability. A comparison of the main metrics is given in Table I.8.

Table I.8. Selected 'green' and economic metrics commonly used for assessing the sustainability and efficiency of a (bio)catalytic reaction.

Economic metrics	**Productivity (g product / L reactor h)**
	Conversion 1 – (g residual substrate / g initial substrate)
	Yield of product on biocatalyst (mole product / mole enzyme)
	Yield of product on substrate (mole product / mole substrate)
	Product concentration (g product / L reactor)
Green chemistry metrics	*E*-factor (kg waste / kg product)
	E^+-factor (*E* + Electrical power + carbon intensity) / kg of desired product
	PMI (g of total chemicals / g of desired product) = (*E*-factor + 1)
	C-factor (g CO_2 equivalents / g product)
	Water intensity (g water used / g product)
	Solvent intensity (g solvent used / g product)

---

[256] a) A. D. Curzons, D. J. C. Constable, D. N. Mortimer, V. L. Cunningham, *Green Chem.* **2001**, *3*, 1–6; b) C. Jiménez-González, C. Ollech, W. Pyrz, D. Hughes, Q. B. Broxterman, N. Bhathela, *Org. Process Res. Dev.* **2013**, *17*, 239–246.

[257] R. A. Sheldon, *ACS Sustain. Chem. Eng.* **2018**, *6*, 32–48.

Different approaches have been explored to enhance the sustainability of chemical processes. These include aqueous-based processes with high substrate loadings,[258] reactions that are completely solvent-free (without the use of either of organic solvent and water),[259] and the utilization of biogenic solvents and deep eutectic solvents.[260] Among these options, solvent-free systems stand out as they offer both environmental benefits and practicability for industrial purposes, although their implementation may not always be feasible. Another approach is to perform multistep (cascade) reactions, which eliminate the need to isolate reaction intermediates.[261] Moreover, continuous flow reaction processes with immobilized enzymes can be implemented, where solvents and water can be recycled, presenting promising and powerful alternatives for achieving sustainability in future chemical processes.[262]

I.8. Design of multicatalytic reactions

Traditionally, synthetic routes involve stepwise reactions with the isolation and purification of intermediates. Nature demonstrates the remarkable efficiency of biocatalysts by combining them in sequence.[263] Emulating this *in vivo* strategy, researchers have combined multiple enzymes *in vitro* to design multi-step transformations in a one-pot fashion (within the same vessel).[264] These multienzymatic cascades, along with chemo- and photo-biocascades[224a,265] (biocatalysts combined with chemo- or photo-catalysts), have been extensively studied for the efficient synthesis of high-added value compounds.

---

[258] a) A. Hinzmann, S. Glinski, M. Worm, H. Gröger, *J. Org. Chem.* **2019**, *84*, 4867–4872; b) H. Gröger, F. Gallou, B. H. Lipshutz, *Chem.Rev.* **2023**, *123*, 5262–5296.

[259] M. Hobisch, M. M. C. H. van Schie, J. Kim, K. R. Andersen, M. Alcalde, R. Kourist, C. B. Park, F. Hollmann, S. Kara, *ChemCatChem* **2020**, *12*, 4009–4013.

[260] a) A. R. Alcántara, P. Domínguez de María, *Curr. Green Chem.* **2018**, *5*, 86–103; b) Á. Mourelle-Insua, I. Lavandera, V. Gotor-Fernández, *Green Chem.* **2019**, *21*, 2946–2951; c) V. Gotor-Fernández, C. E. Paul, *J. Biotechnol.* **2019**, *293*, 24–35; d) S. N. Chanquia, L. Huang, G. G. Liñares, P. Domínguez de María, S. Kara, *Catalysts* **2020**, *10*, 1013.

[261] A. I. Benítez-Mateos, D. Roura Padrosa, F. Paradisi, *Nat. Chem.* **2022**, *14*, 489–499.

[262] P. Díaz-Kruik, S. Gianolio, F. Paradisi, *Chimia* **2023**, *77*, 307–311.

[263] C. S. Jamieson, J. Misa, Y. Tang, J. M. Billingsley, *Chem. Soc. Rev.* **2021**, *50*, 6950–7008.

[264] a) S. Schoffelen, J. C. M. van Hest, *Soft Matter* **2012**, *8*, 1736–1746; b) E. García-Junceda, I. Lavandera, D. Rother, J. H. Schrittwieser, *J. Mol. Catal. B: Enzym.* **2015**, *114*, 1–6; c) R. Siedentop, C. Claaßen, D. Rother, S. Lütz, K. Rosenthal, *Catalysts* **2021**, *11*, 1183.

These methods bring advantages like time and cost savings, improved yields through favorable equilibrium shifts, and the rapid use of unstable intermediates for subsequent reactions.[266] Consecutive processes occurring in one-pot are defined as cascades (or concurrent reactions), when all reagents and catalysts are added from the beginning to the reaction medium under constant reaction conditions. They begin with a substrate and progress through multiple steps, with each product becoming the substrate for the next stage. This is called *linear cascade* (Scheme I.2a).[267] On the other hand, we refer to *sequential processes* when catalysts and reagents are added successively in the same reaction vessel at different operational times, and/or under varying reaction conditions (Scheme I.2b). This strategy still avoids the isolation of intermediate(s), but separate in time the reaction steps. This is the right choice when simultaneous development of two or more stages is incompatible, or when the formation of secondary products must be minimized under specific reaction conditions.

Other reaction cascade assets are worthy to be mentioned:[268] in *orthogonal* cascades, for example, the conversion of a substrate into the desired product is coupled with a second reaction that removes one or more by-products (Scheme I.2c). Furthermore, in *cyclic* cascades, commonly utilized in deracemization processes, one enantiomer from a racemic mixture is converted to an intermediate product, which is then transformed back to the racemic starting material, yielding the unreacted substrate enantiomer as the

---

[265] a) F. F. Özgen, M. E. Runda, S. Schmidt, *ChemBioChem* **2021**, *22*, 790–806; b) S. González-Granda, J. Albarrán-Velo, I. Lavandera, V. Gotor-Fernández, *Chem. Rev.* **2023**, *123*, 5297–5346.

[266] a) Z. Wang, B. S. Sekar, Z. Li, *Bioresour. Technol.* **2021**, *323*, 124551; b) L. Bering, J. Thompson, J. Micklefield, *Trends Chem.* **2022**, *4*, 392–408.

[267] S. Schmidt, A. Schallmey, R. Kourist, in *Enzyme Cascade Design and Modelling*, (Eds.: S. Kara, F. Rudroff), Springer, Berlin (Germany), **2021**, pp. 31–48.

[268] a) E. Ricca, B. Brucher, J. H. Schrittwieser, *Adv. Synth. Catal.* **2011**, *353*, 2239–2262; b) S. P. France, L. J. Hepworth, N. J. Turner, S. L. Flitsch, *ACS Catal.* **2017**, *7*, 710–724.

final product after several cycles (Scheme I.2c). Finally, in the *interconnected* or *parallel* cascades, while a substrate is converted into the desired product, another co-substrate is transformed into a co-product by a parallel enzyme-catalyzed step, which is also synthetically valuable. This strategy can be applied when both biocatalysts share a reciprocal demand for the cofactor, which is therefore regenerated (Scheme I.2c).[269]

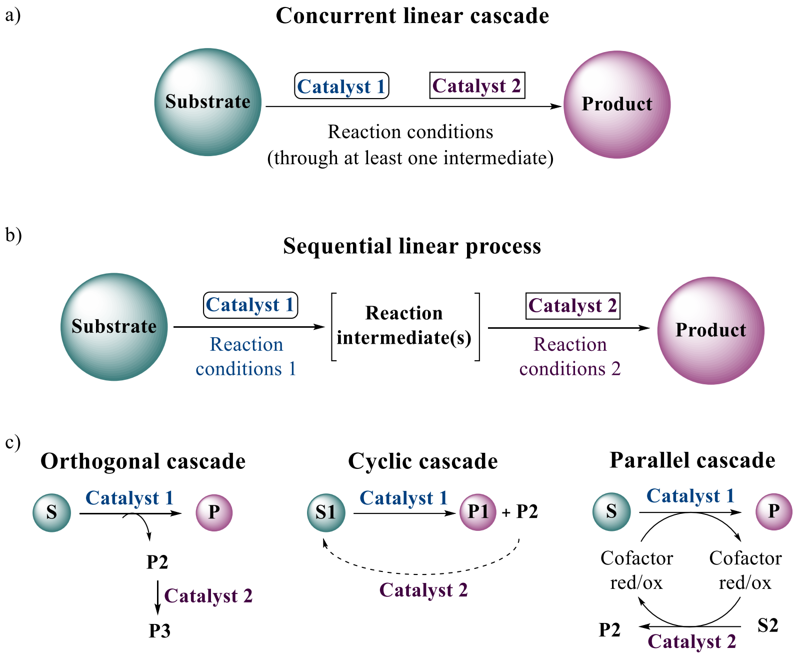
a)
Concurrent linear cascade
Substrate
Catalyst 1
Catalyst 2
Product
Reaction conditions
(through at least one intermediate)
b)
Sequential linear process
Substrate
Catalyst 1
Reaction conditions 1
Reaction intermediate(s)
Catalyst 2
Reaction conditions 2
Product
c)
Orthogonal cascade
S
Catalyst 1
P
P2
Catalyst 2
P3
Cyclic cascade
S1
Catalyst 1
P1 + P2
Catalyst 2
Parallel cascade
S
Catalyst 1
P
Cofactor red/ox
Cofactor red/ox
P2
Catalyst 2
S2

Scheme I.2. General representations for integrated one-pot transformations. Adapted from reference 261.

A representative example applied on the synthesis of furan derivatives is the combination of a galactose oxidase (GOx), a horseradish peroxidase (HRP), and an alcohol dehydrogenase (ADH) for the synthesis of FFCA or

---

[269] a) A. Rioz-Martínez, F. R. Bisogno, C. Rodríguez, G. de Gonzalo, I. Lavandera, D. E. Torres Pazmiño, M. W. Fraaije, V. Gotor, *Org. Biomol. Chem.* **2010**, *8*, 1431–1437; b) A. Bornadel, R. Hatti-Kaul, F. Hollmann, S. Kara, *ChemCatChem* **2015**, *7*, 2442–2445.

FDCA from HMF, according to the cofactor promiscuity of the last enzyme. The co-product of the GOx reaction is hydrogen peroxide (H_2O_2), that is then utilized in the HRP-mediated regeneration of the oxidized nicotinamide cofactor, required by the ADH, enabling an internal cofactor recycling to produce FFCA (Scheme I.3).[270] If the ADH is able to accept a cofactor mimic, namely 1-benzyl-1,4-dihydropyridine-3-carboxamide (BNAH), this compound can be oxidized into the final FDCA product.

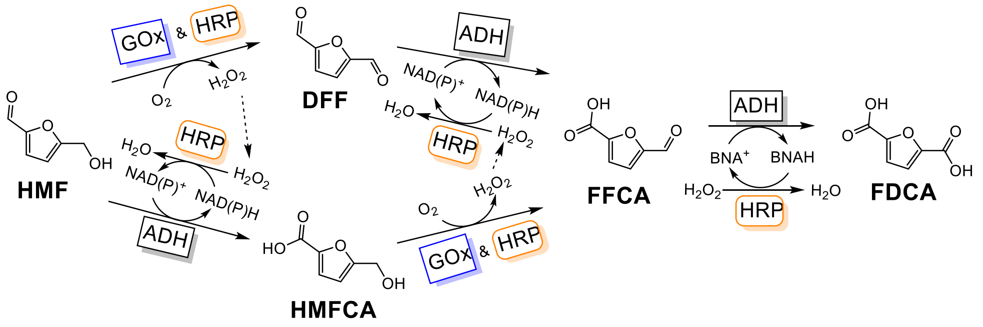
GOx
&
HRP
O2
H2O2
DFF
ADH
NAD(P)+
NAD(P)H
H2O
HRP
H2O2
HMF
OH
O
H2O
HRP
H2O2
NAD(P)+
NAD(P)H
ADH
HO
HMFCA
O2
H2O2
GOx
&
HRP
OH
FFCA
ADH
BNA+
BNAH
H2O2
H2O
HRP
OH
FDCA

Scheme I.3. Dual linear cascade for the synthesis of FFCA or FDCA from HMF.

---

[270] H.-Y. Jia, M.-H. Zong, G.-W. Zheng, N. Li, *ChemSusChem* **2019**, *12*, 4764–4768.

OBJECTIVES

The introduction of this thesis emphasizes the significance of biocatalytic production of furfural and HMF derivatives in the biorefinery context, as well as the crucial need for innovative processes to enable commercialization. In this frame, the main objective of this Doctoral Thesis, included inside the EU network program INTERfaces, is the design of linear cascade transformations for transforming furan-based compounds by the action of multiple enzymes, suitable for large-scale bioconversions. In detail, the search for (novel) enzymes to be applied in the sequential oxidation and transamination of furan-based compounds will be investigated. The primary need will be to establish efficient processes through both reaction engineering and heterologous expression of promising biocatalyst candidates.

The first part will examine laccases as suitable and mild oxidative biocatalysts, exploring evolution approaches to enhance reactivity (rational design and directed evolution) and introducing new oxidative biocatalysts (i.e., Lacc12 laccase). A new colorimetric assay to selectively detect DFF will also be developed as future high-throughput screening method.

In the second part, selected laccases will be combined with amine transaminases to valorize furan derivatives, starting first from furfuryl alcohol as a model substrate. Optimization of each individual step will lead to a one-pot linear sequential process for furfuryl amine production. The process will be extended to HMF amino-derivatives via similar oxidation and transamination sequence. New house-made amine transaminases will be introduced to broaden the range of affordable enzymes for relevant biocatalytic applications.

First part

Laccases: enzyme design and application in oxidative processes

CHAPTER 1

Searching for new laccases from *Pleurotus ostreatus*

Introduction

Oxidoreductases (EC 1), also known as redox enzymes, belong to a major biocatalyst family involved in catalyzing oxidation and reduction reactions in biological systems. These enzymes play a crucial role in various metabolic processes, including energy production, detoxification, and biosynthesis. They transfer electrons from reducing substances to oxidizing substances, facilitated by cofactors like nicotinamide derivatives $NAD(P)^+$, flavin mononucleotide (FMN), heme groups, and others. They drive diverse reactions including hydroxyl and amino group oxidations, carbonyl and imine reductions, and double bond epoxidations. These enzymes are categorized by their electron acceptor, in dehydrogenases, oxidases, and oxygenases.[271] In particular, oxidases drive oxidation reactions on many different substrates using molecular oxygen as the terminal electron acceptor, reducing it to hydrogen peroxide or water, without the need of an external cofactor.[272] In this Doctoral Thesis, laccases, belonging to the oxidase class, will be employed.

1.1.1. Laccases and white biotechnology

Laccases (benzenediol:oxygen oxidoreductase; *p*-diphenol oxidase; EC 1.10.3.2), are blue copper containing oxidases subject of investigation since the late 19th century. They were initially discovered in the exudates of the Japanese lacquer tree, *Rhus vernicifera*, by Yoshida in 1883.[273] Their presence was later confirmed in fungi by Bertrand in 1896,[274] and, since then, similar proteins have been found in both eukaryotes and prokaryotes. Despite its long recognition, laccases gained significant interest in the industrial panorama when research began to focus on enzymatic wood degradation by white-rot fungi. These oxidases have the ability to enzymatically oxidize an extensive array of organic and inorganic substrates through radical generation, including mono-, di-, and polyphenols, aminophenols, methoxyphenols, and even metal complexes. Furthermore, the main action of fungal laccases, tied to the reactions they catalyze, appears to be dichotomous. Indeed, they catalyze both polymerization and depolymerization reactions. This functional duality stems from the existence of diverse isoforms expressed within organisms, found within the same as well as different genera and species.[275] The broad substrate reactivity together with the distinct isoforms, each with their own specific induction patterns and unique biochemical traits, can be exploited for different specific biotechnological applications.[276]

---

[271] A. T. Martínez, F. J. Ruiz-Dueñas, S. Camarero, A. Serrano, D. Linde, H. Lund, J. Vind, M. Tovborg, O. M. Herold-Majumdar, M. Hofrichter, *et al.*, *Biotechnol. Adv.* **2017**, *35*, 815–831.

[272] A. J. C. Wahart, J. Staniland, G. J. Miller, S. C. Cosgrove, *R. Soc. Open Sci.* **2022**, *9*, 211572.

[273] H. Yoshida, *J. Chem. Soc.* **1883**, *43*, 472–486.

[274] S. S. Desai, C. Nityanand, *Asian J. Biotechnol.* **2011**, *3*, 98–124.

1.1.1.1. General features and role in nature

Generally, laccases catalyze the one-electron oxidation process concurrently with the four-electron reduction of molecular oxygen to water.[277] They have been isolated from plants, fungi, and bacteria.[278] Both plant and fungal laccases show a great glycosylation level, with plant laccases exhibiting higher (22% to 45%) compared to fungal laccases (typically 10-25%). Variability is observed in their molecular weight, pH preference, substrate specificity, and other characteristics. They can exist as monomeric, dimeric, or tetrameric proteins in their active holoenzyme state, typically featuring an acidic isoelectric point (pI).[279]

These biocatalysts, whether released externally or found within cells, serve distinct physiological roles. For instance, in plants, they are involved in growth and development processes, cell wall formation and collaborate with peroxidases to initiate lignification.[280] Laccase-like enzymes were also discovered within the cuticles of both larval and adult insects: their phenol oxidase activity is supposed to be related with the process of sclerotization in insects.[281] Moreover, bacterial laccases, found in organisms like *Bacillus subtilis* enhance spore pigmentation, bolstering resistance against stressors like UV radiation and hydrogen peroxide.[282] In bacteria they are also involved in copper homeostasis, morphogenesis, melanisation, and pathogenicity.[283]

---

[275] K. K. Sharma, R. C. Kuhad, *Indian J. Microbiol.* **2008**, *48*, 309–316.

[276] A. D. Moreno, D. Ibarra, M. E. Eugenio, E. Tomás-Pejó, *J. Chem. Technol. Biotechnol.* **2020**, *95*, 481–494.

[277] M. D. Cannatelli, A. J. Ragauskas, *Chem. Rec.* **2017**, *17*, 122–140.

[278] L. Arregui, M. Ayala, X. Gómez-Gil, G. Gutiérrez-Soto, C. E. Hernández-Luna, M. Herrera de los Santos, L. Levin, A. Rojo-Domínguez, D. Romero-Martínez, M. C. N. Saparrat, *et al.*, *Microb. Cell Fact.* **2019**, *18*, 200.

[279] G. Janusz, A. Pawlik, U. Świderska-Burek, J. Polak, J. Sulej, A. Jarosz-Wilkołazka, A. Paszczyński, *Int. J. Mol. Sci.* **2020**, *21*, 966.

Significantly, fungal laccases exhibit dual synthetic and degradative functions. In terms of synthesis, they primarily participate in processes such as fruit body formation, pigmentation, and pathogenesis. Conversely, these enzymes hold a pivotal position in delignification processes.[284] Moreover, they provide protection toward fungal pathogens against detrimental phytoalexins and tannins, rendering them as significant contributors to the virulence of various fungal diseases.[285]

1.1.1.2. Fungal laccases: Structure and mechanism

From an electrochemical perspective, laccases are categorized into three groups based on their T1 site's redox potential (E^0-T1): low, medium, and high-redox potential laccases. The E^0-T1 is influenced by factors like copper-ligand interactions, desolvation effects around the T1 site, electrostatic interactions, and protein folding. Bacterial and plant laccases represent the low-redox potential group with E^0-T1 values below +460 mV

---

[280] Y. Bai, S. Ali, S. Liu, J. Zhou, Y. Tang, *Gene* **2023**, *852*, 147060.

[281] M. J. Gorman, L. I. Sullivan, T. D. T. Nguyen, H. Dai, Y. Arakane, N. T. Dittmer, L. U. Syed, J. Li, D. H. Hua, M. R. Kanost, *Insect Biochem. Mol. Biol.* **2012**, *42*, 193–202.

[282] L. O. Martins, C. M. Soares, M. M. Pereira, M. Teixeira, T. Costa, G. H. Jones, A. O. Henriques, *J. Biol. Chem.* **2002**, *277*, 18849–18859.

[283] a) H. Claus, *Arch. Microbiol.* **2003**, *179*, 145–150; b) D. Singh, S. Rawat, M. Waseem, S. Gupta, A. Lynn, M. Nitin, N. Ramchiary, K. K. Sharma, *Biochem. Biophys. Res. Commun.* **2016**, *469*, 306–312.

[284] A. Sharma, K. K. Jain, A. Jain, M. Kidwai, R. C. Kuhad, *Appl. Microbiol. Biotechnol.* **2018**, *102*, 10327–10343.

[285] V. Lattanzio, V. M. T. Lattanzio, A. Cardinali, *Adv. Res. Phytochem.* **2015**, *661*, 23–67.

vs normal hydrogen electrode (NHE), with a Met residue as the T1-Cu axial ligand. Fungal laccases fall into medium- and high-redox potential categories. Found in ascomycetes and basidiomycetes fungi, they have an E^0-T1 ranging from +460 to +710 mV *vs* NHE, typically featuring a Leu as the non-coordinating axial ligand. High-redox potential laccases are prevalent in basidiomycete white-rot fungi, with E^0-T1 ranging from +730 to +790 mV *vs* NHE.[286] This high-redox potential group is especially significant due to their ability to oxidize a wider substrate range compared to low- and medium-redox potential ones.

1.1.1.3. Laccase from Trametes versicolor

Overall, laccases isolated from fungi (in first place wood-rot basidiomycetes) show high substrate versatility, functional diversity, and potential for various industrial applications that make them particularly appealing for biotechnological use compared to laccases from plants or bacteria. Fungal laccases are extra-cellular glycoproteins, synthetized as monomeric globular structures with a molecular weight of around 60-70 kDa. Typically, they undergo glycosylation, with levels spanning from 10% to 25%, and occasionally exceeding 30% in specific cases.[287]

Their catalytic activity is enabled by the presence of four distinct copper centers within the enzyme structure: one type-1 (T1) copper in addition to three other copper ions forming a trinuclear cluster: one type-2 (T2) and two type-3 (T3).[288] Spectroscopic properties distinguish the different copper centers: T1 copper has a strong absorption around 600 nm, giving the characteristic blue colour to these multicopper oxidases, T2 copper exhibits weak absorption and is active in electron paramagnetic resonance (EPR), while the T3 copper ions are EPR-silent due to antiferromagnetic coupling.

---

[286] C. J. Rodgers, C. F. Blanford, S. R. Giddens, P. Skamnioti, F. A. Armstrong, S. J. Gurr, *Trends Biotechnol.* **2010**, *28*, 63–72.

[287] P. Giardina, V. Faraco, C. Pezzella, A. Piscitelli, S. Vanhulle, G. Sannia, *Cell. Mol. Life Sci.* **2010**, *67*, 369–385.

[288] A. C. Mot, R. Silaghi-Dumitrescu, *Biochem.-Moscow* **2012**, *77*, 1395–1407.

Ligands for type-1 copper involve two histidines (His) and one cysteine (Cys), with an additional axial ligand, usually a methionine (Met), except for certain cases like laccase from *Trametes versicolor* (L*Tv*), where a phenylalanine (Phe) is present or a leucine (Leu) in basidiomycete white-rot fungi.[289] Eight histidines serve as ligands for binding type-2 and type-3 Cu atoms at the T2/T3 cluster, with these amino acid regions being responsible for copper binding and maintaining the protein's three-dimensional structure (Figure 1.1).[290]

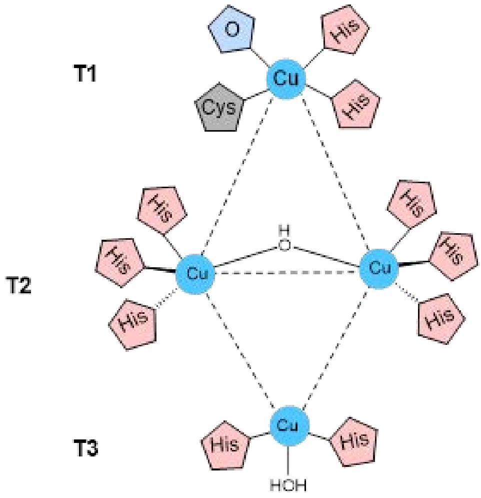

Figure 1.1. Schematic representation of the laccase catalytic site: His, histidine ligand; Cys, cysteine ligand; O, other ligand.

Substrates, such as phenols and aromatic/aliphatic amines, undergo oxidation by T1 copper(II), which is reduced to Cu(I), generating radicals that lead to the formation of dimers, oligomers, and polymers. The extracted electrons are transferred via a conserved His-Cys-His tripeptide motif, to the

---

[289] a) K. Piontek, M. Antorini, T. Choinowski, *J. Biol. Chem.* **2002**, *277*, 37663–37669; b) T. Bertrand, C. Jolivalt, P. Briozzo, E. Caminade, N. Joly, C. Madzak, C. Mougin, *Biochemistry* **2002**, *41*, 7325–7333.

[290] S. V. S. Kumar, P. S. Phale, S. Durani, P. P. Wangikar, *Biotechnol. Bioeng.* **2003**, *83*, 386–394.

T2/T3 site, where molecular oxygen undergoes reduction to form water, regenerating the initial oxidation state of the copper atoms (Figure 1.2).

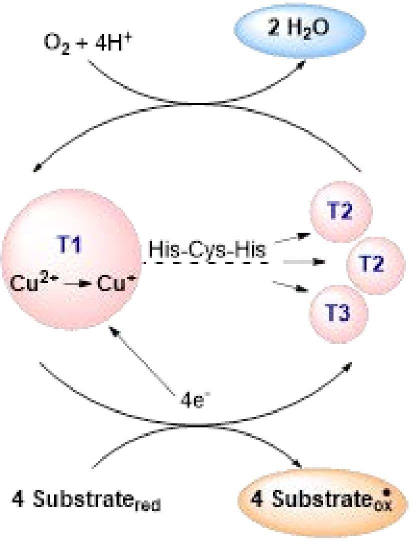

Figure 1.2. Schematic representation of the catalytic cycle of laccases: per each reduced oxygen molecule, two molecules of water are produced and four radicals of the oxidized substrate are generated.

T. versicolor is a fungus that exhibits a remarkable ability to degrade wood. The laccase isolated from this species (L*Tv*), is one of the most representative examples of the blue copper phenol oxidase family from fungi (Figure 1.3), also facilitated due to its commercial availability.

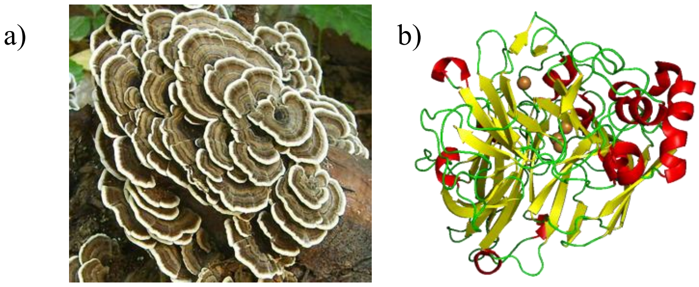

Figure 1.3. a) *T. versicolor* fungus, picture taken from reference 291; b) Crystalline structure of L*Tv* laccase, reported in the Protein Data Bank (PDB), structure 1GYC, https://www.rcsb.org/3d-view/jsmol/1GYC/1.

Its crystalline structure was described in 2002:[289a] it is a monomeric glycoprotein with a molecular mass of 70 kDa, and displays optimal activity within a pH range of 4.5 to 6.0 and a temperature of 25-35 °C, presenting a redox potential of 785 mV.[292]

1.1.1.4. Laccases from Pleurotus ostreatus

The white-rot fungus *Pleurotus ostreatus* (*P. ostreatus*) is a member of the basidiomycetes, and holds significance for both fundamental mycology studies and a range of biotechnological applications.[293] This fungus has been extensively utilized for its capabilities in bioremediation processes and is a valuable source of oxidases, like manganese and other versatile peroxidases, aryl-alcohol peroxidases, and laccases (Figure 1.4).[294]

---

[291] H. Dou, Y. Chang, L. Zhang, **2019**, pp. 361–381.

[292] a) S. Kurniawati, J. A. Nicell, *Bioresour. Technol.* **2008**, *99*, 7825–7834; b) G. Hong, D. M. Ivnitski, G. R. Johnson, P. Atanassov, R. Pachter, *J. Am. Chem. Soc.* **2011**, *133*, 4802–4809; c) J. Margot, C. Bennati-Granier, J. Maillard, P. Blánquez, D. A. Barry, C. Holliger, *AMB Express* **2013**, *3*, 63.

[293] a) A. S. Sekan, O. S. Myronycheva, O. Karlsson, A. P. Gryganskyi, Y. Blume, *PeerJ* **2019**, *7*, e6664; b) M. Kapahi, S. Sachdeva, *Bioresour. Bioprocess.* **2017**, *4*, 32.

[294] R. Cohen, L. Persky, Y. Hadar, *Appl. Microbiol. Biotechnol.* **2002**, *58*, 582–594.

Figure 1.4. The white rot *P. ostreatus* fungus. Picture taken from https://www.mykoweb.com/CAF/species/Pleurotus_ostreatus.html

Notably, different laccase isoenzymes from *P. ostreatus* have been identified, characterized and some of them recombinantly expressed. Their slightly different activities are probably associated with their physiological functions. These isoenzymes form a diverse group of laccases, each with unique properties. LACC10 (POXC) is a produced abundantly under various growth conditions.[295] LACC6 (POXA1b) is a neutral blue laccase with exceptional stability at alkaline pH and a high redox potential, expanding its potential for various biotechnological uses.[296] LACC2 (POXA3) stands out as an atypical heterodimeric laccase, comprising a large subunit similar to other fungal laccases and a small subunit, ssPOXA3, potentially involved in complex stabilization.[297]

1.1.1.5. Laccase-mediator systems (LMSs)

Laccases oxidize target phenols as natural substrates (Scheme 1.1a), with a specific redox potential ranging from 0.5 to 1.0 V *vs* NHE, that is low enough to allow electron abstraction by the T1-Cu atom. Substrates with higher redox potentials or those that struggle to diffuse effectively to the enzyme's active center remain untouched by the laccase. To overcome this limitation, a strategy has emerged using small molecules as intermediate compounds. These molecules are laccase substrates, so they can be oxidized by the enzyme and finally oxidize the desired substrate, being again reduced and able to start a new cycle. Thus, they really act as a bridge between the enzyme and the target substrate, expanding the synthetic capabilities of laccases, particularly those with higher redox potentials. These intermediary compounds are called *mediators*, and when combined with the enzyme, we refer to a laccase-mediator system (LMS, Scheme 1.1b).[277,298]

---

[295] G. Palmeiri, P. Giardina, L. Marzullo, B. Desiderio, G. Nittii, R. Cannio, G. Sannia, *Appl. Microbiol. Biotechnol.* **1993**, *39*, 632–636.

[296] G. Macellaro, M. C. Baratto, A. Piscitelli, C. Pezzella, F. F. de Biani, A. Palmese, F. Piumi, E. Record, R. Basosi, G. Sannia, *Appl. Microbiol. Biotechnol.* **2014**, *98*, 4949–4961.

[297] V. Faraco, C. Ercole, G. Festa, P. Giardina, A. Piscitelli, G. Sannia, *Appl. Microbiol. Biotechnol.* **2008**, *77*, 1329–1335.

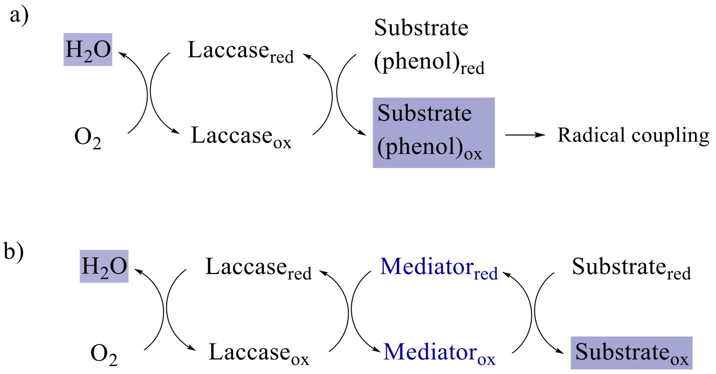

Scheme 1.1. a) Direct oxidation of a substrate using a laccase. b) Laccase-mediated oxidation of a substrate.

A successful redox mediator should be a good substrate for the laccase, and its oxidized form should be stable for a sufficiently prolonged half-life to allow it to oxidize the target compound. Moreover, it should have a high oxidation potential to effectively carry out the oxidation process.[287] The initial

---

[298] a) M. Mogharabi, M. A. Faramarzi, *Adv. Synth. Catal.* **2014**, *356*, 897–927; b) H. Patel, A. Gupte, in *Research Advancements in Pharmaceutical, Nutritional, and Industrial Enzymology*, (Eds.: S. L. Bharati, P. K. Chaurasia), IGI Global, Pensilvania (USA), **2018**, pp. 178–212.

mediator introduced in LMS for delignification of pulp was 2,2’-azino-bis(3-ethylbenzothiazoline-6-sulfonic acid), ABTS.[299] Since then, approximately 100 compounds have been examined to assess their potential in oxidizing lignin or lignin-like structures, both natural or synthetic.[300] Utilizing synthetic mediators in industry faces challenges due to high costs and potential toxicity. Specific lignin-derived phenols have been tested as affordable and eco-friendly “natural” alternatives, showing efficacy in mediating laccase actions, such as dye decolorization,[301] lignin removal from paper pulps,[302] and polycyclic aromatic hydrocarbon oxidation.[303] Representative molecules used as mediators are reported in Figure 1.5.

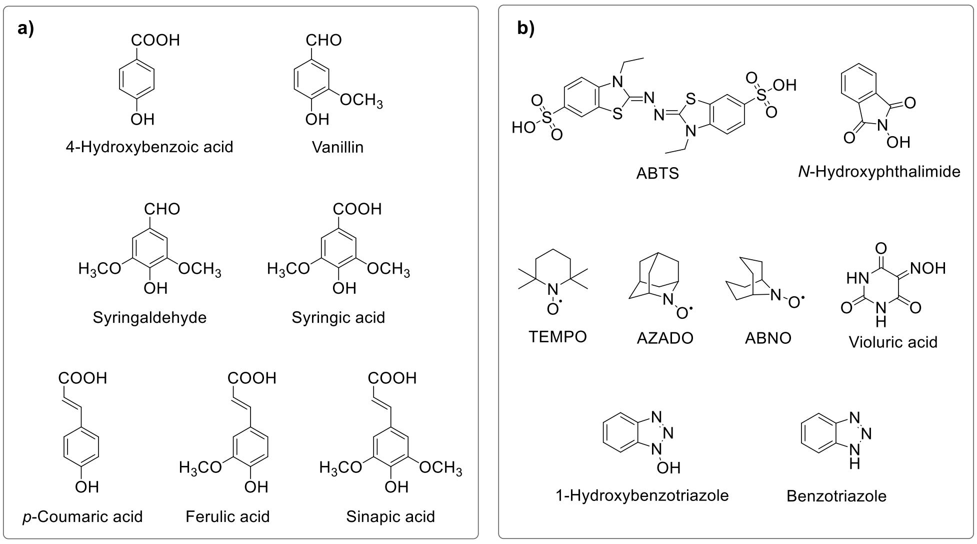
a)
4-Hydroxybenzoic acid
Vanillin
Syringaldehyde
Syringic acid
p-Coumaric acid
Ferulic acid
Sinapic acid
b)
ABTS
N-Hydroxyphthalimide
TEMPO
AZADO
ABNO
Violuric acid
1-Hydroxybenzotriazole
Benzotriazole

Figure 1.5. Natural (**a**) and synthetic (**b**) mediators employed in LMS.

---

[299] R. Bourbonnais, M. G. Paice, *FEBS Lett.* **1990**, *267*, 99–102.

[300] L. P. Christopher, B. Yao, Y. Ji, *Front. Energy Res.* **2014**, *2*, 12.

[301] S. Camarero, A. I. Cañas, P. Nousiainen, E. Record, A. Lomascolo, M. J. Martínez, Á. T. Martínez, *Environ. Sci. Technol.* **2008**, *42*, 6703–6709.

[302] S. Camarero, D. Ibarra, Á. T. Martínez, J. Romero, A. Gutiérrez, J. C. del Río, *Enzyme Microb. Technol.* **2007**, *40*, 1264–1271.

[303] A. I. Cañas, M. Alcalde, F. Plou, M. J. Martínez, Á. T. Martínez, S. Camarero, *Environ. Sci. Technol.* **2007**, *41*, 2964–2971.

Using a mediator offers the possibility to easily convert high-redox potential primary and secondary alcohols (i.e., allylic and benzylic) into the corresponding aldehydes, acids or ketones. The oxidized species produced from the laccase single-electron oxidation play a role in providing hydrogen atoms or electrons in the target organic substances, according to their mechanisms of action. Thus, a mediator usually catalyzes the oxidation of the final compound following two main different routes: (1) Electron Transfer (ET); or (2) radical hydrogen atom transfer (HAT).[304] For instance, ABTS achieves its mediation capacity through ET route, whereas nitroxyl compounds like 1-hydroxybenzotriazole (HBT) follow HAT pathway. The latter is initiated via the oxidation with the laccase-mediated removal of an electron, leading to the automatic release of a proton from the N–OH bond, forming the N–O• radical.[305] A distinct and atypical non-radical ionic mechanism (3) is followed by the nitroxyl radical, 2,2,6,6-tetramethylpiperidine 1-oxyl (TEMPO). When subjected to a laccase-catalyzed oxidation, TEMPO is transformed into the corresponding oxoammonium ion, which subsequently participates in the oxidation of the target molecule.[306] When oxidizing an alcohol, the action of TEMPO is reported to follow different paths at acidic or basic pHs: an alkoxide adduct is produced under basic conditions, while a bimolecular hydride transfer is reported under acidic conditions. At acidic pHs, the reactions are considerably slower than under basic conditions. The mechanisms are not fully elucidated, but higher pH values have demonstrated both thermodynamic and kinetic benefits. In both mechanisms, the stability of the oxoammonium ion emerges as a pivotal factor expediting the reaction, influenced by its interaction with the laccase (Scheme 1.2).[307]

---

[304] J.-R. Jeon, Y.-S. Chang, *Trends Biotechnol.* **2013**, *31*, 335–341.

[305] A. I. Cañas, S. Camarero, *Biotechnol. Adv.* **2010**, *28*, 694–705.

[306] S. A. Tromp, I. Matijošytė, R. A. Sheldon, I. W. C. E. Arends, G. Mul, M. T. Kreutzer, J. A. Moulijn, S. de Vries, *ChemCatChem* **2010**, *2*, 827–833.

[307] J. E. Nutting, M. Rafiee, S. S. Stahl, *Chem. Rev.* **2018**, *118*, 4834–4885.

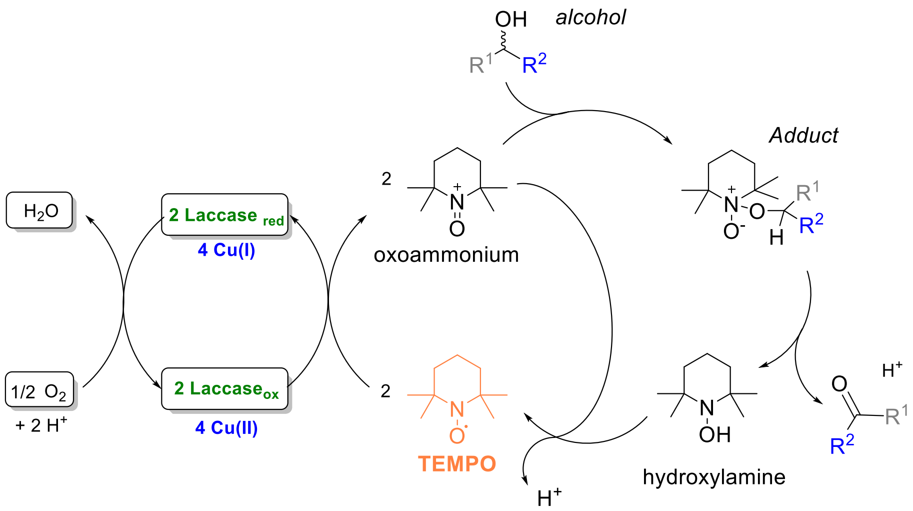

Scheme 1.2. Proposed reaction mechanism of aerobic oxidation of primary alcohols catalyzed by laccase and TEMPO. Adapted from reference 306.

1.1.1.6. Industrial application of laccases

Due to their elevated capacity for nonspecific oxidations and the utilization of readily accessible molecular oxygen as electron acceptor, laccases prove to be valuable biocatalysts for a diverse array of biotechnological uses. The utilization of laccases in industry dates back to 1990s, aiming to replace conventional chemical methods. Given the variability in their properties, numerous laccases have been evaluated across various biotechnological applications in industry.[308]

- Lignocellulosic biorefineries: Laccases are applied in delignification, detoxification, and modification of lignocellulosic materials, improving the following saccharification and fermentation. Laccases combination with pre-treatment methods shows promise in improving sugar yields and bioethanol production.[309]

---

[308] D. Singh, N. Gupta, *Biologia* **2020**, *75*, 1183–1193.

[309] G. Singh, S. Kumar, S. Afreen, A. Bhalla, J. Khurana, S. Chandel, A. Aggarwal, S. K. Arya, *Int. J. Biol. Macromol.* **2023**, *235*, 123840.

- Bio-pulping: Laccases have shown significant promise in the pulp and paper industry, enhancing processes such as pulping, bleaching, deinking, and waste water treatment. These enzymes are applied for delignification, reducing the need for harsh chemicals, and improving paper properties like strength and brightness.[310]

- Medium density fibreboard (MDF): Laccases show promise in catalyzing lignin-based adhesives for MDF production, enhancing their properties through lignin activation. This product, widely used in furniture and other applications, can be modify by covalent cross-linking agents achieved by laccase-mediated modification of lignin.[311]

- Organic synthesis: Laccases are considered excellent green catalysts in chemistry due to their ability to catalyze oxidative transformations using oxygen, and producing water as the sole by-product. They show potential in producing antibiotic precursors and key intermediates for complex synthesis, but their selectivity and stability remain as challenges. They can mediate reactions like dimerization and polymerization, aiding in the synthesis of various compounds, including biaryl derivatives, heterocyclic structures, and conductive polymers.[312]

- Biosensors: Laccases have gained attention in this field for rapid, cost-effective monitoring of phenolic compounds in food, environmental, and medicinal industries. These biosensors utilize laccase enzymes to detect target molecules, producing measurable signals for analysis. They offer advantages in selectivity, sensitivity, and speed, with potential applications ranging from pollutant detection to clinical diagnosis.[313]

- Medical applications, healthcare and cosmetics: Laccases are used in medicinal chemistry for the development of antibiotics, anticancer drugs, and synthesis of cosmetic dyes. Laccases have also shown potential as anti-cancer agents, antioxidants, and agents against pathogens. Laccases also find use in the synthesis of cosmetic products, offering alternatives for hair dyeing and skin lightening, with increasing interest in environmentally-friendly and economically feasible processes.[314]

---

[310] G. Singh, S. K. Arya, *Int. J. Biol. Macromol.* **2019**, *134*, 1070–1084.

[311] W. Sun, M. Tajvidi, C. G. Hunt, B. J. W. Cole, C. Howell, D. J. Gardner, J. Wang, *J. Clean. Prod.* **2022**, *353*, 131659.

[312] I. Bassanini, E. E. Ferrandi, S. Riva, D. Monti, *Catalysts* **2021**, *11*, 26.

[313] M. C. Castrovilli, P. Bolognesi, J. Chiarinelli, L. Avaldi, P. Calandra, A. Antonacci, V. Scognamiglio, *TrAC-Trends Anal. Chem.* **2019**, *119*, 115615.

- Textiles and leather: Laccases aid in traditional bleaching of cotton for improved whiteness, denim finishing, and indigo removal. They offer environmentally friendly alternatives to chemical processes, such as dyeing and bleaching of textiles and leather, resulting in unique colors and improved material properties. Laccases are also used for antimicrobial treatments and fabric modifications, contributing to the development of smart textiles and sustainable dyeing methods.[315]

- Beverages and food: Laccases play a significant role in the beverage and food industries by modifying substrates like phenols, carbohydrates, unsaturated fatty acids, and thiol-containing proteins. In beverages, laccases stabilize wine by removing phenolic compounds, prevent cork taint in wine through enzymatic treatment, and enhance beer shelf-life by reducing haze-forming proteins. In the food sector, laccases improve dough consistency and gluten structures in bakery products, contribute to pectin gelation, and even offer potential in reducing allergenic responses in peanut proteins.[316]

This thriving research field has yielded a range of registered patents and publications.[317] Nonetheless, practical industrial applications demand laccases that remain stable under diverse pH, temperature, and environmental conditions. Although there is high research about the development of laccases working at elevated pH and temperature, as well as for more selective biotransformations, commercial-scale implementation is still hindered by limited knowledge about exact details of enzyme features and mechanisms.

---

[314] S. K. Shin, J. E. Hyeon, Y.-C. Joo, D. W. Jeong, S. K. You, S. O. Han, *Int. J. Biol. Macromol.* **2019**, *129*, 181–186.

[315] A. Zerva, S. Simić, E. Topakas, J. Nikodinovic-Runic, *Catalysts* **2019**, *9*, 1023.

[316] E. Backes, C. G. Kato, R. C. G. Corrêa, R. F. P. Muniz Moreira, R. A. Peralta, L. Barros, I. C. F. R. Ferreira, G. M. Zanin, A. Bracht, R. M. Peralta, *Trends Food Sci. Technol.* **2021**, *115*, 445–460.

[317] V. Lettera, N. Cascelli, A. De Chiaro, G. Sannia, in *Bacterial Laccases: Engineering, Immobilization, Heterologous Production, and Industrial Applications*, (Eds.: M. Yadav, T. Kudanga), Elsevier, Amsterdam (The Netherlands), **2023**, in press.

1.1.2. Laccase mutagenesis

Laccase applications in industrial processes face significant challenges concerning stability, activity, and substrate specificity tailored for relevant purposes. Consequently, researchers have dedicated their efforts to enhance laccase efficiency through the application of molecular engineering techniques, encompassing both directed and random modifications, targeting different regions of the enzyme's active site (Figure 1.6).[318]

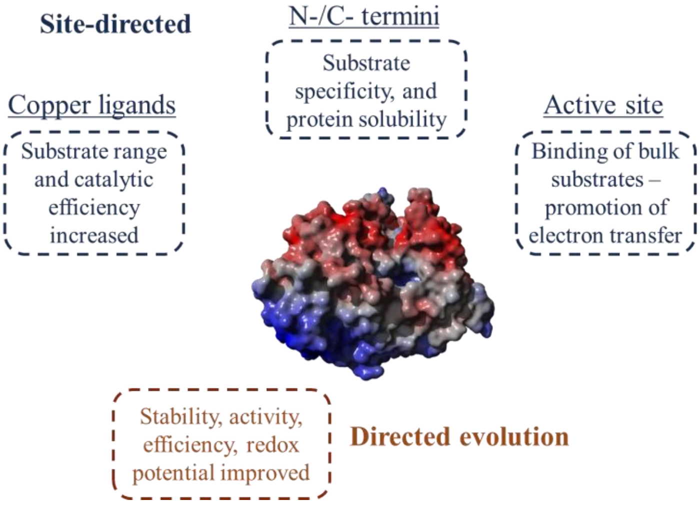
Site-directed
N-/C- termini
Substrate specificity, and protein solubility
Copper ligands
Substrate range and catalytic efficiency increased
Active site
Binding of bulk substrates – promotion of electron transfer
Stability, activity, efficiency, redox potential improved
Directed evolution

Figure 1.6. Properties improved after laccase mutation depending on the target enzyme region investigated.

As disclosed in the Introduction, computational analyses have already demonstrated their robustness in identifying enzyme regions suitable for targeted mutations, thus minimizing the need for extensive screening efforts.

---

[318] I. Stanzione, C. Pezzella, P. Giardina, G. Sannia, A. Piscitelli, *Appl. Microbiol. Biotechnol.* **2020**, *104*, 915–924.

A representative example is the recent achievement of Guallar and Alcalde's research groups: by combining directed evolution with computational design, they produced a tailored variant of a laccase, which exhibited increased activity towards high-redox-potential mediators, enhancing the potential of Cu-T1 from 740 to 790 mV, along with its thermal and acidic stability. The effects were attributed to the substitution of several hydrophobic residues around the Cu-T1 site.[319]

Moreover, Guan and co-workers used rational mutagenesis, guided by a computer-aided design program, to enhance *Bacillus pumilus* CotA laccase's specificity for ABTS and also its thermostability. Surprisingly, the introduced mutations also boosted pH stability through reinforced hydrogen bonding and electrostatic interactions. This modified laccase effectively decolorized industrial dyes under alkaline conditions.[320] Additionally, the variant was optimized for expression in *Pichia pastoris* and successfully applied for detoxifying the carcinogenic dye Evans blue, preventing toxic aniline compounds formation.[321]

POXA1b laccase from *P. ostreatus* underwent multiple rounds of both random and semi-rational mutagenesis.[322] Two improved variants selected for enhanced catalytic activity toward the substrate 2,6-dimethoxyphenol (2,6-DMP), were assessed for their capability to remove complex industrial dyes. These mutants exhibited broader dye degradation specificity compared to the original enzyme, enabling effective decolorization of even stubborn stilbene-type dyes. Interestingly, like in CotA mutagenesis, one of the mutants demonstrated increased stability under both acidic and alkaline pH conditions, and analysis of protein models revealed mutations at the loops adjacent to the substrate-binding pocket, potentially influencing enzyme-substrate interactions.[322a] Several improved variants of the POXA1b laccase were generated through multiple rounds of random mutagenesis, considering various factors like substrate activity and pH stability. These mutants were suitable for wastewater treatment, and seven of them showed better performance in wastewater decolorization under acidic conditions.[322b] Notably, one variant with a higher redox potential than the wild type, displayed improved behaviors in degrading endocrine-disrupting compounds, and in the oxidation of ABTS as mediator.[323]

---

[319] I. Mateljak, E. Monza, M. F. Lucas, V. Guallar, O. Aleksejeva, R. Ludwig, D. Leech, S. Shleev, M. Alcalde, *ACS Catal.* **2019**, *9*, 4561–4572.

[320] Y. Chen, Q. Luo, W. Zhou, Z. Xie, Y.-J. Cai, X.-R. Liao, Z.-B. Guan, *Appl. Microbiol. Biotechnol.* **2017**, *101*, 1935–1944.

[321] J. Xia, Q. Wang, Q. Luo, Y. Chen, X.-R. Liao, Z.-B. Guan, *Process Biochem.* **2019**, *78*, 33–41.

[322] a) A. Miele, P. Giardina, G. Sannia, V. Faraco, *J. Appl. Microbiol.* **2010**, *108*, 998–1006; b) A. Piscitelli, C. Del Vecchio, V. Faraco, P. Giardina, G. Macellaro, A. Miele, C. Pezzella, G. Sannia, *C. R. Biol.* **2011**, *334*, 789–794.

Gupta *et al.* recently highlighted a significant example of a mutated laccase application, emphasizing copper sites T2 and T3 importance. Using directed evolution, they found a truncated *Rheinheimera* sp. laccase variant without a domain containing the T1 copper center that matched wild type's abilities in deinking and degrading indigo dye with external copper. Notably, this variant showed better pH and temperature resistance than the wild type. *In silico* analysis revealed structural differences, including absent beta turns, boosting the variant's stability.[324]

The improvements in laccase variants may not always directly match the enzyme's original desired function. Laccase reactivity is intricate and multifaceted, influenced not only by substrate positioning and active site interactions but also by the potential of the Cu-T1 site to facilitate electron transfer.[325] In conclusion, while engineering laccases offer great potential, a comprehensive understanding of the enzyme's underlying mechanisms is essential for achieving targeted enhancements of their capabilities.

---

[323] G. Macellaro, C. Pezzella, P. Cicatiello, G. Sannia, A. Piscitelli, *Biomed Res. Int.* **2014**, *2014*, 614038.

[324] V. Gupta, S. Balda, N. Gupta, N. Capalash, P. Sharma, *Int. J. Biol. Macromol.* **2019**, *123*, 1052–1061.

[325] V. G. Giacobelli, E. Monza, M. F. Lucas, C. Pezzella, A. Piscitelli, V. Guallar, G. Sannia, *Catal. Sci. Technol.* **2017**, *7*, 515–523.

Results and Discussion

1.2.1. Rational mutagenesis of POXA1b laccase: Docking studies

Although *P. ostreatus* laccases exhibit intriguing characteristics, they do not directly oxidize furan molecules, which are the compounds of interest in this doctoral thesis. POXA1b was selected for evolution experiments, in order to point out an improved variant able to oxidize furan molecules such as HMF, owing to its remarkable activity and stability. A bioinformatics study was performed using the YASARA program and molecular docking to assess potential obstacles at the enzyme's active site that could affect the binding of primary alcohol molecules. This analysis helped to identify interactions and possible substrate placement errors in the active site.[326] This approach holds promise for conducting a targeted mutagenesis experiment at specific sites.

The initial investigation focused on understanding the oxidation pathway of HMF to DFF, as illustrated in Scheme 1.3.[327] Notably, the CH_2OH group, from which the initial electron transfer occurs, needs to be strategically positioned in close proximity to the Cu-T1 site.

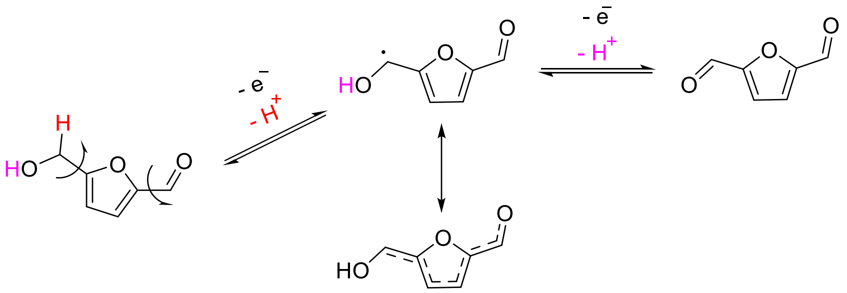

Scheme 1.3. Possible oxidation pathway from HMF to DFF.

This arrangement is crucial and must be further reinforced by essential interactions between the molecule and specific side chain residues within the active site. These interactions were previously outlined by Bertrand *et al.*[289b] The enzymatic active site was defined and used as a reference for conducting docking simulations with various substrates:

---

[326] a) E. Krieger, G. Vriend, *Bioinform.* **2014**, *30*, 2981–2982 (License version 20.10.4); b) E. Krieger, G. Vriend, *J. Comput. Chem.* **2015**, *36*, 996–1007.

[327] R. Trammell, K. Rajabimoghadam, I. Garcia-Bosch, *Chem. Rev.* **2019**, *119*, 2954−3031.

- ABTS: non-phenolic highly studied substrate, for validating the models and the cell manually built around the active site;
- Resorcinol: phenolic substrate, as a reference for bonds, interactions, positions, and energy values;
- TEMPO: non-phenolic substrate, applied as mediator in this project;
- HMF and furfuryl alcohol, as target compounds.

The two catalytic residues surrounding Cu1 His456 and Asp205 (referenced by POXA1b numbering), have consistently been demonstrated and employed as benchmarks to validate the accurate positioning of molecules. This validation is achieved by calculating relative distances between these residues and the substrate under study. Notably, these amino acids are highly conserved within laccase active sites and play distinct roles: His456 facilitates an efficient electron transfer, while Asp205 stabilizes radical substrate intermediates.[328]

Due to its large size and pronounced hydrophobic nature, ABTS fitted perfectly within the enzymatic active site, resulting in a robust binding energy. Additionally, essential stabilizing interactions within the active site, such as π-π stacking and hydrophobic interactions, contributed to minimal dissociation values. The affinity, expressed as binding energy, was comparable to values reported in existing literature,[329] as determined with AutoDock software (Figure 1.7). Thus, the constructed model was deemed reliable for subsequent analyses.

---

[328] P. M. H. Kroneck, in *Multi-Copper Oxidases*, (Ed.: A. Messerschmidt), World Scientific, London (UK), **1997**, pp. 391−407.

[329] Y. Cárdenas-Moreno, L. A. Espinosa, J. C. Vieyto, M. González-Durruthy, A. del Monte-Martinez, G. Guerra-Rivera, M. I. Sánchez López, *Ann. Proteom. Bioinform.* **2019**, *3*, 1–9.

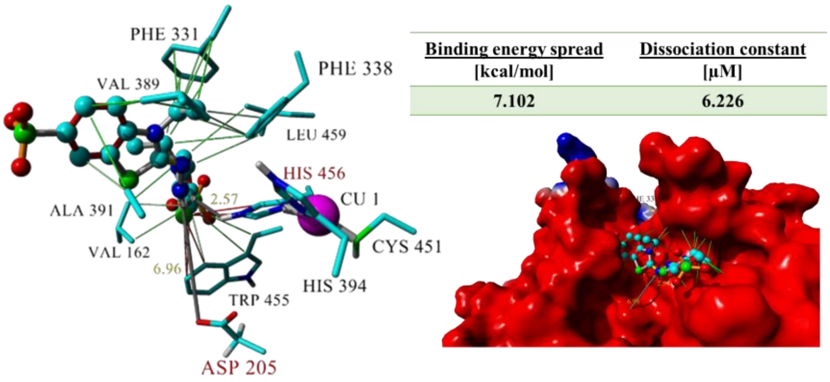

Binding energy spread [kcal/mol]	Dissociation constant [μM]
7.102	6.226

Figure 1.7. YASARA representation of the best conformation of POXA1b and ABTS from the docking studies based on the binding energy (Kcal/mol) and dissociation constant (μM). Hydrophobic interactions between the amino acids and ABTS are shown in green, π-π interactions in red, H-bonds as yellow dot lines, and distances from catalytic residues (in red) appear in yellow.

The affinity of resorcinol for the active site was lower compared to that of ABTS. Nevertheless, the energy binding value remained high, indicating its classification as a good laccase substrate. Conversely, the dissociation constant for resorcinol was notably higher than that of ABTS. This discrepancy arises from the presence of fewer stabilizing interactions between the molecule and the side chain residues within the active site. This reduced number of interactions allowed a greater freedom of movements to resorcinol within the active site, while still maintaining a strong binding interaction in its potentially active conformation. This arrangement enabled an efficient electron transfer (as illustrated in Figure 1.8).

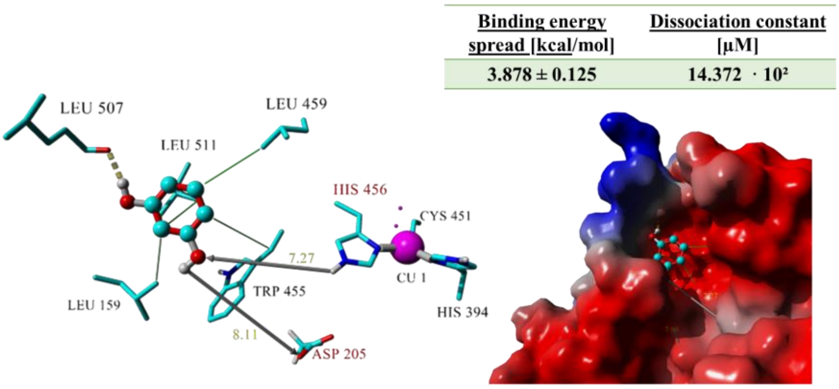
LEU 507
LEU 459
LEU 511
HIS 456
CYS 451
7.27
CU 1
LEU 159
TRP 455
HIS 394
8.11
ASP 205

Binding energy spread [kcal/mol]	Dissociation constant [µM]
3.878 ± 0.125	14.372 · 10²

Figure 1.8. YASARA representation of the best conformation of POXA1b and resorcinol from the docking studies based on the binding energy (Kcal/mol) and dissociation constant (µM). Color codes for interactions, amino acid residues, and distances are described in Figure 1.7.

Interestingly, a similar pattern emerged when the docking for TEMPO as substrate was analyzed (as illustrated in Figure 1.9). This indicated a favorable binding in the correct orientation and an acceptable dissociation constant, both contributing to stabilize the molecule in an active conformation for the enzymatic oxidation.

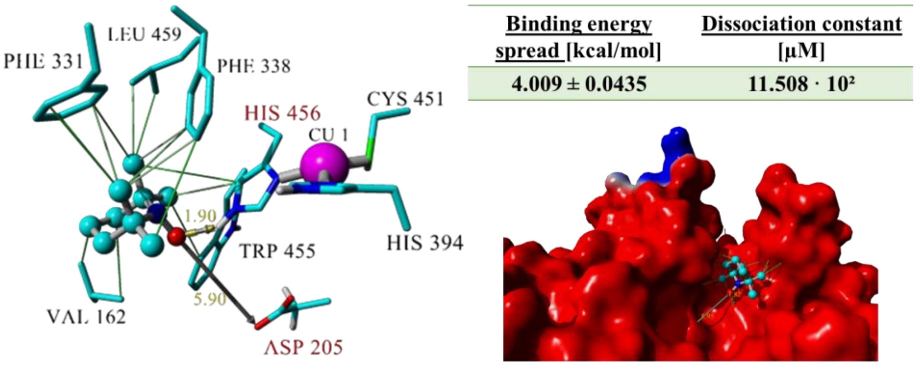
PHE 331
LEU 459
PHE 338
HIS 456
CYS 451
CU 1
1.90
TRP 455
HIS 394
5.90
VAL 162
ASP 205

Binding energy spread [kcal/mol]	Dissociation constant [µM]
4.009 ± 0.0435	11.508 · 10²

Figure 1.9. YASARA representation of the best conformation of POXA1b and TEMPO from docking studies based on the binding energy (Kcal/mol) and dissociation constant (µM). Color codes for interactions, amino acid residues, and distances are described in Figure 1.7.

Upon conducting docking studies with HMF, two interesting conformations were attained. Both predictions exhibited similar favourable binding energies, indicating a suitable substrate conformation and orientation (as shown in Figure 1.10). However, they revealed a higher dissociation constant compared to the previously values. This result suggested that while HMF can enter and interact with the Cu-T1 centre of the POXA1b active site, it struggled to maintain an active conformation for an adequate duration.

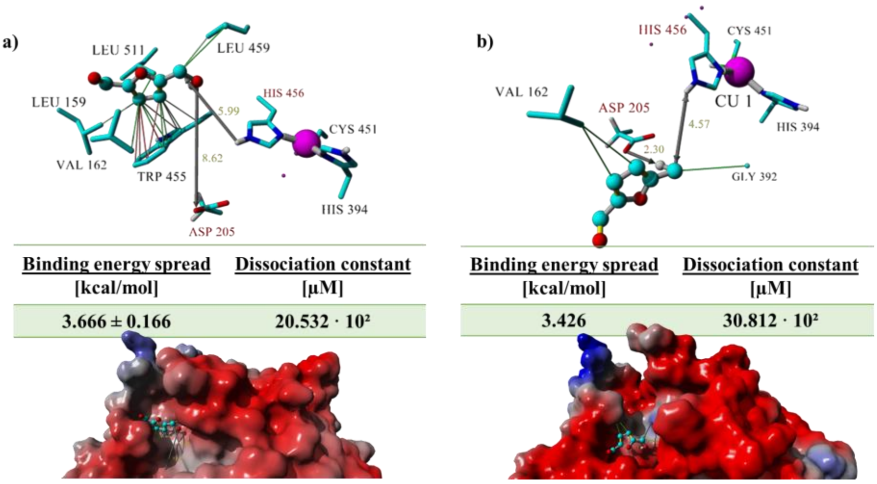

Binding energy spread [kcal/mol]	Dissociation constant [μM]
3.666 ± 0.166	$20.532 \cdot 10^2$

Binding energy spread [kcal/mol]	Dissociation constant [μM]
3.426	$30.812 \cdot 10^2$

Figure 1.10. YASARA representations of the best conformations of POXA1b and HMF from docking studies based on the binding energy (Kcal/mol) and dissociation constant (μM). Color codes for interactions, amino acid residues, and distances are described in Figure 1.7.

Of particular interest is the prediction shown in Figure 1.10b, which shows a closer interaction with the enzyme. However, it lacked stabilization due to the limited engagement of side chain residues within the substrate. This limitation led to a higher dissociation constant for the complex.

A noteworthy observation across all these intermediates was the involvement of the tryptophan residue at position 455. Its interaction with the substrates suggested a possible role in stabilizing their conformations and consequently in reducing the dissociation constants. Intriguingly, HMF encountered hindrance due to this bulky residue when shifting into the position illustrated in Figure 1.10b. While this intermediate might facilitate a stronger interaction with Cu-T1, it was likely a less stable system.

Applying the same analysis to furfuryl alcohol, yielded even less favorable binding energies when considering the substrate orientation. Furthermore, the resulting huge dissociation constant value strongly suggested an unfavorable interaction within the active site, indicating a poor binding (Figure 1.11).

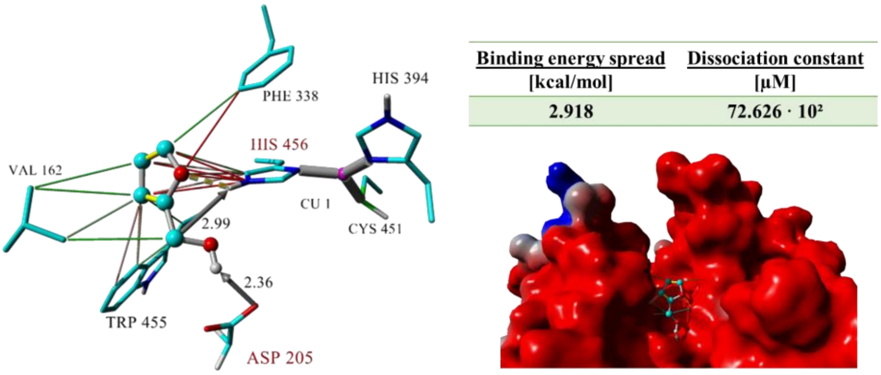

Binding energy spread [kcal/mol]	Dissociation constant [μM]
2.918	$72.626 \cdot 10^2$

Figure 1.11. YASARA representation of the best conformation of POXA1b and furfuryl alcohol from docking studies based on the binding energy (Kcal/mol) and dissociation constant (μM). Color codes for interactions, amino acid residues, and distances are described in Figure 1.7.

Summing up the key outcomes from the initial bioinformatics analysis for predicting furan-based substrate interactions:

- HMF's affinity for the active site was comparable to other recognized substrates, indicating its potential suitability for oxidation. However, less stable interactions might result from the molecule's lower hydrophobicity.

- The proximity of HMF to the Cu-T1 active centre was hindered by tryptophan at position 455, which played a role in stabilizing the active orientations of substrate molecules.
- Furfuryl alcohol's interactions were less favourable compared to the other substrates, suggesting limitations for its oxidation reaction.

Following the first evidences of the bioinformatics approach, the closest position of HMF to the Cu-T1 active center, while less stable, encountered obstruction from Trp455. This residue appeared pivotal in stabilizing the active orientation for other substrates. Consequently, a new enzymatic variant structure was generated using the YASARA tool to compare the binding energies. Hence, Trp455 was changed by an alanine in order to maintain the hydrophobic nature of the active site while reducing the steric hindrance posed by the side chain (Figure 1.12). The goal was to facilitate the entry for the substrate into the enzyme's active site, and enable it to remain there for a sufficient duration to undergo the desired oxidation process.

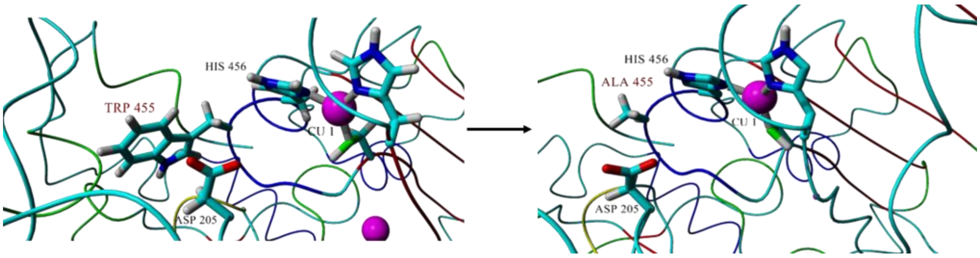

Figure 1.12. *In silico* change of Trp455 position by Ala using YASARA tool.

The analysis employed the AutoDock system within the YASARA software, assessing binding energies in Kcal/mol and dissociation constants in µM for selected substrates: ABTS, resorcinol, TEMPO, HMF, and furfuryl alcohol. Distances to His456 and Asp205 were also measured, as these catalytic residues are known for their key roles in the electron transfer and substrate stabilization (Table 1.1).

Table 1.1. Binding energy (Kcal/mol), dissociation constant (µM), and distances (Å) from the catalytic residues of POXA1b (His 456 and Asp 205). Values were compared when applying both Trp455 and Ala455 enzyme models.

Substrate	AA_455	Binding energy spread (kcal/mol)	Dissociation constant (µM)	His-456 distance (Å)	Asp-205 distance (Å)
ABTS	Trp	7.10	6.23	2.57	6.96
	Ala	6.85 ± 0.62	9.60	3.85	6.72
Resorcinol	Trp	3.88 ± 0.12	$14.37 \cdot 10^2$	7.27	8.11
	Ala	4.12 ± 0.32	$9.31 \cdot 10^2$	7.87	6.28
TEMPO	Trp	4.01 ± 0.043	$11.51 \cdot 10^2$	1.90	5.90
	Ala	3.84	$15.32 \cdot 10^2$	4.30	9.61
Furfuryl alcohol	Trp	2.92	$72.63 \cdot 10^2$	2.99	2.36
	Ala	3.41 ± 0.25	$31.56 \cdot 10^2$	6.74	4.91
HMF	Trp	3.67 ± 0.17	$20.53 \cdot 10^2$	5.99	8.62
	Ala	3.92 ± 0.36	$13.43 \cdot 10^2$	7.04	3.53

*For AutoDock a ligand efficiency ≥0.35 and a dissociation constant of 1200-270 µM indicate good bindings.

Reducing the side-chain residue size at position 455, negatively influenced the interaction with larger substrates like ABTS. This change increased the dissociation constants and slightly affected the binding energies, attributed to the role of tryptophan in constraining the substrate within the active conformation. The reduced hindrance in the entrance channel facilitated the entry of smaller substrates like resorcinol. This led to better interactions and closer positions to the catalytic residues.

Conversely, TEMPO binding was negatively affected as worse values were obtained for both parameters. Furfuryl alcohol maintained a relatively high dissociation constant but showed a reduced binding energy, indicating a more stable binding, though its position was still slightly distant from the catalytic center. The absence of Trp455 led to a substantial shift of HMF towards Asp205, possibly indicating a new open channel in the active site. This change in HMF's position led to a halved dissociation constant with comparable values to resorcinol.

In light of these inconclusive insights, solely pursuing direct site mutagenesis to enhance substrate stabilization within the active site might overlook other important aspects of the enzyme functionality, thus probably leading to unsuccessful variants. To face challenges in targeting correct mutations on POXA1b to recognize both HMF and furfuryl alcohol as substrates, a directed evolution strategy was therefore devised.

1.2.2. Development of a high-throughput screening procedure for DFF detection

The objective of the directed evolution on POXA1b laccase was to discover enzyme variants with higher redox potentials capable of specifically oxidizing HMF, the focal point of this PhD research. However, the absence of effective screening methods that could selectively identify the desired product formation posed a hurdle to establish the mutagenesis approach.

To overcome this obstacle, the initial step in our mutagenesis process was to “begin with the end”. This involved identifying a rapid, simple, and feasible technique for selectively detecting the formation of the desired reaction product, 2,5-diformylfuran (DFF), following the catalytic oxidation *in vitro*. The initial concept was to choose a compound capable of reacting with a dialdehyde like DFF, resulting in the formation of a detectable product (observable through UV-Vis spectra or as a precipitate).

This method was designed to yield a precise and sensitive outcome in relation to the substance being analyzed, while effectively avoiding potential interferences from the substrate (HMF) and any other potential by-products derived from the oxidation of HMF (FFCA, FDCA, or HFCA). The suggested approach for quickly detecting DFF involved the creation of a test based on the polymerization of the dialdehyde with an aromatic diamine, specifically 1,4-phenylenediamine (referred to as *para*-phenylenediamine or PPD). In fact, previously, the formation of polymeric Schiff bases through the reaction of diamines with dialdehydes, including DFF, has been reported.[330] These demonstrations served as proof-of-concept for the development of novel bio-derived polymeric substances.[331] Nevertheless, their potential as colorimetric agents for creating a selective DFF detection assay has never been reported.

The aldehyde moiety of HMF can also react with PPD, yielding the corresponding imine. Although this imine could dimerize, it cannot fully polymerize due to the terminal hydroxyl group, although these species might still impact the color generation. For a selective color-driven DFF screening, the formed conjugated structures from PPD and HMF had not to interfere at the UV/Vis absorption profile (Scheme 1.4).

---

[330] a) C. Méalares, A. Gandini, *Polym. Int.* **1996**, *40*, 33–39; b) T. Xiang, X. Liu, P. Yi, M. Guo, Y. Chen, C. Wesdemiotis, J. Xu, Y. Pang, *Polym. Int.* **2013**, *62*, 1517–1523; c) G. Li, K. Yu, J. Noordijk, M. H. M. Meeusen-Wierts, B. Gebben, P. A. M. oude Lohuis, A. H. M. Schotman, K. V. Bernaerts, *Chem. Commun.* **2020**, *56*, 9194–9197.

[331] a) Z. Hui, A. Gandini, *Eur. Polym. J.* **1992**, *28*, 1461–1469; b) J. Ma, M. Wang, Z. Du, C. Chen, J. Gao, J. Xu, *Polym. Chem.* **2012**, *3*, 2346–2349.

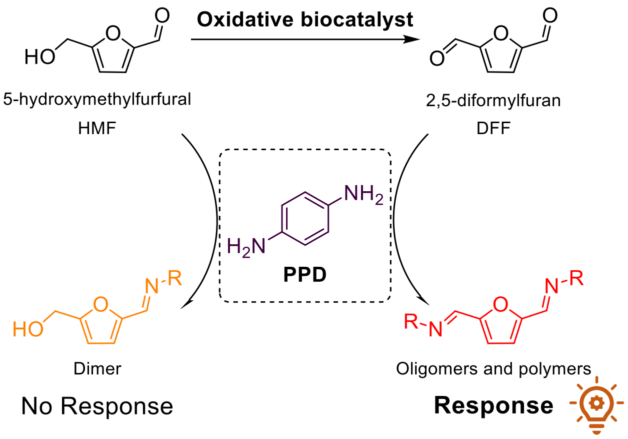
Oxidative biocatalyst
HO
O
5-hydroxymethylfurfural
HMF
2,5-diformylfuran
DFF
NH2
H2N
PPD
N-R
R-N
Dimer
Oligomers and polymers
No Response
Response

Scheme 1.4. Illustration of the devised high-throughput screening technique outlined in this study. The oxidation of HMF results in the accumulation of DFF. Subsequently, the introduction of PPD facilitates the targeted identification of DFF.

The incubation took place in an aqueous environment at a mildly basic pH (100 mM KPi buffer, pH 7.5), facilitating Schiff base formation. In the initial phase, individual spectrophotometric UV/Vis analyses of HMF, DFF, and PPD at a concentration of 20 µM validated that each compound exhibited minimal absorption in the visible spectrum (beyond 380 nm, Figure 1.13a). HMF and DFF were separately incubated with PPD, using concentrations up to 100 µM for each. A distinct response was seen exclusively for DFF in the 350–500 nm wavelength range (Figure 1.13b).

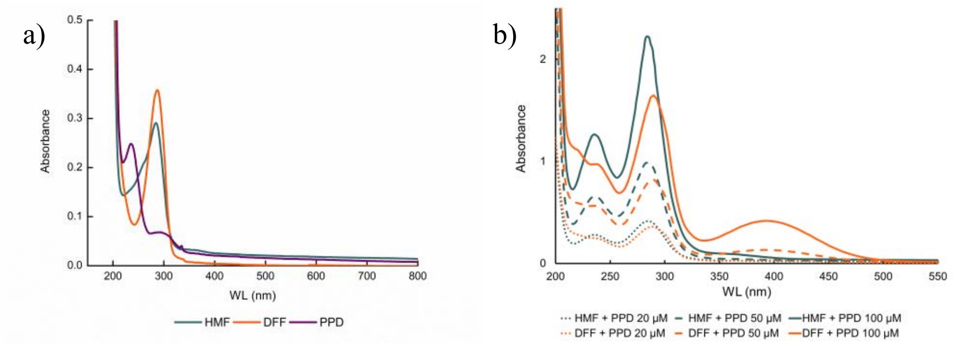

Figure 1.13. UV/Vis spectra of: a) HMF, DFF and PPD (20 µM each); b) HMF (substrate) or DFF (product) at 20, 50 and 100 µM incubated with PPD (same concentration) in KPi buffer 100 mM, pH 7.5.

To simulate the reaction progress, a mixture of HMF (4.9 mM) and DFF (100 µM) was created, mimicking 2% HMF conversion into DFF. Comparative incubations were conducted for individual compounds with PPD. The distinctive peak profile arising from DFF and PPD interaction (red line, Figure 1.14) confirmed earlier observations of an absorbance shift towards 450–500 nm. In contrast, the reaction between HMF and PPD yielded lower absorbance values (green line, Figure 1.14), representing the assay background noise under specific conditions. Interestingly, a similar trend emerged at the 500–600 nm range when HMF reacted with PPD in the presence of small DFF amounts (purple line, Figure 1.14), leading to a higher overall absorbance due to the polymer contribution from DFF.

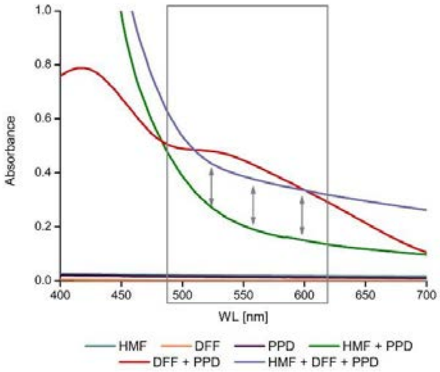

Figure 1.14. UV-Vis spectra of HMF, DFF, PPD, and their mixtures.

The formation of Schiff polymers resulting from the interaction between DFF and PPD, even at small quantities, played a pivotal role in the prominent color development observed (Figure 1.15). While the presence of HMF alone led to an orange precipitate (panel a), a distinct red precipitate was formed when PPD was introduced during DFF incubation (panel b), and similarly in the case of a mixed HMF and DFF solution (panel c). Furthermore, the intensity of color in the assay exhibited a clear correlation with the amount of DFF, with higher concentrations yielding more intense red solutions (panel d). Given that the main shifts in the colorimetric response with respect to HMF were within the 500–600 nm range of the visible spectrum, the wavelength of 500 nm was selected for method validation and assay sensitivity evaluation.

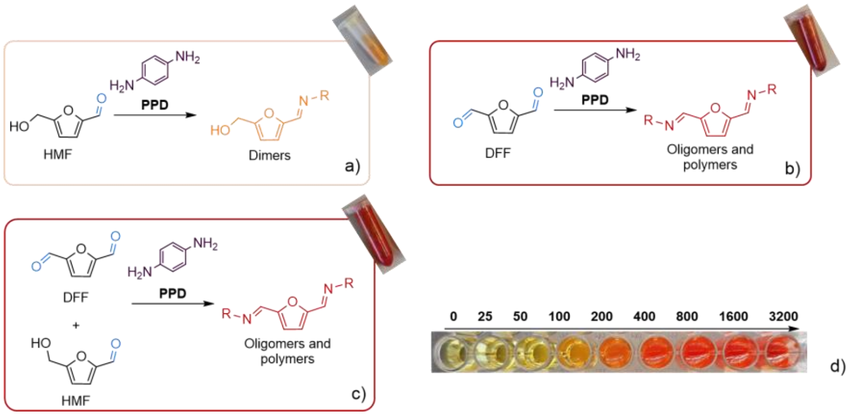
HO
HMF
H$_2$N
NH$_2$
PPD
HO
N-R
Dimers
a)
DFF
PPD
R-N
N-R
Oligomers and polymers
b)
DFF
+
HO
HMF
PPD
R-N
N-R
Oligomers and polymers
c)
0
25
50
100
200
400
800
1600
3200
d)

Figure 1.15. Different colors of the precipitates formed when PPD (1 equivalent) was incubated with HMF (panel a), DFF (panel b), or in an equimolar HMF:DFF mixture (panel c). Shift in color observed at increasing DFF concentrations (units in µM in the *in vitro* system, panel d).

The assay's linearity was determined by measuring absorbance changes with increasing analyte concentrations in a multiwell scale. Dimethylsulfoxide (DMSO) was used as cosolvent for enhancing HMF and DFF solubilities at higher concentrations.[332] However, DMSO's interference with DFF detection resulted in delayed response times, necessitating a fixed 15% v/v DMSO concentration. Then, the assay's linearity was established in both plain buffer (100 mM KPi, pH 7.5) and DMSO-buffer systems, up to 200 µM of DFF (Figure 1.16). In DMSO-buffer conditions, regression analysis indicated a slightly improved slope, hinting at a DFF solubility threshold in plain buffer and a more consistent system in the presence of DMSO.

---

[332] a) G. Tsilomelekis, T. R. Josephson, V. Nikolakis, S. Caratzoulas, *ChemSusChem* **2014**, *7*, 117–126; b) S. Despax, C. Maurer, B. Estrine, J. Le Bras, N. Hoffmann, S. Marinkovic, J. Muzart, *Catal. Commun.* **2014**, *51*, 5–9.

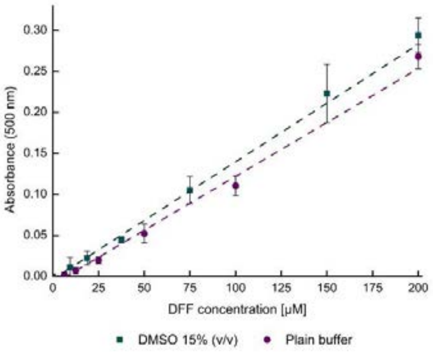

Figure 1.16. Linearity of the colorimetric assay at different concentrations of DFF (0–200 µM) in plain buffer (KPi 100 mM, pH 7.5, purple line) or with DMSO (15% v/v, green line). The data shown are representative of experiments performed by triplicate.

To assess the assay's sensitivity, the limits of detection (LOD) and quantification (LOQ) were determined in multiwell plates for both conditions (plain buffer and with 15% v/v DMSO). Remarkably, the HTS method demonstrated remarkable capability in detecting DFF in both media. Notably, the LOD and LOQ values for the DMSO-water system (8.4 µM and 25.5 µM, respectively) were marginally lower than those calculated in plain buffer (Table 1.2).

Table 1.2. Calibration curve regression analysis for determination of LOD and LOQ of the colorimetric assay in plain buffer or with 15% v/v DMSO.

Reaction system	Linear range (µM)	Calibration curve[a]	SD of calibration curve	LOD (µM)	LOQ (µM)
Plain Buffer[b]	6–200	A = 0,0008 * C – 0,0003	$2.182 * 10^{-3}$	8.8	26.7
DMSO 15% (v/v)	6–300	A = 0,0014 * C – 0,0038	$3.556 * 10^{-3}$	8.4	25.5

[a] A: Absorbance value; C: concentration. [b] KPi buffer 100 mM, pH 7.5.

As commented before, the oxidative conversion of HMF into DFF can lead to the formation of various derivatives, due to the presence of reactive alcohol and aldehyde groups, affording FFCA, FDCA, and HFCA, which might be present in the reaction mixture (Figure 1.17).[333] Thus, the interference in DFF detection of these by-products, along with unreacted HMF, was evaluated. DMSO (15% v/v) was utilized to ensure solubility of all furan derivatives. Various mixtures of putative side products and DFF at different concentrations were prepared to simulate conditions encountered in enzymatic transformations. None of the investigated side products exhibited significant absorbance contributions at 500 nm when incubated with PPD (Figure 1.18). In combination with DFF, these compounds did not interfere with the analyte detection (grey lines in panels a-d, Figure 1.18), as evident from the reference response with only DFF (orange lines in panels a-d, Figure 1.18).

---

[333] a) S. M. McKenna, S. Leimkühler, S. Herter, N. J. Turner, A. J. Carnell, *Green Chem.* **2015**, *17*, 3271–3275; b) M. M. Cajnko, U. Novak, M. Grilc, B. Likozar, *Biotechnol. Biofuels* **2020**, *13*, 66; c) K. Saikia, A. K. Rathankumar, P. S. Kumar, S. Varjani, M. Nizar, R. Lenin, J. George, V. K. Vaidyanathan, *J. Chem. Technol. Biotechnol.* **2022**, *97*, 409–419.

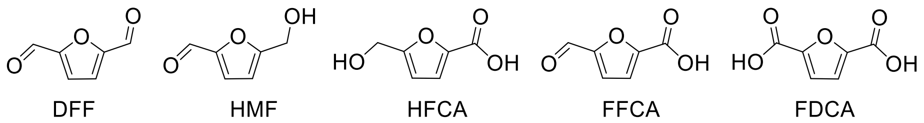

Figure 1.17. Structures of the tested compounds: HMF, 5-hydroxymethylfurfural; DFF, 2,5-diformylfuran; HFCA, 5-hydroxymethyl-2-furancarboxylic acid; FFCA, 5-formyl-2-furancarboxylic acid; FDCA, 2,5-furandicarboxylic acid.

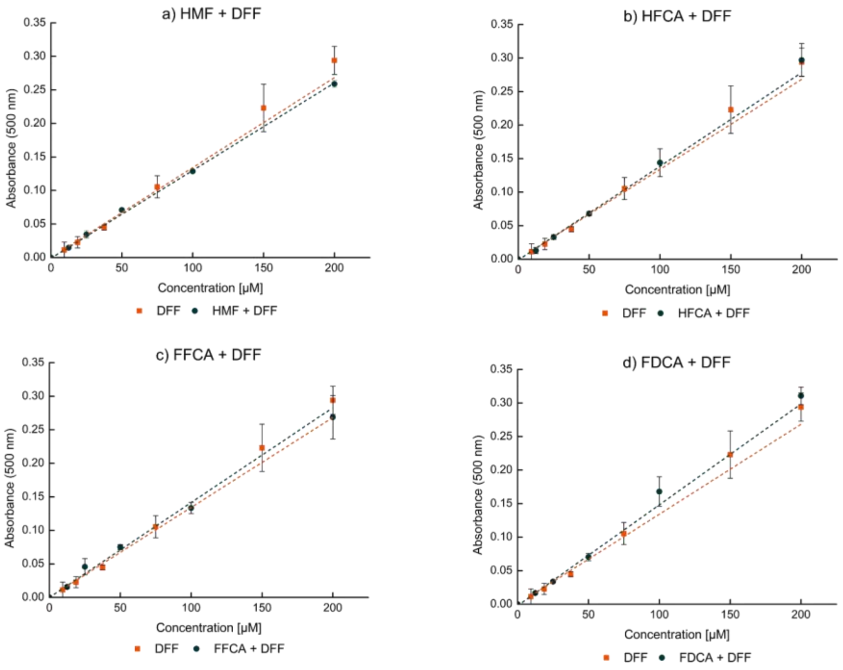

Figure 1.18. Effect of: a) HMF, b) HFCA, c) FFCA, and d) FDCA in the DFF colorimetric assay. Grey line: side-product + DFF + PPD (as equimolar mixtures). Orange line: DFF + PPD. The data shown are representative of experiments performed by triplicate.

To demonstrate the assay's robustness, Z' values were determined for each pair of DFF and side product. This parameter offers insight into the assay's effectiveness and is employed to assess its quality without real samples, aiding in further development and optimization.[334] The calculated values for each combination fell within the range of 0.60–0.72, confirming the method's reliability in identifying positive outcomes (Table 1.3). These values are acceptable when exceeding 0.5, aligning with, for example, the range reported by Straathof and colleagues in the setup of an HTS assay for amino acid decarboxylase activity detection.[335]

Table 1.3. Z' values calculated for each couple of compounds (DFF + side-product).

Side-product combined with DFF	Z' value
HMF	0.72
HFCA	0.68
FFCA	0.60
FDCA	0.70

All these results robustly establish our colorimetric assay as a swift, sensitive, and user-friendly tool for high-throughput screening in the conversion of HMF to DFF under mild aqueous conditions. The assay detects the analyte at low concentrations, even in the presence of DMSO as a co-solvent, and it is not interfered by other co-products that could emerge from HMF oxidation.

---

[334] a) J.-H. Zhang, T. D. Y. Chung, K. R. Oldenburg, *J. Biomol. Screen.* **1999**, *4*, 67–73; b) J. Inglese, C. E. Shamu, R. K. Guy, *Nat. Chem. Biol.* **2007**, *3*, 438–441; c) J. Inglese, R. L. Johnson, A. Simeonov, M. Xia, W. Zheng, C. P. Austin, D. S. Auld, *Nat. Chem. Biol.* **2007**, *3*, 466–479.

[335] R. Médici, P. Domínguez de María, L. G. Otten, A. J. J. Straathof, *Adv. Synth. Catal.* **2011**, *353*, 2369–2376.

1.2.3. Colorimetric assay validation in the detection of DFF from real oxidation of HMF by LMSs

Following the assessment of the assay with DFF and its mixtures containing various HMF derivatives, the method was successfully employed in an actual transformation scenario. Since it was designed as HTS to be used in the screening of a library of laccase mutant for detecting DFF production from HMF, the formation of DFF by oxidation of HMF using three different LMSs with TEMPO as mediator was tested (Scheme 1.5).

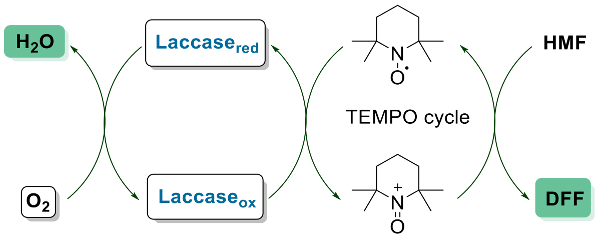

Scheme 1.5. Overview of the laccase/TEMPO system to oxidize HMF.

Hence, three fungal laccases, the one from *Trametes versicolor*, and POXA1b and POXC from *P. ostreatus* were used. For assessing the validity of the colorimetric assay on real samples, initial rates of the three different LMSs for DFF production were also measured (Figure 1.19)

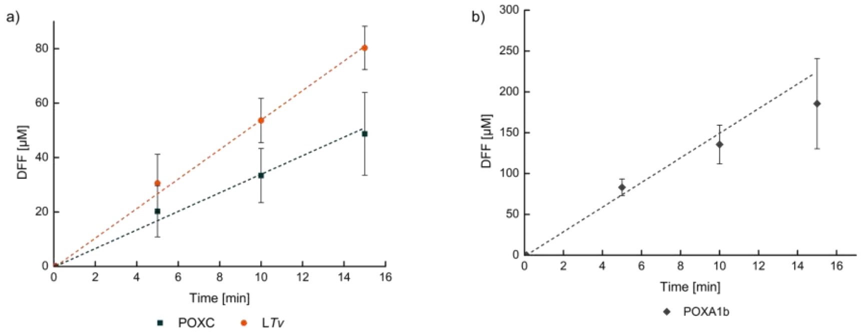

Figure 1.19. Time course of DFF production from HMF (40 mM) using the colorimetric assay at 30 °C under optimum conditions for each laccase: a) POXC (pH 6.5, 0.25 U, grey dots) and L*Tv* (pH 5, 0.25 U, orange dots); b) POXA1b (pH 5.5, 2.5 U), DMSO 15% v/v, and TEMPO (20 mol%). The data are representative of experiments performed in triplicate and are presented as mean standard deviation.

Comparing the initial DFF production rates among the three distinct LMSs, highlighted their varying efficiency in terms of TEMPO recycling. The potential for DFF overoxidation during rapid recycling was also evident. Thus, lower enzyme quantities were employed for the faster systems (0.25 U for POXC and L*Tv*). Conversely, the slower reaction of the POXA1b system necessitated an enzyme increase to 2.5 U, ensuring robust DFF detection within identical time intervals. The initial rates of DFF production using different LMSs were normalized per unit of enzyme (Table 1.4).

Table 1.4. Initial rate calculations for DFF production from HMF, applying the three LMSs. DFF was detected with the colorimetric method under the reported conditions, and its concentration was obtained by interpolation in the calibration curve.

Laccase	**Reaction conditions**[a]	**Initial rate for DFF production from HMF** (μmol DFF·min^{-1}·U^{-1})
L*Tv*	Citrate buffer, 100 mM, pH 5	21.7
POXC	Phosphate buffer, 100 mM, pH 6.5	13.9
POXA1b	Citrate buffer, 100 mM, pH 5.5	5.3

[a] [HMF]= 40 mM, TEMPO (20 mol%), DMSO (15% v/v).

Among the three LMSs, the L*Tv*-mediated system showcased notably rapid DFF production at short reaction times. Similarly, the POXC-mediated reactions generated efficiently DFF. However, in the case of the POXA1b-mediated system, lower DFF accumulation was observed, closely linked to the swiftness of this laccase in promptly reoxidizing TEMPO.

In conclusion, the assay's applicability extended to real DFF production from HMF oxidation. Moreover, it proved capable of evaluating kinetic parameters for different HMF-oxidizing enzymes by tracking DFF accumulation over time in the reaction mixture. Thus, its application as a HTS tool for evaluating a panel of laccase variants to directly oxidize HMF was pursued.

1.2.4. Directed evolution towards novel POXA1b variants

Directed evolution of POXA1b was performed choosing *Saccharomyces cerevisiae* as expression system for heterologous production and random mutagenesis with error prone PCR as technique. Three sets of mutagenic PCRs were set up according to the three mutation rates (Figure 1.20a). When a linear vector and fragment that share ending DNA sequences are transformed in *S. cerevisiae* cells, they can undergo recombination that restores the circular topology of the plasmid (Figure 1.20b). Hence, it has been shown that fragments with a complementarity of 50-100 bp (25-40 for smaller fragments), are enough for the recombination system to work.[336]

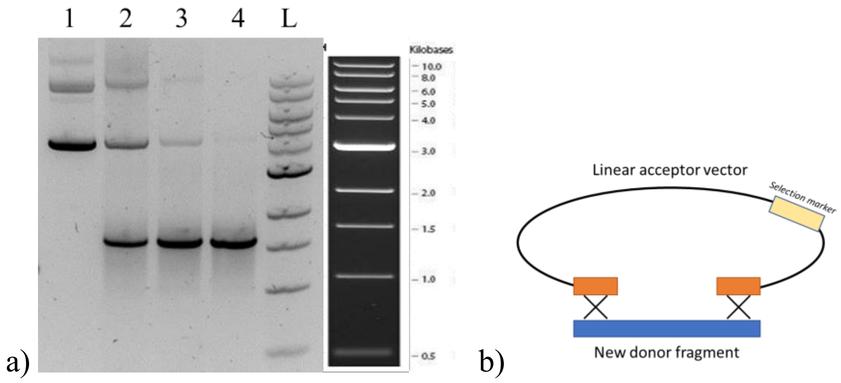

Figure 1.20. a) Agarose gel showing the mutagenic PCR product (POXA1b) amplified from pSAL4-POXA1b. Lane 1: pSAL4-POXA1b plasmid-control template of PCR (7,374 kb). Lanes 2-3-4: low, medium, high mutation frequency PCR products (POXA1B mutants: 1,626 kb). L: 1 kb DNA ladder. b) Scheme of the homologous recombinant system in *S. cerevisiae*.

Recombinant *S. cerevisiae* clones were successfully achieved. A few of them were visible in the high-frequency mutation rate transformants. This is because a high number of mutations incorporated into the gene sequence of the fragment could lead to families with fewer end-compatible gene mutants. This, in turn, hinders the homologous recombination event in the yeast. A total of 548 clones were picked and tested on plates in the presence of ABTS for qualitative screening purposes. Out of these, 424 clones exhibited a low to medium mutation rate, while 124 clones displayed a high mutation rate.

---

[336] C. K. Raymond, T. A. Pownder, S. L. Sexson, *BioTechniques* **1999**, *26*, 134–141.

Among the 424 clones with a low-medium mutation rate, 93 showed an oxidation halo (thus, positive hits). Similarly, out of the 124 clones with a high mutation rate, 29 yielded positive results in the ABTS qualitative screening (Figure 1.21).

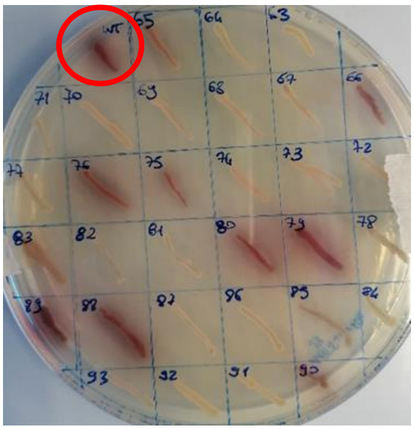

Figure 1.21. Yeast cells secreting randomly mutated POXA1b laccases in the oxidation experiment with ABTS. Wild-type POXA1b is indicated by a red circle.

Furthermore, a microscale quantitative ABTS assay was conducted for the ABTS-positive clones that were identified through the qualitative plate assay (Figure 1.22). The activities of the chosen mutants exhibited a broad spectrum, highlighting significant heterogeneity within the analyzed library. Among the various variants, three mutants (indicated by the green arrows), exhibited notably increased activity towards the model phenolic substrate ABTS in comparison to the wild-type POXA1b. Specifically, these mutants (53, 114, and 342) displayed enhancements in activity by approx. 0.5-fold, 1-fold, and 1.5-fold, respectively.

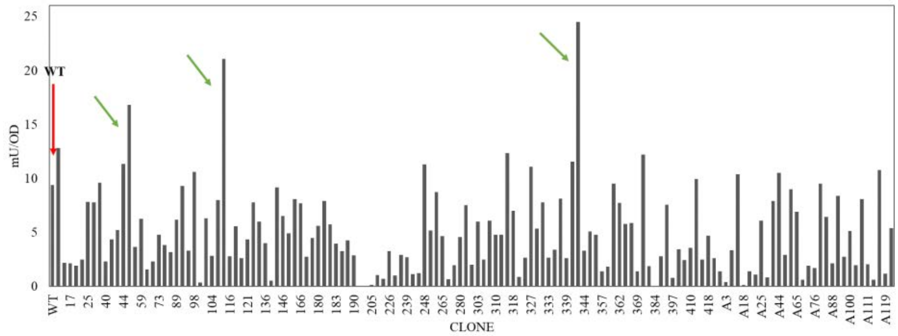

Figure 1.22. ABTS screening of the library of POXA1b random mutants. ABTS activity was standardized for OD_{600} of cell density (0.3-0.8), for being independent of the yeast growth for each variant. Red arrow: wild-type POXA1b; Green arrows: improved variants for ABTS-activity.

Despite the potential negative outcomes from the ABTS screening, all 548 clones were cultivated in the expression medium and subsequently subjected to an assay involving HMF, the target molecule. For measuring DFF production, the previously established colorimetric method was utilized. Among them, six laccase variants exhibited a comparable response in the colorimetric assay, leading to a shift towards an orange hue. This color change indicated a potential oxidation of HMF into DFF (Table 1.5).

Interestingly, two variants, namely POXA1b_MUT_116 and POXA1B_MUT_128, displayed positive results in the HMF assay while yielding negative results in the ABTS assay. Notably, all mutants that were identified as positive for HMF oxidation screening exhibited reduced activity against ABTS. This observation confirms the initial visual analysis conducted on plates, suggesting the occurrence of possible alterations in substrate affinity.

Table 1.5. Colorimetric ABTS and HMF oxidation assay results on the 7 positive mutants of POXA1b towards HMF. Control: 1,4-phenylenediamine + growth medium. Screening: ABTS assay in plate and HMF assay in microplate; %: measured value in preparative 1 mL scale.

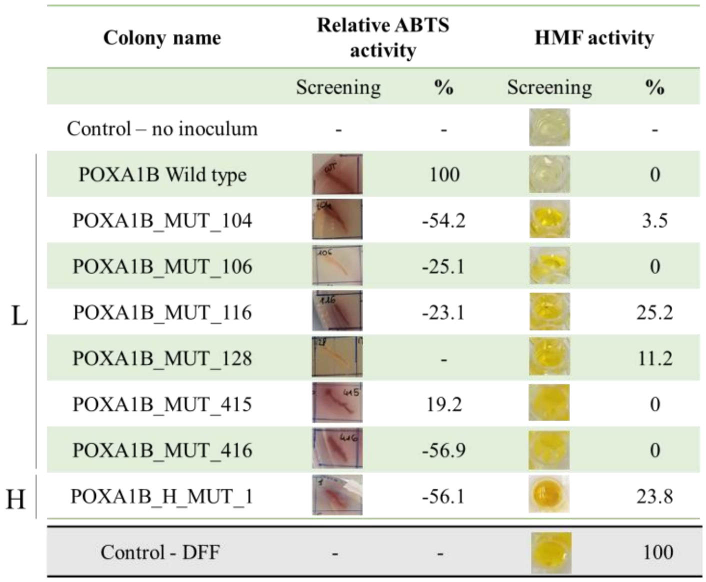

	Colony name	**Relative ABTS activity**		**HMF activity**	
		Screening	%	Screening	%
	Control – no inoculum	-	-		-
L	POXA1B Wild type		100		0
	POXA1B_MUT_104		-54.2		3.5
	POXA1B_MUT_106		-25.1		0
	POXA1B_MUT_116		-23.1		25.2
	POXA1B_MUT_128		-		11.2
	POXA1B_MUT_415		19.2		0
	POXA1B_MUT_416		-56.9		0
H	POXA1B_H_MUT_1		-56.1		23.8
	Control - DFF	-	-		100

To confirm the direct oxidation of HMF into DFF, preparative assays were conducted *in vitro* using the selected mutants. Both the blank reaction crude (HMF incubated in growth SD medium in the presence of secreted wild-type POXA1b), and the control buffer exhibited partial conversion of HMF. Conversely, HMF remained stable in plain buffer. Interestingly, a reduction of HMF into its diol form appeared to merge solely in the presence of the growth medium. These signals persisted across all other reaction crudes. Unfortunately, no significant presence of DFF was detected for any of the selected POXA1b variants.

Laccases are characterized by highly conserved, functionally essential, and expansive regions. Achieving an elevation in redox potential demands considerable mutations within the active site. However, only a limited number of positions can be mutated without compromising overall activity. In this instance, despite detecting few variants with greater activity towards the commonly used ABTS substrate, the size of the POXA1b library was inadequate to yield an evolved variant with a sufficiently elevated redox potential for the conversion of HMF to DFF.

Experimental Section

1.3.1. General information

Commercially available HMF was purchased from Manchester Organics. DFF, FFCA, HFCA, FDCA were purchased from Sigma-Aldrich. L*Tv* laccase was obtained from Sigma-Aldrich. ABTS was purchased from AppliChem GmbH (Germany) and was used as the substrate to measure the laccase activity.

The *Escherichia coli* strain Top 10 (F-mcrA D (mrr-hsdRMS-mcrBC) f80lacZDM15 DlacX74 deoR recA1 araD139 D (ara-leu) 7697 galU galK rpsL (StrR) endA1 nupG) was used in all DNA manipulation for plasmid amplification and preservation. For medium composition, "%" must be considered as w/v.

The medium used for growing *E. coli* was the rich medium Luria-Bertani (LB, tryptone 1%, NaCl 1%, yeast extract 0.5%), and the temperature 37 °C. Selective medium was supplemented with 100 mg/L of ampicillin, while solid medium with 15% w/v of agar (Difco). *E. coli* TOP10 competent cells were prepared as follow: one single colony of TOP10 cells is scraped from a fresh LB agar plate and inoculate 5–10 mL of sterile LB. After an overnight culture at 37 °C, 200 rpm the cells were inoculated at final concentration of 0.1 OD_{600}/mL (Optical Density at 600 nm) in 50 mL of sterile LB and culture at 37 °C with shaking at 200 rpm until OD/mL of 0.5–0.7 (mid log phase) was reached. The 50 mL-culture was split equally between sterile centrifuge tubes and cells collected by centrifugation for 10 minutes at 4000 rpm, 4 °C. Supernatant was discarded and 20 mL of sterile, ice-cold 100 mM $CaCl_2$ added to each cell pellet gently resuspended. The cells were allowed to chill on ice for approx. 15 minutes. The washed cells were collected by centrifugation for 10 minutes at 4000 rpm at 4 °C and the supernatant discarded. 5 mL of sterile, ice-cold 100 mM $CaCl_2$ supplemented with 15% v/v sterile glycerol were added to each cell pellet. After resuspending the cells, they are divided into 80–100 µL aliquots in sterile, ice-cold Eppendorf tubes. The chemically competent can be stored at –80 °C for at least 1 year. The transformation efficiency was quantified by transforming the cells with a known amount (40–80 ng) of PUC18 plasmid a high copy-number vector used as standard plasmid carrying on the ampicillin resistance gene, and count the number of transformant colonies.

After 30 min in ice, a mixture of chemically competent TOP10 cells and DNA was placed at 42 °C for 90 s (heat shock) and then placed back in ice for 1 min. Fresh LB medium was added and the transformed cells were incubated at 37 °C for 40 min (180 rpm). A more concentrated bacteria suspension (9:10 of volume) and a more diluted one (1:10 volume) were plated onto agar plates with ampicillin as antibiotic for selection of positive colonies. Two controls of the transformation experiment with sterile water were made, one plating heated shocked cells onto agar plates without selection (positive control) for assessing the vitality of the competent cells, and the other onto selective plates (negative control). No colonies (or few) have been detected in the latter, meaning the absence of spontaneous resistant cells or other contaminants.

1.3.2. Yasara predictions: Homology modelling and molecular docking experiments

POXA1b structure was generated through prime homology modelling respect to *LTv* automatically selecting 1GYC.pdb as a template (60% of sequence identity).[337] Predicted binding conformations are reported with specific docking scores. Autodock Vina was used in those experiments, Gibbs free energy of binding as docking score and dissociation constant of the molecule (K_D) registered as program output. For AutoDock and VINA algorithm, a ligand efficiency >=0.35 and a dissociation constant of 1200-270 μM indicate good bindings.[338] The ligands were built using the SMILE strings function of YASARA and the docking was performed selecting the definition cell around the active site of POXA1b 3D structure in order to have a more reliable prediction of the interaction.[339] The results were analysed and interpreted using YASARA Structure licence tool, taking in consideration the positioning previsions closer to His456 and Asp205 as reference catalytic active site side chain residues.[288] Molecular graphics were created with YASARA (www.yasara.org) and POVRay (www.povray.org).

---

[337] M. P. Jacobson, D. L. Pincus, C. S. Rapp, T. J. F. Day, B. Honig, D. E. Shaw, R. A. Friesner, *Proteins* **2004**, *55*, 351–367.

[338] O. Trott, A. J. Olson, *J. Comput. Chem.* **2010**, *31*, 455–461.

1.3.3. Assay for laccase activity

ABTS ($\varepsilon_{420} = 36{,}000\ M^{-1}\ cm^{-1}$) test was performed at room temperature in 100 mM citrate buffer pH 3.0 with 2 mM final concentration of the substrate and a suitable amount of the enzyme necessary to obtain an absorbance of 0.5–1 after approximately 1 min. The resulted increasing coloured radical cation ($ABTS^{+\bullet}$) was tracked using a UV-Vis spectrophotometer at 420 nm. One unit of laccase activity was defined as the enzyme amount oxidizing 1 μmol of substrate per min.[340]

1.3.4. High-throughput screening method

A suitable volume (150 μL) of a solution containing DFF and the other components at appropriate concentrations, dissolved in KPi buffer 100 mM pH 7.5 (when present, DMSO was used at 15% v/v) was transferred into a 96-well plate. 1,4-Phenylenediamine was then added as reactant to each well (50 μL, 5 mM), shifting towards orange color according to DFF concentration of the sample up to obtain a reddish precipitate. The plates were kept at room temperature (20-25 °C) for 5 min, and the increase in the absorbance at 500 nm was measured with a UV/Vis spectrophotometer. The limit of absorption was set up to the formation of the precipitate, which caused a heterogeneous solution.

---

[339] J. Wang, R. M. Wolf, J. W. Caldwell, P. A. Kollman, D. A. Case, *J. Comput. Chem.* **2004**, *25*, 1157–1174.

[340] A. Piscitelli, P. Giardina, C. Mazzoni, G. Sannia, *Appl. Microbiol. Biotechnol.* **2005**, *69*, 428–439.

1.3.5. Determination of Z' values

The Z' value was calculated using positive (DFF in this case) and negative reference controls (side products). Z' values for by-product/DFF pairs close to 1.0 demonstrate the robustness of the method. To evaluate the overall performance of the assay and its application in a HTS format, values obtained either at 200 µM of DFF or the corresponding side-product as positive and negative reference controls were used.[334] The Z' values of each side-product–DFF pair was calculated using the following equation:

$$Z' = 1 - \frac{3SD_{\mathrm{DFF}} + 3SD_{\mathrm{side\ product}}}{|mean_{\mathrm{DFF}} - mean_{\mathrm{side\ product}}|}$$

1.3.6. Reaction progress curves for the LMSs and initial rate measurements

To prevent leakages when spreading small volumes, the reagents were combined beforehand, and then placed in the multiplate. The reaction progress curve was obtained dispensing in each well 125 µL of the reaction mixture, consisting of 30 U of laccase per mmol of substrate for POXA1b, 4 U per mmol of substrate for L*Tv* and POXC laccases, 20 mol% of TEMPO as mediator (mol of mediator per mol of substrate), and 40 mM of HMF as starting concentration (it was selected after trials at different HMF amounts). Citrate buffers 100 mM, pH 5 and 5.5, were used for L*Tv* and POXA1b laccases, respectively, and KPi buffer 100 mM, pH 6.5, for POXC. All the reaction mixtures were incubated in a 96-well plate at 30 °C, under vigorous stirring. The reaction was stopped by enzyme inactivation adding an aqueous 10 M NaOH solution (25 µL), and then PPD (40 mM) was added. The mixture was incubated for 5 min at rt without shaking and finally the absorbance at 500 nm was measured.

1.3.7. Cloning vector

The design of the expression vector was made with SnapGene Viewer. pSAL4 plasmid carrying on POXA1b coding gene was used as scaffold for directed evolution of POXA1b laccase: it was propagated in *E. coli* TOP10 cells, and the expression was carried on *Saccharomyces cerevisiae* (Figure 1.23).

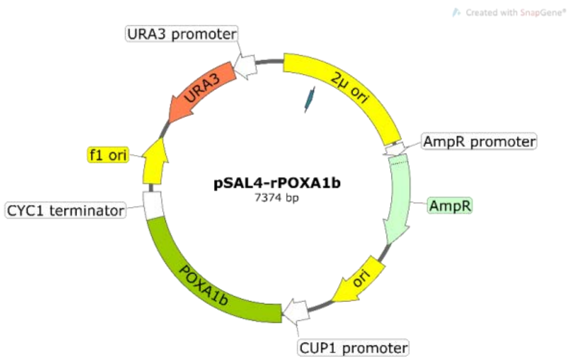
Created with SnapGene
URA3 promoter
URA3
2µ ori
f1 ori
AmpR promoter
pSAL4-rPOXA1b
7374 bp
CYC1 terminator
AmpR
ori
POXA1b
CUP1 promoter

Figure 1.23. pSAL4 vector with wild-type POXA1b laccase coding gene. 2µ ori: yeast 2µ plasmid origin of replication; AmpR promoter: promoter of AmpR coding gene; AmpR: coding gene for *bla* gene, β-lactamase, conferring resistance to ampicillin, carbenicillin, and related antibiotics; Ori: bacterial plasmid origin of replication; CUP1 promoter and CYC1 terminator: inducible metallothionein gene promoter regulated by Cu^{2+} and transcription terminator respectively from *S. cerevisiae;* f1 ori: f1 bacteriophage origin of replication; URA3 promoter: *S. cerevisiae* promoter of URA3 coding gene; URA3: orotidine-5'-phosphate decarboxylase, required for uracil biosynthesis, and yeast auxotrophic marker.

1.3.8. Nucleic acid manipulation

Oligonucleotide primers were designed complementary to POXA1b gene in pSAL4 vector for the mutagenic PCR in the directed evolution experiment (Table 1.6).

Table 1.6. Forward (*Fw*) and reverse (*Rev*) primers. Tm: melting temperature. Nucleotides in bold are complementary to the POXA1b cDNA sequence.

Primer	Nucleotide Sequence	Tm
Fw	5'**ATTCAAGCTTATGGCGGTTGCATTCGTTGC** 3'	66 °C
Rev	5'TTACTC**TCATGCTTTCAATGGCGCAGGCAGACG**3'	67 °C

1.3.8.1. Digestion with restriction enzymes

The mutagenic PCR products and pSAL4 cloning vector were hydrolyzed with opportune restriction enzymes (Promega), SmaI and BglII, respectively. Due to the different buffer and incubation temperatures, the hydrolysis reactions were performed separately using 5 U of enzyme for each µg of DNA. Firstly, SmaI was incubated with buffer J at 25 °C for 2.5 h, while BglII with buffer D incubating at 37 °C for 2.45 h. Between the first and the second hydrolysis, the linear plasmid was extracted and purified from agarose gel with QIAquick Gel Extraction Kit from Quiagen as specified by the manufacturer. The final linear vector was again purified from the reaction mixture after agarose gel separation using the same procedure. The agarose gel, made of 0.8% agarose in tris-acetate-EDTA (TAE) buffer, was stained with GelRed intercalant agent. The electrophoresis was conducted in TAE (40 mM Tris-acetate, 1 mM EDTA, pH 8) at 80 V, and the gel was finally revealed under UV by using ChemiDoc gel imaging system. DNA was then extracted from the gel according to the protocol, eluted in pure water and quantified by Thermo Scientific NanoDrop spectrophotometer.

While the short fragment consisting of the POXA1b original core (969 pb) was removed from pSAL4-POXA1b plasmid, both desired extreme ends of the gene were kept in order to promote the subsequent *in vivo* recombination, as explained in the main text, leaving 155 bp at the 5'-end and 475 bp at the 3'-end of the original cDNA sequence and recovering a new plasmid of 6,405 kb (Figure 1.24).

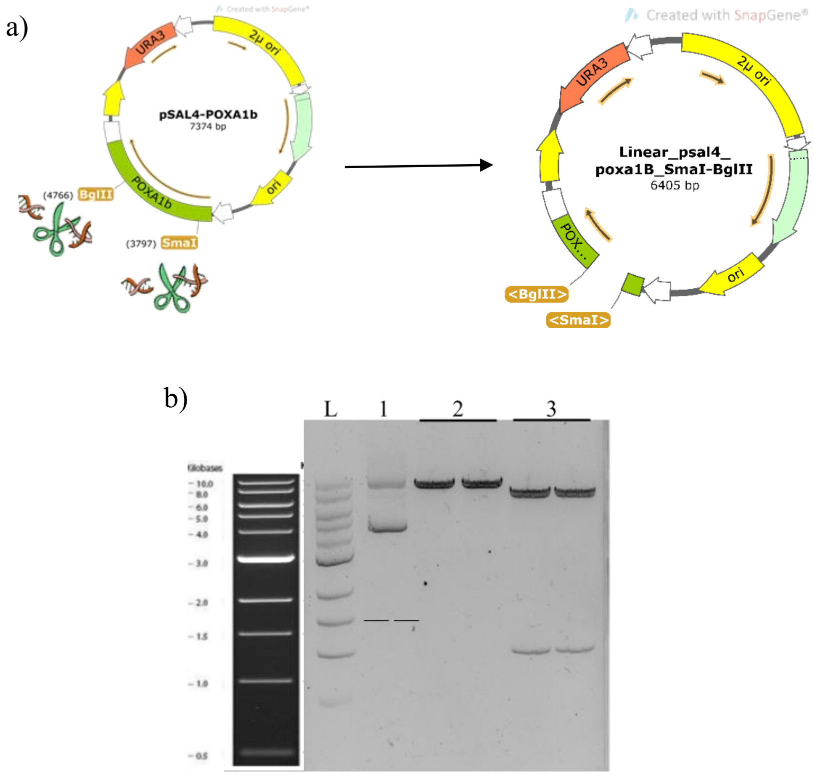
a)
pSAL4-POXA1b
7374 bp
URA3
2μ ori
POXA1b
ori
(4766) BglII
(3797) SmaI
Linear_psal4_
poxa1B_SmaI-BglII
6405 bp
POX...
<BglII>
<SmaI>
Created with SnapGene
b)
L
1
2
3
Kilobases
10.0
8.0
6.0
5.0
4.0
3.0
2.0
1.5
1.0
0.5

Figure 1.24. a) Linearization of pSAL4-POXA1B after SmaI-BglII double cut. A fragment of 969 pb is released after the double cut. b) Agarose gel showing the linear vector after SmaI - BglII hydrolysis. Lane L: 1 kb DNA ladder. Lane 1: pSAL4-rPOXA1b plasmid-control template of PCR (7,374 kb). Lane 2: pSAL4 linear – from single cut with SmaI (7,374 kb). Lane 3: pSAL4 linear – from double cut with SmaI-BglII (6,405 kb + 969 pb).

1.3.8.2. Randomly mutated gene library construction

The pSAL4-POXA1b coding plasmid was isolated using the MiniPrep kit supplied by Quiagen®, from *E. coli* TOP10 cells. The plasmid was used as template for the testing PCR. The final analysis of the amplification reaction was conducted on agarose gel, thus confirming the presence of the amplified

POXA1b gene, with the expected molecular weight, of almost 1614 kb, while no amplification was observed in the absence of the template (Figure 1.25).

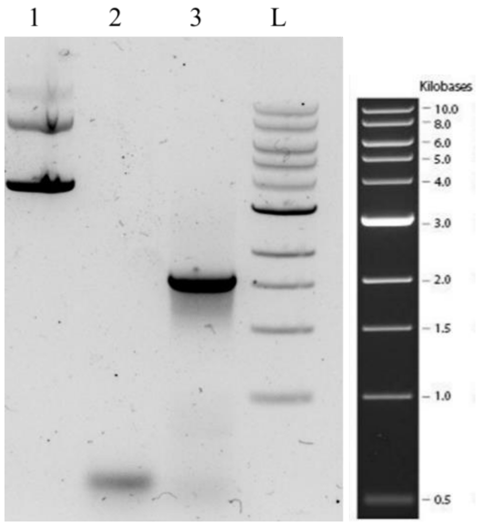
1
2
3
L
Kilobases
10.0
8.0
6.0
5.0
4.0
3.0
2.0
1.5
1.0
0.5

Figure 1.25. Agarose gel showing the PCR product (POXA1b) amplified from pSAL4-POXA1b with the designed primers. Lane 1: pSAL4-POXA1b plasmid-control template of PCR (7,374 kb). Lane 2: Control of PCR-no template. Lane 3: PCR product: POXA1B fragment (1,626 kb). Ladder: 1 kb DNA ladder.

Hence, the PCR cycle was set up as follows:

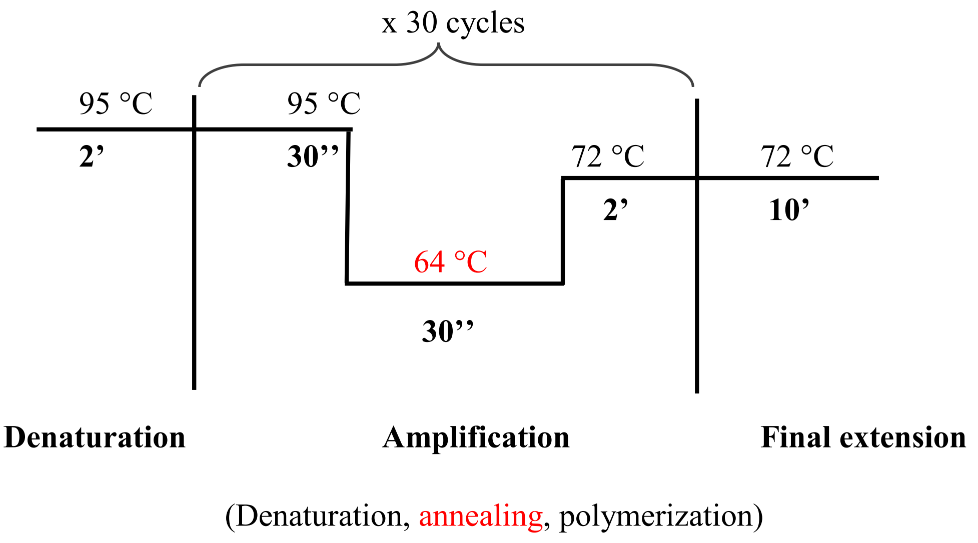
x 30 cycles
95 °C
2'
95 °C
30''
64 °C
30''
72 °C
2'
72 °C
10'
Denaturation
Amplification
Final extension
(Denaturation, annealing, polymerization)

The PCR products and the cloning vectors were hydrolyzed with the opportune restriction enzymes (Promega), SmaI and BglII, respectively, and isolated as reported in Section 1.3.8.1. The final linear vector was again purified from the reaction mixture after agarose gel separation. The electrophoresis was conducted in TAE (40 mM Tris-acetate, 1 mM EDTA, pH 8) at 80 V and the gel was finally revealed under UV by using ChemiDoc gel imaging system. DNA was then extracted from the gel according to the protocol, eluted in pure water and quantified by Thermo Scientific NanoDrop spectrophotometer.

1.3.8.3. PCR

Mutazyme® II DNA polymerase (GeneMorphII Random mutagenesis kit, Agilent) was the enzyme used for random prone PCR. The mutagenic PCR reaction was carried on using the SimpliAmp Thermal Cycler (Thermo Fisher Scientific) and the amplification program as showed in Section 1.3.8.2. The amount of each PCR component is reported in Table 1.7.

Table 1.7. Amount of PCR components.

Component	Initial concentration	Final concentration/amount
Mutazyme II DNA polymerase	125 U/µL	2.5 U/µL
Mutazyme II Reaction buffer	10X	1X
dNTP mix	40 mM	400 µM
Oligo: Forward Primer	10 µM	0.5 µM
Oligo: Reverse Primer	10 µM	0.5 µM
Template - DNA	797.4 ng/µL	10–50–100 ng
Nuclease-Free Water	-	Up to 50 µL final

The predicted mutation frequencies depended on the initial target amount of DNA, meaning "target" as DNA to be amplified, not the total amount of the DNA template.

Mutation rate	Mutation frequency (mutations/kb)	Initial target amount (ng)
Low	0–4.5	500–1000
Medium	4.5–9	100–500
High	9–16	0.1–100

1.3.8.4. Saccharomyces cerevisiae: Host of mutagenesis

The *S. cerevisiae* strain used for heterologous expression was W303-1A (MAT ade2-1, his3-11, 15, leu2-3, 112, trp1-1, ura3-1, can1-100). The medium formulated for growing wild-type *S. cerevisiae* was the rich medium YPD: 1% yeast extract, 2% bacto tryptone, 2% glucose. Solid medium contained 15% of agar. Transformed yeast was grown in the SD medium containing:

Components of SD medium

Yeast nitrogen base w/o AA	0.67%
Casamino acids	0.5%
Tryptophan	40 mg/L
Adenine	30 mg/L
Succinate buffer pH 5.3	50 mM
Glucose	2%
Copper sulfate	0.6 mM

LiOAc single-stranded carrier DNA/PEG method was used for *S. cerevisiae* transformation with the pSAL4 vector and mutagenic PCR fragments. The protocol was revised from the first version of Ito and co-workers[341] and discussed by Gietz and Woods.[342]

The yeast strain was inoculated into 5 mL of YPD medium and incubated overnight at 30 °C. The titer of the culture was determined by measuring the OD_{600} of the cells, counting that a suspension containing 1 x 10^6 cells/mL will give an OD_{600} of 0.1. An appropriate volume of suspension was transferred into 50 mL of pre-warmed YPD medium (250 mL flask) to reach a final cell density of 5 x 10^6 cells/mL (0.5 OD/mL). The flask was incubated on a rotary shaker at 30 °C and 200 rpm to allow the cells to complete at least 2 divisions, but not more than 4. For the *S. cerevisiae* strain used in these experiments, it took 8–10 h. When the cell titer was at least 2 x 10^7 cells/mL (1.6 OD/mL), the cells were harvested by centrifugation, washed in 25 mL of sterile water and then again in 1 mL. Cells were vortex-mixed in 1.0 mL of sterile clean water. 100 µL samples (~10^8 cells) were pipetted into 1.5-mL microcentrifuge tubes, one for each transformation, centrifuged at top speed for 30'', and the supernatant was discarded. 1 mL of Li-Acetate 0.1 M was added, the suspension vortex-mixed and incubated for 5 min at 30 °C. The preparation was centrifuged at top speed for 30 s, and the supernatant discarded. 360 µL of the transformation mix as maximum was added, consisting of: 300 µL PEG 4000 [50% (w/v)], LiOAc (1.0 M), 25 µL boiled single-stranded DNA (4.0 mg/mL), and 35 µL of DNA (1.5 µg minimum, for maintaining a high recombination efficiency). The cells were resuspended by vigorous vortex-mixing allowing the complete homogeneity of the mixtures. The tubes were incubated in a 42 °C water bath for 20–40 min, then centrifuged at top speed for 30 s and the transformation mix was removed. The cells were resuspended in 1.0 mL of sterile water. Appropriate dilutions of the cell suspension were plated onto SD medium and the plates incubated for 3–4 days.

---

[341] H. Ito, Y. Fukuda, K. Murata, A. Kimura, *J. Bacteriol.* **1983**, *153*, 163–168.

[342] R. D. Gietz, R. A Woods, *Methods Enzymol.* **2002**, *350*, 87–96.

After the transformation with the POXA1b variant library, only the positive clones were able to grow in absence of uracil, each of them keeping the close plasmid expressing one single variant of POXA1b. Plate assay for assessing the activity of the variants was performed on solid selective medium supplemented with 0.2 mM ABTS and incubating the plates at 28 °C for 4 days. For the flask scale growths, pre-cultures (3 mL) were grown on SD medium in a 15 mL Falcon tube for 16 h. A suitable volume of suspension to reach a final OD_{600} value of 0.5 was then used to inoculate 250 mL Erlenmeyer flasks containing 50 mL of SD medium. All cultures were conducted at 28 °C on a rotary shaker at 230–250 rpm.

For the growth in multi-well plates, related to the library screening, single clones were picked and transferred into 96-well plates containing 50 µL of SD medium per well. Plates were incubated at 28 °C and 600 rpm in a shaker for 24 h. After that time, 150 µL of SD was added to each well and the plates were incubated under the same conditions for other 24 h. The plates were sealed with an acetate film in order to prevent evaporation. The plates were, then, centrifuged for 5 min at 4,000 rpm, 4 °C and a suitable volume of supernatant was transferred to a new 96-well plate for performing the colorimetric HMF screening.

1.3.8.5. DNA gel electrophoresis

The mutagenized PCR products and the linear pSAL4 vector were separated and analysed on agarose gel 0.8% w/v. The electrophoresis was conducted in TAE (40 mM tris-acetate pH 8, 1 mM EDTA) at 80 V. To visualize DNA, 0.5 mg/L Gel Red was added to the agarose gel. DNA fragments were visualized with ultraviolet light (365 nm). PCR products and linear plasmid were extracted and purified from agarose gel with the Quiagen® kit from as specified by the manufacturer.

CHAPTER 2

Design and expression of a new laccase: Lacc12

Introduction

Current laccase production from natural sources cannot meet rising market demand due to low yield production and incompatibility with growth conditions of the microorganisms under standard industrial fermentation processes. This involves not just the bioprocess, but also downstream phases. Recombinant protein expression in easily cultivable hosts boosts productivity, reduces costs, and offers potentially scalable industrial applications.[343] Moreover, GRAS microbial hosts, "Generally Regarded as Safe", can be selected for producing proteins isolated also from harmful species. Hence, choosing the right heterologous expression system is pivotal for successful, economical protein production.

Since the beginning of 1990s, recombinant expression of laccases has been a matter of research of many groups. Bacteria (like *E. coli*) and yeasts (*Saccharomyces cerevisiae*, *Pichia pastoris*) have been exploited for heterologous expression due to their ability to rapidly achieve high cell densities with simple media.[344] Yeasts are particularly valuable when dealing with unstable or biologically inactive proteins produced in bacteria. They also become indispensable when post-translational modifications, like glycosylations and the proper formation of disulfide bonds, not possible to achieve in bacteria, are necessary, as is the case for fungal laccases.[345]

2.1.1. Laccase production in yeasts: Focus on *Pichia pastoris*

At the beginning of this century, the first results of expressing fungal laccases in non-conventional yeasts like *Kluyveromyces lactis*, *Yarrowia*

---

[343] C. Pezzella, F. Autore, P. Giardina, A. Piscitelli, G. Sannia, V. Faraco, *Curr. Genet.* **2009**, *55*, 45–57.

[344] a) B. Schilling, R. M. Linden, U. Kupper, K. Lerch, *Curr. Genet.* **1992**, *22*, 197–203; b) S. Kajita, S. Sugawara, Y. Miyazaki, M. Nakamura, Y. Katayama, K. Shishido, Y. Iimura, *Appl. Microbiol. Biotechnol.* **2004**, *66*, 194–199; c) K. Kataoka, H. Komori, Y. Ueki, Y. Konno, Y. Kamitaka, S. Kurose, S. Tsujimura, Y. Higuchi, K. Kano, D. Seo, T. Sakurai, *J. Mol. Biol.* **2007**, *373*, 141–152.

[345] L. Liu, H. Yang, H. Shin, R. R. Chen, J. Li, G. Du, J. Chen, *Bioengineered* **2013**, *4*, 212–223.

lipolytica, and *Pichia methanolica* were reported.[340,346] Successively, *S. cerevisiae* and *P. pastoris* have been introduced for highly glycosylated laccase recombinant expression. Despite both bacterial and fungal laccases have been recombinantly expressed in different systems, in general this class of enzyme is difficult to express heterologously and purify in an active form.[347] Moreover, significant production yield variability exists due to differences in expressed cDNAs and host selection for heterologous expression. For instance, POXC and POXA1b laccases have shown higher expression in *K. lactis* than in *S. cerevisiae*,[340] whereas POXA3 from the same source exhibited the opposite pattern.[343] Interestingly, POXA1b is actively and abundantly produced in *P. pastoris* (Figure 2.1),[348] whereas POXC less.[349]

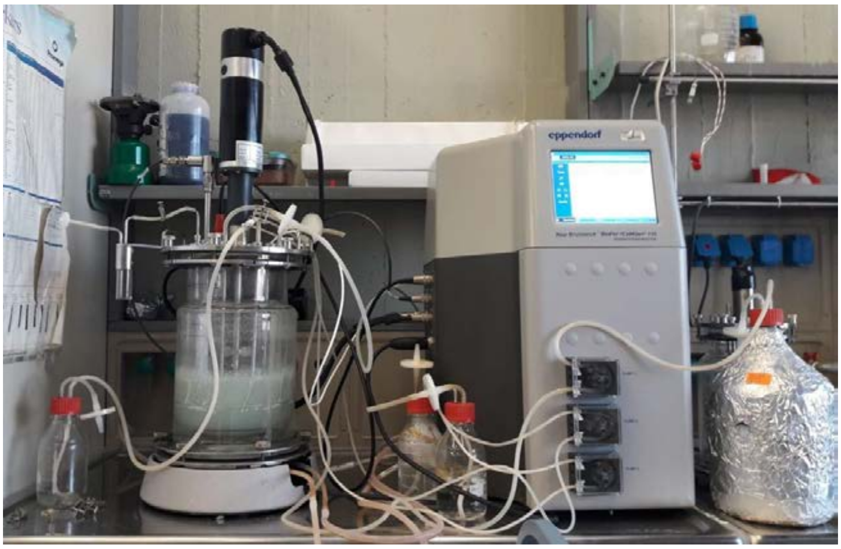

Figure 2.1. POXA1b production from *P. pastoris* in 5 L-scale fermenter.

---

[346] a) C. Jolivalt, C. Madzak, A. Brault, E. Caminade, C. Malosse, C. Mougin, *Appl. Microbiol. Biotechnol.* **2005**, *66*, 450–456; b) M. Guo, F. Lu, J. Pu, D. Bai, L. Du, *Appl. Microbiol. Biotechnol.* **2005**, *69*, 178–183.

[347] B. G. Ergün, P. Çalık, *Bioprocess Biosyst. Eng.* **2016**, *39*, 1–36.

[348] C. Pezzella, V. G. Giacobelli, V. Lettera, G. Olivieri, P. Cicatiello, G. Sannia, A. Piscitelli, *J. Biotechnol.* **2017**, *259*, 175–181.

[349] Q. Song, X. Deng, R.-Q. Song, *Microorganisms* **2020**, *8*, 601.

The effectiveness of the methylotrophic yeast *P. pastoris* in recombinant enzyme expression is attributed to the ease of genetic manipulation, secretion of recombinant proteins, rapid growth to high cell densities in minimal medium and the ability to provide essential post-translational modifications. These benefits make it as the perfect candidate for the recombinant production of industrial enzymes at large scale.[350]

Furthermore, this yeast exhibits minimal secretion of native proteins. Thus, extracellular production of recombinant enzymes can simplify purification procedures and significantly decrease downstream costs.[351] Signal sequences for protein secretion into the expression media can be utilized. Laccases are secreted by native eukaryotic producers, such as filamentous *fungi*, due to the presence of an N-terminal signal prepropeptide. It facilitates the movement of laccase through the secretory pathway and out of cells. Certain hosts, including yeasts, identify and utilize native fungal signal sequences to achieve laccase secretion. In addition, various yeast signal peptides have also been employed to efficiently facilitate the laccase secretion from yeast cells. Among them, *S. cerevisiae* α-mating factor (α-factor),[352] *SUC2*,[353] *XPR2*,[354] or xylanase secretion signal sequences can be mentioned.[355]

The success of *P. pastoris* as a platform for heterologous enzyme production hinges on its robust and tightly regulated alcohol oxidase 1 promoter (pAOX1). This promoter has been utilized to express a diverse array of enzymes, including laccases, at great levels (Figure 2.2).

---

[350] M. Ahmad, M. Hirz, H. Pichler, H. Schwab, *Appl. Microbiol. Biotechnol.* **2014**, *98*, 5301–5317.

[351] a) T. Vogl, A. Glieder, *New Biotech.* **2013**, *30*, 385–404; b) A. Massahi, P. Çalık, *J. Theor. Biol.* **2015**, *364*, 179–188.

[352] D. M. Mate, D. Gonzalez-Perez, R. Kittl, R. Ludwig, M. Alcalde, *BMC Biotechnol.* **2013**, *13*, 38.

[353] A. Klonowska, C. Gaudin, M. Asso, A. Fournel, M. Réglier, T. Tron, *Enzyme Microb. Technol.* **2005**, *36*, 34–41.

[354] C. Madzak, L. Otterbein, M. Chamkha, S. Moukha, M. Asther, C. Gaillardin, J.-M. Beckerich, *FEMS Yeast Res.* **2005**, *5*, 635–646.

[355] N. Nishibori, K. Masaki, H. Tsuchioka, T. Fujii, H. Iefuji, *J. Biosci. Bioeng.* **2013**, *115*, 394–399.

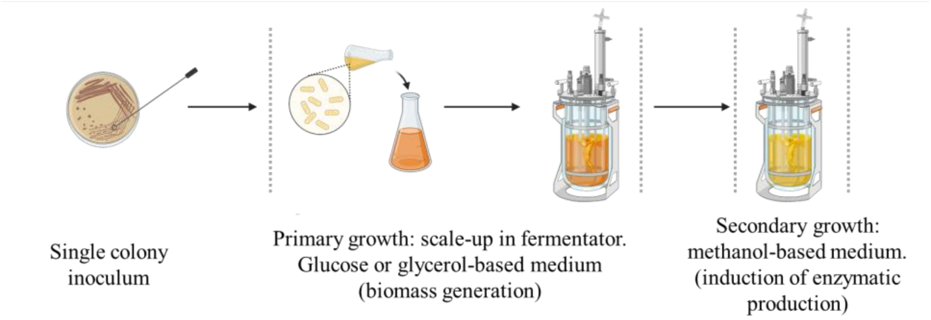
Single colony
inoculum
Primary growth: scale-up in fermentator.
Glucose or glycerol-based medium
(biomass generation)
Secondary growth:
methanol-based medium.
(induction of enzymatic
production)

Figure 2.2. Process flow scheme of heterologous production of enzymes in *P. pastoris* yeast using pAOX1 promoter-type vectors. Elements of the figures were obtained from www.biorender.com.

However, gene synthesis regulated by pAOX1 relies on methanol presence, which bring operative working risks and is not suitable for food processes. To address this challenge, various innovative alternative promoters have emerged, including the constitutive glyceraldehyde 3-phosphate dehydrogenase promoter (pGAP), enolase promoter (pENO1), and inducible promoters such as dihydroxyacetone synthase (pDAS), formaldehyde dehydrogenase (pFLD1), glutathione-dependent formaldehyde dehydrogenase (FLD), and isocitrate lyase (pICL1).[356]

Despite yeasts are promising organisms for the heterologous expression of laccases, optimization steps are necessary to reach acceptable levels of protein. There are various methods for controlling expression and secretion levels, broadly categorized into two branches: regulation during the construction of the recombinant gene, and optimization of yeast cultivation and final enzyme production.

According to the type of promoter, *P. pastoris* expression vectors can be categorized into two main groups: inducible expression vectors, which include pPIC9, pHIL-S1, pPICZ, and pYAM75P, and constitutive expression vectors, such as pHIL-D2, pHWO10, and pGAPZ. The promoter within the inducible vectors triggers gene expression exclusively when methanol is present. On the other hand, the promoter within the constitutive vectors does not necessitate induction and offers robust operability, remarkable stability, and enhanced safety.

---

[356] a) I. Safder, S. Khan, I. Islam, M. K. Ali, Z. Bibi, M. Waqas, *Biomed. Lett.* **2018**, *4*, 1–14; b) A. T. Özçelik, S. Yılmaz, M. Inan, in *Recombinant Protein Production in Yeast*, *Methods in Molecular Biology*, (Eds.: B. Gasser, D. Mattanovich), Vol. 1923, Springer, New York (USA), **2019**, pp. 97–112.

Optimizing laccase production and activity in yeast cells typically includes using appropriate growth media with nitrogen sources, maintaining optimal pH, reducing cultivation temperature, and optimizing copper levels (Figure 2.3).

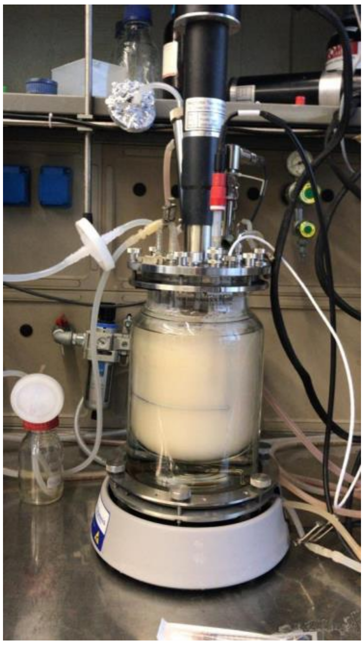

Figure 2.3. High-density growth of *P. pastoris* cells after growth conditions optimization.

To lower production and purification costs, strategies involve employing a robust constitutive promoter paired with an efficient secretion signal sequence, or optimizing DNA codons specific to the yeast host.[357] However, for laccase heterologous expression, to generalize production conditions is difficult; the success of each method to be tested depends on factors like the laccase gene, yeast species, and strains involved.

2.1.2. Lacc12: A promising laccase. Gene isolation

In 2010, Lettera and co-workers discovered a new laccase originating from the fruiting body of *P. ostreatus*, expressed during the development of the fruit body, being possibly involved in the process itself. This enzyme presents 68% identity with a laccase found in *Cyathus bulleri* (ABW75771), as well as to laccase2 from *Coprinopsis cinerea* (AAR01243), and 67% identity with POXC. The K_m value of Lacc12 for standard laccase substrates adheres to the sequence syringaldazine > 2,6-DMP > ABTS, and its affinity for typical substrates align and is in comparable order of magnitude with those of other recognized members within the same enzyme family.[358] However, it was shown to be expressed at low levels after with several production steps from its native source.

Thus, recombinant production of Lacc12 was needed. Apart from the characterization, to set-up larger scale biotransformations with this unexplored laccase, it is essential to engage in its heterologous expression.

---

[357] Z. Antošová, H. Sychrová, *Mol. Biotechnol.* **2016**, *58*, 93–116.

[358] V. Lettera, A. Piscitelli, G. Leo, L. Birolo, C. Pezzella, G. Sannia, *Fungal Biol.* **2010**, *114*, 724–730.

Results and Discussion

2.2.1. Recombinant Lacc12 production: Inducible *vs* constitutive expression

The first strategy embraced for Lacc12 recombinant expression regarded the choose of the expression vector: the house-made PJGGαKR and pPICZB were selected for constitutive and inducible laccase production, respectively. The predicted protein sequence of Lacc12 contains an N-terminal secretion signal (23 amino acids), which is a typical secretion sequence recognized by the native organism. In the case of constitutive expression, both Lacc12 genes, with and without the intrinsic sequence were performed in PJGGαKR vector, which already carried on the typical α secretion signal. The sequence with the intrinsic signal for secretion will be called signal Lacc12 from now on.

Despite the presence of numerous colonies in *P. pastoris* transformation (Figure 2.4), unfortunately no activity was revealed in ABTS plates, maybe due to inefficiency of protein synthesis or correct folding (Figure 2.5).

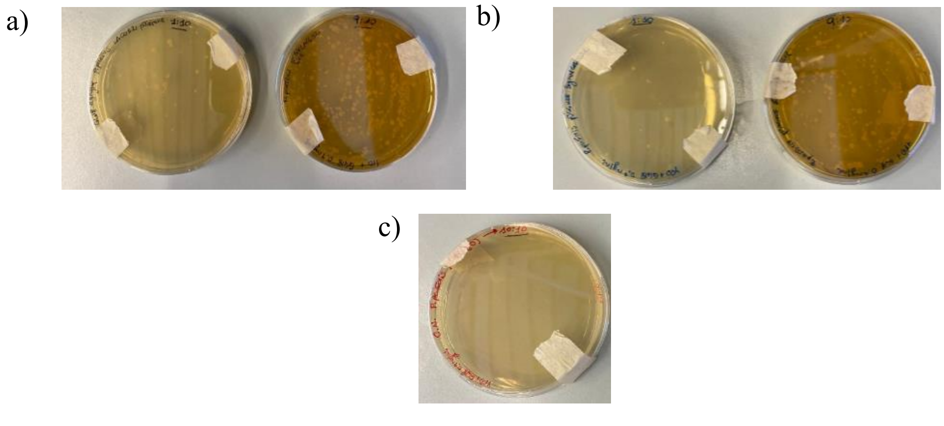

Figure 2.4. Result of the transformation on *P. pastoris* with: a) pJGGαKR-Lacc12, and b) pJGGαKR Lacc12-signal. c) Negative control: transformation with water assured the absence of resistant cells or other contaminants.

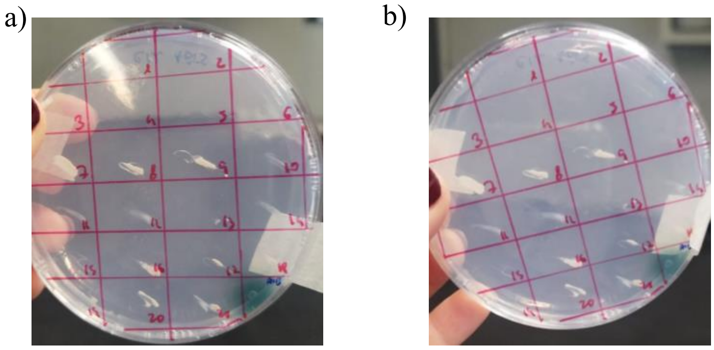

Figure 2.5. ABTS assay on plate. a) Lacc12, and b) signal-Lacc12. The green spot is the positive control (*P. pastoris* expressing POXA1b laccase).

SDS-PAGE analyses of samples collected after 5 days of fermentation (Figure 2.6) confirmed the complete absence of recombinant proteins both in cell pellets and supernatants. Thus, the first easiest strategy for achieving Lacc12 recombinant expression was to change the vector from a constitutive system to an inducible one (pPICZB).

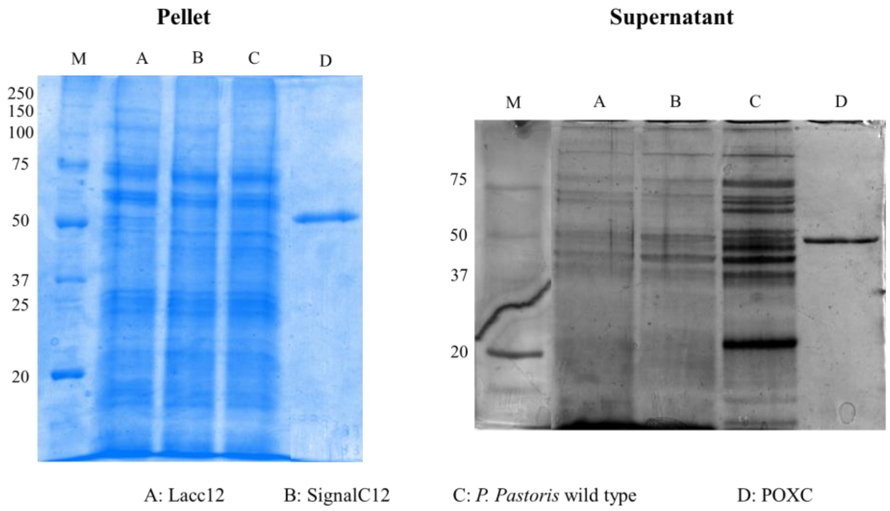
Pellet
M
A
B
C
D
250
150
100
75
50
37
25
20
Supernatant
M
A
B
C
D
75
50
37
20
A: Lacc12
B: SignalC12
C: P. Pastoris wild type
D: POXC

Figure 2.6. SDS-PAGE gels on pellet (left panel) and supernatant (right panel) of Lacc12 (A.), Lacc12 signal (B.) and *P. pastoris* wild type as control (C.). POXC (D.) was added as reference.

For the inducible experiments, Lacc12 gene was successfully cloned into pPICZB under the control of AOX1 promoter with a ligase event in *E. coli* TOP10 cells. *P. pastoris* recombinant cells carrying on the pPICZB-Lacc12 gene were achieved. The efficiency of PmeI (integrated in AOX1 promoter site) linearized vector transformation was almost double than the one linearized with BsiWI (integrated in AOX1 terminator). This evidence suggested a potentially higher recombination efficiency at the AOX1 promoter site. Intriguingly, the majority of these strains were capable of thriving at the highest tested Zeocin concentration. No significant differences were observed when the gene was integrated at the AOX1 promoter (achieved through PmeI hydrolysis of the vector), or at the AOXI terminator (achieved through BsiWI hydrolysis of the vector). Colonies number 3 and 28 from PmeI-clones, and number 8, 14, and 21 from BsiWI ones gave oxidation halo on ABTS agar plates after 7 days of incubation (Figure 2.7). Notably, these selected colonies also demonstrated the capability to thrive in the presence of 1 mg/mL of Zeocin.

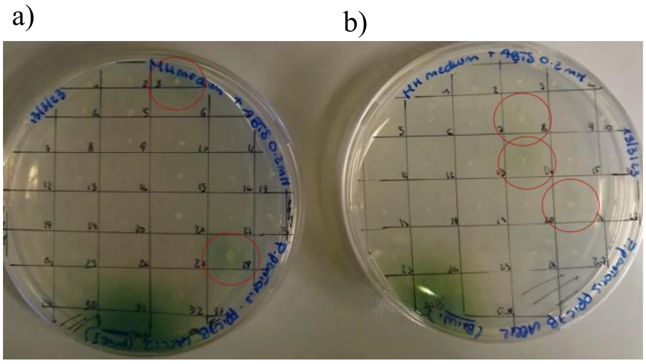

Figure 2.7. ABTS assay on plate. a) Lacc12 (PmeI hydrolysis), and b) Lacc12 (BsiWI hydrolysis). The green spot in the lower part of the plate is the positive control (*P. pastoris* expressing POXA1b laccase).

After a span of 10 days, nearly all the colonies exhibited the ability to oxidize ABTS, signifying their production in an active form. However, the colony demonstrating the highest rate of ABTS oxidation was chosen for further cultivation in a smaller scale (20 mL within a 100-mL flask), aiming to evaluate the laccase production, wherein methanol was introduced daily to induce the process.

Heterologous proteins are typically expressed at temperatures ranging from 20 °C to 30 °C in *P. pastoris*. Multiple studies have demonstrated that temperature constitutes a crucial variable in the *Pichia* expression system, affecting protein stability in relation to folding and activity.[359] Thus, colonies were initially cultivated on a small scale (20 mL culture broth) at both 28 and 23°C, using methanol as carbon source and protein synthesis inducer.

Samples collected at 4 days already revealed the initial activity profiles of the secreted laccase. Among the colonies, BsiWI 21, PmeI 3, and PmeI 28 displayed moderate activities towards ABTS (shown in Figure 2.8). Colony BsiWI 8 was excluded due to the absence of significant activity detection, whereas the activity of colony BsiWI 14 was four-times lower than that of the others. In Figure 2.8a, the activity values have been reported as absolute activity (normalized per OD_{600} of cells). There was no detectable ABTS activity in the supernatant of wild-type *P. pastoris*. Despite the growth profiles being similar, including that of the wild-type *P. pastoris* it is worth noting that samples collected from cultures at 23 °C exhibited higher activity accumulation compared to those grown at 28 °C. This difference could possibly be attributed to the laccase's instability at higher temperatures or the difficulties associated with achieving a proper folding at elevated temperatures. Park and co-workers already investigated Lacc12 laccase production using another vector system at a higher temperature. Our activity profiles of Lacc12 detected at fourth and fifth day of fermentation is in the values that they reported before optimizing their system.[360]

---

[359] (a) F. Hong, N. Q. Meinander, L. J. Jönsson, *Biotechnol. Bioeng.* **2002**, *79*, 438–449; b) B. Gasser, M. Maurer, J. Rautio, M. Sauer, A. Bhattacharyya, M. Saloheimo, M. Penttilä, D. Mattanovich, *BMC Genomics* **2007**, *8*, 179; c) P. Li, A. Anumanthan, X.-G. Gao, K. Ilangovan, V. V. Suzara, N. Düzgüneş, V. Renugopalakrishnan, *Appl. Biochem. Biotechnol.* **2007**, *142*, 105–124.

[360] M. Park, M. Kim, S. Kim, B. Ha, H.-S. Ro, *Mycobiology* **2015**, *43*, 280–287.

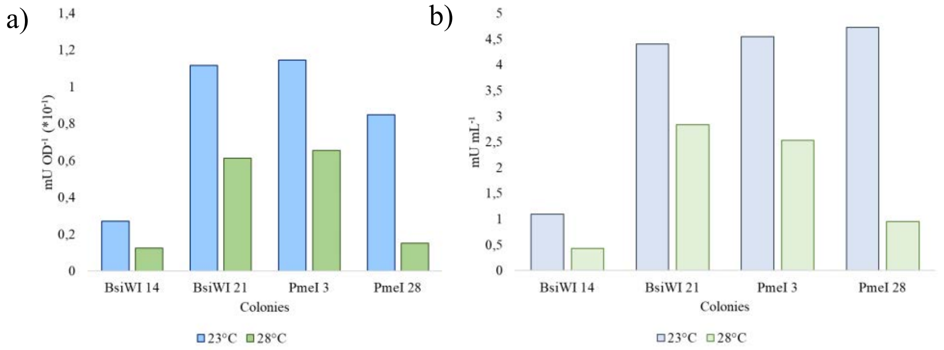

Figure 2.8. Lacc12 activity profile (supernatants) of the selected recombinant *P. pastoris* colonies: a) normalized, and b) non-normalized, for cellular optical density. Yeast cells were grown for 4 days either at 23 °C (blue lines) and 28 °C (green lines) with intermittent addition of 1.5% (v/v) methanol every 24 h.

The cultures were subsequently analyzed after 5 days of incubation. ABTS activity profiles of colonies grown at 28 °C resulted to be < 5.0 mU/mL, and thus, they are not presented. Similarly, the BsiWI 14 colony did not exhibit an increased laccase secretion, leading to its exclusion from further studies. On the other hand, BSIWI 21, PmeI 3, and PmeI 28 colonies grown at 23 °C accumulating the laccase in the range of 3.5–6.0 mU/mL (Figure 2.9). The necessity for lower temperatures for laccase production could potentially be attributed to the inaccurate folding of the laccase that can occur at higher temperatures.

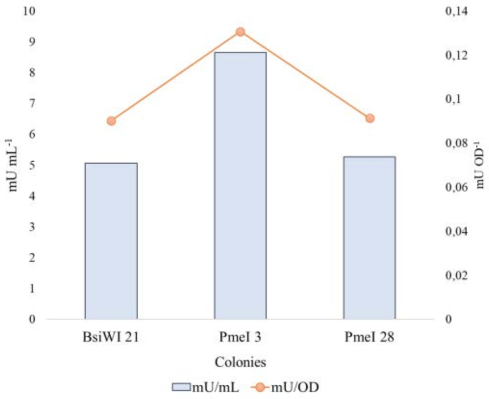

Figure 2.9. Lacc12 activity profile (supernatants) in the recombinant *P. pastoris* colonies after 5 days of fermentation at 23 °C.

The supernatants were subsequently subjected to dialysis, and SDS-PAGE gel electrophoresis was performed to visualize the protein overexpression and determine the apparent molecular weight (Figure 2.10). Based on these preliminary tests, the most promising Lacc12 producer appears to be PmeI 3, with the protein exhibiting an apparent size of 75 kDa.

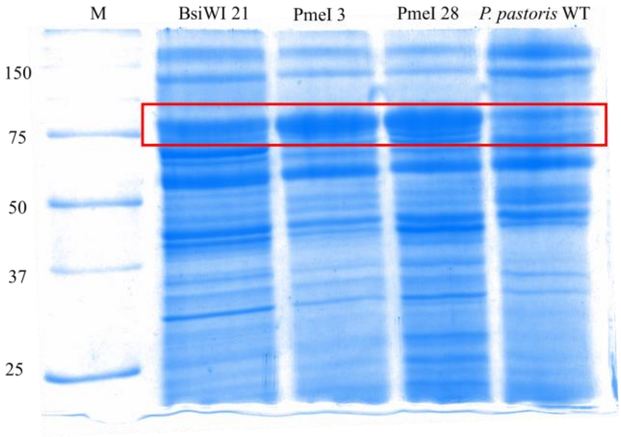

Figure 2.10. SDS-PAGE of the supernatants of the selected colonies (BsiWI 21, PmeI 3, and PmeI 28) compared with *P. pastoris* background. The overexpression is framed in red.

Experimental Section

2.3.1. General information

ABTS was purchased from AppliChem GmbH (Germany) and was used as the substrate to measure laccase activity. 2,6-DMS was obtained from Sigma Aldrich.

E. coli TOP10 cells were used for vector manipulation and amplification. *P. pastoris* cells were used for protein expression. The growth of both microorganisms was performed in different media reported below ("%" considered as w/v):

- LB low salt medium (*E. coli*, only when the vector carried on Zeocin resistance): 1% tryptone, 0.5% yeast extract, 0.5% NaCl, 1.5% agar.
- LB medium (*E. coli*, with vector carrying on geneticin resistance): 1% tryptone, 0.5% yeast extract, 1% NaCl, 1.5% agar.
- YPDS medium (*P. pastoris*, complex medium): 1% yeast extract, 2% peptone, 2% glucose, 1 M sorbitol, 2% agar.
- MD/MM minimal medium (*P. pastoris*, minimal medium for plate screening): 1.34% YNB (w/o amino acid, with ammonium sulfate), 4×10^{-5}% biotin, 2% glucose or glycerol for PJGG carrying vector clones, 0.5% methanol for pPICZB ones.
- BMGY/BMMY (*P. pastoris*, medium for flasks' growth): 1% yeast extract, 2% peptone, 100 mM potassium phosphate pH 6.0, 1.34% YNB (w/o amino acid, with ammonium sulfate), 4×10^{-5}% biotin, 1% glycerol or glucose for PJGG carrying vector clone, or 0.5% methanol for pPICZB ones.

Lysis buffer-BB used for *P. pastoris* cell lysis was the following: 50 mM sodium phosphate pH 7.4, 1 mM PMSF, 1 mM EDTA, 5% glycerol.

2.3.2. Lacc12 constitutive expression

pJGGαKR vectors carrying on the different Lacc12 sequences were obtained from GenScript Biotech (The Netherlands), and processed as follows.

2.3.2.1. Cloning vector

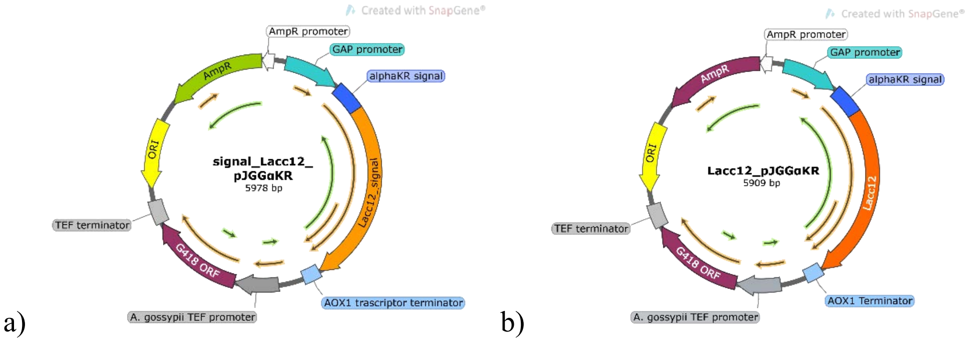
Created with SnapGene®
AmpR promoter
GAP promoter
alphaKR signal
AmpR
ORI
signal_Lacc12_
pJGGαKR
5978 bp
Lacc12_signal
TEF terminator
G418 ORF
A. gossypii TEF promoter
AOX1 trascriptor terminator
a)
Created with SnapGene®
AmpR promoter
GAP promoter
alphaKR signal
AmpR
ORI
Lacc12_pJGGαKR
5909 bp
Lacc12
TEF terminator
G418 ORF
A. gossypii TEF promoter
AOX1 Terminator
b)

Figure 2.11. pJGGαKR vectors with Lacc12 and Lacc12 signal.

The design of the expression vector was made with a free licence of SnapGene Viewer (Figure 2.11). The clonal genes syntheses with codon optimization for *Pichia* expression were purchased from GenScript. The features of the pJGGαKR vector are: G418 ORF: confers resistance to Geneticin; ORI: bacterial plasmid origin of replication; AmpR: β-lactamase coding gene which confers resistance to ampicillin; alphaKR signal: α-factor mating secretion signal for enzyme production in yeast; TEF1 promoter and terminator: promoter and terminator signals for EF-1α in *S. cerevisiae*; AOX1 terminator: terminator of the synthesis of AOX1 gene in *P. pastoris*, being the recognized sequence for the integration of the plasmid into the yeast genome; GAP promoter: inducible promoter, potentiated by glycerol.

2.3.2.2. DNA manipulation

The vector was linearized in order to be used for *P. pastoris* transformation. The hydrolysis reaction was performed separately using 10 U of enzyme each µg of DNA for a total amount of 4 µg of vector, and incubated with buffer NEB3.1 at 55 °C for 4 h. After verifying the complete vector hydrolysis by Agarose gel electrophoresis, the linear vector was purified with QIAquick Gel Extraction Kit from Quiagen as specified by the manufacturer. The agarose gel (0.8% agarose in TAE buffer) was stained with GelRed intercalant agent. The electrophoresis was conducted in TAE (40 mM Tris-acetate, 1 mM EDTA, pH 8) at 80 V, and the gel was finally revealed under UV by using ChemiDoc gel imaging system.

2.3.2.3. Pichia pastoris: Recombinant laccase production

The protocol for inducing the competence in *P. pastoris* cells is reported herein: 5 mL of YPD in 15-mL conical tube was inoculated with one well-isolated colony off a fresh YPD agar; the inoculum was kept at 30 °C and 200 rpm overnight. The cells were diluted into 25 mL of fresh YPD to a starting concentration of OD_{600} <0.2 and grow at 30 °C, 200 rpm for almost 5.30 h in a baffled 250-mL flask. Cells were then harvested at an OD_{600} of approx. 1.5. Culture was kept on ice for 15 min. Cooled cells were centrifuged at 4 °C and 2.000 rpm for 5 min and re-suspended in 2 mL YPD-Hepes (1.6 mL YPD + 0.4 mL 1 M Hepes pH 6.8). 75 µL freshly made 1 M 1,4-dithiothreitol (DTT) to the YPD/Hepes/cell suspension was slowly added and cells rocked at 100 rpm for 25 min at 28 °C. Samples containing DTT were diluted by adding 40 mL ice-cold water in a 50-mL Falcon tube, and cells kept at 0–4 °C. Then, cells were pelleted twice by centrifugation at 2,200 rpm for 5 min in a refrigerated centrifuge at 4 °C, and the supernatant discarded. The preparation was washed in sterile, ice-cold 1 M sorbitol twice and cells re-suspended in 20 mL of 1 M sorbitol, centrifuged as above and the supernatant well discarded. 300 µL of ice-cold 1 M sorbitol was added to the final pellet and the cells were re-suspended completely. The final cell suspension was kept on ice. These competent cells were used immediately, or frozen in chilled tubes for storage at −80 °C for approx. 6 months.[361]

Electroporation was selected for cloning the expression vectors into *P. pastoris* cells as linear DNA molecules. The DNA "ends" facilitate integration into the *P. pastoris* genome to create a stable expression strain by a single "cross-over" event. PJGGαKR vector is linearized at the BsiWI site in the AOX1 terminator, and it is integrated into the AOX1 terminator site in the yeast genome resulting also in a duplication of the terminator sequence.

PJGGαKR vector has been linearized at the BsiWI site in the AOX1 terminator (AOX promoter has been replaced with GAP promoter), and it is integrated into a multiple AOX1 terminator site in the yeast genome resulting also in a duplication of the terminator sequence. PJGGαKR vectors are preserved in *E. coli* TOP10 cells. After plasmid isolation from 20 mL of *E. coli* TOP10 cell culture, the vector is linearized with a BsiWI restriction enzyme, purified, the right concentration was achieved with ethanol precipitation protocol up to an appropriate concentration for the following steps, and used for transforming *P. pastoris* competent cells according to the following protocol:

- Add DNA (300–1000 μg) to thawed competent cells. DNA volumes up to 5 μL per 30 μL of E-comp cells are recommendable for higher transformation yields, as larger volumes may result in lower numbers of transformants. Most importantly, reduce the amount of salt/ions added to the E-comp cells.

- Mix gently and transfer the entire sample to an ice-cold sterile electroporation cuvette. Keep the cuvette/sample on ice.

- Rapidly, remove the sample cuvette from the ice and place it between the electrodes in the "shock chamber" of the electroporation device, activate and discharge the device.

---

[361] K. Madden, I. Tolstorukov, J. Cregg, in *Genetic Transformation Systems in Fungi*, (Eds.: M. A. van den Berg, K. Maruthachalam), Vol. 1, Springer International Publishing, Cham (Switzerland), **2015**, pp. 87–91.

- After the electroporation discharge, add approx. 1 mL of *Pichia* Electroporation Recovery Solution (PERS) to the cuvette, mix it with the cells and then transfer the sample from the cuvette to a sterile 2-mL micro-centrifuge tube for incubation.

- Incubate the samples at 28–30 °C, shaking at 100 rpm for 3 h.

- Spread the cells onto YPD-agar plates with G418 antibiotic (0.9 mg/mL) for the selection.

- Incubate the plates at 30 °C for 2–3 days.

2.3.3. Lacc12 inducible expression

Lacc12 sequence with its intrinsic secretion signal at N-termini was synthesized in commercial PMK vector and kept in TOP10 competent cells (Figure 2.12). The gene was properly designed in order to allow its cloning into the expression plasmids after sequential hydrolysis with EcoRI-KpnI restriction enzymes.

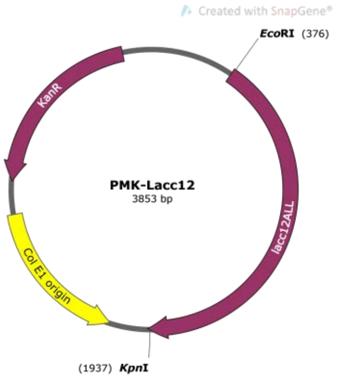

Figure 2.12. The characteristic elements of PMK vector are: KanR: confers bacterial resistance to kanamycin; and Col E1 origin: bacterial plasmid origin of replication.

2.3.3.1. Cloning vector

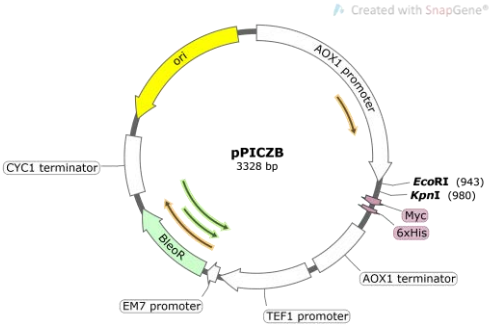
Created with SnapGene®
ori
AOX1 promoter
pPICZB
3328 bp
CYC1 terminator
EcoRI (943)
KpnI (980)
Myc
6xHis
BleoR
AOX1 terminator
EM7 promoter
TEF1 promoter

Figure 2.13. pPICZB empty vector.

The characteristic elements of pPICZB vector (Figure 2.13) are: BleoR: phleomycin coding gene from *Streptoalloteichus hindustanus*, conferring resistance to Zeocin®; ORI: bacterial plasmid origin of replication; TEF1 promoter and CYC1 terminator: promoter and terminator signals for EF-1α in *S. cerevisiae* transcription and terminator for CYC1; EM7 promoter: synthetic bacterial promoter; AOX1 promoter and terminator: strong methanol inducible promoter and terminator of the synthesis of AOX1 gene in *P. pastoris*, being the recognized sequences for the integration of the plasmid into the yeast genome; Myc: Myc (human c-Myc oncogene) epitope tag; and 6xHis: 6xHis epitope tag.

It is worthy to mention that microorganisms (both yeast or bacteria) carrying this vector achieve the ability to grow in presence of Zeocin® at different concentrations (25 µg/mL for bacteria, 100–2000 µg/mL for yeast).

2.3.3.2. DNA manipulation

pPICZB empty vector (3328 Kb) and the Lacc12 gene (1561 Kb) were restricted with EcoRI-KpnI in two sequential steps (Figure 2.14). The Lacc12 gene was cloned into pPICZB under the control of AOX1 promoter with a ligase event *in vitro*. *E. coli* TOP10 recombinant cells were transformed with the ligated product for assuring vector preservation and amplification prior to *P. pastoris* recombinant construction. 6 colonies were selected for confirming the success of the ligation event and grown in 3 mL of LB low salt with Zeocin®. The presence of the insert in the vector was verified by PCR (primers designed on the sequence of Lacc12 gene). After growing the clone in 50 mL LB-MS broth, a great amount of the final recombinant plasmid pPICZB-Lacc12 (4852 Kb) was isolated using Quiagen MiniPrep Kit as reported by the supplier.

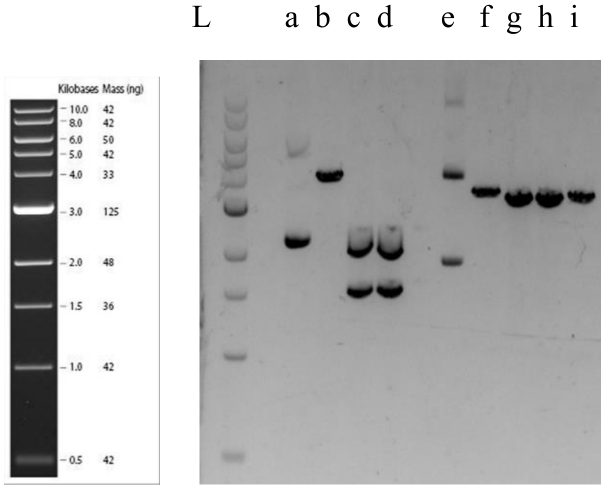

Figure 2.14. Agarose gel on ligase products. L: Ladder, molecular marker; a: PMK-Lacc12; b: PMK-Lacc12 vector single cut with KpnI (3853 Kb); c-d: PMK-Lacc12 double cut with KpnI-EcoRI releasing Lacc12 gene (1561 Kb); e: empty pPICZB vector; f: single cut pPICZB vector with KpnI; g-i (3328 Kb): pPICZB double cut with KpnI-ECORI (3291 Kb).

The pure pPICZB vector was linearized in order to be used for *P. pastoris* transformation with two different restriction enzymes, BsiWI and PmeI, in order to verify which system allowed to have higher laccase expression. The former linearizes the vector in multiple AOX1 terminator, while the latter at AOX1 promoter, respectively.

The hydrolysis reaction was performed separately using 10 Units of enzyme each µg of treated DNA for a total amount of 4 µg of vector. BsiWI hydrolysis was performed in buffer NEB®3.1 at 55 °C for 4 h, PmeI hydrolysis in CutSmart® buffer at 37 °C for 4 h. After verifying the complete vector hydrolysis by agarose gel electrophoresis, the linear vector was purified with QIAquick Gel Extraction Kit from Quiagen as specified by the manufacturer. The agarose gel (0.8% agarose in TAE buffer) was stained with GelRed intercalant agent (Figure 2.14). The electrophoresis was conducted in TAE buffer (40 mM Tris-acetate, 1 mM EDTA, pH 8) at 80 V and the gel was finally revealed under UV by using ChemiDoc gel imaging system.

2.3.3.3. Pichia pastoris: Recombinant laccase production

pPICZB vector is preserved in *E. coli* TOP10 cells. After plasmid isolation from 20 mL of *E. coli* TOP10 cell culture, the vector was linearized with both relative restriction enzymes, purified, and both linear systems were used for transforming *P. pastoris* competent cells according to the protocol reported in Section 2.3.2.3.

30 single colonies from both growths were scraped from each system from 1:10 dilution plate, and tested at growing antibiotic concentrations (0.5 and 1 mg/mL) for qualitatively selecting the ones that had multiple integration events of the vector.

For liquid inoculum, all cultures were conducted in baffled flasks (1:5 volume medium-air) with 100 µg/mL of Zeocin® and incubated on rotary shakers at 28 °C and 180–200 rpm. The selected recombinant clones were scraped from YPDS plates and pre-inoculated in 3 mL BMGY medium. This pre-culture was overnight grown at 28 °C on a rotary shaker (250 rpm) and used to inoculate 100-mL shaken baffled flasks containing 20 mL of BMMY to get a starting OD_{600} value of 1.0. The pre-inoculum excess was kept at –80 °C in sterile glycerol 15% (v/v). Cells were grown up to for 7 days on a rotary shaker (250 rpm) at 28 °C, and culture supernatants periodically recovered and assayed for laccase activity. 1.5% methanol was daily added to the culture to induce protein expression and compensate solvent evaporation. Small-scale expression conditions may not be optimal for all the proteins. For this reason, apart from ABTS assay, SDS-PAGE (combined with Comassie or Silver stain) was used for determining in a first asset, the success of expression.

2.3.4. *P. pastoris* cell lysis

Cells were pelleted at 5,000 rpm, after 30 min and 4 °C. Supernatants were dialyzed and concentrated as described below, and cell pellets were kept on ice. Pellets were then washed in 400 µL of BB, and re-suspended in BB (20 µL per 1.0 OD_{600} cells). An equal volume of acid-washed glass beads was added (size 0.5 mm, 200 mg, until only a meniscus is visible). It should be estimated an equal volume by displacement. Cells were vortexed 30 s, then incubated on ice for 30 s for 8 total vortexing cycles (4 min). Cells were boiled for 5 min and pelleted at maximum speed for 10 min at 4 °C. The clear supernatant was transferred to a fresh microcentrifuge tube. The vortex step was repeated again adding other 100 µL of BB to residual cell pellets. All the recovered supernatants were joined and assayed with the Bradford assay for estimating the total amount of total proteins. In general, *Pichia* cell lysates should contain 5–10 µg/mL of protein.

2.3.5. Protein manipulation: Laccase assays and SDS-PAGE gel

ABTS assay was performed as reported in 1.3.3. Laccase activity towards DMP was assayed in a mixture containing 1 mM DMP in the McIlvaine's citrate-phosphate buffer adjusted to pH 5.0. Oxidation of DMP was followed by absorbance increase at 477 nm (ε_{477}= 14800 M^{-1} cm^{-1}).[362]

For the ABTS plate assay for assessing the constitutive expression of Lacc12, recombinant clones of *P. pastoris* were obtained on solid YPD medium with G418 antibiotic (0.9 mg/mL) and supplemented with 0.2 mM ABTS: each colony was scraped from the YPD selective agar and plated onto a ABTS selective plate. Plates were incubated at 28 °C for at least 3 days, and positive colonies showing oxidative halo (dark purple) were propagated. Recombinant cells transformed with the same plasmid carrying on an active laccase (POXA1b) was used as positive control.

---

[362] H. Wariishi, K. Valli, M. H. Gold, *J. Biol. Chem.* **1992**, *267*, 23688–23695.

Plate assays for assessing Lacc12 inducible expression were performed on solid minimal MM medium with Zeocin® antibiotic (0.1 mg/mL) and supplemented with 0.2 mM ABTS and 0.6 mM $CuSO_4$ for helping to preserve the laccase folding: around 30 colonies for each linearized system (BsiWI and PmeI) were scraped from the YPD selective agar and plated onto YPDS selective plates at higher antibiotic concentration first and then onto ABTS selective ones. Plates were incubated at 28 °C for at least 5 days, until positive colonies showed oxidative halo (green). 100 μL of pure methanol were added daily to the plate lid in order to compensate the solvent evaporation within the days. The first colonies oxidizing ABTS on plate were selected for propagation. Recombinant cells transformed with the same plasmid carrying on an active laccase (POXA1b) were used as positive control.

For protein visualization onto SDS-gel, cell supernatants were dialyzed against Trizma buffer, 50 mM pH 7.5, for removing the salts and concentrated 10X with Amicon® Ultra-5 KDa MCWO. Cell pellets were lysed as reported above. 20 μL of supernatant or recovered cell lysate were mixed with 5 μL 5X SDS-PAGE Gel Loading buffer (Sample Buffer). The samples (7–15 μg of total protein, measured by the Bradford assay) were boiled for 10 min, and maximum 20 μL were loaded per well onto 10% acrylamide in TRIS/glycine buffer gel. Polyacrylamide (10%) gel electrophoresis in 0.1% SDS was carried out as described by Laemmli.[363] The same samples were loaded twice: one gel was then stained (Comassie or silver staining).

---

[363] U. K. Laemmli, *Nature* **1970**, *227*, 680–685.

Second part

Bienzymatic cascades to obtain valuable furan derivatives

CHAPTER 3

Valorization of furfuryl alcohol via oxidation towards furfural using laccases followed by biotransamination towards furfuryl amine

Introduction

Furfuryl amine (**1d**), in particular, serves as an essential building block in the synthesis of various pharmaceuticals and agrochemicals.[364] **1d** can be synthesized from amination of furfural (**1b**), which can be obtained directly from biomass sources or chemically through the oxidation of furfuryl alcohol (**1a**). Beyond its role in resins, solvents, and agricultural chemicals, **1a** can also serve as a valuable substrate for **1b** synthesis through the oxidation of its alcohol moiety.[365] Additionally, the pursuit of selective and sustainable enzymatic approaches for the production of furan derivatives holds immense appeal. This is because biocatalysts offer enhanced selectivity and specificity compared to chemical reagents, and they operate under environmentally friendly reaction conditions.

Apart as intermediate in the amine synthesis, **1b** offers unique opportunities as chemical platform for other high-added value compounds. Traditionally, the difficulty in achieving aldehyde **1b** formation via oxidation consists of its susceptibility to overoxidation, leading to the accumulation of 2-furoic acid (**1c**), being a challenging process that deserves further investigation and requires optimization (Scheme 3.1).[366]

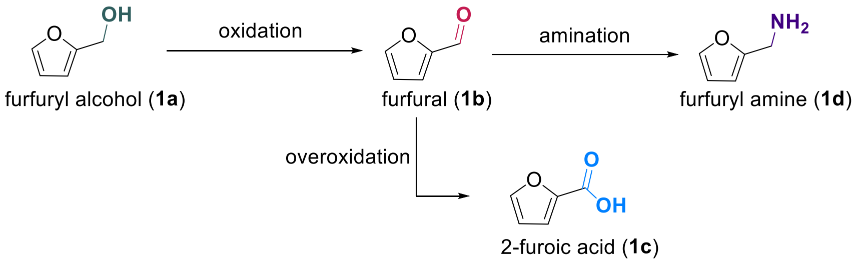

Scheme 3.1. Possible chemical approaches for the synthesis of furfural (**1b**), 2-furoic acid (**1c**), and fufuryl amine (**1d**) from furfuryl alcohol (**1a**).

---

[364] J. Zhu, G. Yin, *ACS Catal.* **2021**, *11*, 10058–10083.

[365] G. Gómez Millán, H. Sixta, *Catalysts* **2020**, *10*, 1101.

[366] a) J. J. Dong, E. Fernández-Fueyo, F. Hollmann, C. E. Paul, M. Pesic, S. Schmidt, Y. Wang, S. Younes, W. Zhang, *Angew. Chem. Int. Ed.* **2018**, *57*, 9238–9261; b) N. Li, M. H. Zong, *ACS Catal.* **2022**, *12*, 10080–10114.

3.1.1. Transferases

Transferases (EC2) are a group of enzymes responsible for the transfer of a functional group from one molecule to another. The diversity of functional groups transferred and the range of reactions catalyzed by transferases underscore their significance in biochemistry and molecular biology. Enzymes belonging to this family, in fact, are involved in maintaining cellular homeostasis, regulating biological processes, and ensuring the proper functioning of living organisms.

Amongst the functional groups that enzymes from this class can transfer, the most significant ones include:

- Phosphate groups ($-PO_4^{3-}$): Kinases are the enzymes involved in the transfer of phosphate groups from ATP, crucial in cellular signalling.

- Methyl groups ($-CH_3$): Methyltransferases shuttle methyl groups, vital for epigenetic modifications and gene expression regulation.

- Amino groups ($-NH_2$): Aminotransferases transfer amino groups in amino acid metabolism.

- Acyl groups (-COR): Acyltransferases shuttle acyl groups, central in lipid metabolism.

- Sugar residues: Glycosyltransferases transfer sugar moieties, essential in carbohydrate and glycoprotein biosynthesis.

With respect to nomenclature, the second digit within the code number assigned to transferases conveys information about the general type of functional group being transferred (“2.1”: one-carbon group; "2.2" aldehydic or ketonic group, "2.3" acyl group). Meanwhile, the third digit in the code provides additional details about that specific group (i.e., 2.1.1" for methyltransferases and "2.1.2" for formyltransferases). An exception is the case of enzymes that transfer phosphorus-containing groups (2.7): the third digit serves to specify the nature of the acceptor group rather than the transferred group.

In many cases, the donor of the reaction is a cofactor (or coenzyme) linked with the group to be transferred. A special case is that of the transaminases (EC 2.6.1), used in this study.

3.1.1.1. Transaminases (TAs)

Transaminases (TAs) or aminotransferases belong to the group of transferases and catalyze the reversible transfer of an amino group from a donor (usually a primary amine) to an acceptor (a carbonyl compound such as a ketone, an aldehyde, or a keto acid), needing pyridoxal 5'-phosphate (PLP) as cofactor, a form of vitamin B6 covalently bound in the enzyme active site (Scheme 3.2).[367]

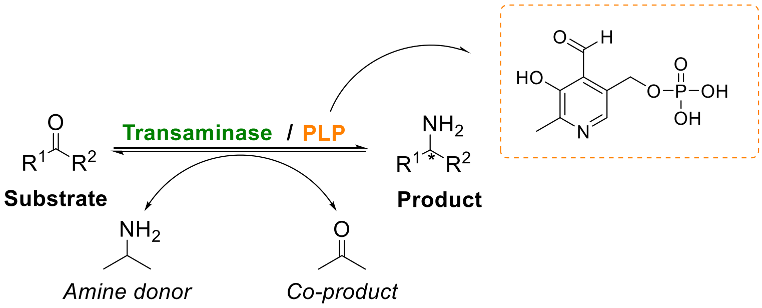

Scheme 3.2. The typical reaction carried out by ATAs involving the reversible transfer of the amino group from an amine donor to an acceptor molecule (carbonyl compound), with the aid of PLP as cofactor.

The origins of transamination can be traced to 1930 when Needham and colleagues first noticed the connection between the levels of amino acids like L-glutamic acid and L-aspartic acid in the breast muscles of pigeons.[368] Since them, researchers focused on investigating the reaction mechanism of TAs[369] and identifying the specific substrates with the objective to exploit their potential in amination and cascade reactions.[370] With advancements in structural biology, an expanding database of three-dimensional ATA structures was discovered, accompanied by a precise mapping of their active sites.[371] Moreover, ATAs engineering was utilized to improve enzymatic stability and activity towards various substrates.[372] These findings have strengthened the application of TAs across multiple sectors.[373]

---

[367] I. Slabu, J. L. Galman, R. C. Lloyd, N. J. Turner, *ACS Catal.* **2017**, *7*, 8263–8284.

[368] D. M. Needham, *Biochem. J.* **1930**, *24*, 208–227.

[369] K. E. Cassimjee, B. Manta, F. Himo, *Org. Biomol. Chem.* **2015**, *13*, 8453–8464.

Transaminases can be classified into three major groups based on the nature of the substrate they can act on. First, α-transaminases (α-TAs), highly specific, only accept substrates that have a carboxylic acid group at the α position to the amino group. On the other hand, ω-transaminases (ω-TAs) transfer amino groups to/from terminal positions that are separated by at least one carbon atom from the carboxylic acid group. Finally, amine transaminases (ATAs) represent the most versatile category as they can work with carbonyl substrates without necessitating the presence of a carboxylic acid group in the molecule. Therefore, the latter are the most commonly used in organic synthesis.

PLP-dependent enzymes fall into seven different fold-types (I–VII). Although these enzymes exhibit broad substrate specificities, ω-transaminases are present in only two distinct classes: (*S*)-selective enzymes, which are categorized under protein fold-type I, and (*R*)-selective enzymes, which belong to protein fold-type IV.[374]

---

[370] a) M. Fuchs, J. E. Farnberger, W. Kroutil, *Eur. J. Org. Chem.* **2015**, *2015*, 6965–6982; b) H. Land, P. Hendil-Forssell, M. Martinelle, P. Berglund, *Catal. Sci. Technol.* **2016**, *6*, 2897–2900.

[371] a) J.-S. Shin, B.-G. Kim, *J. Org. Chem.* **2002**, *67*, 2848–2853; b) F. Steffen-Munsberg, C. Vickers, A. Thontowi, S. Schätzle, T. Tumlirsch, M. S. Humble, H. Land, P. Berglund, U. T. Bornscheuer, M. Höhne, *ChemCatChem* **2013**, *5*, 150–153; c) N. van Oosterwijk, S. Willies, J. Hekelaar, A. C. T. van Scheltinga, N. J. Turner, B. W. Dijkstra, *Biochemistry* **2016**, *55*, 4422–4431.

[372] M. S. Weiß, I. V. Pavlidis, P. Spurr, S. P. Hanlon, B. Wirz, H. Iding, U. T. Bornscheuer, *ChemBioChem* **2017**, *18*, 1022–1026.

[373] a) E. E. Ferrandi, D. Monti, *World J. Microbiol. Biotechnol.* **2018**, *34*, 13; b) S. A. Kelly, S. Pohle, S. Wharry, S. Mix, C. C. R. Allen, T. S. Moody, B. F. Gilmore, *Chem. Rev.* **2018**, *118*, 349–367.

3.1.1.2. General reaction mechanism

In 2002, Shin and Kim proposed the architecture of a TA active site by examining the connection between substrate structure and reactivity. They utilized a transaminase sourced from *Vibrio fluvialis* JS17 for their analysis.[371a] ATAs are active either as homo dimers or in higher oligomeric forms. Each monomer has a single active site located at the junction of the two subunits with amino acid residues from both monomers involved into its architecture, assessing its functionality.[375] Each active site is characterized by a region for binding the cofactor (phosphate group binding cup) and a region for binding the substrate.[376] To account for substrate specificity and stereoselectivity, a two-site attaching model for the substrate-binding region was suggested. This model comprises both a large (L) pocket and a small (S) pocket. Typically, the L pocket can accommodate larger substituents, with hydrophobic and carboxylate groups, whereas the S pocket is limited to accepting a small group (Figure 3.1). The S pocket was found to be critical in substrate recognition, more than in catalytic performance, preventing bulky substituents from binding.[377] Consequently, efforts in rational design often focus on modifying the S binding pocket to accept bulkier substituents.[378]

---

[374] K. Szmejda, T. Florczak, I. Jodłowska, M. Turkiewicz, *Biotechnol. Food Sci.* **2017**, *81*, 23–34.

[375] M. S. Humble, K. E. Cassimjee, M. Håkansson, Y. R. Kimbung, B. Walse, V. Abedi, H.-J. Federsel, P. Berglund, D. T. Logan, *FEBS J.* **2012**, *279*, 779–792.

[376] A. I. Denesyuk, K. A. Denessiouk, T. Korpela, M. S. Johnson, *Biochim. Biophys. Acta-Proteins Proteomics* **2003**, *1647*, 234–238.

[377] E. S. Park, J. S. Shin, *Enzyme Microb. Technol.* **2011**, *49*, 380–387.

[378] a) L. Skalden, C. Peters, J. Dickerhoff, A. Nobili, H.-J. Joosten, K. Weisz, M. Höhne, U. T. Bornscheuer, *ChemBioChem* **2015**, *16*, 1041–1045; b) D. X. Jia, C. Peng, J. L. Li, F. Wang, Z. Q. Liu, Y. G. Zheng, *Appl. Biochem. Biotechnol.* **2021**, *193*, 3624–3640; c) S. J. Novick, N. Dellas, R. Garcia, C. Ching, A. Bautista, D. Homan, O. Alvizo, D. Entwistle, F. Kleinbeck, T. Schlama, T. Ruch, *ACS Catal.* **2021**, *11*, 3762–3770.

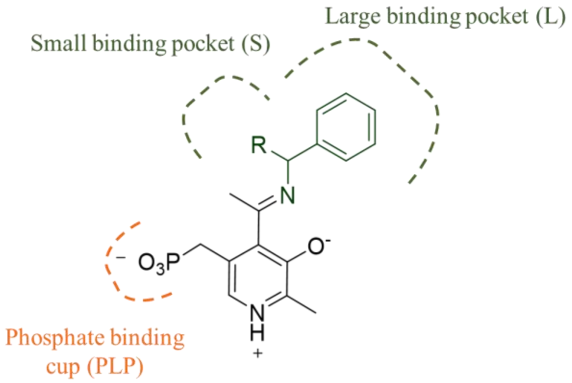

Figure 3.1. General active site architecture of an ATA with a substrate and the PLP cofactor bound during the transference of the amino group.

The reaction mechanism of TAs has been extensively investigated for aspartate aminotransferase; nevertheless, it can be extended to other types of TAs. They follow a ping-pong bi-bi catalytic reaction mechanism, which can also be viewed as the action of two separate half-transaminations: the first oxidative deamination of the amine donor and the following reductive amination of an amine acceptor (Scheme 3.3, green and purple sides, respectively).

First, PLP is covalently linked to the lysine residue within the active site of the transaminase through an imine bond, resulting in the formation of the internal aldimine intermediate. The stability of this intermediate is reinforced by the presence of either aspartate (Asp) or glutamate (Glu).[379] The amine donor initially binds to the active site of the enzyme and it undergoes a transaldimination with the amino group donor (for example, L-alanine), forming an external aldimine (1). This leads to the transfer of the amino group from alanine to the PLP-transaminase complex. Subsequently, the free lysine of the active site facilitates the isomerization of the double bond in the external aldimine, resulting in the formation of a ketimine (2). This intermediate undergoes a hydrolysis process, and pyridoxamine 5’-phosphate (PMP) and the co-product of the transamination process (pyruvic acid, in this case) are produced (green side of Scheme 3.3). Once the co-product is released, PMP links to the amine acceptor (a ketone, for example), leading to the formation of a new ketimine intermediate (3), which is then converted into an external aldimine through isomerization, aided by the catalytic lysine (4, Scheme 3.3, purple side). Finally, the external aldimine reacts with the catalytic lysine, producing the transamination product, with the regeneration of PLP ready for a following cycle. Thus, only catalytic amounts of this cofactor are required for transaminase reactions.[369]

---

[379] A. C. Eliot, J. F. Kirsch, *Annu. Rev. Biochem.* **2004**, *73*, 383–415.

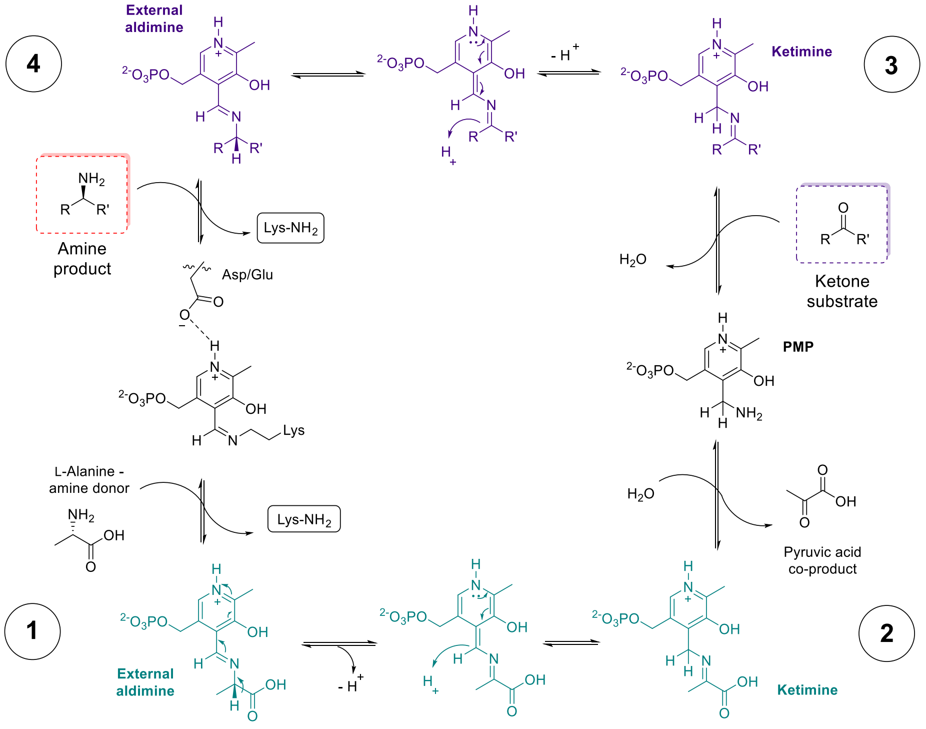
External aldimine
4
- H+
Ketimine
3
Amine product
Lys-NH2
Asp/Glu
H2O
Ketone substrate
PMP
Lys
L-Alanine - amine donor
Lys-NH2
H2O
Pyruvic acid co-product
1
External aldimine
- H+
Ketimine
2

Scheme 3.3. Transaminase reaction mechanism using L-alanine as amine donor. The lysine in the scheme is the catalytic lysine in the ATA active site.

3.1.1.3. Thermodynamic aspects of the transamination reaction

The thermodynamic efficiency of this reaction depends on the energy levels between the pairs of amine donor and amine acceptor, as well as the target product and carbonyl co-product. It is common knowledge that the transamination of a carbonyl compound using an amino acid as the amine donor is thermodynamically unfavorable.[380] Therefore, a shift of the reaction equilibrium towards the amine compound direction is necessary. The choice of the amine donor can play a crucial role; as well, the removal of products *in situ* or the utilization of cascade reactions, have effectively tackled the hinders of the unfavorable reaction equilibrium for amine synthesis.

As such, the most widely employed amine donor is alanine, the natural amino group donor of many transaminases. As universal donor, alanine is accepted from almost every wild-type TA. The co-product of transamination reaction is pyruvic acid. However, the accumulation of pyruvic acid at high concentrations inhibits the enzyme.[381] To shift the reaction equilibrium in the desired direction, several enzymatic methods have been developed based on the quasi-irreversible conversion of pyruvate.[382] As examples, alanine dehydrogenase (AlaDH) has been used for regenerating again alanine from pyruvic acid, ensuring a continuous supply of the amine donor (Scheme 3.4a).[383] Thus, the cost of the amine donor can be reduced up to 97%, and the *E*-factor decreased with improvements in the atom efficiency.[384] However, it requires other enzymes (like glucose dehydrogenase) to regenerate the nicotinamide cofactor used by AlaDH. Otherwise, lactate dehydrogenase (LDH) can be used to reduce pyruvic acid into lactic acid using NAD(P)H and its regeneration system (Scheme 3.4c).[385] In these examples, the use of additional enzymes for regenerating the cofactors leads to further complications of the overall biocatalytic process. Another strategy is the removal of pyruvic acid by decarboxylation catalyzed by pyruvate decarboxylase (PDC), thus yielding CO_2 and acetaldehyde (Scheme 3.4c).[386] Without the need of an external cofactor, and due to CO_2 volatility, the latter should be the most convenient choice, driving the reaction equilibrium in the desired direction almost irreversibly.[387] However, the presence of the acetaldehyde as by-product can inhibit the TA or might get aminated itself, yielding another undesired side product (ethanamine), thereby decreasing the efficiency of the reaction.

---

[380] a) P. Tufvesson, J. S. Jensen, W. Kroutil, J. M. Woodley, *Biotechnol. Bioeng.* **2012**, *109*, 2159–2162; b) M. T. Gundersen, R. Abu, M. Schürmann, J. M. Woodley, *Tetrahedron: Asymmetry* **2015**, *26*, 567–570; c) B. Manta, K. E. Cassimjee, F. Himo, *ACS Omega* **2017**, *2*, 890–898.

[381] a) M. S. Malik, E.-S. Park, J.-S. Shin, *Appl. Microbiol. Biotechnol.* **2012**, *94*, 1163–1171; b) F. Steffen-Munsberg, C. Vickers, H. Kohls, H. Land, H. Mallin, A. Nobili, L. Skalden, T. van den Bergh, H.-J. Joosten, P. Berglund, M. Höhne, U. T. Bornscheuer, *Biotechnol. Adv.* **2015**, *33*, 566–604.

[382] R. C. Simon, N. Richter, E. Busto, W. Kroutil, *ACS Catal.* **2014**, *4*, 129–143.

[383] D. Koszelewski, I. Lavandera, D. Clay, G. M. Guebitz, D. Rozzell, W. Kroutil, *Angew. Chem. Int. Ed.* **2008**, *47*, 9337–9340.

[384] N. Richter, J. E. Farnberger, D. Pressnitz, H. Lechner, F. Zepeck, W. Kroutil, *Green Chem.* **2015**, *17*, 2952–2958.

Apart from alanine, isopropylamine (IPA) has emerged as an interesting amine donor industrial choice; it is cheaper and it lacks chirality, being able to be used with both (*S*)- and (*R*)-selective ATAs. Moreover, there is no need for additional enzymes to manage with pyruvic acid, since the only resulting co-product is acetone (Scheme 3.4d). Both compounds, residual amine donor and co-product, can be later on easily removed due to their low boiling points, which facilitates downstream in scaling-up processes (for IPA, 32 °C; for acetone, 56 °C).[388] However, when using IPA as amine donor, a large molar excess (>40 equivalents) is needed to shift the reaction equilibrium towards the desired amine formation, unless acetone is *in situ* removed.[389] Additionally, effectively eliminating low concentrations of acetone (<100 mM) from a reaction, without removing other volatile substances, is challenging. Moreover, IPA can be used only with a limited number of natural transaminases, due to its small size and strong nucleophilicity which can interfere with active site's amino acids, potentially causing inhibition at high amine concentrations. To tackle these challenges, many natural transaminases have undergone genetic modifications using molecular biology techniques. These alterations have enabled these enzymes to catalyze various reactions using IPA as the amine donor.[390]

---

[385] A. Telzerow, J. Paris, M. Håkansson, J. González-Sabín, N. Ríos-Lombardía, H. Gröger, F. Morís, M. Schürmann, H. Schwab, K. Steiner, *ChemBioChem* **2021**, *22*, 1232–1242.

[386] M. D. Truppo, N. J. Turner, J. D. Rozzell, *Chem. Commun.* **2009**, 2127–2129.

[387] M. Höhne, S. Hühl, K. Robins, U. T. Bornscheuer, *ChemBioChem* **2008**, *9*, 363–365.

[388] P. Kelefiotis-Stratidakis, T. Tyrikos-Ergas, I. V. Pavlidis, *Org. Biomol. Chem.* **2019**, *17*, 1634–1642.

[389] P. Tufvesson, C. Bach, J. M. Woodley, *Biotechnol. Bioeng.* **2014**, *111*, 309–319.

---

[390] A. W. H. Dawood, M. S. Weiß, C. Schulz, I. V. Pavlidis, H. Iding, R. O. M. A. de Souza, U. T. Bornscheuer, *ChemCatChem* **2018**, *10*, 3943–3949.

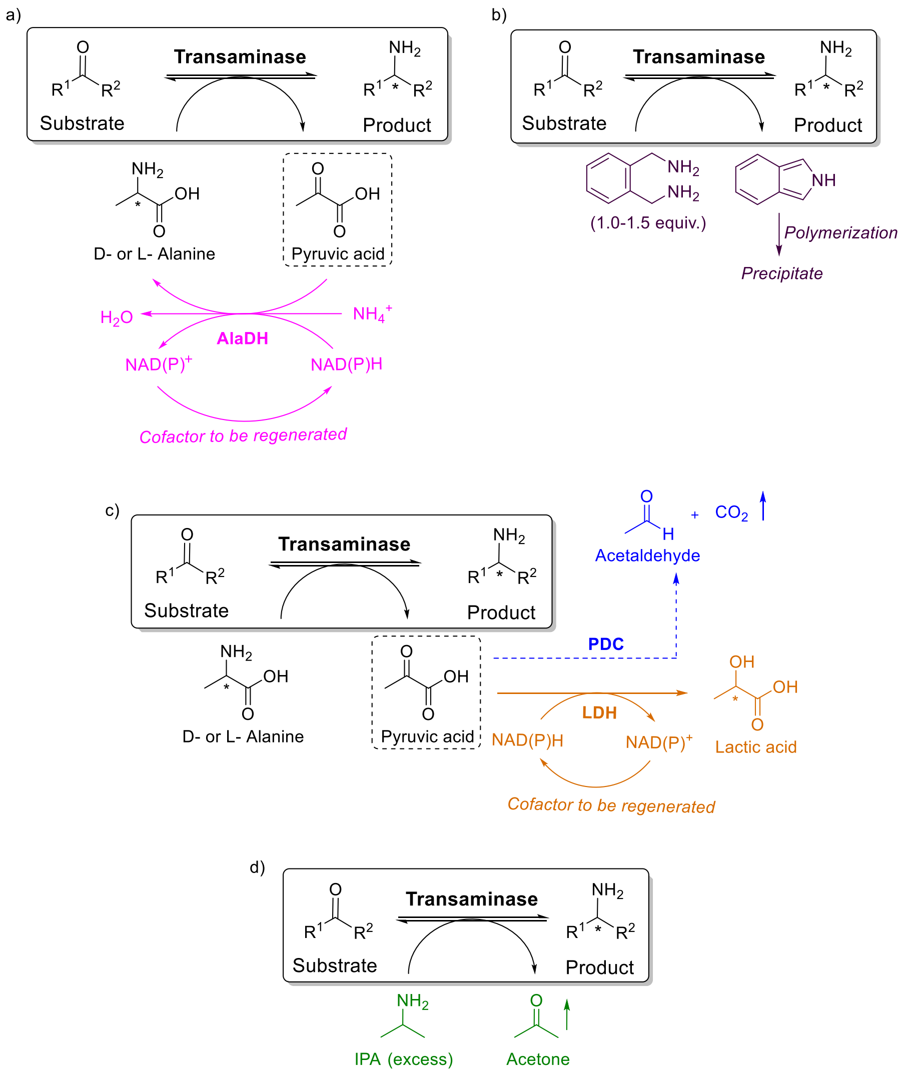
a)
Transaminase
Substrate
Product
D- or L- Alanine
Pyruvic acid
H2O
NH4+
AlaDH
NAD(P)+
NAD(P)H
Cofactor to be regenerated
b)
Transaminase
Substrate
Product
(1.0-1.5 equiv.)
Polymerization
Precipitate
c)
Transaminase
Substrate
Product
D- or L- Alanine
Pyruvic acid
Acetaldehyde
CO2
PDC
LDH
NAD(P)H
NAD(P)+
Lactic acid
Cofactor to be regenerated
d)
Transaminase
Substrate
Product
IPA (excess)
Acetone

Scheme 3.4. Different strategies used to shift the equilibrium of the transamination reaction towards the amination product.

In recent years, research has also focused on alternatives to alanine and IPA in biotransamination reactions, the so-called *smart amine donors*. Diamines have been commonly employed, such as xylylenediamine (XDA, Scheme 3.4b), and the biological derivatives putrescine, cadaverine, and spermidine. They are required in nearly equimolar amounts compared to the carbonyl substrate, since these types of donors undergo spontaneous cyclization or polymerization once the transamination is completed.[391] Thus, they can shift the chemical equilibrium of the reaction toward the formation of the amine in a quasi-irreversible manner. The by-product can easily be removed from the reaction mixture due to precipitation.

3.1.1.4. Amine transaminases in industry

Transaminases have attained much attention because of their key biocatalytic role in chiral drug production. Around 40% of currently available pharmaceuticals, indeed, consist of compounds with at least one amine functionality, highlighting their crucial role in the pharmaceutical industry.[392] Hence, enzymatic synthesis of chiral pharmaceuticals using TAs provides an eco-friendly alternative to traditional chemical methods, such as asymmetric hydrogenation of a Schiff base, C−H insertion, diastereoisomeric crystallization, and nucleophilic addition.[392a,393] In essence, ATAs contribute significantly to the efficient and sustainable synthesis of key compounds used in pharmaceutical and agrochemical applications.

For preparative production of chiral amines and amino acids using TAs, different strategies can be applied, including the kinetic resolution of a racemic mixture with a theoretical yield of the enantioenriched product of ≤50%, and the asymmetric production of one single enantiomer from the corresponding prochiral ketone with up to 100% theoretical yield. Also, deracemization of a racemic mixture into one enantiomer in a theoretical yield of up to 100% can be designed using stereocomplementary TAs (Scheme 3.5).[394]

---

[391] a) A. Gomm, W. Lewis, A. P. Green, E. O'Reilly, *Chem. Eur. J.* **2016**, *22*, 12692–12695; b) S. E. Payer, J. H. Schrittwieser, W. Kroutil, *Eur. J. Org. Chem.* **2017**, *2017*, 2553–2559; c) C. A. McKenna, M. Štiblariková, I. De Silvestro, D. J. Campopiano, A. L. Lawrence, *Green Chem.* **2022**, *24*, 2010–2016.

[392] a) D. Ghislieri, N. J. Turner, *Top. Catal.* **2014**, *57*, 284–300; b) O. I. Afanasyev, E. Kuchuk, D. L. Usanov, D. Chusov, *Chem. Rev.* **2019**, *119*, 11857–11911.

[393] D. Sakamoto, I. Gay Sánchez, J. Rybáček, J. Vacek, L. Bednárová, M. Pazderková, R. Pohl, I. Císařová, I. G. Stará, I. Starý, *ACS Catal.* **2022**, *12*, 10793–10800.

[394] A. M. Bezborodov, N. A. Zagustina, *Appl. Biochem. Microbiol.* **2016**, *52*, 237–249.

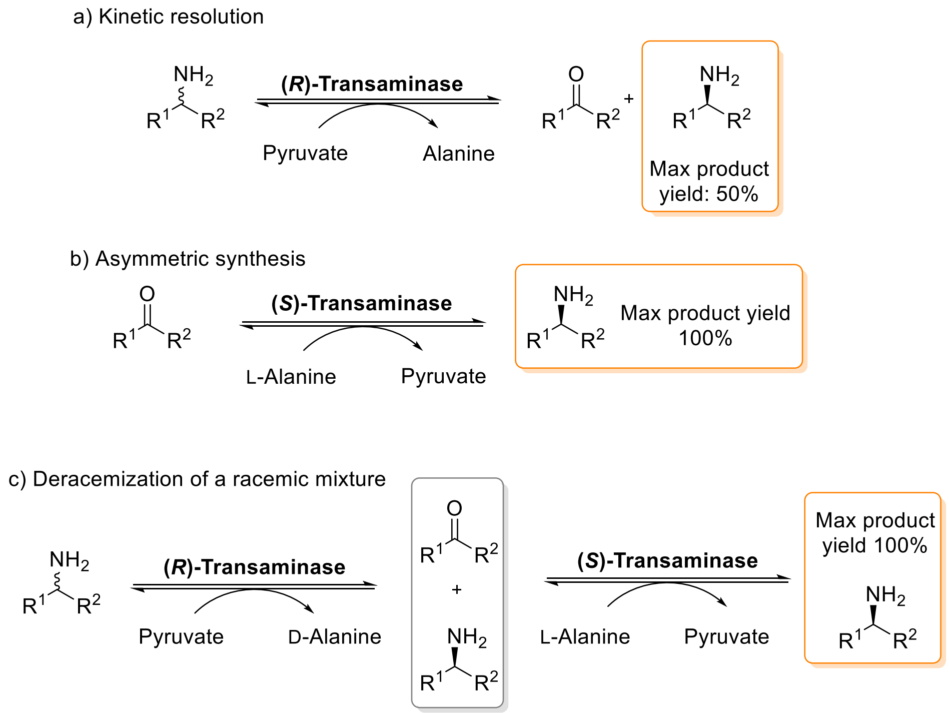
a) Kinetic resolution
NH2
R1
R2
(R)-Transaminase
Pyruvate
Alanine
O
+
Max product yield: 50%
b) Asymmetric synthesis
(S)-Transaminase
L-Alanine
Pyruvate
Max product yield 100%
c) Deracemization of a racemic mixture
(R)-Transaminase
Pyruvate
D-Alanine
(S)-Transaminase
L-Alanine
Pyruvate
Max product yield 100%

Scheme 3.5. TA-catalyzed reactions of interest in industry: a) Kinetic resolution of a racemic amine using, e.g. pyruvate as an amine acceptor; b) asymmetric synthesis of a chiral amine from a prochiral ketone using, e.g. L-alanine as amine donor; and c) deracemization of racemic amines using stereocomplementary TAs.

The most representative example of a TA application in the pharmaceutical sector is the production of the antidiabetic drug sitagliptin. In this scenario, researchers from Merck, in collaboration with those from Solvias and Codexis, set-up the direct asymmetric synthesis of the antidiabetic chiral amine sitagliptin from its prochiral ketone precursor using ArRmut11-TA, an amine transaminase sourced from *Arthrobacter* sp. (Scheme 3.6).[395] The wild-type enzyme did not convert efficiently the substrate due to the hindrance of the bulky side groups of the ketone. To overcome this challenge, a combination of computational design and directed evolution techniques was employed. This approach involved modifying the enzyme's large binding pocket within the active site to accommodate the substrate, and subsequently, further enhancing the enzyme's activity and stability. IPA was selected as cheap amine donor, and removal of acetone was performed, in order to achieve a more favorable reaction equilibrium.

---

[395] C. K. Savile, J. M. Janey, E. C. Mundorff, J. C. Moore, S. Tam, W. R. Jarvis, J. C. Colbeck, A. Krebber, F. J. Fleitz, J. Brands, *et al.*, *Science* **2010**, *329*, 305–309.

The reaction achieved a 92% yield with a purity exceeding 99.95% enantiomeric excess. Overall yield of sitagliptin was improved, productivity boosted by 53%, and total waste reduced by 19%, compared to the previous methodology.[396] The use of the TA-catalyzed system effectively replaced at that time the previous expensive method, which involved rhodium-catalyzed asymmetric enamine hydrogenation and specialized high-pressure hydrogenation equipment (250 psi).

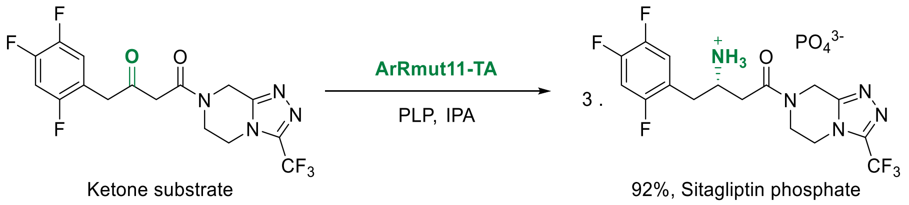

Scheme 3.6. Enzymatic synthesis of Sitagliptin via transamination.

Researchers at Pfizer in 2017 applied a transaminase for achieving the asymmetric amination of β-tetralone to produce a crucial chiral amine intermediate, used as gamma secretase inhibitor precursor (Scheme 3.7).[397] The reaction exhibited good yield and selectivity, it was performed on multikilogram scale, involving a minimal enzyme loading and IPA as amine donor. Without the need of any organic cosolvent, the reaction was set-up as a slurry-to-slurry reaction, since it was observed that the desired amine product precipitated as phosphate salt during the reaction, facilitating its isolation. Additionally, the reaction was executed under a nitrogen atmosphere to prevent the oxidation of the β-tetralone core. This also facilitated the removal of acetone, the by-product of the reaction, thereby promoting high conversion rate.

---

[396] A. A. Desai, *Angew. Chem. Int. Ed.* **2011**, *50*, 1974–1976.

[397] M. Burns, C. A. Martinez, B. Vanderplas, R. Wisdom, S. Yu, R. A. Singer, *Org. Process Res. Dev.* **2017**, *21*, 871–877.

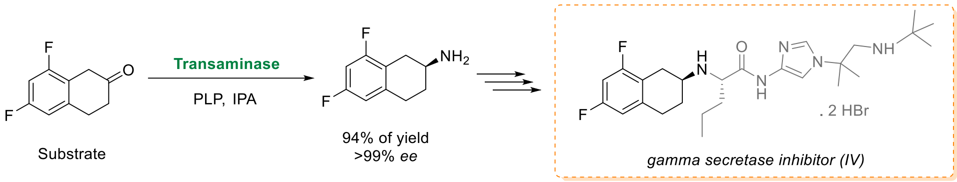

Scheme 3.7. Chiral amine intermediate production for gamma secretase inhibitor (IV) via asymmetric transaminase synthesis.

Researchers from Merck & Co. collaborated with Codexis to evolve a transaminase enzyme for a dynamic kinetic resolution process for the production of a chiral lactam building block, a crucial component in making ubrogepant, a calcitonin gene-related peptide receptor antagonist.[398] The enzyme screening was conducted at pH 10.5 to induce epimerization at the ketone's α-stereocenter. Multiple rounds of evolution on a selected transaminase allowed to improve selectivity at the C-4 and C-5 chiral centers and increased its tolerance to high DMSO cosolvent concentrations and up to 20-fold increasing substrate loading, thus being possible to decrease the enzyme loading by 20-fold. The enzyme operated effectively in a 1:1 DMSO:buffer mixture at 55 °C. During the reaction, the amino ester formed spontaneously cyclized into a lactam intermediate. This cyclization was facilitated by the basic pH and elevated temperature, shifting the transaminase equilibrium towards the desired product. The optimized process was successfully scaled up in high yield and selectivity on a 198 g scale (Scheme 3.8).

---

[398] N. Yasuda, E. Cleator, B. Kosjek, J. Yin, B. Xiang, F. Chen, S.-C. Kuo, K. Belyk, P. R. Mullens, A. Goodyear, *et al.*, *Org. Process Res. Dev.* **2017**, *21*, 1851–1858.

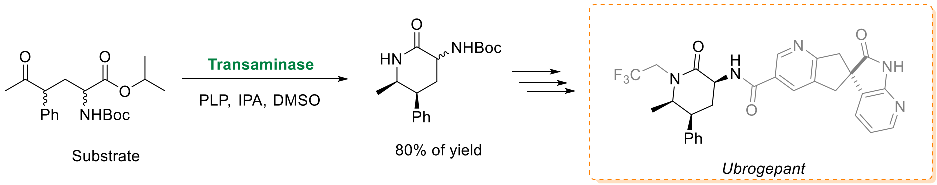

Scheme 3.8. Dynamic Kinetic Resolution process catalyzed by a transaminase to synthesize a chiral lactam intermediate for the preparation of ubrogepant.

Very recently, at Merck & Co., a transaminase was used to synthesize an amine-based precursor essential for the synthesis of the chiral tetrahydropyran structure found in the reversible Bruton's tyrosine kinase inhibitor nemtabrutinib.[399] Starting from the sustainable feedstock Cyrene, which already had one of the desired stereocenters, a commercially available Codexis enzyme was employed. This TA played a crucial role in introducing the amine and establishing the desired diastereomeric center. In the final process, a high substrate loading of 100 g/L was utilized. This process was successfully tested on a 50-g scale, resulting in the isolation of the desired amine with both high yield and selectivity (Scheme 3.9).

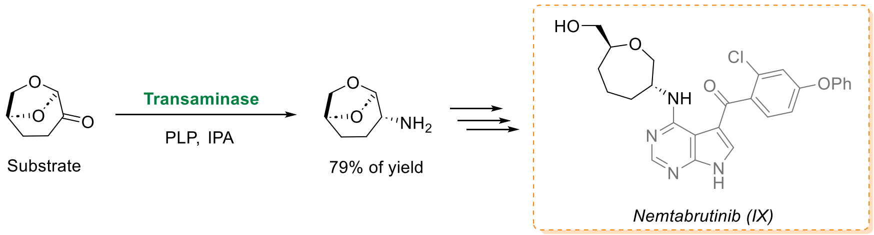

Scheme 3.9. Asymmetric synthesis of a chiral amine intermediate for the production of nemtabrutinib from bio-based Cyrene applying a transaminase-catalysed process.

---

[399] N. Kuhl, B. W. H. Turnbull, Y. Ji, R. T. Larson, M. Shevlin, C. K. Prier, C. K. Chung, R. Desmond, E. Guetschow, C. Q. He, *et al.*, *Green Chem.* **2023**, *25*, 606–613.

3.1.2. Laccases and ATAs in one-pot processes

In our research group, laccase-mediator systems have been effectively used for different purposes such as deracemization of racemic (hetero)aromatic alcohols into their single enantiomers,[400] or converting them into amines, in sequential approach, with alcohol dehydrogenases or transaminases, respectively.[401] In all of these biotransformations, the oxidation step was carried out with low initial substrate concentrations (25–50 mM) and a high amount of TEMPO as mediator (33 mol%). Otherwise, the transamination step was set-up selecting IPA as amine donor in great excess (1 M). The concurrent cascade could not be set-up, due to the observed loss of activity shown by TEMPO in the presence of IPA.

With this background in mind, we envisaged to extend this sequential approach to furan-based compounds. Thus, a one-pot sequential system was designed towards **1d** synthesis from **1a** through **1b,** combining laccases (with the aid of mediators) and transaminases as biocatalysts (Scheme 3.10).

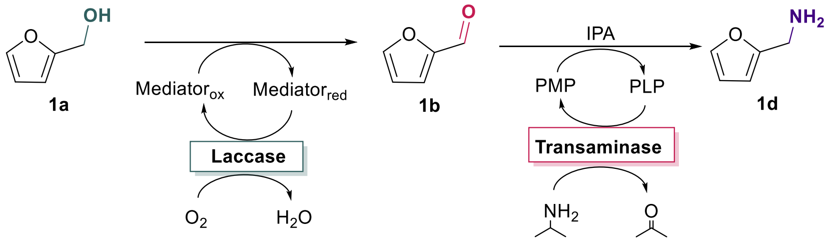

Scheme 3.10. One-pot bienzymatic sequential approach for the synthesis of **1d** combining a laccase-mediator system and a transaminase reaction (selecting IPA as amine donor).

---

[400] a) K. Kędziora, A. Díaz-Rodríguez, I. Lavandera, V. Gotor-Fernández, V. Gotor, *Green Chem.* **2014**, *16*, 2448–2453; b) A. Díaz-Rodríguez, N. Ríos-Lombardía, J. H. Sattler, I. Lavandera, V. Gotor-Fernández, W. Kroutil, V. Gotor, *Catal. Sci. Technol.* **2015**, *5*, 1443–1446; c) S. González-Granda, D. Méndez-Sánchez, I. Lavandera, V. Gotor-Fernández, *ChemCatChem* **2020**, *12*, 520–527.

[401] a) L. Martínez-Montero, V. Gotor, V. Gotor-Fernández, I. Lavandera, *Green Chem.* **2017**, *19*, 474–480; b) J. Albarrán-Velo, I. Lavandera, V. Gotor-Fernández, *ChemBioChem* **2020**, *21*, 200–211; c) J. Albarrán-Velo, I. Lavandera, V. Gotor-Fernández, *Mol. Catal.* **2020**, *493*, 111087.

Results and Discussion

3.2.1. Study of the first reaction step: Laccase oxidation of 1a into 1b

The two reaction steps, oxidation and transamination, were analyzed separately in a first attempt, in order to improve each single reaction step. Three laccases were selected for the oxidation step: the two laccases from *Pleurotus ostreatus* (POXA1b and POXC) and the one from *Trametes versicolor* (L*Tv*). Each of them possessing distinct characteristics such as thermal stability, specific activity, and redox potential (785 mV, 690 mV, and 650 mV, respectively), were investigated for their ability to oxidize furfuryl alcohol (**1a**) into furfural (**1b**), with a special focus in avoiding the overoxidation into 2-furoic acid (**1c**, Scheme 3.11).

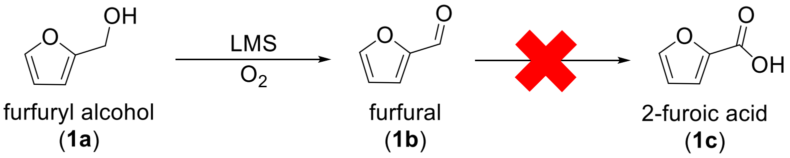

Scheme 3.11. Selective biooxidation of furfuryl alcohol into furfural using a LMS under aerobic conditions.

3.2.1.1. POXA1b, POXC and LTv laccases as object of investigation: Enzymatic stability studies

The three laccases were first assessed for their stability under optimal conditions: the residual activity at their respective optimal pH levels and 30 °C was assessed (Figure 3.2). POXA1b exhibited a notably high half-life at pH 5.5, retaining its full enzymatic activity for a duration of 8 days. Notably, POXA1b has been previously recognized as one of the most heat-resistant laccases, with a half-life of 3 hours at 60 °C and pH 7, and a remarkable 30-day stability at 25 °C and pH 9. On the other hand, POXC displayed a half-life of approximately 20 hours at pH 6, which is consistent with prior findings concerning this enzyme. Meanwhile, L*Tv* exhibited an impressive half-life of nearly 70 hours at pH 5, which aligns with previous reports highlighting the enzyme's stability over a few days under these conditions.[402]

These preliminary results highlighted that POXA1b is more appropriate when extended reaction durations are required. L*Tv*, on the other hand, is well-suited for the same reaction conditions but with shorter time frames. On the other hand, POXC showed the ability to function in less acidic pH environments, which makes it suitable for combining with subsequent reaction steps at higher pH levels, although its enzymatic activity is retained for a shorter duration.

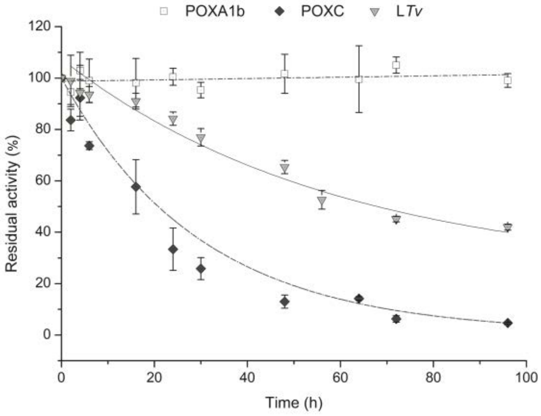

Figure 3.2. Residual activity of L*Tv* (▼), POXA1b (□) and POXC (♦) at pH 5, 5.5, and 6.5, respectively, at 30 ºC.

3.2.1.2. Mediator screening

Initially, a relatively high substrate concentration of 100 mM was employed; as expected, none of the three enzymes exhibited direct oxidation of the substrate, even with a constant supply of extra oxygen. Thus, a panel of 26 potential laccase mediators (5 mol%), both synthetic and naturally derived, was examined (Table 3.1).

---

[402] R. Hürmüzlü, M. Okur, N. Saraçoğlu, *Int. J. Biol. Macromol.* **2021**, *192*, 331–341.

Table 3.1. Mediator screening for the oxidation of **1a.**

Mediator	**Nature of the mediator**	**Conversion (%)[a]**		
		T. versicolor **(pH 5)**	**POXC (pH 6.5)**	**POXA1b (pH 5.5)**
TEMPO	Synthetic	58	47	31
4-Hydroxy-TEMPO	Synthetic	40	7	2
4-Acetoamido-TEMPO	Synthetic	18	3	2
NHA	Synthetic	<1	1	<1
ABTS	Synthetic	6	1	<1
HBT	Synthetic	9	1	<1
HPI	Synthetic	4	1	<1
AZADO	Synthetic	<1	<1	<1
Violuric acid	Synthetic	<1	<1	2
Gallic acid	Natural	<1	<1	<1
Vanillic acid	Natural	<1	<1	<1
Acetosyringone	Natural	<1	2	2
Acetovanillone	Natural	<1	<1	<1
Caffeic acid	Natural	<1	1	<1
Syringaldehyde	Natural	<1	1	1
Vanillin	Natural	<1	<1	1
p-Coumaric acid	Natural	<1	1	<1
Syringol	Natural	<1	1	<1
PHP	Natural	<1	1	<1
Cathecol	Natural	<1	<1	<1
Vanillyl alcohol	Natural	<1	<1	<1
Ethyl vanillin	Natural	<1	<1	<1
Guaiacol	Natural	<1	<1	<1
Sinapic acid	Natural	<1	<1	<1
Resorcinol	Natural	<1	<1	<1
Ferulic acid	Natural	<1	<1	<1

[a] Conversion values (%) were measured by GC analysis by comparison to standard curves based on the peak area of each compound. In all cases, only furfural was observed as product.

Among the various compounds tested, only few proved to be effective in catalyzing this oxidative reaction after 16 h of incubation at 30 °C, primarily (2,2,6,6-tetramethylpiperidin-1-yl)oxyl radical (TEMPO) and its derivatives like 4-hydroxy-TEMPO and 4-acetamido-TEMPO. For all three tested laccases, TEMPO emerged as the most efficient mediator, yielding moderate conversions into **1b** (31–58%). Consequently, TEMPO was chosen for further optimization studies.

The result obtained with the L*Tv*-TEMPO system (58% conversion) was in line with expectations, as it is one of the most widely explored laccase-mediated oxidative methods and has previously been used to oxidize primary and secondary alcohols into their corresponding carbonyl compounds.[403] However, efficient processes for the oxidation of furfuryl alcohol using laccases have been relatively scarce. There have been few reports where TEMPO[404] or its derivatives, such as 4-acetamido-TEMPO[405] or AZADO,[406] were employed in combination with L*Tv* for the oxidation of **1a** under an oxygen atmosphere. Unfortunately, these approaches often required high enzyme loadings, yielded low conversions, or necessitated large quantities of the mediator.

Furthermore, Waghmode and co-workers reported the oxidation of several alcohols, including furfuryl alcohol, using TEMPO in conjunction with *Tricholoma giganteum* laccase. However, this method required the use of 75 mol% of TEMPO and 1,500 U/mL of the enzyme at 37 °C to achieve quantitative furfural accumulation.[407] These challenges prompted us to explore other laccases, such as those from *P. ostreatus*, to achieve this transformation more efficiently.

---

[403] S. Riva, *Trends Biotechnol.* **2006**, *24*, 219–226.

[404] M. Mifsud, A. Szekrényi, J. Joglar, P. Clapés, *J. Mol. Catal. B: Enzym.* **2012**, *84*, 102–107.

[405] I. W. C. E. Arends, Y.-X. Li, R. A. Sheldon, *Biocatal. Biotransform.* **2006**, *24*, 443–448.

[406] C. Zhu, Z. Zhang, W. Ding, J. Xie, Y. Chen, J. Wu, X. Chen, H. Ying, *Green Chem.* **2014**, *16*, 1131–1138.

[407] A. R. Jadhao, H. Patel, K. M. Kodam, A. Gupte, S. B. Waghmode, *Tetrahedron* **2022**, *128*, 133114.

3.2.1.3. pH optimization

The pH impact on the oxidation of **1a** (100 mM) into **1b** using the LMS with TEMPO as the mediator was thoroughly investigated. In the case of L*Tv*, which belongs to the blue copper phenol oxidase family found in fungi, it is well-known that this type of laccase performs optimally under acidic conditions.[292c] Previous experiences with the L*Tv*-TEMPO system applied to the oxidation of various alcohol substrates had established that pH values in the range of 4.5 to 5 were optimal.[400a] Consequently, we selected pH 5 for further transformations involving L*Tv*.

Our focus then turned to the two laccases sourced from *P. ostreatus*. We examined the oxidation reactions using a mediator loading of 10 mol% (Figure 3.3). POXA1b exhibited activity in a pH range similar to that of L*Tv*, with optimal conditions found at pH 5.5. On the other hand, the LMS employing POXC displayed activity over a broader pH range, spanning from pH 5.0 to 8.0, with an optimum at pH 6.5. Encouragingly, after 16 hours at 30 °C, we were able to achieve conversions of nearly 70% and 90% with POXA1b and POXC, respectively.

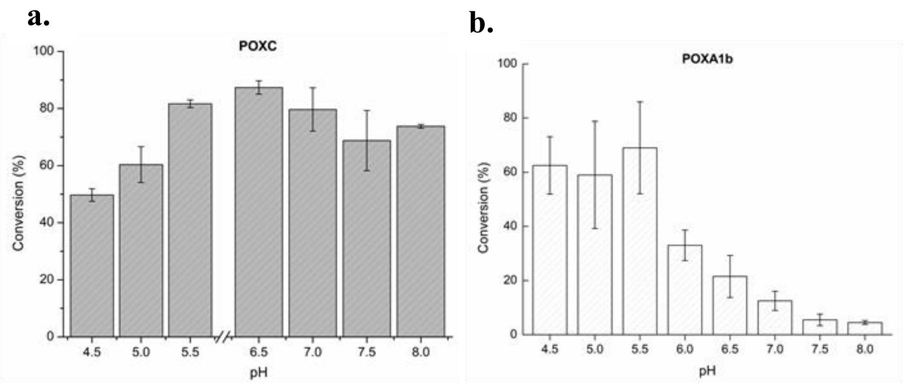

Figure 3.3. Study of the pH influence in the oxidation of furfuryl alcohol (100 mM) using TEMPO as mediator (10 mol%) at 30 ºC after 16 h using POXC (**a**) and POXA1b (**b**) laccases (5.8 U/mL). Buffer Na-Citrate (50 mM) for pH 4.5–5.5; buffer KPi (50 mM) for pH 6–7.5; buffer Tris-HCl (50 mM) for pH 8. Conversions were calculated by GC analyses of the reaction crude mixtures.

Most of the laccase-TEMPO applications are effective only at acidic pHs, thus reducing the possible combinations of these systems with other enzymes in cascade assets. Moreover, pH also influences the TEMPO efficiency in oxidizing the substrates. Basic pHs have not been often applied for laccase-TEMPO mediated oxidations, since under these conditions most of the tested laccases are not very active. Conversely, TEMPO in combination with POXC may efficiently be applied at pH up to 8.0, potentially overcoming these limits.

3.2.1.4. Influence of mediator and laccase concentrations

The performance of the oxidative LMS with the three laccases was assessed, each operating at its optimal pH. TEMPO loading was varied, ranging from 10 to 33 mol%, as well as the concentration of the laccase (ranging from 2.9 to 5.8 U/mL) in the oxidation of **1a** (100 mM) into **1b**. In some instances, particularly when higher amounts of TEMPO were used, we observed the co-production of 2-furoic acid (**1c**), which resulted from the overoxidation of furfural.

We compared the overall performances, considering both the desired formation of **1b** and the accumulation of **1c** (Table 3.2). The undesired formation of the carboxylic acid **1c** to some extent (ranging from 8% to 25%, as seen in entries 1, 2, 4, and 5) was mainly observed with the L*Tv*-TEMPO system. Selective oxidation of **1a** into **1b** was observed when lower mediator concentrations were used (entries 3 and 6, at 10 mol%). It can be due to the fact that the oxidation of **1b** to **1c** proceeds through the hydrate form of the aldehyde. This reaction is catalyzed under acidic pH conditions, and since the L*Tv* laccase works more effectively at low pHs, the overoxidation process is favored.

Conversely, due to a lower reaction rate and the selection of higher pH levels, no overoxidation of **1b** was observed when using laccases from *P. ostreatus*, even at high mediator and enzyme concentrations (as in entry 1, with 33 mol% TEMPO). This difference can also be attributed to the lower redox potential of POXC (690 mV) and POXA1b (650 mV) compared to L*Tv* (785 mV). As a result, using 58 U/mmol$_s$ of the laccase, we obtained comparable results for L*Tv* and POXC with TEMPO (10 mol%, entry 3). However, higher mediator loadings (20–33 mol%) yielded better results with both *P. ostreatus* laccases (entries 1 and 2), achieving complete conversion into **1b** without the formation of co-product **1c**.

Table 3.2. Comparison of furfural production applying the LMS at different TEMPO concentrations (mol%) and laccase loadings (U/mL) after 16 h at 30 ºC.

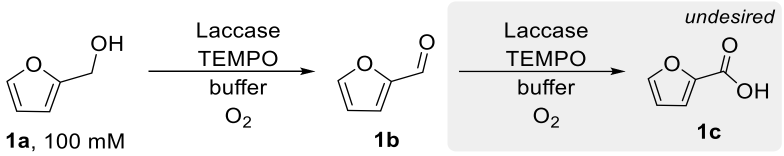

Entry	Enzyme (U/mmol$_s$)	TEMPO (mol%)[b]	L*Tv* (%)[a]		POXC (%)[a]		POXA1b (%)[a]	
			1b	**1c**	**1b**	**1c**	**1b**	**1c**
1	58	33	80	20	99	<1	99	<1
2		20	89	11	99	<1	99	<1
3		10	99	<1	97	<1	48	<1
4	29	33	75	25	74	<1	80	<1
5		20	92	8	56	<1	60	<1
6		10	98	<1	55	<1	58	<1

[a] Conversion values were calculated by GC analyses of the crude reaction mixtures using calibration curves. [b] Referred to the amount of alcohol **1a**.

We conducted a comprehensive analysis of the performance, cost-effectiveness, and purity of the three laccases with the aim of selecting the optimal oxidative system for coupling with a subsequent reaction, specifically an ATA-catalyzed biotransamination.

In terms of cost analysis, it became evident that integrating POXC and POXA1b was a more economically advantageous choice. L*Tv* from Sigma Aldrich, which was utilized in this study, has a cost of 0.21 € per unit (excluding handling and shipping charges), whereas both *P. ostreatus* laccases from BioPox are priced at 0.10 € per unit (including handling and shipping costs). Additionally, L*Tv* displayed a specific activity for ABTS close to 100 U/mg, indicating the possible presence of other contaminant proteins that could interfere with undesired secondary reactions. In contrast, both POXC and POXA1b exhibited specific activities for ABTS of 670 and 550 U/mg, respectively, suggesting a higher degree of enzyme homogeneity for both laccases.

Taking all of these factors into consideration, we opted to proceed with *P. ostreatus* laccases for further experimentation.

3.2.1.5. Optimization of the mediator amount

The effect of lowering the TEMPO concentration was also investigated in order to optimize a system with the lowest possible amount of the chemical oxidant (Figure 3.4). Interestingly, we achieved conversions of up to 95% towards **1b**, even with just 5 mol% of the mediator after 72 h, or using a 10 mol% TEMPO after 48 h when employing the POXA1b system (Figure 3.4a). Similarly, the POXC system allowed us to achieve complete conversion of **1b** with 20 mol% of the mediator after only 16 h, or by using 10 mol% of TEMPO after 24 h (Figure 3.4b).

However, when using 2.5 mol% of the oxidant, the POXA1b-TEMPO system resulted in low conversion levels (<5%). In contrast, the POXC-TEMPO system yielded a significant 60% furfural production after 24 h under these conditions.

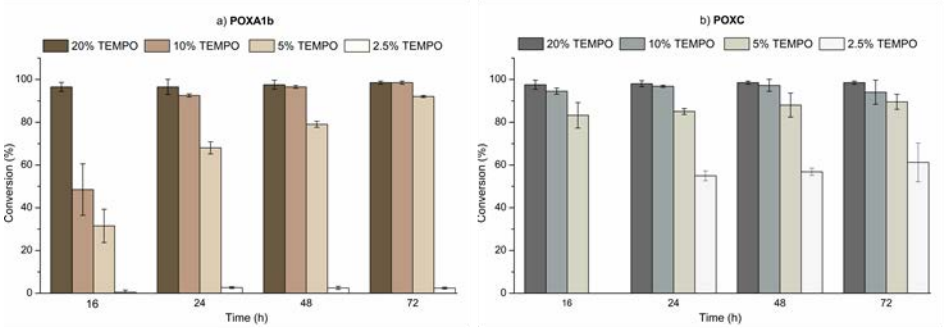

Figure 3.4. Conversion of **1a** (100 mM) into **1b** mediated by TEMPO (2.5–20 mol%) and POXA1b (**a**) and POXC (**b**) at different reaction times (16–72 h).

It is important to remark that the transformation mediated by POXC proceeded rapidly, achieving high conversions in 16 h. In contrast, reactions catalyzed by POXA1b progressed more slowly, especially when 5 mol% and 10 mol% of the mediator were used. However, in the case of POXC, there were no significant changes observed after this initial 16 h, whereas reactions catalyzed by POXA1b exhibited increasing conversion values over time. These results align with the higher stability observed for POXA1b compared to POXC, underscoring the potential of the former for potential oxidative transformations. Once again, it is important to mention that carboxylic acid **1c** was not detected in these experiments.

3.2.1.6. Co-solvent screening

To demonstrate the versatility and practicality of the *P. ostreatus* laccase-TEMPO systems with 10 mol% of TEMPO, we conducted tests in the presence of various co-solvents at a concentration of 10% v/v. We evaluated the residual activity of these systems in both water-miscible and immiscible organic solvents (Figure 3.5). After 16 h at 30 °C, POXA1b exhibited partial stability, with more than 60% of its initial activity remaining in the presence of most solvents. Importantly, its catalytic performance remained intact. Notably, in biphasic systems with solvents like *tert*-butyl methyl ether (MTBE) and cyclohexane, significantly higher conversion rates (ranging from 60% to 80%) were observed compared to the reaction in plain buffer (40%). Conversely, POXC was more sensitive to the presence of all immiscible solvents, and its oxidative performance was negatively impacted, typically retaining less than 30% of its initial activity in most of the tested solvents. For this enzyme, ethyl acetate (EtOAc), MTBE, and cyclohexane provided the best results in terms of conversions into **1b** (ranging from 80% to 90%), which were similar to those observed in the plain buffer. In summary, most of the solvents were compatible with the POXA1b-TEMPO system, whereas only a few could be effectively integrated into the POXC-TEMPO oxidative system. Interestingly, both enzymes showed a preference for immiscible organic co-solvents over miscible ones, suggesting their potential applicability with more lipophilic substrates.

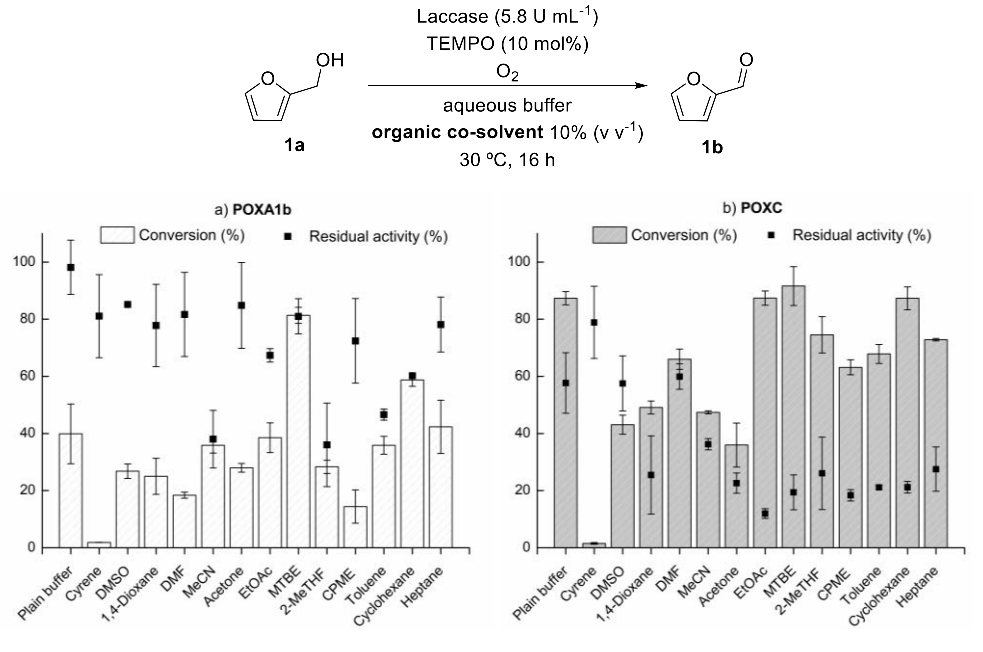

Figure 3.5. *Bars*: Conversion of **1a** (100 mM) into **1b** using POXA1b-TEMPO (**a**) and POXC-TEMPO systems (**b**) with 10 mol% of the mediator after 16 h at 30 ºC in the presence of different organic solvents (10% v/v). The error is the result of two independent sets of reactions. *Dots* (■): Residual activity of the corresponding laccase in the analyzed solvent measured against ABTS.

On one hand, a laccase-TEMPO oxidation system that can achieve complete conversions into furfural under less acidic pH conditions within 16 h was investigated. On the other hand, a system with similar performance but at extended reaction times (72 h) was provided, using a highly stable laccase, reducing the mediator concentration to as low as 5 mol%. Additionally, both systems responded differently to the presence of co-solvents. POXA1b's activity remained unaffected in the presence of most common water-miscible and immiscible organic solvents at a concentration of 10% v/v, which can enhance the solubility of hydrophobic substrates.

3.2.2. Study of the second reaction step: Transamination of 1b into 1d

Furfural was employed as the model substrate to set-up the transaminase reaction with various amine transaminases: 28 commercial ATAs from Codexis and 17 recombinant *E. coli* cells encoding an ATA which were already available at our research group were tested.

3.2.2.1. Broadening the panel of biocatalysts: Recombinant expression of new ATAs in E. coli

Plasmids containing the gene of eight novel ATAs from Prof. Kourist at the University of Graz were readily accessible in our laboratory. Following an extensive literature search, a well-defined transformation protocol was established for their recombinant expression.

The nucleotide sequences of the 8 ATAs was obtained by PCR and verified through sequencing and compared to a nucleotide database using BLAST alignment to confirm their accuracy. Following this verification, plasmid transformation experiments were initiated.

The ATAs were successfully expressed in *E. coli* recombinant cells. However, due to the exceptionally high activity of T7 RNA polymerase, some basal level expression of the gene of interest was observed in certain non-induced ATA recombinant cell systems, especially evident after 16 h of incubation (Figure 3.6b), and even in the absence of IPTG addition. Upon analyzing the SDS-PAGE gel obtained after 6 h of inducing the whole cell system (Figure 3.6a), it was evident that the overexpression was highly successful in yielding a substantial amount of the target proteins.

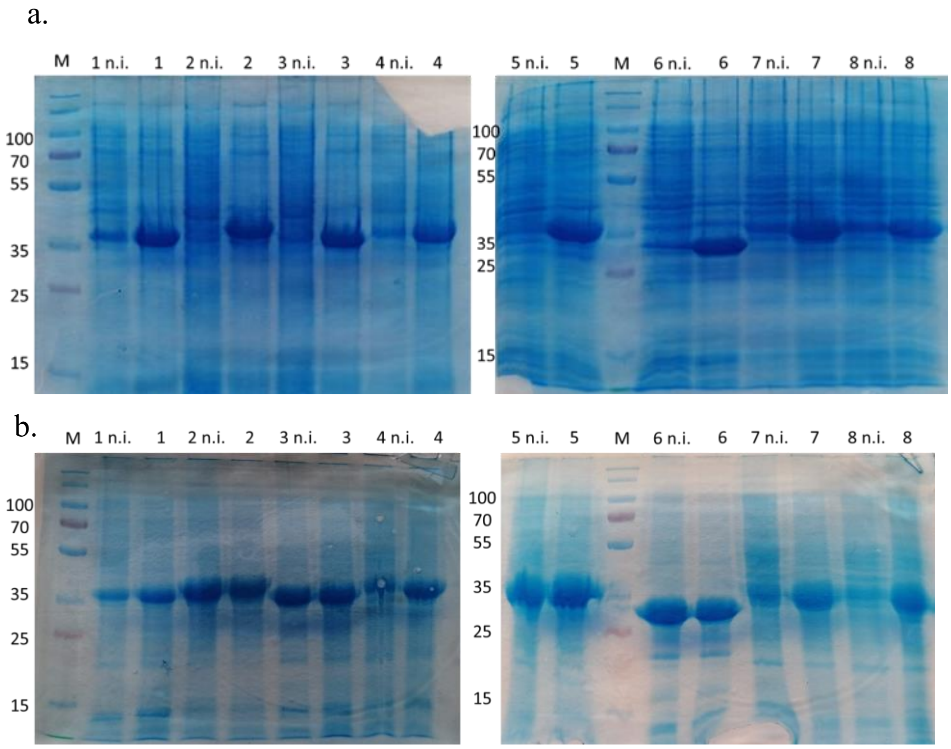

Figure 3.6. SDS-PAGE gel of the whole recombinant cells expressing Kourist's ATAs after 6 h of induction (a.) and 16 h (b.). ATAs overexpressing systems have been named as 1–8. M: molecular weight marker (kDa); 1–8 n.i.: non-induced system; 1–8: induced system with 0.1 mM IPTG.

3.2.2.2. ATA screening for 1d biosynthesis

The recombinant ATAs were produced growing the *E. coli* recombinant cells, inducing the protein production, and recovering the dry cell powder after lyophilization. An assay on all the new batches produced was conducted following by GC the production of acetophenone from 1-phenylethylamine in the presence of pyruvic acid within the time, thus assessing the units of ATAs per milligram of cells (around 2 U). The enzymatic reactions were carried out in parallel with one blank reaction (sample with no ATA), for having the GC peaks scenario as background to check if the appearance/disappearance of the peaks in real reaction crudes were due to the enzyme action or not. The reaction conditions were set-up as reported in Scheme 3.12.

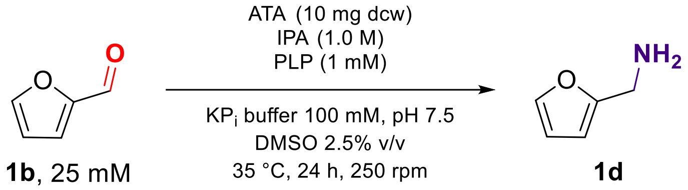

Scheme 3.12. Sum up of the selected transamination reaction conditions for the conversion of furfural into furfuryl amine.

In the blank sample, the complete absence of the expected peak corresponding to the substrate, furfural, was compensated by the appearance of a single, more retained peak. This phenomenon was attributed to the high reactivity of IPA (used in excess to drive the equilibrium towards amine synthesis) with the aldehyde group of furfural, resulting in the formation of an imine compound due to the basic treatment of the reaction crudes before injection at GC, as confirmed by NMR analysis.

The presence of this unique peak was interpreted as residual substrate in all reaction samples. By comparing the intensity to the peak corresponding to furfuryl amine (previously identified in the GC spectrum by injecting a chemically synthesized reference), the conversion percentages for each tested ATA were determined. The substrate concentration was set at 25 mM, and among the 28 commercial amine transaminases, only three exhibited conversions of less than 10% (Table 3.3), while the rest afforded quantitative conversions.

Table 3.3. Screening of commercial transaminases with **1b** after 24 h at 35 °C.

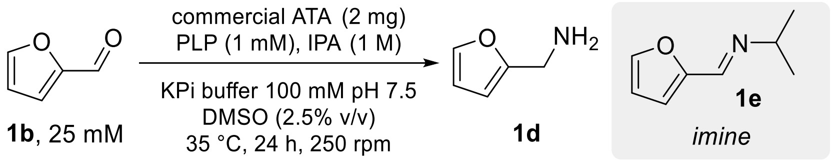
commercial ATA (2 mg)
PLP (1 mM), IPA (1 M)
KPi buffer 100 mM pH 7.5
DMSO (2.5% v/v)
35 °C, 24 h, 250 rpm
1b, 25 mM
1d
1e
imine

Entry	ATA	1d (%)[a]	1b (%)[a]	1e (%)[a]
1	ATA-013	>99	<1	<1
2	ATA-024	>99	<1	<1
3	ATA-025	>99	<1	<1
4	ATA-033	>99	<1	<1
5	ATA-113	>99	<1	<1
6	ATA-200	>99	<1	<1
7	ATA-217	>99	<1	<1
8	ATA-234	>99	<1	<1
9	ATA-237	>99	<1	<1
10	ATA-238	>99	<1	<1
11	ATA-251	>99	<1	<1
12	ATA-254	>99	<1	<1
13	ATA-256	>99	<1	<1
14	ATA-260	>99	<1	<1
15	ATA-301	>99	<1	<1
16	ATA-303	>99	<1	<1
17	ATA-412	>99	<1	<1
18	ATA-415	>99	<1	<1
19	TA-P1-A06	>99	<1	<1
20	TA-P1-B04	>99	<1	<1
21	TA-P1-F03	>99	<1	<1
22	TA-P1-G05	>99	<1	<1
23	TA-P1-G06	>99	<1	<1
24	TA-P2-A07	>99	<1	<1
25	TA-P2-B01	>99	<1	<1
26	TA-P2-A01	10	<1	90
27	ATA-117	9	<1	91
28	ATA-007	5	<1	95

[a] Compound percentage values were calculated by GC analyses of the crude reaction mixtures using calibration curves.

Additionally, out of the 17 in-house overexpressed ATAs, three achieved a conversion lower than 31%, three achieved a conversion of 57–

76%, while the other yielded complete conversions into furfuryl amine. The best results were attained with ATAs from ArS-TA,[408] Cv-TA,[409] ArRmut11-TA,[395] Bm-TA,[371c,410] its variant S119G (BmS119G-TA),[411] and a variant from *Vibrio fluvialis* (Vf-mut).[412] Other enzymes such as the ones from ArR-TA,[413] Vf-TA,[414] and At-TA,[415] afforded lower product formation (4–66%). As well, most of the new made-in-house ATAs (TA1-TA5) shown low conversion values more related to low recognition of IPA, chosen in this reaction system as amine donor. Only TAs 6–8 gave higher conversion values (70–92%, Table 3.4).

---

[408] U. Kaulmann, K. Smithies, M. E. B. Smith, H. C. Hailes, J. M. Ward, *Enzyme Microb. Technol.* **2007**, *41*, 628–637.

[409] S. Pannuri, S. V. Kamat, A. R. M. Garcia, PCT Int. Appl. WO 2006063336 A2 20060615, **2006**

[410] D. Koszelewski, M. Göritzer, D. Clay, B. Seisser, W. Kroutil, *ChemCatChem* **2010**, *2*, 73–77.

[411] B. Z. Costa, J. L. Galman, I. Slabu, S. P. France, A. J. Marsaioli, N. J. Turner, *ChemCatChem* **2018**, *10*, 4733–4738.

[412] F. Cabirol, A. Gohel, S. H. Oh, D. Smith, B. Wong, J. LaLonde, PCT Int. Appl. WO 2011159910A2 20111222, **2011**.

[413] A. Iwasaki, Y. Yamada, N. Kizaki, Y. Ikenaka, J. Hasegawa, *Appl. Microbiol. Biotechnol.* **2006**, *69*, 499–505.

[414] J.-S. Shin, B.-G. Kim, *Biotechnol. Bioeng.* **1999**, *65*, 206–211.

[415] M. Höhne, S. Schätzle, H. Jochens, K. Robins, U. T. Bornscheuer, *Nat. Chem. Biol.* **2010**, *6*, 807–813.

Table 3.4. Furfural biotransamination results using overexpressed ATAs in *E. coli* after 24 h at 35 ºC.

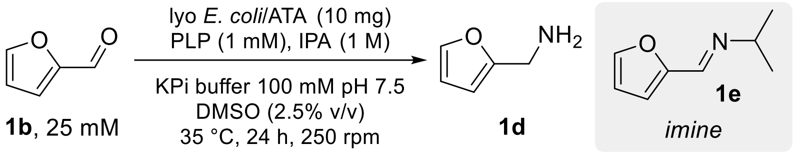
lyo *E. coli*/ATA (10 mg)
PLP (1 mM), IPA (1 M)
KPi buffer 100 mM pH 7.5
DMSO (2.5% v/v)
35 °C, 24 h, 250 rpm
1b, 25 mM
1d
1e
imine

Entry	ATA	1d (%)[a]	1b (%)[a]	1e (%)[a]
1	Cv-TA	>99	<1	<1
2	ArS-TA	>99	<1	<1
3	ArRmut11-TA	>99	<1	<1
4	Bm-TA	>99	<1	<1
5	BmS119G-TA	>99	<1	<1
6	Vf-mut-TA	>99	<1	<1
7	ArR-TA	57	<1	43
8	Vf-TA	66	<1	34
9	At-TA	4	<1	96
10	TA1	21	<1	80
11	TA2	3	<1	97
12	TA3	29	<1	71
13	TA4	<1	<1	98
14	TA5	31	<1	69
15	TA6	70	<1	30
16	TA7	76	<1	24
17	TA8	92	<1	8

[a] Compound percentage values were calculated by GC analyses of the crude reaction mixtures after basic extraction using calibration curves.

In a new set of experiments, biotransamination of **1b** at higher substrate concentrations (50–200 mM) was investigated. The reactions were performed with the same amount of the lyophilized *E. coli* cells overexpressing only the best ATA candidates (entries 1–6, Table 3.4), while keeping the remaining reaction conditions constant (KPi buffer 100 mM pH 7.5, DMSO 2.5% v/v, and IPA 1 M, as amine donor). Among the panel of enzymes, only Cv-TA and ArS-TA catalyzed efficiently the transformation into **1d** with a percentage of 70–75% at 150 mM of **1b**. Significant drops of product formation were attained for transamination reactions catalyzed by ATAs from *Bacillus megaterium* and *Vibrio fluvialis* (Figure 3.7).

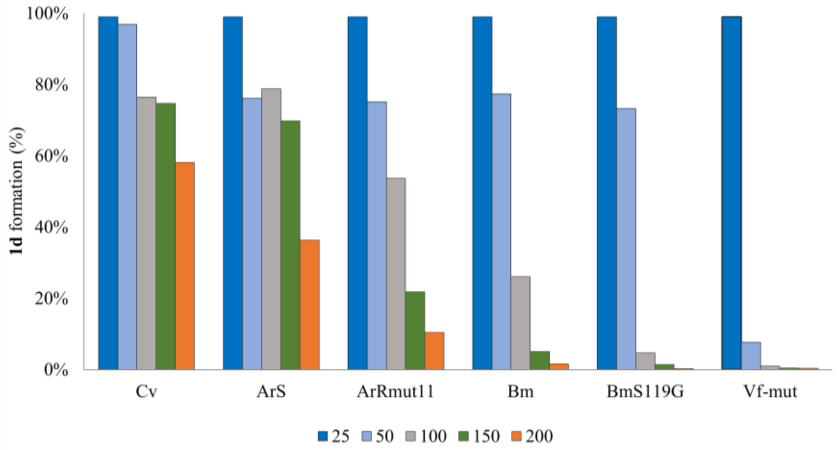

Figure 3.7. Transamination of furfural (**1b**) with increasing concentrations of the substrate (50–200 mM) at pH 7.5. Amine **1d** percentage values were determined by GC analyses of the crude reaction mixtures after basic extraction using calibration curves.

Due to the potential for aldehyde compounds to react with proteins, there is a possibility of ATA inactivation at high **1b** concentrations. To address this concern, a stepwise approach adding the inhibiting substrate can be employed. As a demonstration of this concept, an experiment was designed using *E. coli*/ArS-TA, where **1b** was added incrementally (50 mM per addition) at intervals of 0, 3, 6, and 9 h, resulting in a final concentration of 200 mM after 24 h. The conversion into amine **1d** at the end reached 95%, a significant improvement compared to the previous result of 36% obtained with a direct addition of 200 mM (as shown in Figure 3.7). This experiment served as a promising starting point for future process optimization experiments.

3.2.2.3. pH influence in 1d biosynthesis

Transamination reactions using IPA as an amine donor pose challenges and complications when dealing with highly reactive substrates, like aldehydes. These issues result in undesired by-products, as illustrated in Scheme 3.13.

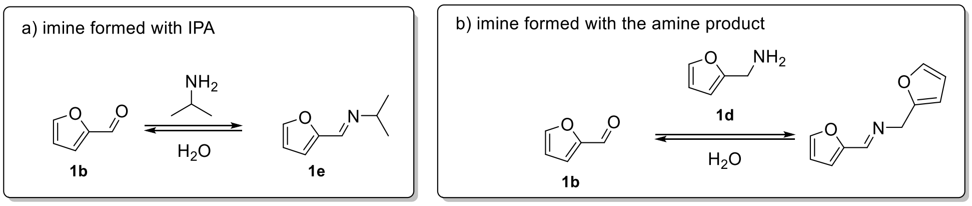

Scheme 3.13. Different reaction possibilities to form imines in the biotransamination of aldehyde **1b** showed in the present study due to the: a) presence of IPA; b) presence of the amine product.

On one hand, the amine acceptor **1b** reacts with IPA to create imine **1e**, which was previously observed in previous biotransformations (Scheme 3.13a). On the other hand, the desired amine product **1d** can combine with the remaining substrate, leading to the formation of an extra imine species (Scheme 3.13b).

Given that imine bond formation is reversible, particularly in aqueous solutions, we explored whether pH levels could influence these ATA-catalyzed processes. The presence of imine compounds might hinder the desired reaction by reducing the concentration of the available aldehyde species in the reaction mixture. Since imines are more likely to be formed at basic pH conditions, using a more acidic reaction medium might enhance these biotransaminations by minimizing, to some extent, the presence of unwanted imine compounds. To test this concept, ATA-catalyzed reactions with **1b** at various concentrations was performed, using the best enzymes previously identified for this substrate, and conducing the reactions in a 100 mM KPi buffer at pH 6.5 (Figure 3.8).

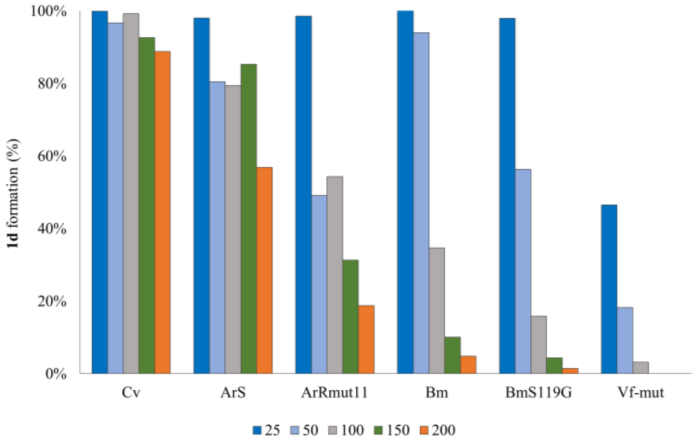

Figure 3.8. Transamination of furfural (**1b**) at increasing concentrations of the substrate (50–200 mM) at pH 6.5. Conversion values of the crude reaction mixtures were determined by GC using calibration curves.

In general, higher conversions towards the desired amine product **1d** were achieved for almost all ATAs, which supports our hypothesis concerning the equilibrium between aldehyde and imine and its effect on the desired reaction. Notably, we achieved particularly positive results with Cv-TA and ArS-TA when compared to pH 7.5 (Figure 3.7). However, for Bm-TA and its mutant, slightly lower conversions were observed, which can be attributed to the reduced stability or activity of these biocatalysts under more acidic pH conditions. Nonetheless, the impact of pH on the biotransformation of furan-based aldehydes like **1b** was clearly evident from the results, highlighting the importance of carefully considering this parameter, especially when using a highly nucleophilic amine donor like IPA.

3.2.3. One-pot sequential synthesis of 1d from 1a at preparative scale

In order to show the applicability of the laccase-TEMPO systems with POXA1b and POXC, we pursued the production of furfuryl amine from **1a** through a one-pot oxidation-transamination sequence. Traditional chemical synthesis methods often involve harsh procedures that can produce imines as intermediate compounds, leading to the formation of undesired by-products, which can impact the final purity and yield of the desired compound.[416]

In this sequential approach, 50 mg of substrate **1a** was used and the transamination was done using amine transaminase from *Chromobacterium violaceum*. The transaminase reaction was conducted with an excess of IPA as the amine donor (1 M concentration). The transamination of the furfural intermediate occurred following the oxidation step in the same reaction vessel. We achieved this by simply adding the ATA, PLP as the cofactor, and IPA as the amine donor (Scheme 3.14). To adjust the pH for the second step, we introduced the amine donor in the form of a phosphate salt.

The one-pot/two-step system was successfully set-up by utilizing *P. ostreatus* laccases and TEMPO. This system allowed for the quantitative production of the furfural intermediate, which was subsequently transformed into furfuryl amine using Cv-TA and IPA, resulting in an impressive overall conversion rate of 99%. The final product, **1d**, was obtained with excellent purity through a liquid-liquid extraction process, eliminating the necessity for additional purification steps, and achieving a 48% isolated yield.

---

[416] M. K. Saini, S. Kumar, H. Li, S. A. Babu, S. Saravanamurugan, *ChemSusChem* **2022**, *15*, e202200107.

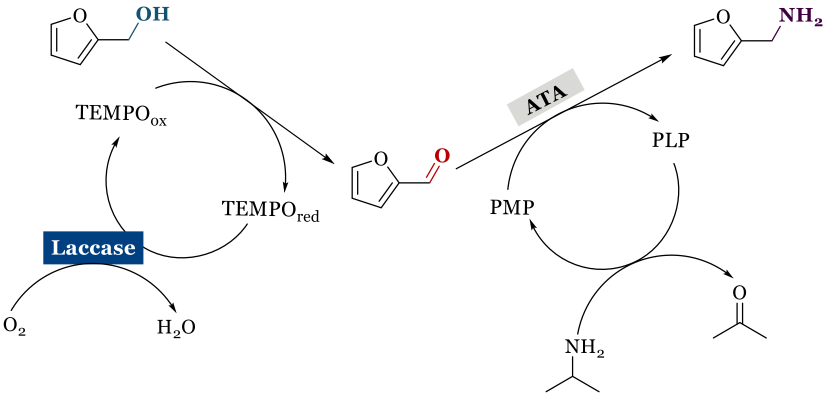

Scheme 3.14. One-pot bienzymatic sequential approach for the synthesis of **1d** using a laccase-TEMPO system and Cv-TA. Reaction conditions: Laccase POXC/POXA1b (58 U/mmol$_s$ **1a**), oxygenated phosphate/citrate buffer (50 mM, pH 6.5/5.5), TEMPO (20 mol%), 30 °C, 16 h, 250 rpm. Then, Cv-TA (10 mg DCW), KPi buffer (pH 6.5, 100 mM), PLP (1 mM), $(IPA)_3PO_4$ (330 mM), 30 °C, 24 h, 250 rpm.

3.2.4. Environmental impact of the preparative biosynthesis of 1d

The environmental impact of the sequential system for the synthesis of **1d** was assessed using the *E*-factor concept.[253b] The focus of the evaluation was on how the reaction conditions, waste generation, and the work-up process contributed to the overall impact. The downstream process was responsible for 89% of the overall environmental impact. Product extraction using organic solvents accounted for over 70% of this impact, while water contributed 24% (Figure 3.9). Excluding the solvents, the *E*-factor for the cascade transformation was found to be 22.5, which is consistent with values obtained for similar oxidative systems.[401a,417] To improve the environmental footprint of the laccase/TEMPO-ATA cascade protocol, it would be possible to implement a continuous extraction method to reduce solvent usage, potentially increasing the product yield. Additionally, using immobilized

---

[417] L. Martínez-Montero, A. Díaz-Rodríguez, V. Gotor, V. Gotor-Fernández, I. Lavandera, *Green Chem.* **2015**, *17*, 2794–2798.

mediator and cofactors would allow the reuse of the aqueous medium for multiple cycles, further reducing its impact on the environment.

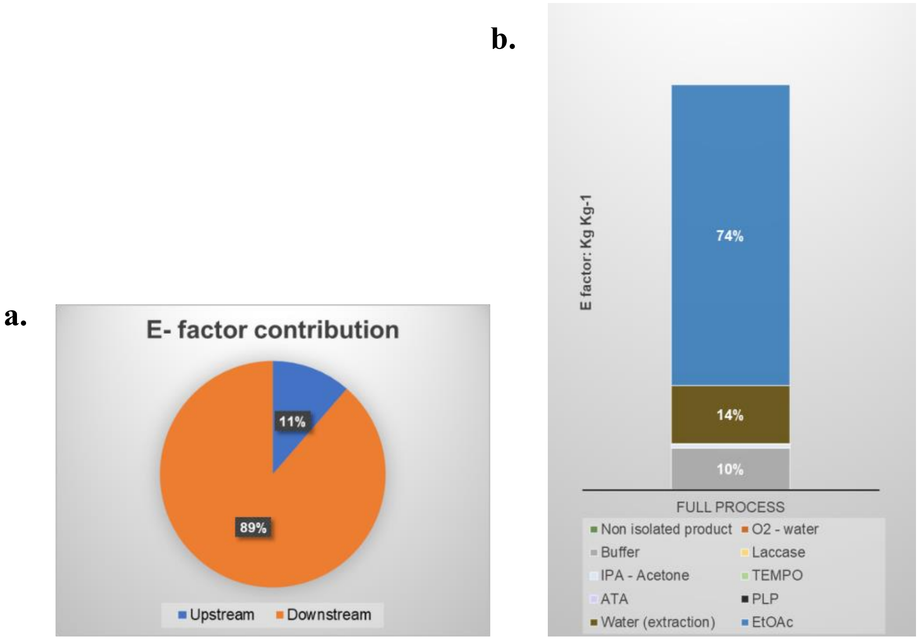

Figure 3.9. Contribution (%) to the *E*-factor (including solvents) for upstream and downstream of the process (**a**) and for each element (**b**) for the sequential oxidation and amination of **1a** into **1d**.

Experimental Section

3.3.1. General information

Non-commercially available furfuryl alcohol (**1a**) was chemically synthesized exhibiting physical and spectral data in agreement with those reported in the literature (as described in procedures and characterization data given below). The oxidation step mediated by the laccase-TEMPO catalytic system was performed open-to-air using a (19 x 130 x 3) mm tube under magnetic stirring, while for the transamination step, the tube was sealed. The following measurement units were used in this Experimental Section: U of enzyme: Enzymatic units per mL of solution; Mediator (mol%): (mmol mediator/mmol substrate) x 100.

All chemicals were either purchased from commercial sources. Commercially available furfural and furfuryl amine were purchased from Sigma-Aldrich and used as standards. Commercially available aldehyde **1b** and amine **1d** were purchased from Sigma-Aldrich and used as standards. NMR spectra were recorded on a Bruker AV300 MHz spectrometer including ^{1}H and ^{13}C. All chemical shifts (δ) are reported in parts per million (ppm) and referenced to the residual solvent signal. Gas chromatography (GC) analyses were performed on an Agilent HP6890 GC chromatograph equipped with a FID detector and DB-1701 column from Agilent (30 m x 0.25 mm x 0.25 µm). Multiplicities of signals in the ^{1}H-NMR spectra are the following: s = singlet, d = doublet, t = triplet, q = quartet, dd = doublet of doublets

L*Tv* was obtained from Aldrich (103 U/mg). Recombinant POXA1b from *P. ostreatus*[358] expressed in the yeast *Pichia pastoris* under the control of the AOX1 promoter (induced by glycerol, 550 U/mg),[348] and POXC laccase produced from *P. ostreatus*[295] (670 U/mg), were provided by BioPox srl.

Cv-TA, ArR-TA, ArS-TA, ArRmut11-TA, Bm-TA, BmS199G-TA, Vf-mut-TA, Vf-TA, and At-TA were recombinantly expressed in *E. coli* BL21(DE3) cells (Invitrogen), using ampicillin or kanamycin as antibiotic.

3.3.2. Synthesis of reference materials

3.3.2.1. Synthesis of alcohol 1a

Furfuryl alcohol (**1a**) was synthesized by the procedure described by Gładkowski and co-workers.[418] A solution of $NaBH_4$ (170.2 mg, 4.5 mmol) in water (1 mL) was added dropwise at 0 °C to a stirring solution of furfural (288 mg, 3 mmol) in MeOH (10 mL). The reaction mixture was first stirred for 1 h in an ice bath and then for additional 2 h at room temperature. Afterwards, the reaction was quenched by the addition of hot water (5 mL) was added, the product was extracted with CH_2Cl_2 (3 x 15 mL), and the combined organic phases were washed with brine (5 mL). The organic layer was dried over anhydrous Na_2SO_4, filtered and the solvent was evaporated under reduced pressure. The reaction crude containing the alcohol was purified by column chromatography on silica gel (40% EtOAc/Hexane), yielding the alcohol **1a** as a yellowish oil (120 mg, 80% yield). The spectral data of **1a** were in accordance with the ones reported in the literature.

3.3.2.2. Synthesis of carboxylic acid 1c

2-Furoic acid (**1c**) was synthesized according to the protocol described by Das and Chakraborty.[419] Under nitrogen atmosphere, ^{t}BuOOH (70% in water, 0.26 mL, 2 mmol) was added to a stirred solution of $CuBr_2$ (11.16 mg, 0.05 mmol) and furfural **1b** (1 mmol) in MeCN (2.5 mL). The reaction progress was monitored using TLC analysis (20% EtOAc/Hexane) until the aldehyde was consumed. The solvents were removed using a rotary evaporator, and the mixture was treated with an aqueous $NaHCO_3$ saturated solution. Then, the solution was extracted with EtOAc (2 x 2 mL), collecting the aqueous layer that was acidified using a 2 M aqueous HCl solution until acidic pH was reached, and extracted with EtOAc (2 x 2 mL). The organic layers were combined, dried over anhydrous Na_2SO_4, filtered and concentrated under vacuum in a rotatory evaporator. Finally, the reaction crude was purified by column chromatography on silica gel (40% EtOAc/Hexane), obtaining the carboxylic acid **1c** as a brownish powder (140 mg, 70% yield). The spectral data of **1c** were in accordance with the ones reported in the literature.

---

[418] W. Gładkowski, A. Skrobiszewski, M. Mazur, M. Siepka, A. Pawlak, B. Obmińska-Mrukowicz, A. Białońska, D. Poradowski, A. Drynda, M. Urbaniak, *Tetrahedron* **2013**, *69*, 10414–10423.

[419] R. Das, D. Chakraborty, *Appl. Organomet. Chem.* **2011**, *25*, 437–442.

3.3.3. General procedure for the LMS oxidation of 1a into 1b

In a test tube open to air, TEMPO was added to a solution of **1a** (0.1 mmol, 100 mM) in an oxygen-saturated buffer (50 mM, at the proper pH). The reaction mixture was magnetically stirred for a few minutes to dissolve all the reagents, and a buffered solution with laccases from L*Tv* or *P. ostreatus* (5.8 U/mL) was then added. The mixture was magnetically stirred (250 rpm) for additional 16 h at controlled temperature (30 °C). After this time, the product was extracted with EtOAc (2 x 2 mL), the organic phases were combined, dried over anhydrous Na_2SO_4 and filtered. An aliquot was taken for the determination of the degree of conversion by GC analysis.

3.3.4. Stability study of laccases

Laccase stability was measured at 30 °C and 300 rpm (magnetic stirring) employing the appropriate buffer and pH for the later oxidation reaction: L*Tv*: Na-Citrate buffer 50 mM, pH 5; POXA1b: Na-Citrate buffer 50 mM, pH 5.5; POXC: KPi buffer 50 mM, pH 6.5. This study was conducted starting with the same concentration of laccases (6 U/mL and 60 U/mg).

The protein concentration was determined using the BioRad Protein Assay (BioRad), with BSA as standard.

3.3.5. Mediator screening

In a test tube open to air, the corresponding mediator (5 mol%) was added to a solution of the alcohol **1a** (0.1 mmol, 100 mM) in a monophasic oxygen-saturated buffer with DMF (10% v/v) as cosolvent (L*Tv*: Na-Citrate buffer 50 mM, pH 5. POXA1b: Na-Citrate buffer 50 mM, pH 5.5. POXC laccase: KPi buffer 50 mM, pH 6.5). The reaction mixture was magnetically stirred for a few minutes to dissolve all the reagents, and a volume corresponding to 5.8 U/mL of buffered solution with the laccases was then added. POXC laccase was provided in solution (NaPi buffer 50 mM, pH 6.5), meanwhile POXA1b as lyophilized powder, that was resuspended in the appropriate buffer for each reaction. The mixture was magnetically stirred (300 rpm) for additional 16 h at controlled temperature (30 °C). After this time, the aqueous mixture was acidified using a 2 M aqueous HCl solution, and extracted with EtOAc (2 x 2 mL). The organic phases were combined, dried over anhydrous Na_2SO_4 and filtered, and an aliquot was taken for the determination of the degree of conversion by GC analysis. DMF was selected in a first attempt as a water miscible co-solvent for allowing the homogenization of the reaction medium in the presence of all the studied mediators.

3.3.6. pH influence in the LMS oxidation of 1a

In a test tube open to air, TEMPO (10 mol%) was added to a solution of **1a** (0.1 mmol, 100 mM) in an oxygen-saturated buffer (50 mM). The buffers used for all the pHs were the following: Buffer Na-Citrate for pH 4.5–5.5; buffer KPi for pH 6–7.5; buffer Tris-HCl for pH 8. The reaction mixture was magnetically stirred for a few minutes to dissolve all the reagents, and a solution with the corresponding laccase (5.8 U/mL) was then added, and the mixture was magnetically stirred (250 rpm) for additional 16 h at controlled temperature (30 °C). After this time, the product was extracted with EtOAc (2 x 2 mL), the organic phases were combined, dried over anhydrous Na_2SO_4

and filtered. Finally, an aliquot was taken for the determination of the degree of conversion by GC analysis.

3.3.7. Optimization of the mediator and laccase amounts in the LMS oxidation of 1a

In a test tube open to air, different amounts of TEMPO (10, 20 and 33 mol%) were added to a solution of **1a** (0.1 mmol, 100 mM) in an oxygen-saturated buffer (50 mM, L*Tv*: Na-Citrate buffer, pH 5; POXA1b: Na-Citrate buffer, pH 5.5; POXC laccase: KPi buffer, pH 6.5). The reaction mixture was magnetically stirred for a few minutes to dissolve all the reagents, and the corresponding laccase (2.9 or 5.8 U/mL) was then added. The reaction conditions, work-up and analysis were kept the same as described in Section 3.3.3.

3.3.8. Study of the solvent influence in the LMS oxidation of 1a

In a test tube open to air, TEMPO (10 mol%) was added to a solution of **1a** (0.1 mmol, 100 mM) in a monophasic or biphasic mixture of an oxygen-saturated buffer (50 mM, Na-Citrate buffer, pH 5.5 for POXA1b; KPi buffer, pH 6.5 for POXC), and the organic solvent (10% v/v, for a total volume of 1 mL). The reaction mixture was magnetically stirred for few minutes to dissolve all the reagents, then the corresponding laccase (5.8 U/mL) was added, and the mixture was magnetically stirred (250 rpm) for additional 16 h at 30 °C. After this time, the product was extracted with EtOAc (2 x 2 mL), the organic phases were combined, dried over anhydrous Na_2SO_4 and filtered. Finally, an aliquot was taken for the determination of the degree of conversion by GC analysis.

3.3.9. New recombinant ATAs panel expression (TAs 1–8)

3.3.9.1. Transformation protocol

Transformation of *E. coli* (DE3) cells: Competent *E. coli* BL21 (DE3) cells (Invitrogen/ThermoFisher Scientific, Carlsbad, CA, U.S.A.) were transformed with the vectors encoding the ATAs. The transformation protocol has been performed according to the heat shock protocol. The cells were later grown at 37 °C in TB medium supplemented with ampicillin (100 µg/mL) or kanamycin (40 µg/mL). 70 µL of the saturated broth of each recombinant cell were plated in terrific broth medium agar supplemented with the proper antibiotic and incubated overnight at 37 °C and 200 rpm. One single recombinant colony of each ATA was again grown overnight and stubs have been made from the saturated growths broths in 70% glycerol and preserved at –80 °C.

3.3.9.2. Protein expression and SDS-PAGE

One single colony of each recombinant cell was inoculated in 3 mL of terrific broth medium supplemented with the proper antibiotic overnight. Each recombinant system cell was inoculated in fresh TB medium supplemented with antibiotic for a final concentration of 0.1 OD/mL and growths were performed at 37 °C and 200 rpm in an orbital shaker. ATA expression was induced with 0.1 mM of IPTG at an OD_{600} between 0.6 and 0.8 and carried out at 25 °C and 150 rpm overnight. SDS gel page was done for confirming that the overexpression was performed after 6 h of induction.

3.3.9.3. Cell lysis

The cells were harvested at 4,000 g for 15 min and washed in the proper lysis buffer, disrupted by sonication (Branson Sonifier S-250, 2.5 minutes, 1 sec on/4 sec off, 80% output-amplitude), and centrifuged at 50,000 g for 1 h.

The cleared lysates were filtered through 0.45 µm syringe filter, concentrated and UV-activity assay were conducted. The protein concentration of the lysate was determined by the Bradford assay. The cell-free lysate was stored at –20 °C.

Consequently, the repertoire of in-house-produced ATAs available for the screening was expanded as detailed in Table 3.5.

Table 3.5. House-made ATAs used in this contribution.

Name	**ATA coding gene from**
Cv-TA	*Chromobacterium violaceum*
ArS-TA	*Arthrobacter citreus*
ArRmut11-TA	*Arthrobacter* sp. ATA-117 mutant
Bm-TA	*Bacillus megaterium*
BmS119G-TA	S119G mutant from *Bacillus megaterium*
Vf-mut-TA	mutant from *Vibrio fluvialis*
ArR-TA	*Arthrobacter* sp. KNK168
Vf-TA	*Vibrio fluvialis*
At-TA	*Aspergillus terreus*
TA1	*Pseudocardia acaciae*
TA2	*Shinella* sp.
TA3	*Tetrasohaera japonica*
TA4	*Exophiala sideris*
TA5	*Exophiala xenobiotica*
TA6	*Tetrasohaera japonica*
TA7	*Exophiala xenobiotica*-variant 1
TA8	*Exophiala xenobiotica*-variant 2

3.3.9.4. Enzymatic characterization

Suitable growth protocols and lysis buffers were established for the 8 transaminases (Table 3.6).[385] This preparation set the stage for future experiments involving reaction trials using the partially characterized crude cell-free lysates.

Table 3.6. Selected buffer and pH for lysis of recombinant *E. coli* expressing TAs 1–8.

ATA	Lysis conditions
TA1	50mM MES buffer, pH 6
TA2	50 mM MES buffer, pH 6
TA3	50 mM MOPS buffer, pH 7
TA4	100 mM KPi buffer, pH 7.5
TA5	50 mM MES buffer, pH 6
TA6	50 mM MOPS buffer, pH 7
TA7	100 mM KPi buffer, 7.5
TA8	100 mM KPi buffer, 7.5

3.3.10. General protocol for in-house ATAs recombinant expression

3.3.10.1. General protocol for the recombinant expression of (S)-selective (Cv-TA and ArS-TA) and (R)-selective transaminases (ArR-TA and ArRMut11-TA)

For the recombinant expression of the (*S*)- and (*R*)-ATAs on *E. coli*, a colony was selected, and cells were grown overnight in LB medium supplemented with ampicillin (120 µg/mL for *S*-ATAs or 100 µg/mL for *R*-ATAs) at 37 °C and 200 rpm. 250 mL of fresh LB medium was inoculated with a final cell concentration of 0.1 OD_{600}, and ampicillin (90 µg/mL for *S*-ATAs or 120 µg/mL for *R*-ATAs) was added, and the cells were grown at 37 °C and 200 rpm. ATAs expression was induced with 0.5 mM of IPTG at 0.5–0.7 OD_{600}, and for *S*-ATAs an additional amount of ampicillin was added (30 µg/mL). Induction was continued at 20 °C and 120 rpm for 16 h in the case of (*S*)-ATAs, and 5 h for (*R*)-ATAs. After that time, the cells were harvested by centrifugation at 4,000 g and 4 °C for 20 min, and washed twice with 100 mM potassium phosphate buffer, pH 7.5. Cells were frozen with nitrogen liquid and lyophilized. The crude whole cells-containing ATAs were stored at 4 °C, being stable for several months.

3.3.10.2. General protocol for the recombinant expression of Bm-TA and BmS119G-TA

For the expression of Bm-TA and BmS119G-TA on *E. coli* recombinant strain, a single colony was selected and grown overnight in LB medium (supplemented with ampicillin, 100 µg/mL) at 37 °C and 220 rpm. The starting culture was used to inoculate 500 µL of fresh LB medium supplemented with 50 µg/mL ampicillin in 2-L Erlenmeyer flasks. The cultures were incubated at a rotary shaking rate of 220 rpm at 37 °C. The recombinant protein expression was induced by adding 0.2 mM of IPTG when OD_{600} reached 0.6–0.8. The cell cultures were incubated at 18 °C for 16 h. The cells were then harvested by centrifugation at 4,000 g and 4 °C for 20 min, and washed twice with 100 mM potassium phosphate buffer, pH 7.5. Cells were frozen with nitrogen liquid and lyophilized. The crude whole cells-containing ATAs were stored at 4 °C, being stable for several months.

For the CFE, cell pellets were resuspended (1 g of wet cell paste per 10 mL HEPES buffer 100 mM, pH 8.0), containing PLP (1 mM) and imidazole (5 mM). The cell pellets were lysed in an iced bath by ultrasonication (20 cycles of 20 s on and 20 s off). After centrifugation (4 °C, 16,000 g, 20 min) the CFE was stored at –20 °C.

3.3.10.3. General protocol for the recombinant expression of Vf and Vf-mut-TA

For the expression of Vf-TA on *E. coli* recombinant strain, a single colony was selected and grown overnight in LB medium supplemented with kanamycin (50 µg/mL) at 37 °C and 220 rpm. The starting culture was used to inoculate fresh LB medium containing 50 µg/mL. The cultures were incubated at a rotary shaking rate of 220 rpm at 37 °C. The recombinant protein expression was induced by adding IPTG (1 mM), when the OD_{600} reached 0.5–0.8. After 5 h of induction, the cells were harvested and disrupted by sonication. The cells were then harvested by centrifugation at 4,000 g and 4 °C for 20 min, and washed twice with 100 mM potassium phosphate buffer, pH 7.5. The crude whole cells frozen with nitrogen liquid and lyophilized, and then stored at 4 °C, being stable for several months.

3.3.10.4. General protocol for the recombinant expression of At-TA

For the expression of At-TA on *E. coli* recombinant strain, a single colony was selected and grown overnight at 37 °C and 220 rpm in LB medium supplemented with ampicillin (100 μg/mL). The starting culture was used to inoculate fresh LB medium supplemented with ampicillin (100 μg/mL). Cells were incubated initially at 37 °C on an orbital shaker until OD_{600} reached 0.7. The recombinant protein expression was induced by adding IPTG (0.1 mM). At the same time, the incubation temperature was decreased to 20 °C, and cultivation continued for 20 h. The cells were then harvested by centrifugation at 4,000 g and 4 °C for 20 min, and washed twice with 100 mM potassium phosphate buffer, pH 7.5. Cells were frozen with nitrogen liquid and lyophilized. The crude whole cells-containing ATAs were stored at 4 °C, remaining stable for several months.

3.3.11. Evaluation of the apparent activity for *E. coli*/TA whole cells

The activity of the ATA lyophilized pellets was assayed employing enantiopure (*S*)-1-phenylethylamine (**2a**) as substrate (100 mM, Scheme 3.15).[420]

---

[420] U. K. Laemmli, *Nature* **1970**, *227*, 680–685.

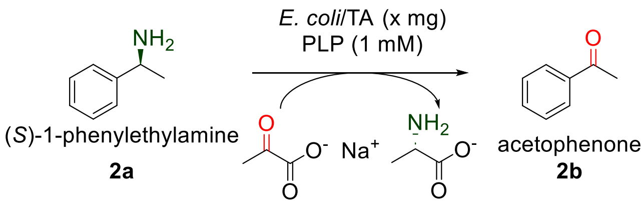

Scheme 3.15. Deamination of (*S*)-1-phenylethylamine with sodium pyruvate for TA activity determination.

Lyophilized *E. coli* cells containing the heterologously expressed TA (10 mg) were added in a 2.0-mL Eppendorf tube and rehydrated in 1 mL of KPi buffer (100 mM, pH 7.0) containing PLP (1 mM) and sodium pyruvate (100 mM) in an Eppendorf orbital thermo-shaker for 30 min at 30 °C and 700 rpm. Then, the substrate **2a** (100 mM, 12.1 μL) was added and mixed carefully (t = 0 min). The reactions were stopped after the set-up times (30 s, 60 s, 90 s, 120 s, 180 s, 240 s, 300 s) by addition of an aqueous NaOH 10 M solution (200 μL). One sample for each time point was prepared. Then, the mixture was extracted with EtOAc (2 x 500 μL). The combined organic extracts were dried with anhydrous Na_2SO_4 and subjected to GC-FID analysis. The slope of the linear function that fitted the points collected during the first minute was used to calculate the specific value of apparent enzyme activity expressed in U/mg [μmol min^{-1} mg^{-1} cells)].

In the cascade reaction, 50 mg of these whole cells were employed, which corresponded to 10 U/mL of Cv-TA.

The exact values of the other measured ATAs are reported in Table 3.7.

Table 3.7. Units measured for ATAs used in furfural transformations.

Abbreviation	Original organism description	Enzyme form	Units[a,b]
Cv	*Chromobacterium violaceum*	Lyophilized cell powder	0.084
ArR	*Arthrobacter* sp. (*R*)-selective	Lyophilized cell powder	0.15
ArS	*Arthrobacter citreus* / HisTag	Lyophilized cell powder	0.02

[a] 1 unit is defined as 1 μmol of formed product per min. [b] U/mg of *E. coli* lyophilized cells.

3.3.12. General procedure for the biotransamination of 1b into 1d

Reactions were performed on a total reaction volume of 1 mL, in an Eppendorf vial, containing the substrate (25–200 mM), DMSO (2.5% v/v), PLP (1 mM), potassium phosphate buffer (100 mM, pH 7.5), IPA (1 M), and the corresponding *E. coli* lyophilized cells heterologously expressing the corresponding ATA (10 mg). The reaction mixture was incubated at 35 °C and 250 rpm for 24 h, and then stopped by the addition of an aqueous NaOH solution (10 M, 200 μL). The mixture was extracted twice with EtOAc (2 x 500 μL), and the organic layers were separated by centrifugation (2 min, 11,350 rpm). Later, they were combined and dried over Na_2SO_4. Degrees of conversions were determined by GC.

3.3.13. Biotransamination of furfural adding the substrate in a stepwise manner

The reaction was performed on a total reaction volume of 1 mL, in an Eppendorf vial, containing the substrate (50 mM), DMSO (2.5% v/v), PLP (1 mM), potassium phosphate buffer (100 mM, pH 7.5), IPA (1 M), and *E. coli* lyophilized cells heterologously expressing ArS-TA (10 mg). The reaction mixture was incubated at 35 °C and 250 rpm for 3 h. Furfural (50 mM each addition) was again added after 3, 6, and 9 h (final concentration of 200 mM), and the reaction was incubated at 35 °C and 250 rpm for a total time of 24 h. Then it was stopped by the addition of an aqueous NaOH solution (10 M, 200 μL). The mixture was extracted twice with EtOAc (2 x 500 μL), and the organic layers were separated by centrifugation (2 min, 11,350 rpm). Later, they were combined and dried over Na_2SO_4. Degree of conversion was determined by GC, obtaining a conversion of furfuryl amine of 95%.

3.3.14. Cascade protocol to transform 1a into 1d

In a test tube open to air, TEMPO (20 mol%) was added to a solution of **1a** (9.8 mg, 100 mM) in an oxygen-saturated buffer (5 mL, KPi buffer pH 6.5 for POXC, citrate buffer pH 5.5 for POXA1b). The reaction mixture was magnetically stirred for a few minutes to dissolve all the reagents, then the laccase (5.8 U/mL) was added, and the mixture was stirred for additional time at 30 °C. After 16 h, PLP (1 mM), and $(IPA)_3PO_4$ (330 mM) were added to the mixture containing furfural (**1b**) as intermediate. The addition of this concentrated salt provided IPA to the reaction medium and increased the pH from the initial value to approximately 6.5. No further pH adjustment was required for the biotransamination reaction. Finally, whole cells expressing Cv-TA (10 mg) were added. No pH changes were observed in the KPi buffer after residual POXC action. The tube was closed and the reaction mixture was vigorously shaken for 24 h, at 250 rpm and 35 °C in an orbital shaker. After this time, the reaction was stopped by addition of an aqueous HCl 6 M solution (2 mL, pH 2). Degree of conversion into amine **1d** was determined by GC analysis. The acidified solution was extracted with EtOAc (4 x 5 mL). The resulting aqueous layer was basified by adding NaOH aqueous 10 M solution until pH 13, and extracted with EtOAc (4 x 5 mL). The organic layers were combined, washed with brine (5 mL), dried over anhydrous Na_2SO_4 and filtered. After evaporation of the solvent under reduced pressure, the corresponding amine was obtained pure as yellow oil (24 mg, 48% isolated yield), confirmed by NMR analysis.

3.3.15. EATOS calculations

E-factor calculations (Figure 3.9) were estimated considering the wastes (kg or L) of materials for producing 1 kg of furfuryl amine (**1d**) as product.

3.3.16. Analytics

3.3.16.1. GC analyses

For laccase-mediated reactions, in a 2.0 mL Eppendorf vial, the reaction mixture (1 mL) was taken and extracted with EtOAc (3 x 0.5 mL), and the combined organic layers were next washed by brine (1 mL), and dried over anhydrous Na_2SO_4, filtered and analyzed by GC (Table 3.8).

For the transaminase reactions, the mixture was treated with aqueous NaOH solution (10 M, 200 µL), then extracted twice with EtOAc (2 x 500 µL), and the organic layers were separated by centrifugation (2 min, 11,350 rpm). Later, they were combined and dried over Na_2SO_4.

For the determination of conversion values in laccase-mediated oxidations and the following transamination, the following GC column was used: Agilent DB-1701 (30 m x 0.25 cm x 0.25 µm, 12.2 psi N_2).

Table 3.8. Retention times for compounds **1a-1e**, **2a** and **2b** obtained by GC analysis.

Entry	Compound	Column	Program[a]	Retention time (min)
1	**1a**	DB-1701	90/0/2/130/3/30/200/2	4.5
2	**1b**	DB-1701	90/0/2/130/3/30/200/2	3.9
3	**1c**	DB-1701	90/0/2/130/3/30/200/2	16.2
4	**1d**	DB-1701	90/0/2/130/3/30/200/2	3.3
5	**1e**	DB-1701	90/0/2/130/2/30/200/2	6.0
6	**2a**	DB-1701	80/6.5/10/160/5/20/200/2	10.1
7	**2b**	DB-1701	80/6.5/10/160/5/20/200/2	11.4

[a] GC programme: initial temp. (ºC) / time (min) / ramp (ºC/min) / temp. (ºC) / time (min) / ramp (ºC/min) / final temp. (ºC) / time (min).

3.3.16.2. Calibration curves of compounds 1a-d, 2a, and 2b

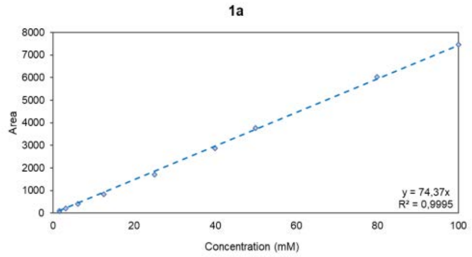

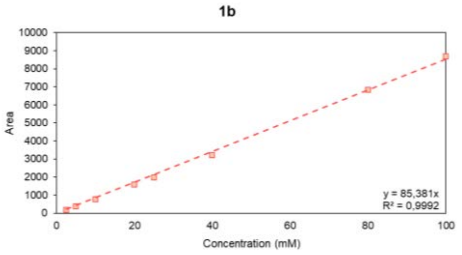

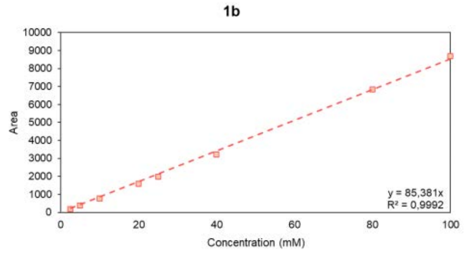

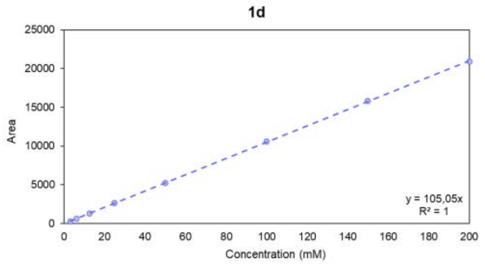

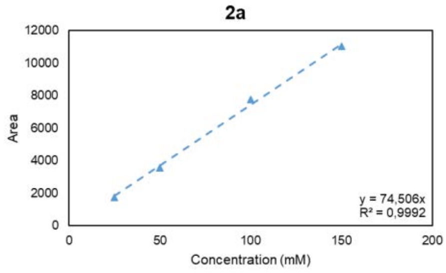

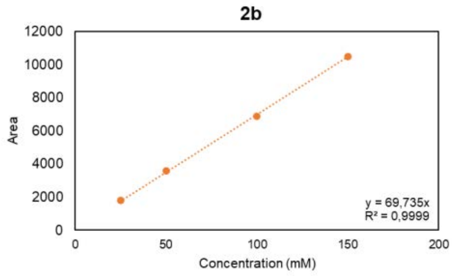

3.3.17. Compounds characterization

Furfuryl alcohol (1a)

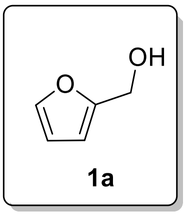

1a

Yellowish oil (80%).

Molecular formula: $C_5H_6O_2$

Molecular weight: 98.10 g/mol

^{1}**H NMR** (300 MHz, $CDCl_3$) δ 7.40 (d, J= 1.9 Hz, 1H), 6.34 (dd, J= 3.3, 1.9 Hz, 1H), 6.29 (d, J= 3.2 Hz, 1H), 4.61 (s, 2H), 1.82 (s, 1H, OH).

^{13}**C NMR** (75 MHz, $CDCl_3$) δ 154.1 (C), 142.7 (CH), 110.5 (CH), 107.9 (CH), 57.6 (CH_2).

2-Furoic acid (1c)

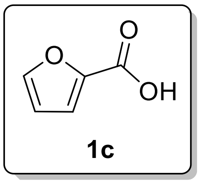

1c

White powder (70%).

Molecular formula: $C_5H_4O_3$

Molecular weight: 112.08 g/mol

^{1}H NMR (300 MHz, $CDCl_3$, TMS) δ 10.16 (br s, 1H, OH), 7.63 (m, 1H), 7.31 (d, J= 3.4 Hz, 1H), 6.55 (dd, J= 3.5, 1.7 Hz, 1H).

^{13}C NMR (75 MHz, $CDCl_3$, TMS) δ 164.2 (C), 147.9 (CH), 144.5 (C), 120.6 (CH), 112.8 (CH).

Furfuryl amine (1d)

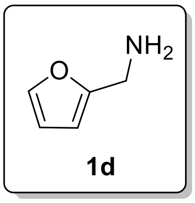

1d

Yellowish oil (48%).

Molecular formula: C_5H_7NO

Molecular weight: 97.12 g/mol

^{1}H NMR (300 MHz, $CDCl_3$, TMS) δ 7.36 (d, J= 1.8 Hz, 1H), 6.32 (t, J= 3.2 Hz, 1H), 6.15 (d, J= 3.2 Hz, 1H), 3.83 (s, 2H).

^{13}C NMR (75 MHz, $CDCl_3$, TMS) δ 156.5 (C), 141.5 (CH), 110.1 (CH), 104.9 (CH), 39.2 (CH_2).

1-(Furan-2-yl)-*N*-isopropylmethanimine (1e)

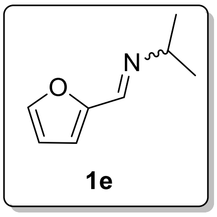

1e

Isolated from the blank reaction (without ATA) of **1b** in presence of IPA. Yellow oil (70%).

^{1}H-NMR (300 MHz, $CDCl_3$, TMS) δ 8.01 (s, 1H), 7.41 (d, *J* = 1.8 Hz, 1H), 6.62 (d, *J* = 3.4 Hz, 1H), 6.36 (dd, *J* = 3.2, 1.5 Hz, 1H), 3.39 (hept, *J* = 6.3 Hz, 1H), 1.17 (d, *J* = 6.4 Hz, 6H).

^{13}C-NMR (75 MHz, $CDCl_3$, TMS) δ 150.6 (C), 146.5 (CH), 143.9 (CH), 113.3 (CH), 110.9 (CH), 61.2 (CH), 23.6 ($2CH_3$).

CHAPTER 4

Chemoenzymatic synthesis of HMF derivatives applying LMSs and ATAs

Introduction

2,5-Bis(aminomethyl)furan (BAMF, **3f**) and 5-aminomethyl-2-furoic acid (AMFC, **3g**) are highly relevant compounds in the context of sustainable and bio-based chemistry (Scheme 4.1).[421] Their versatility and eco-friendly characteristics make them valuable intermediates compounds in chemical industry, aiming to reduce the environmental impact of the products obtained by their manufacture without affecting their performance and economic viability. Interestingly, both BAMF and AMFC can be obtained from HMF (**3a**), thus demonstrating the versatility of the latter as a renewable feedstock.

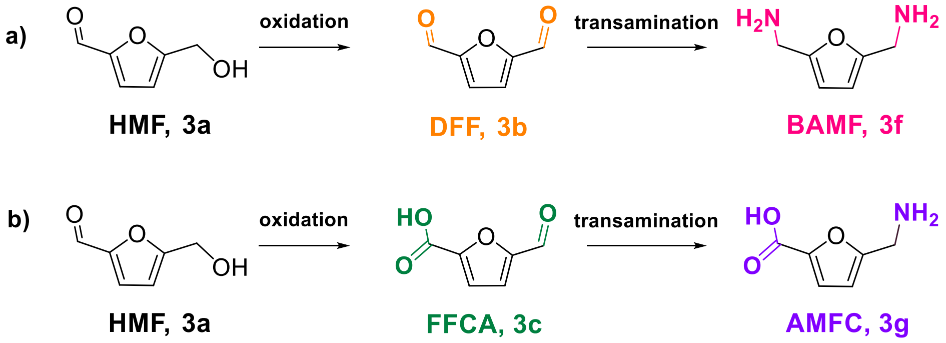

Scheme 4.1. a) **3f**, and b) **3g** biosynthesis from **3a**.

Regarding BAMF synthesis, the process typically begins with the oxidation of HMF to form DFF. Following that, DFF can be enzymatically aminated with the assistance of ATAs. Conversely, in the case of AMFC synthesis, the initial step involves the conversion of HMF into FFCA (**3a**) as an intermediate, which can then undergo a transaminase-catalyzed reaction to affoard AMFC.

---

[421] a) A. Lancien, R. Wojcieszak, E. Cuvelier, M. Duban, P. Dhulster, S. Paul, F. Dumeignil, R. Froidevaux, E. Heuson, *ChemCatChem* **2021**, *13*, 247–259; b) C. C. Truong, D. K. Mishra, Y. Suh, *ChemSusChem* **2023**, *16*, e202201846.

BAMF and AMFC can be used in fields such as pharmaceuticals and polymers. In particular, BAMF is an interesting monomer for various functionalized material, like Nonisocyanate polyurethanes (NIPUs) and functional cross-linked materials derived therefrom (Scheme 4.2).[422]

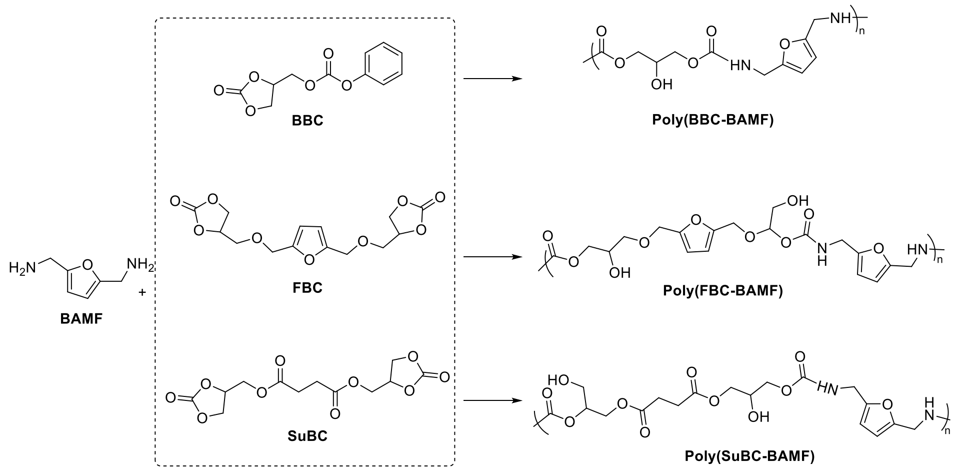

Scheme 4.2. Synthesis of main-chain NIPUs utilizing BAMF and 3-furan-based bis(cyclic carbonates): phenoxycarbonyloxymethyl ethylene carbonate (BBC), hydroxymethylfuran bis(cyclic carbonate) (FBC), and succinate bis(cyclic carbonate) (SuBC).

AMFC has drawn increasing attention as precursor of poly(5-aminomethyl-2-furoic acid, PAMF) after direct polymerization (Scheme 4.3). The achieved polymer showed exceptional properties comparable with commercialized materials.[423]

---

[422] P. S. Choong, N. X. Chong, E. K. W. Tam, A. M. Seayad, J. Seayad, S. Jana, *ACS Macro Lett.* **2021**, *10*, 635–641.

[423] a) A. W. Lankenau, M. W. Kanan, *Chem. Sci.* **2020**, *11*, 248–252; b) C. P. Woroch, I. W. Cox, M. W. Kanan, *J. Am. Chem. Soc.* **2023**, *145*, 697–705.

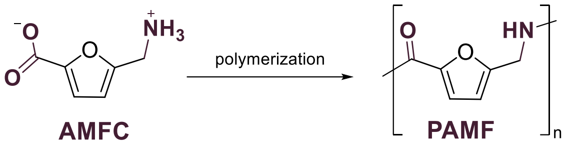

Scheme 4.3. Ploymerization of AMFC to obtain PAMF.

4.1.1. Oxidized derivatives obtained from HMF

As previously explained, the presence of two functional groups in HMF plays a significant role in its heightened reactivity. Consequently, HMF serves as a crucial foundational compound for the production of various valuable industrial chemicals, including BAMF and AMFC, which are obtained through oxidative reactions involving compounds like DFF, FFCA, FDCA, and HFCA as intermediated (Figure 4.1). Moreover, oxidized chemicals derived from HMF are bio-platform molecules (intermediates) for useful materials in the industrial context.

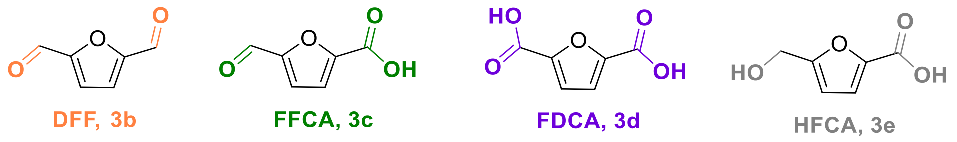

Figure 4.1. Oxidized compounds achievable from HMF.

The challenge for HMF oxidation into these compounds lies in the adequate catalyst selection and controlling the reaction conditions (temperature, pression and solvent)[424] to transform HMF into a desired product while minimizing the formation of unwanted byproducts.

---

[424] M. Ventura, A. Dibenedetto, M. Aresta, *Inorg. Chim. Acta* **2018**, *470*, 11–21.

Numerous research efforts are aimed at developing more efficient and selective catalytic processes for the conversion of HMF, as it has significant potential for the production of renewable chemicals and biofuels.[425]

Owing to the disadvantages linked to conventional chemical processes for HMF conversion, there has been a growing interest in the biotransformation of HMF into its derivatives. Despite numerous efforts focused on whole-cell and biocatalytic HMF conversion, limits of these studies lie in their predominant confinement to laboratory-scale operations, due to relatively modest yields of the end products, and the reduced economic and industrial viability associated with these biocatalytic approaches.

4.1.1.1. DFF (3b)

DFF has been effectively converted into valuable compounds, contributing to the creation of promising materials. Numerous efforts have been made to optimize reaction conditions in this regard.[426] Most of the approaches for DFF accumulation include HMF oxidation catalysed by metals and various solid catalysts in organic solvents, or in water[427] or using sugar oxidases like galactose oxidase, mainly working in high solvent reaction systems.[428]

Sheldon and co-workers reported the first example of biocatalytic conversion of HMF into DFF by using a chloroperoxidase obtained from *Caldariomyces fumago*, while hydrogen peroxide was present as a reactant.[429] This process yielded a 53% DFF output in just 2.5 h with the concomitant production of various by-products.

---

[425] a) Z. Zhang, P. Zhou, in *Production of Platform Chemicals from Sustainable Resources. Biofuels and Biorefineries*, (Eds.: X. Fang, Z. Smith, Jr., R. Qi), Springer Nature Singapore, **2017**, pp. 171–206; b) S. Hameed, L. Lin, A. Wang, W. Luo, *Catalysts* **2020**, *10*, 120; c) J. T. Cunha, A. Romaní, L. Domingues, *Catalysts* **2022**, *12*, 202.

[426] W. Zhang, H. Qian, Q. Hou, M. Ju, *Green Chem.* **2023**, *25*, 893–914.

[427] P. H. Tran, *ChemSusChem* **2022**, *15*, e202200220.

[428] T. Haas, J. C. Pfeffer, K. Faber, M. Fuchs, US 2014/0120587 A1, **2014**.

[429] M. P. J. van Deurzen, F. van Rantwijk, R. A. Sheldon, *J. Carbohydr. Chem.* **1997**, *16*, 299–309.

Additionally, Li and co-workers utilized *Candida boidinii* alcohol oxidase in combination with catalase to facilitate the oxidation of HMF, resulting in a DFF yield of 43% within 72 h.[430] Due to the activating influence of horseradish peroxidase on galactose oxidase, Carnell and co-workers established a biocatalytic setup comprising horseradish peroxidase, galactose oxidase, and catalase. This system resulted in an 88% DFF yield at pH 7.5, compared to the 77% at pH 6.5 and 56% in deionized water, emphasizing the role of the solvent.[431] Finally, Turner and co-workers reported the utilization of an engineered galactose oxidase for the oxidation of HMF obtaining DFF in 92% yield.[432]

DFF, characterized by two identical aldehyde groups, shows significant potential as a precursor for the production of pharmaceuticals, fuel and polymers.[433] First of all, it is the intermediate for BAMF production.[434] A significant hurdle in the synthesis of BAMF from HMF, utilizing DFF as an intermediate, is the design of a complete enzymatic pathway with high yield that ensure the accumulation of the desired product and that would not require harsh conditions or the addition of dangerous reagents. These challenges, particularly pertaining to the transamination of DFF into BAMF, have been thoroughly investigated in this Doctoral Thesis.[435]

In 2015, Mascal and his team successfully achieved the synthesis of furan-2,5-dicarbonyl chloride (FDCC) by DFF oxidation with *tert*-butyl hypochlorite, reaching 80% yield. FDCC was proved to be useful as an intermediate for making furoate ester biofuels in ethanol leading to diethyl furan-2,5-dicarboxylate in 76% yield through a two-step process.[436]

---

[430] Y. Z. Qin, Y. M. Li, M. H. Zong, H. Wu, N. Li, *Green Chem.* **2015**, *17*, 3718–3722.

[431] S. M. McKenna, P. Mines, P. Law, K. Kovacs-Schreiner, W. R. Birmingham, N. J. Turner, S. Leimkühler, A. J. Carnell, *Green Chem.* **2017**, *19*, 4660–4665.

[432] W. R. Birmingham, A. T. Pedersen, M. Dias Gomes, M. B. Madsen, M. Breuer, J. M. Woodley, N. J. Turner, *Nat. Commun.* **2021**, *12*, 4946.

[433] G. D. Yadav, R. V. Sharma, *Appl. Catal. B: Environ.* **2014**, *147*, 293–301.

[434] N. T. Le, A. Byun, Y. Han, K. I. Lee, H. Kim, *Green Sustain. Chem.* **2015**, *5*, 115–127.

[435] A. Pintor, N. Cascelli, A. Volkov, V. Gotor-Fernández, I. Lavandera, *ChemBioChem*, doi: 10.1002/cbic.202300514.

[436] S. Dutta, L. Wu, M. Mascal, *Green Chem.* **2015**, *17*, 3737–3739.

As well, Fu and co-workers developed a powerful Pd catalyst supported by hydroxyapatite for biomass-derived furfural hydrogenation, achieving a quantitative yield into 2,5-bis(hydroxymethyl)-tetrahydrofuran from DFF at 60 °C.[437] The former finds important applications in resin, polymer, and synthetic fiber manufacturing.

2,5-Dicyanofuran[438] and 2,5-bis(aminomethyl)furan,[439] are key monomers for polymer synthesis, which were prepared by Xu and co-workers through oximation of DFF. Both compounds led to the corresponding dioxime that was later chemically converted into 2,5-bis(aminomethyl)furan through dehydration and hydrogenation processes, respectively. Other relevant compounds achieved from DFF are reported in Scheme 4.4.

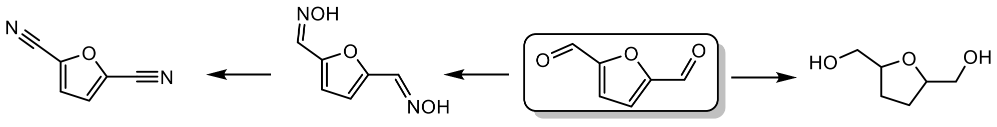

3b

Scheme 4.4. Chemicals derived from DFF.

One of the direct uses of DFF as building block for polymers formation was disclosed by Dhers *et al.*[440] for the synthesis of a polyimine vitrimer derived from fructose, which allows an entirely renewable carbon content of 100% by blending DFF with a mixture of dimeric and trimeric amines in three-step process and without a catalyst need. This process relied on imine bonds as covalent dynamic connections (Scheme 4.5). The resulting dynamic films due to covalent bond rearrangements offers unique properties and potential applications, exhibiting rapid stress relaxation at room temperature and stability in both basic and acidic environments.

---

[437] C. Li, G. Xu, X. Liu, Y. Zhang, Y. Fu, *Ind. Eng. Chem. Res.* **2017**, *56*, 8843–8849.

[438] Y. Xu, X. Jia, J. Ma, J. Gao, F. Xia, X. Li, J. Xu, *ACS Sustain. Chem. Eng.* **2018**, *6*, 2888–2892.

[439] Y. Xu, X. Jia, J. Ma, J. Gao, F. Xia, X. Li, J. Xu, *Green Chem.* **2018**, *20*, 2697–2701.

[440] S. Dhers, G. Vantomme, L. Avérous, *Green Chem.* **2019**, *21*, 1596–1601.

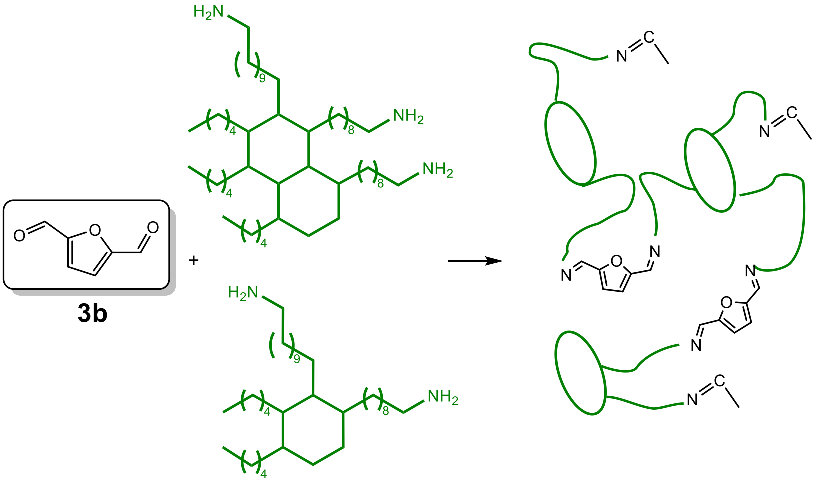

Scheme 4.5. The production of DFF-based polyimine vitrimer with a mixture of dimeric and trimeric amines, known as DTA.[440]

4.1.1.2. FFCA (3c)

Research on FFCA production is constrained by the challenges of achieving selectivity in its synthesis, as FFCA is primarily formed through the partial oxidation of HMF. Early research on FFCA production was pioneered by Domínguez de María and Guajardo, utilizing a catalytic system consisting of lipase B from *Candida antarctica* (CAL-B) and TEMPO for the oxidation of HMF. This method resulted in a 52% FFCA yield in 24 h when using *t*-butanol as the solvent.[441]

Similarly, Martínez and co-workers found an aryl alcohol oxidase from *Pleurotus eryngii* was effective in partially oxidizing HMF, leading to a 98%

---

[441] P. Domínguez de María, N. Guajardo, *ChemSusChem* **2017**, *10*, 4123–4134.

FFCA yield within 4 h.[442] Additionally, Dijkman and Fraaije employed HMF oxidase from *Methylovorus* sp. MP688, which produced a 92% FFCA yield from HMF after 5 h.[443] To boost FFCA production, Zhang identified a laccase (CotA-TJ102) from *Bacillus subtilis* capable of selectively oxidizing HMF affording a 98.5% FFCA yield in 12 h with complete HMF conversion.[444]

Recently, TEMPO was used in the metal-free synthesis of DFF and FDCA with acid promoters in *t*-BuOH as solvent, and the role of different acid additives in the product distribution was discussed. The hydration degree of aldehyde intermediates was key to control the selectivity of the reaction through carboxylic acid derivatives.[445] In addition, Li and co-workers showed how reaction engineering can lead to acidic production of HMF derivatives from laccase/TEMPO system, using the laccase from *Trametes versicolor*. Thus, DFF undergoes hydration with water to form the gem-diol and over-oxidization to the carboxylic acid FFCA, the salt composition and ionic strength of the buffer influencing more than the pH of the reaction on the FFCA formation and later FDCA accumulation.[446]

Wang and co-workers developed a piezocatalytic method for HMF oxidation into FFCA with 96% conversion and 70% FFCA yield.[447] Nitrogen doped carbon spheres with wrinkled cages as metal-free catalysts led to achieve FFCA from HMF with 92.3% conversion and 90.5% selectivity.[448] Finally, a task-oriented Anderson-type polyoxometalate and DES coupling system was demonstrated as an adequate and reusable system for HMF oxidation into FFCA (97% yield).[449]

---

[442] J. Carro, P. Ferreira, L. Rodríguez, A. Prieto, A. Serrano, B. Balcells, A. Ardá, J. Jiménez-Barbero, A. Gutiérrez, R. Ullrich, *et al.*, *FEBS J.* **2015**, *282*, 3218–3229.

[443] W. P. Dijkman, M. W. Fraaije, *Appl. Environ. Microbiol.* **2014**, *80*, 1082–1090.

[444] C. Zhang, X. Chang, L. Zhu, Q. Xing, S. You, W. Qi, R. Su, Z. He, *Int. J. Biol. Macromol.* **2019**, *128*, 132–139.

[445] X. Li, R. Zhu, *Appl. Catal. A: Gen.* **2022**, *636*, 118600.

[446] A. D. Cheng, M. H. Zong, G. H. Lu, N. Li, *Adv. Sustain. Syst.* **2021**, *5*, 2000297.

[447] Z. Chen, H. Zhou, F. Kong, M. Wang, *Appl. Catal. B: Environ.* **2022**, *309*, 121281.

[448] J. Zhu, C. Yao, A. Maity, J. Xu, T. Zhan, W. Liu, M. Sun, S. Wang, V. Polshettiwar, H. Tan, *Chem. Commun.* **2021**, *57*, 2005–2008.

[449] Y. Sun, K. Yang, Z. Zhu, T. Su, W. Ren, H. Lü, *Chem. Commun.* **2022**, *58*, 8105–8108.

Chemical catalysts for the production of FFCA via selective oxidation of 5-HMF as CuO-CeO_2, Ru/Al_2O_3, and MnO_2–$NaHCO_3$ mixed oxides were also employed. These catalysts, when combined with molecular oxygen as the oxidizing agent in an aqueous solution, exhibited excellent performance in terms of both selectivity and conversion.[195b,450]

FFCA has applications in the synthesis of surfactants and resins. Moreover, it has distinctive structural characteristics that have been reported well-suited for the synthesis of drug derivatives (Scheme 4.6).[451]

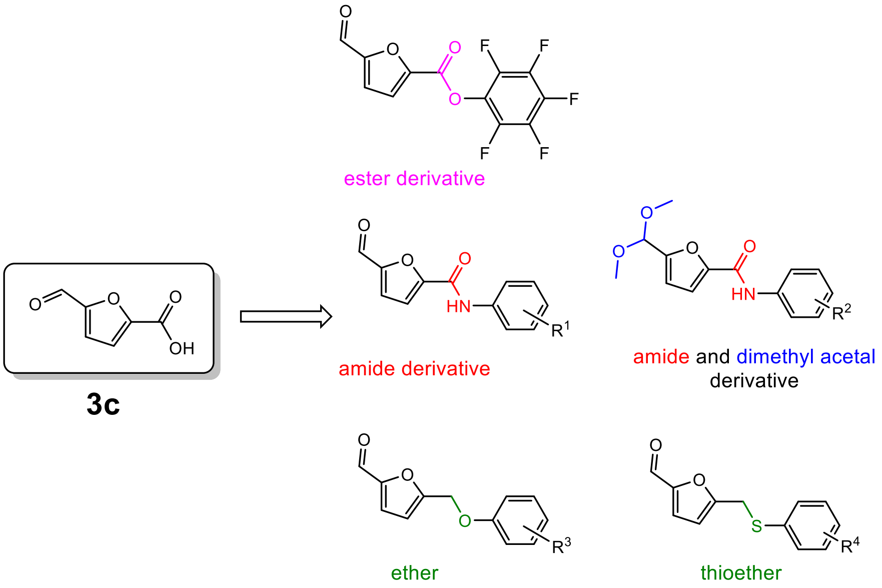
ester derivative
3c
amide derivative
amide and dimethyl acetal derivative
ether
thioether
HN
R1
R2
R3
R4
OH
F
S

Scheme 4.6. Structure of FFCA-based drug derivatives.

---

[450] a) A. D. da Fonseca Ferreira, M. Dorneles de Mello, M. A. P. da Silva, *Ind. Eng. Chem. Res.* **2019**, *58*, 128–137; b) E. Hayashi, Y. Yamaguchi, K. Kamata, N. Tsunoda, Y. Kumagai, F. Oba, M. Hara, *J. Am. Chem. Soc.* **2019**, *141*, 890–900.

[451] D. Zhao, T. Su, Y. Wang, R. S. Varma, C. Len, *Mol. Catal.* **2020**, *495*, 111133.

4.1.1.3. FDCA (3d)

The conversion of HMF into FDCA requires a series of consecutive oxidation steps, which can lead to a complex reaction medium due to the wide array of potential intermediate products that may form during the process.[452] The transformation of HMF into FDCA involves a two-step process. Initially, the alcohol group in HMF undergoes oxidation to form the corresponding aldehyde, which is subsequently oxidized to produce FDCA. Various reaction systems, employing both enzymatic and chemoenzymatic approaches were explored utilizing either isolated enzymes or whole-cell systems.

Various methods have been investigated for oxidizing HMF to FDCA, including electrocatalysis, photocatalysis, and the use of metal oxides as catalysts.[453] As well, innovative processes have been reported, including electrochemical and photochemical, as well as the application of microwave assistance, continuous flow systems, along with alternative methods involving noble and non-noble metals supported on various materials.[454]

Amongst all, biocatalysis is considered the ideal methodology for sustainable and environmentally friendly FDCA production. In one of the early examples, dating back to 2013, a cascade reaction was proposed, involving the initial oxidation of HMF with TEMPO to yield DFF. Subsequently, DFF was oxidized to FDCA using peracetic acid, which was generated *in situ* by CAL-B.[455]

Using oxidoreductases, Koopman and co-workers reported the first example of whole-cell biotransformation of HMF into FDCA, using a recombinant strain of *Pseudomonas putida* S12. They attributed the biotransformation process to a gene coding for an oxidoreductase enzyme.[456] Recently, whole-cell biocatalysis was applied in a cascade reaction to convert HMF into FDCA by co-expressing vanillin dehydrogenase and HMF/furfural oxidoreductase in *Escherichia coli*.[457]

---

[452] H. Yuan, H. Liu, J. Du, K. Liu, T. Wang, L. Liu, *Appl. Microbiol. Biotechnol.* **2020**, *104*, 527–543.

[453] D. Troiano, V. Orsat, M. J. Dumont, *ACS Catal.* **2020**, *10*, 9145–9169.

[454] a) C. Chen, L. Wang, B. Zhu, Z. Zhou, S. I. El-Hout, J. Yang, J. Zhang, *J. Energy Chem.* **2021**, *54*, 528–554; b) T. Su, D. Zhao, Y. Wang, L. Hongying, R. S. Varma, C. Len, *ChemSusChem* **2021**, *14*, 266–280.

[455] M. Krystof, M. Pérez-Sánchez, P. Domínguez de María, *ChemSusChem* **2013**, *6*, 826–830.

A cascade reaction employing a LMS system and a whole cell catalyst was studied by Troiano and co-workers, achieving the successful oxidation of HMF into FDCA. The laccase from *Trametes versicolor* and TEMPO in combination with *Trichoderma reesei* whole-cell filamentous fungus achieved the best results with a FDCA molar yield of 88% after 80 h.[458]

Another cascade approach reported is the three-enzyme sequence using galactose oxidase, unspecific peroxygenase, and aryl alcohol oxidase, resulting in an 80% yield of FDCA.[459]

More recently, Kara and co-workers reported a one-pot biocatalytic cascade for the synthesis of FDCA from HMF in biphasic and microaqueous conditions using galactose oxidase to first produce DFF, which was subsequently subjected to oxidation with peracetic acid formed from ethyl acetate by CAL-B catalyzed perhydrolysis.[460]

In an alternative approach, immobilized cells of *Burkholderia cepacia* H-2 were used to resolve the issue of HMF inhibition in the biofuel production process from lignocellulose waste. The microorganism, able to convert HMF into FDCA, was an effective solution for the removal of HMF in the liquor.[461]

A newly discovered enzyme, 5-hydroxymethylfurfural oxidase (HMFO), was applied to catalyze the oxidation of HMF into FDCA in a single reaction step.[443] Later on, the efficient whole-cell biotransformation of HMF into FDCA was achieved by using a strain of *Pseudomonas putida* (S12) engineered to express HMFO.[462]

---

[456] F. Koopman, N. Wierckx, J. H. de Winde, H. J. Ruijssenaars, *Proc. Natl. Acad. Sci.* **2010**, *107*, 4919–4924.

[457] X. Wang, X. Y. Zhang, M. H. Zong, N. Li, *ACS Sustain. Chem. Eng.* **2020**, *8*, 4341–4345.

[458] D. Troiano, V. Orsat, M.-J. Dumont, *Bioresour. Technol.* **2022**, *344*, 126169.

[459] A. Karich, S. Kleeberg, R. Ullrich, M. Hofrichter, *Microorganisms* **2018**, *6*, 5.

[460] M. Milić, E. Byström, P. Domínguez de María, S. Kara, *ChemSusChem* **2022**, *15*, e202102704.

[461] J.-Y. Tsai, P.-Y. Lu, C.-F. Yang, *Biocatal. Biotransform.* **2022**, *40*, 275–285.

Overall, there have been several attemps for the biocatalytic methods to production of FDCA, however many of these approaches require additional refinements to enhance productivity and cost-efficiency for large-scale applications.[453] The industrial interest in FDCA is well documented in a recent patent review about its biotechnological production strategies.[463] FDCA, in fact is one of the twelve key value-added platform chemicals derived from biomass identified by the U.S. Department of Energy.[464] For instance, it is utilized in the production of amides, thermosetting materials, polyesters, resins, and plasticizers, which have broad applications in the manufacturing of everyday-use products. FDCA serves as a precursor to terephthalic acid, the major component together with ethylene glycol (EG) in the production of PEF.[192a,465] PEF has been employed in polymer synthesis either alone and combined with PET, potentially serving as a renewable substitute for entirely PET-based commercial polymers that are typically derived from the transesterification and subsequent polymerization of terephthalic acid (TPA) and EG (Figure 4.2).[466] Moreover, the polycondensation of pure FDCA, 1,6-hexanediol and 1,2-propanediol resulted in a co-polyester used as 3D-printed material.[467]

---

[462] C. Hsu, Y. Kuo, Y. Liu, S. Tsai, *Microb. Biotechnol.* **2020**, *13*, 1094–1102.

[463] M. Milić, P. Domínguez de María, S. Kara, *EFB Bioecon. J.* **2023**, *3*, 100050.

[464] T. Werpy, G. Petersen, US Department of Energy, United States, **2004**. doi: 10.2172/15008859.

[465] a) J. Zhang, J. Li, Y. Tang, L. Lin, M. Long, *Carbohydr. Polym.* **2015**, *130*, 420–428; b) E. Barnard, J. J. Rubio Arias, W. Thielemans, *Green Chem.* **2021**, *23*, 3765–3789.

[466] K. Loos, R. Zhang, I. Pereira, B. Agostinho, H. Hu, D. Maniar, N. Sbirrazzuoli, A. J. D. Silvestre, N. Guigo, A. F. Sousa, *Front. Chem.* **2020**, *8*, 585.

[467] Y. Geng, Z. Wang, X. Hu, Y. Li, Q. Zhang, Y. Li, R. Wang, L. Zhang, *Eur. Polym. J.* **2019**, *114*, 476–484.

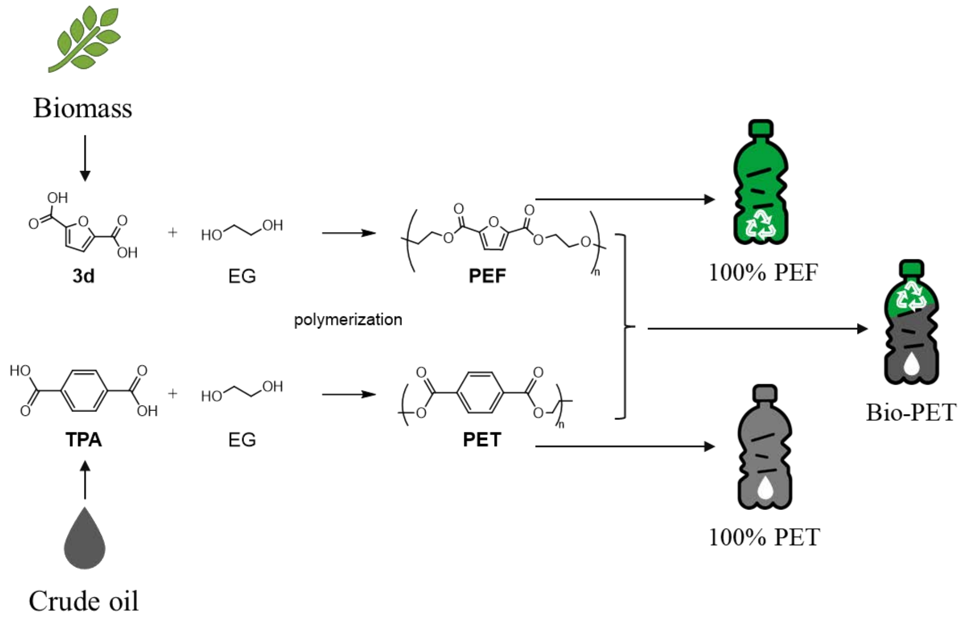
Biomass
3d
EG
PEF
polymerization
TPA
EG
PET
Crude oil
100% PEF
Bio-PET
100% PET

Figure 4.2. PEF and PET synthesis and manufacture of renewable PEF bottles, multilayer PEF and PET bottles (Bio-PET) and PET bottles (adapted from www.renewable-carbon.eu/graphics).

PEF and related materials obtained from FDCA are environmentally friendly polyester alternatives that have found increasing applications in the manufacturing sector (Figure 4.3).[468]

---

[468] S. Singhal, S. Agarwal, M. P. Mudoi, N. Singhal, R. Singh, *Biomass Convers. Biorefinery* **2021**, doi: 10.1007/s13399-021-01871-6.

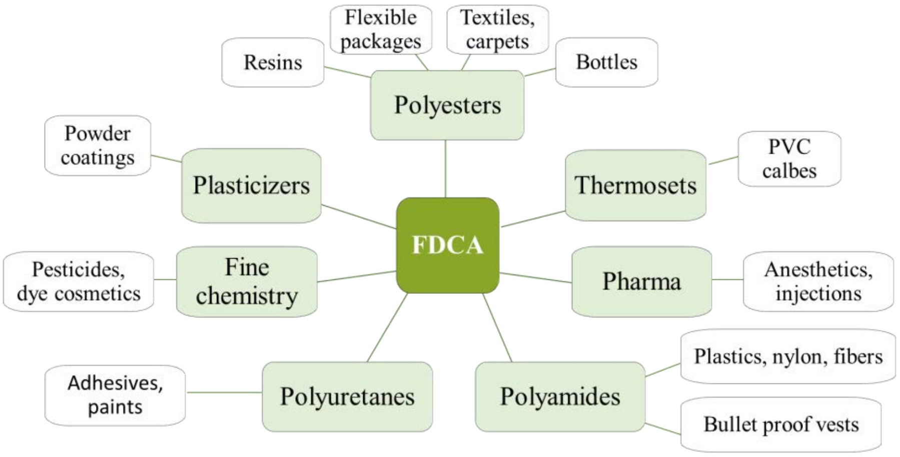
FDCA
Polyesters
Resins
Flexible packages
Textiles, carpets
Bottles
Plasticizers
Powder coatings
Thermosets
PVC calbes
Fine chemistry
Pesticides, dye cosmetics
Pharma
Anesthetics, injections
Polyuretanes
Adhesives, paints
Polyamides
Plastics, nylon, fibers
Bullet proof vests

Figure 4.3. Different compounds achieved from FDCA as chemical platform.

4.1.1.4. HFCA (3e)

HFCA is obtained by the selective oxidation of the aldehyde group of HMF. Metal catalysts such as silver oxide surfaces[469] and cobalt based MOFs[470] have been reported for HFCA production from HMF. Nevertheless, biocatalytic routes are currently more investigated, due to their sustainability and the achievement of higher yields. For instance, lipase-mediated HMF oxidation was proved as a highly advantageous method for HFCA production by Domínguez de María and co-workers, yielding a 76% HFCA yield in 24 h when using ethyl acetate as the acyl donor, hydrogen peroxide and CAL-B.[455] Then, Li and his team utilized *Escherichia coli* derived xanthine oxidase in the presence of air, obtaining 94% yield of HMF oxidation into HFCA after 7 h. Additionally, another oxidation system was assayed for HMF with horse liver alcohol dehydrogenase and hydrogen peroxide, which, under optimized conditions, yielded an 81% HFCA production after 60 h.[430]

---

[469] a) D. Zhao, D. Rodriguez Padron, R. Luque, C. Len, *ACS Sustain. Chem. Eng.* **2020**, *8*, 8486–8495; b) C. A. Celaya, R. Oukhrib, M. A. El Had, Y. Abdellaoui, H. A. Oualid, H. Bourzi, R. Chahboun, D. Zhao, S. M. Osman, V. S. Parmar, C. Len, *Mol. Catal.* **2022**, *519*, 112117.

[470] M. Bordeiasu, A. Ejsmont, J. Goscianska, B. Cojocaru, V. I. Parvulescu, S. M. Coman, *Appl. Catal. A: Gen.* **2023**, *657*, 119147.

Recently, Hatti-Kaul and co-workers reported a remarkable 98% yield of HFCA within 12 h by using *Gluconobacter oxydans* to oxidize HMF under pH-controlled conditions.[471] Similarly, Ouyang and his team used *Pseudomonas putida* KT2440 whole cells for the HMF selective oxidation, obtaining a 96.8% yield from 160 mmol/L HMF within 12 h and 100% HFCA yield from 140 mmol/L in just 6 h at 35 °C.[472] Meanwhile, the optimization of reaction parameters opened up new possibilities for large-scale HFCA production. For instance, Zhang and co-workers explored the use of *Deinococcus wulumuqiensis* R12 for HMF oxidation, achieving a 90% yield when processing 300 mmol/L HMF in a fed-batch asset after 20 h.[473] Similarly, Chang's research team utilized *Pseudomonas aeruginosa* PC-1 to convert HMF into HFCA, yielding 90.1% within just 6 h, increasing substrate concentration from 100 to 721 mmol/L HFCA in fed-batch modality.[474] More recently, the same research group identified the aldehyde dehydrogenase responsible for HMF oxidation, subsequently amplified in *E. coli*. In particular, the engineered *E. coli* strain displayed an impressive tolerance to HMF (up to 300 mM): when applied in a fed-batch process, 547.8 mM HFCA was produced from 600 mM HMF within 19 h only, paving the way for promising industrial production of HFCA.[475]

HFCA was applied in the enzymatic synthesis of furan-based oligoesters, using ε-caprolactone as a co-monomer[193] or for the preparation of plasticizers tested on poly(vinyl chloride).[476]

---

[471] M. Sayed, S. H. Pyo, N. Rehnberg, R. Hatti-Kaul, *ACS Sustain. Chem. Eng.* **2019**, *7*, 4406–4413.

[472] Q. Xu, Z. Zheng, L. Zou, C. Zhang, F. Yang, K. Zhou, J. Ouyang, *Bioprocess Biosyst. Eng.* **2020**, *43*, 67–73.

[473] R. Cang, L. Q. Shen, G. Yang, Z. D. Zhang, H. Huang, Z. G. Zhang, *Catalysts* **2019**, *9*, 526.

[474] X. Pan, S. Wu, D. Yao, L. Liu, L. Zhang, Z. Yao, Y. Pan, S. Chang, B. Li, *React. Chem. Eng.* **2020**, *5*, 1397–1404.

[475] S. Chang, S. Zhang, T. Chen, L. Xu, S. Ge, B. Li, C. Yun, G. Zhang, X. He, X. Pan, *Mol. Catal.* **2023**, *538*, 112966.

[476] Y. Hao, A. Tian, J. Zhu, J. Fan, Y. Yang, *Ind. Eng. Chem. Res.* **2020**, *59*, 18290–18297.

4.1.2. Current challenges in the enzymatic modification of HMF (3a)

Biorefinery sector has recently prioritized HMF and its derivatives due to their versatile applications. While various chemical methods have been developed to produce furanic derivatives, they often come with environmental issues, challenging reaction conditions, and by-product generation. Therefore, exploring alternatives routes for HMF conversion is crucial. Novel biotransformation pathways have been set-up to generate chemicals like FDCA, DFF, HFCA, FFCA, and latest BAMF and AMFC, among others. However, these biotransformation processes face limitations, primarily due to HMF's toxicity that inhibits microorganism growth and enzymatic activity. Challenges also include side-product formation, the absence of simple separation techniques, and catalyst regeneration.

To make the commercial-scale production of HMF derivatives feasible, in-depth investigation into metabolic mechanisms and rate-limiting steps in HMF conversion is needed to engineer innovative biotransformation pathways in microorganisms. Enhancing microbial HMF conversion can be achieved through modifying proteins to accelerate substrate conversion and improve the overall transformation rate. For industrial viability, it is essential to analyze enzyme stereochemical structures and active sites, in order to design new biocatalytic pathways for HMF conversion. Metabolic engineering of microorganisms can enhance enzyme yields and activities related to HMF transformation. In terms of cost-effectiveness, immobilizing enzymes and whole cells through efficient and cost-friendly methods is crucial for easy recovery, reducing overall process costs. Robust biocatalytic systems are needed to counteract the toxicity of furan aldehydes, which can inhibit enzyme actions. Exploring cost-effective downstream processing techniques that allow simple and uncontaminated recovery of HMF derivatives is essential. Optimizing cascade reactions for HMF biotransformation can prevent the accumulation of intermediate products. Lastly, considering the high cost of HMF and its derivatives, it is essential to explore new biotransformation approaches with industrial feasibility for cost-effective production. Therefore, further research in enzyme, metabolic, and chemical engineering, along with process design, is currently a need to address the challenges in HMF biotransformation, enabling the development of environmentally friendly and industrially viable technologies for high-value HMF derivative production.

Results and Discussion

4.2.1. Transamination of DFF (3b) into BAMF (3f)

In order to study the production of furan diamines, the transamination of **3b** in **3f** was investigated (Scheme 4.7). The standard established reaction conditions were utilized, which involved IPA (1 M) as the amine donor in a KPi buffer with a pH of 7.5 and DMSO (2.5% v/v) as a co-solvent, necessary due to the relatively low solubility of **3b** in aqueous medium. Before performing the enzymatic screening, we carried out solubility tests with amine **3f**, which revealed that the product of our reaction had high solubility in water, making it difficult to extract using various organic solvents. Consequently, similar to amine **3g**, we opted for reverse phase HPLC as the analytical method to monitor the reaction. This method was selected to accurately measure the concentrations of the substrate **3b** and product **3f** in biotransaminations.

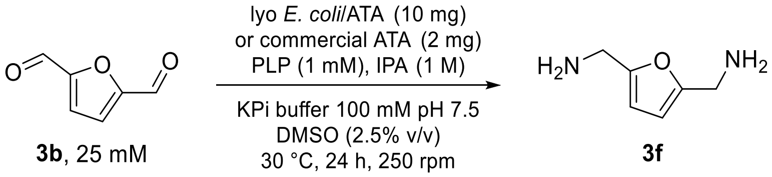

Scheme 4.7. Reaction conditions for biotransamination of **3b** into **3f**.

A blank reaction, performed without the addition of enzyme, once again confirmed that **3b** was completely converted into the diimine derivative **3h** in the reaction mixture (Scheme 4.8). This was due to the high reactivity of IPA with the aldehyde groups in the aqueous medium, as already observed for furfural (see Section 3.2.3.3) and supported by NMR studies (see Section 4.3.9).

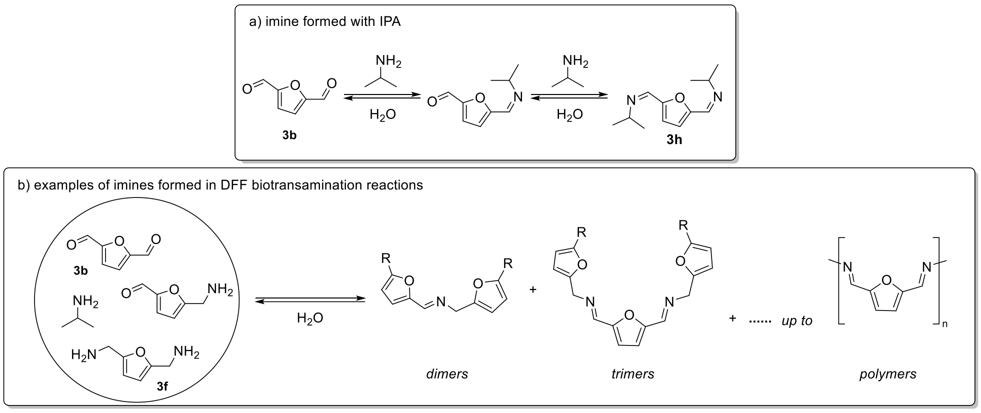
a) imine formed with IPA
NH2
H2O
3b
3h
b) examples of imines formed in DFF biotransamination reactions
3b
NH2
3f
R
dimers
trimers
+ ...... up to
n
polymers

Scheme 4.8. Different reaction possibilities for (poly)imines formation in the biotransamination of dialdehyde **3b** showed in the present study due to the: presence of: a) presence of IPA; b) The amine product **3f** and amino aldehyde intermediate.

During our investigations, we observed three different scenarios in the monitorization of the studied transformations, outlined in Figure 4.4.

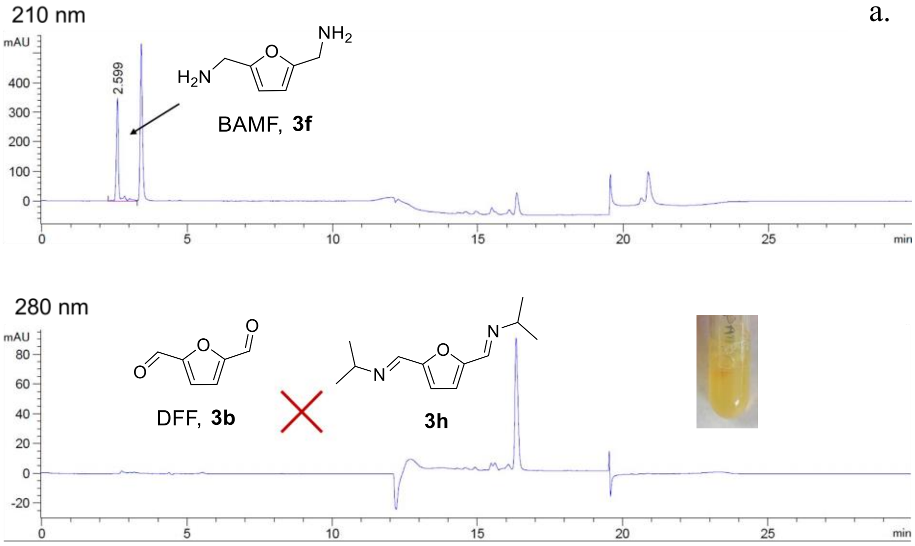

Figure 4.4.

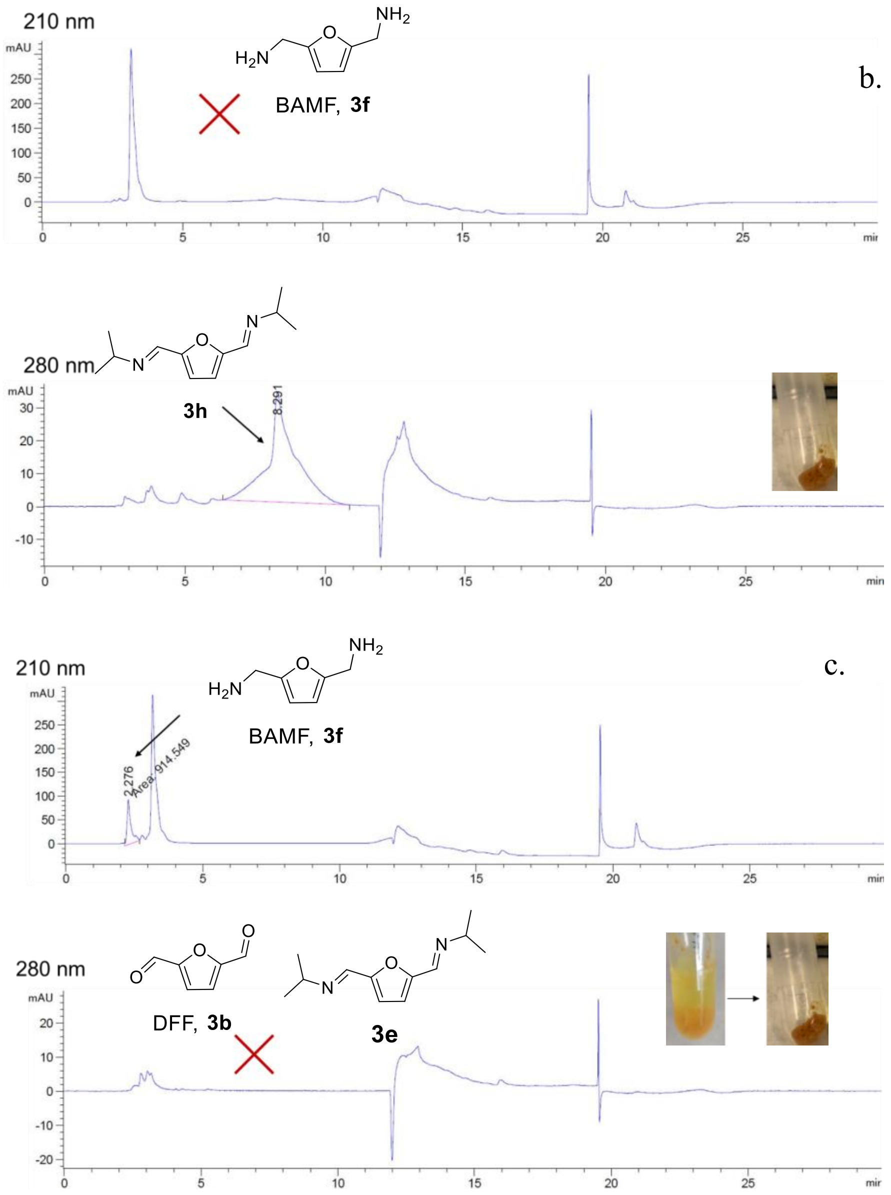

Figure 4.4. (cont) HPLC chromatograms and reaction crudes of DFF (25 mM) biotransamination reactions ater 24 h using Bm-TA (Panel a, full conversion into **3f**), TA-P2-A07 (Panel b, no conversion towards **3f**), and Vf-mut-TA (Panel c, partial formation of **3f**, 44%). The peak detected at 3.2 min (210 nm) is the co-solvent DMSO. Reaction crudes shows precipitate formation in case of low conversion of **3b** into **3f** (Panels b and c), while clearer crudes are observed when full production of **3f** is attained (Panel a).

In cases of quantitative conversions into diamine **3f** (detected at 210 nm), were achieved, no residual diimine was found. In reaction mixtures with very low formation of **3f** (less than 10%), diimine was the main compound observed at 280 nm. Conversely, in reaction mixtures with partial conversions into **3f**, little or no diimine residue was present, and the mass balance of the reaction was not closed, indicating the possible presence of other intermediates. Furthermore, the precipitation of a residue in the Eppendorf tubes was observed in these reaction mixtures (as shown in Figure 4.4), suggesting the formation of oligomeric or polymeric species.

4.2.1.1. ATAs screening

After the study of the crude mixture profiles, a screening of different ATAs was performed. Limited information is available in the existing literature regarding the study of **3b** in combination with ATAs.[477] Therefore, a comprehensive screening of various transaminases was conducted, including commercially available ones from Codexix Inc. (ATA-xxx and TA-P1-xxx), to determine which enzymes performed the best (Table 4.1). The source of all the transaminases is reported in Table 3.5. Diamine **3f** percentage values were calculated by reverse phase HPLC analyses of the crude reaction mixtures using calibration curves (see Section 4.3.8.2).

---

[477] A. Dunbabin, F. Subrizi, J. M. Ward, T. D. Sheppard, H. C. Hailes, *Green Chem.* **2017**, *19*, 397–404.

Table 4.1. Screening of ATAs for the transamination of **3b** (25 mM) after 24 h at 35 °C.

Entry	ATA	3f (%)[a]	Entry	ATA	3f (%)[a]
1	Cv-TA	89	**18**	ATA-200	58
2	ArS-TA	91	**19**	ATA-217	1
3	ArRmut11-TA	>99	**20**	ATA-234	26
4	Bm-TA	>99	**21**	ATA-237	64
5	BmS199G-TA	>99	**22**	ATA-238	55
6	Vf-mut-TA	44	**23**	ATA-254	61
7	ArR-TA	22	**24**	ATA-256	50
8	Vf-TA	<1	**25**	ATA-260	41
9	At-TA	<1	**26**	ATA-301	21
10	ATA-251	97	**27**	ATA-303	70
11	ATA-025	>99	**28**	ATA-412	33
12	ATA-007	1	**29**	ATA-415	79
13	ATA-024	95	**30**	TA-P1-A06	53
14	ATA-033	81	**31**	TA-P1-B04	40
15	ATA-013	67	**32**	TA-P1-F03	34
16	ATA-113	62	**33**	TA-P1-G05	31
17	ATA-117	8	**34**	TA-P1-G06	49

[a] Product formation values were measured by reverse phase HPLC analyses of the crude reaction mixtures using calibration curves.

Five ATAs, ArRmut11-TA, Bm-TA, BmS119G-TA, ATA-025, ATA-251 (entries 3, 4, 5 and 11), demonstrated remarkable efficiency in catalyzing the formation of diamine **3f** with over 96% conversion, as indicated in Table 4.1. These enzymes included the commercial ones.

4.2.1.2. Reaction intensification

The five enzymes showing better conversion values were selected to investigate the impact of higher substrate concentrations ranging from 50 to 200 mM (Figure 4.5).

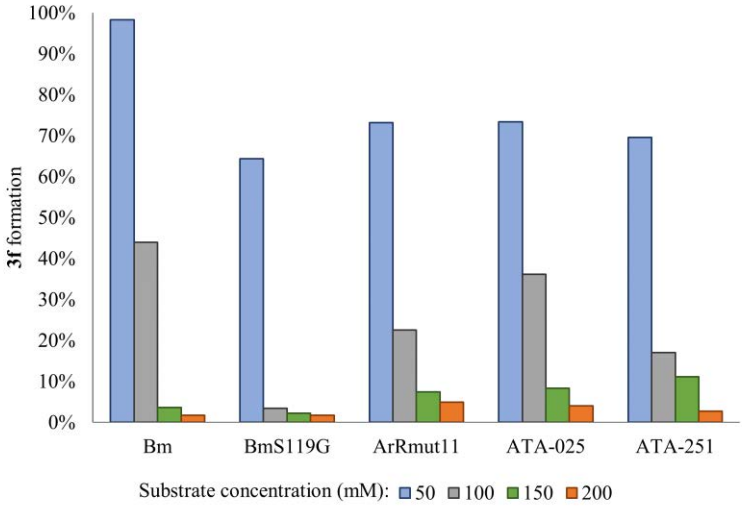

Figure 4.5. Transamination of DFF (**3b**) at increasing concentrations of the substrate (50–200 mM), pH 7.5, IPA 1 M. Percentage values of **3f** were determined by reverse phase HPLC analyses of the crude reaction mixtures using calibration curves.

Among these enzymes, only Bm-TA was able to achieve quantitative conversion into **3f** at a 50 mM concentration of DFF. However, the other ATAs yielded the diamine **3h** with 60-70% conversion at this concentration. Unfortunately, when we increased the substrate concentrations further, a significant decrease in the formation of **3f** was observed, suggesting that these enzymes were not efficient in converting DFF at higher loadings. To address this and enhance solubility in the reaction mixture, the amount of DMSO was increased from 2.5% to 5% v/v for 100 mM and 150 mM substrate concentrations, while 10% v/v was selected for 200 mM DFF to enhance solubility in the reaction mixture, but this adjustment did not lead to improved results.

As mentioned previously, in all the reaction mixtures, the residual DFF disappeared, forming the diimine **3h** appearing a solid residue. Another factor to take into consideration is that the amount of IPA remained constant in these experiments, and this affected the reaction equilibrium. Initially, a 1:20 ratio of substrate to IPA (at 25 mM of substrate concentration, with 2 reactive aldehyde groups per molecule) was considered, but this ratio gradually decreased to 1:2.5 as the DFF concentration increased to 200 mM in the experiments with higher substrate concentration.

4.2.1.3. pH influence on 3f synthesis

It is evident that when performing transamination using IPA as the amine donor with **3b** unwanted reactions occur. In the case of DFF, the overall situation is exceptionally complex. Besides the reaction equilibria with IPA (as depicted in Scheme 4.8a), due to the presence of two reactive aldehyde groups in each DFF molecule, various other imine-type intermediates may exist, some of which could undergo oligomerization and polymerization processes (as illustrated in Scheme 4.8b). In fact, this complexity has been observed in prior research involving transaminases[477] and metal-catalyzed reductive aminations.[434]

Also in this case, as a proof of concept, we repeated the ATA-catalyzed reactions with aldehyde **3b** at different concentrations with the best enzymes previously found for each substrate using KPi buffer 100 mM pH 6.5 as reaction medium, having proved that pH influences the imine formation (Figure 4.6). The amount of co-solvent was adjusted for 50 and 100 mM of **3b** concentration.

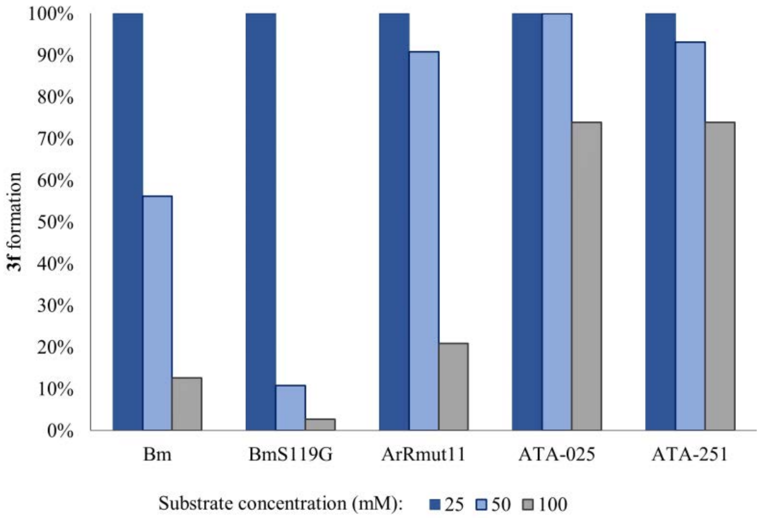

Figure 4.6. Transamination of DFF (**3b**) at increasing concentrations of the substrate (25–100 mM) at pH 6.5 and IPA 1M. The amount of the co-solvent DMSO was adjusted according to **3b** concentration, as disclosed in the main text.

As observed for furfural transamination, higher conversions towards the corresponding diamine product **3f** was observed, especially remarkable were the positive results obtained with ATA-025 and ATA-251, in comparison with the results observed at pH 7.5. These evidences support our assumption regarding the aldehyde/imine equilibrium and its influence on the target reaction, underlining the necessity for a thorough examination of this factor becomes especially crucial when employing a highly nucleophilic amine donor, such as IPA.

4.2.2. Study of the LMS oxidation of HMF (3a)

In order to synthetize oxidative derivatives from HMF, LMSs were investigated, selectig L*Tv* and *P. ostreatus* (POXA1b and POXC) laccases. In case of LMS oxidation of HMF, **3b** overoxidation into FFCA (**3c**) was a significant concern. It is crucial to highlight that the overoxidation of DFF into **3c** was facilitated by the hydration conditions of DFF within the buffered catalyzed system. Our experimental findings unequivocally confirmed that DFF was initially produced as a product of the HMF oxidation reaction but promptly underwent overoxidation to yield the monocarboxylic acid **3c**.

A series of experiments were conducted to investigate the impact of varying buffer strength on the product distribution in the oxidation of HMF with LMSs. Concurrent control experiments were also carried out. These control trials demonstrated that HMF remained stable in the absence of laccase or TEMPO. This indicated that TEMPO could not undergo re-oxidation without the presence of laccase. Furthermore, when TEMPO was absent, no significant oxidation products were observed. This lack of observable oxidation products can be attributed to the inability of both laccases to recognize HMF as a substrate. These results underscore the essential role that each component in the catalytic system plays in the oxidation process.

As the reaction progressed, the absence of HFCA was consistently observed, indicating that FFCA, DFF and FDCA were the predominant compounds detected in the reaction mixture (Scheme 4.9). To ensure the accuracy of the conversion values reported from here on, as well as product distribution, we also performed ^{1}H-NMR analysis of selected samples, which assessed that the relative concentrations of various components in the reaction crudes corresponded to the ones measured by HPLC. Thus, the latter was selected as analytics to quantify the furan derivatives.

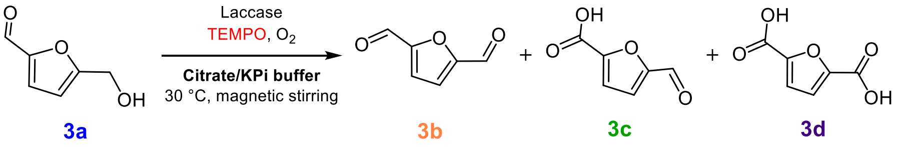

Scheme 4.9. LMS oxidation of HMF and the products detected in the reaction crudes. Laccase and TEMPO loadings as well as buffer concentration were the investigated parameters.

4.2.2.1. Influence of the buffer strength

Influence of buffer strength (50 and 100 mM) was investigated in FFCA (**3c**) accumulation for L*Tv* and *P. ostreatus* laccases (POXA1b and POXC, Figure 4.7). The reactions mediated by POXA1b and L*Tv* were conducted under their optimal conditions that are citrate buffer with pH values of 5.5 and 5, respectively. On the other hand, for the POXC-mediated reactions, a KPi buffer with a pH 6 was chosen, as it had yielded the best results for furfuryl alcohol oxidation.

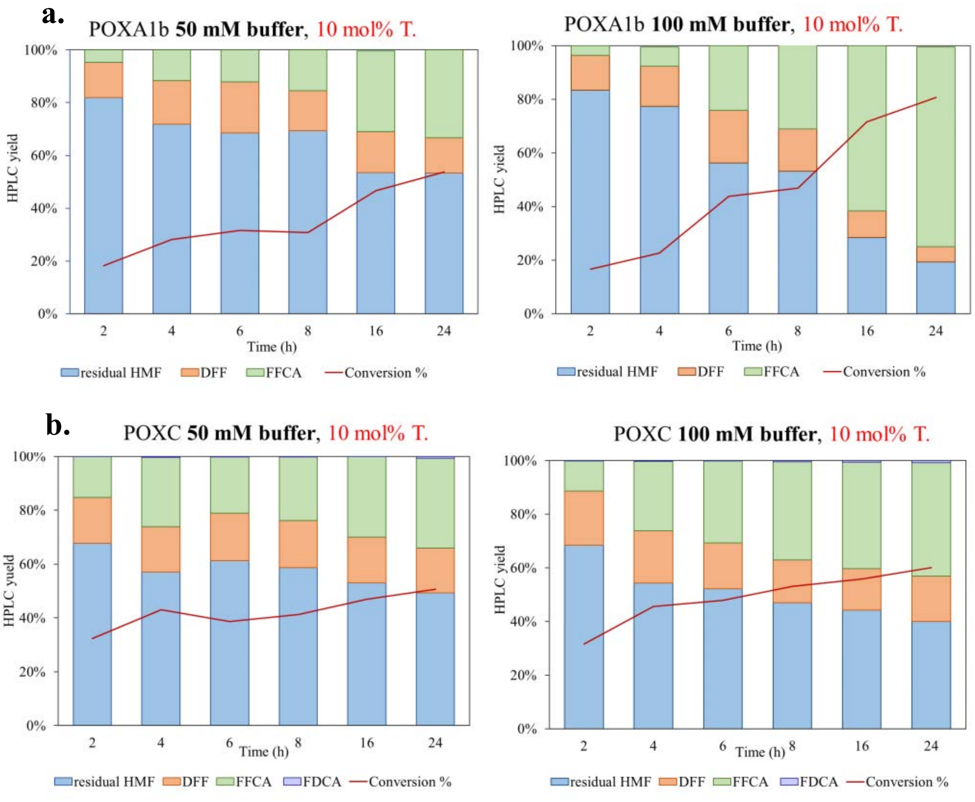

Figure 4.7. Conversion (%) of HMF in DFF, FFCA, FDCA and HFCA mediated by the laccase-TEMPO system using (**a**) POXA1b and (**b**) POXC, investigating the buffer strength (50–100 mM) influence on the accumulation of the different possible products. Conversions were measured by RP-HPLC using an external standard.

A lower buffering capacity of 50 mM had a notable impact on the overall conversion of HMF, which was observed to be around 50% for both systems. This decrease in conversion was likely due to several factors, including enzyme instability, the decomposition of the oxoammonium cation of TEMPO resulting from pH changes caused by the formation of the acidic over-oxidation product. In this particular situation, both DFF and FFCA were present in the reaction mixture from short reaction times.

In the case of the POXA1b system, the oxidation appeared to progress slowly up to 8 h, with a notable acceleration in conversion observed at 16 and 24 h. During this time, FFCA accumulation reached 33%. DFF was initially observed at 20% at 6 h, followed by its gradual depletion over the next 14 h.

Conversely, the POXC system seemed to reach a more modest equilibrium around 8 h, with a maximum of 33% FFCA accumulation and 15% DFF, which remained relatively constant throughout the observed reaction times. At each observed time point, the pH was monitored, revealing a gradual drop in pH after 4 h due to FFCA accumulation in the reaction medium. The POXA1b system exhibited a considerable tolerance for the pH decrease, as evidenced by continuous HMF conversion even in this weak buffering system.

By increasing the buffer strength to 100 mM, in the POXA1b system, 80% of HMF conversion was achieved, with 74% FFCA and 6% residual DFF accumulation at 24 h of reaction. This confirmed that DFF acted as a transient intermediate in the overall reaction complex. In contrast, the KPi buffer system appeared less tolerant to the increase in FFCA accumulation, causing a drop in pH from 6.5 to pH 4 after only 8 h. Nonetheless, the POXC system continued to work slowly up to 16 h, reaching 60% HMF conversion, 43% FFCA, and 17% DFF. The pH in this system remained relatively stable, reaching pH 4 after 24 h.

The oxidation of HMF using L*Tv* laccase has been previously documented in several papers as an efficient system, especially when used in conjunction with great quantities of TEMPO. This combination has proven to be effective in producing FDCA as the main oxidative compound.[333b,478]

In our experiments, we conducted a series of similar trials to assess the impact of buffer concentration on the reaction. Given that L*Tv*, like POXA1b, operates effectively under acidic conditions with a working pH of 5.0, we tested citrate buffer concentrations of 50 mM and 100 mM. The enzyme amount was consistently set at 58 U/mmol$_s$ (Figure 4.8).

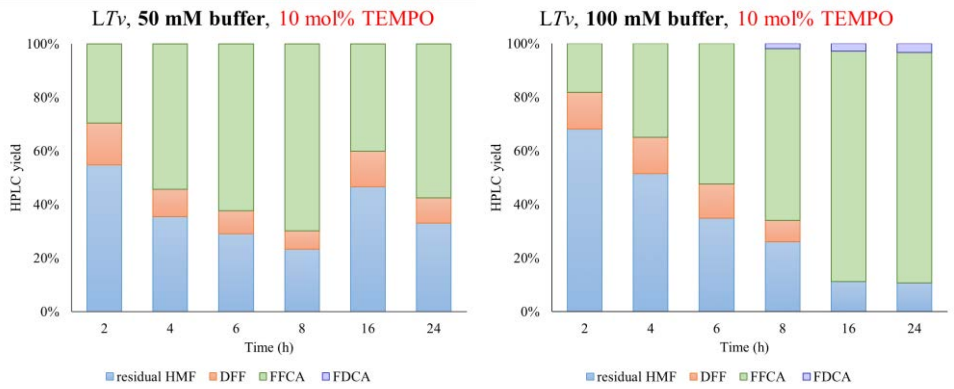

Figure 4.8. Conversion of HMF into the oxidized derivatives mediated by TEMPO in the presence of L*Tv* at 50 mM and 100 mM of citrate buffer concentration and TEMPO at 10 mol%.

Compared to what it was observed for the other *P. ostreatus*-mediated reactions, a lower buffering capacity (50 mM) did not strongly affect the overall HMF conversions, which at 24 h was assessed at 50% in presence of just 10 mol% of TEMPO. This case served as confirmation of TEMPO's relative stability, even when the reaction led to the attainment of acidic pH levels due to the formation of carboxylic acid-oxidized compounds. The enhanced capacity of L*Tv* for recycling TEMPO was reaffirmed when the

---

[478] a) Z. Y. Yang, M. Wen, M. H. Zong, N. Li, *Catal. Commun.* **2020**, *139*, 105979; b) J. Wei, L. Yang, W. Feng, *Enzyme Microb. Technol.* **2023**, *162*, 110144.

buffer concentration was raised to 100 mM, FDCA accumulation reaching 85%.

In case of *P. ostreatus* laccases, a higher buffer concentration was tested, in order to try to improve the performances for both systems, due to higher buffering powder, and then lower pH reduction (Figure 4.9).

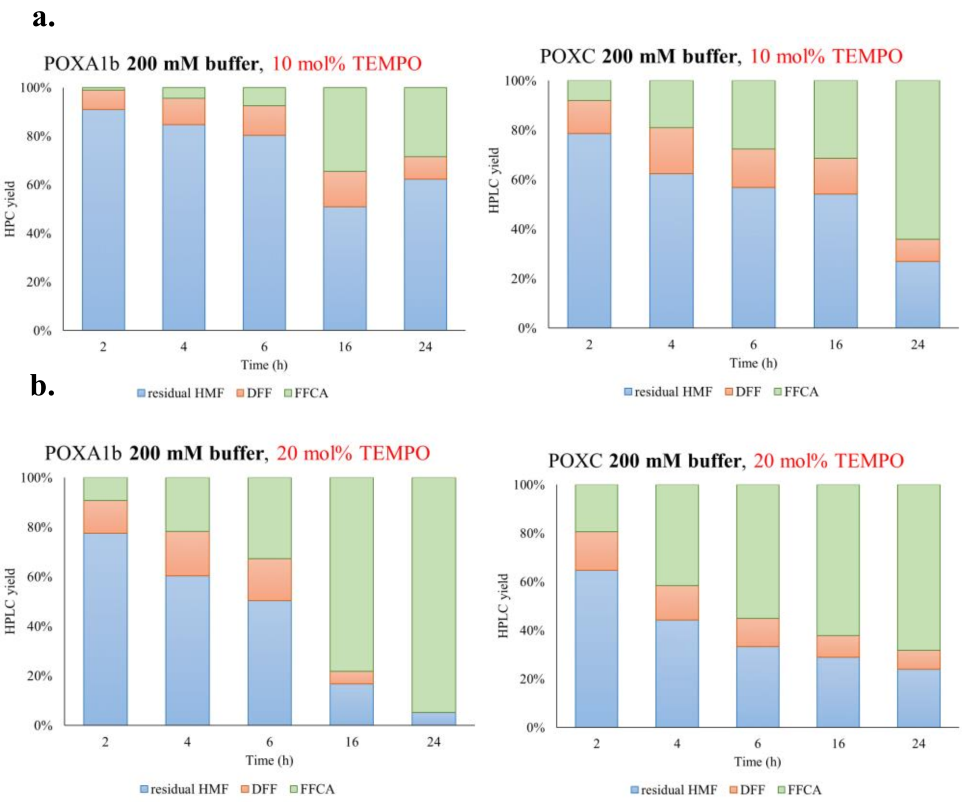

Figure 4.9. Conversion of HMF into oxidized derivatives mediated by TEMPO in the presence of POXA1b and POXC at 200 mM of buffer concentration and TEMPO at 10 mol% (**a**) or 20 mol% (**b**).

The data from POXA1b-mediated reactions shows results similar to those previously obtained at a buffer concentration of 100 mM. This similarity is primarily attributed to the preserved enzymatic activity at acidic pH levels. On the other hand, the POXC system enabled the achievement of

70% HMF conversion at both 10 and 20 mol% of TEMPO, with a 65% accumulation of FFCA after 24 h. This highlights the crucial role of the buffer in the reaction system for POXC, as its activity significantly decreases at low pH values.

4.2.2.2. Influence of the mediator amount

Influence of varying the mediator's quantity in the reaction was also investigated, specifically within the range of 10–20 mol%. Previous research had suggested that increasing the concentration of oxy-radicals like TEMPO and ABNO could lead to enhancements in HMF conversion and product yields.[479] In the case of POXA1b, it was observed that a higher mediator amount (20%) had a slight positive effect on the accumulation of FFCA over time, while minimal effects were observed for POXC (Figure 4.10).

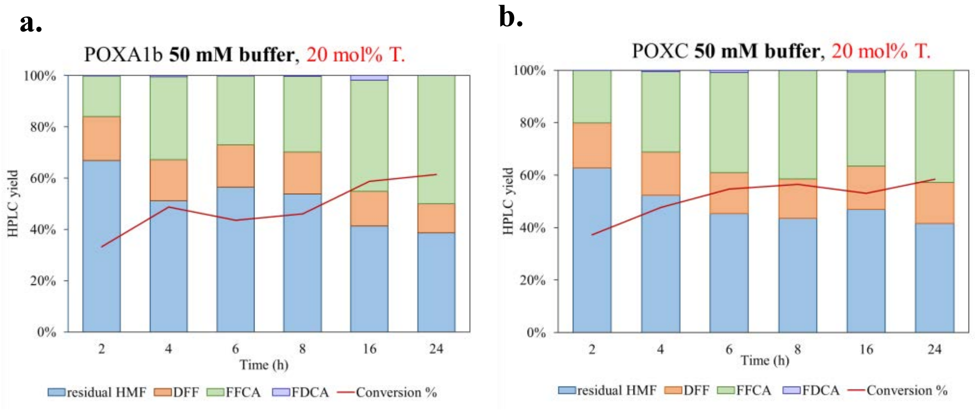

Figure 4.10. Conversion (%) of HMF into DFF, FFCA, FDCA and HFCA mediated by a laccase-TEMPO system using POXA1b (**a**) and POXC (**b**), investigating the mediator amount (20 mol%) influence on the accumulation of the different possible products. Conversions were measured by RP-HPLC using an external standard.

---

[479] a) A. Dijksman, A. Marino-González, A. M. Payeras, I. W. C. E. Arends, R. A. Sheldon, *J. Am. Chem. Soc.* **2001**, *123*, 6826–6833; b) L. Wang, S. S. Shang, G. Li, L. Ren, Y. Lv, S. Gao, *J. Org. Chem.* **2016**, *81*, 2189–2193.

Regarding the L*Tv*-mediated oxidation of HMF, overall HMF conversions sharply increased to 99% when the amount of TEMPO was raised to 20 and 33 mol% (Figure 4.11).

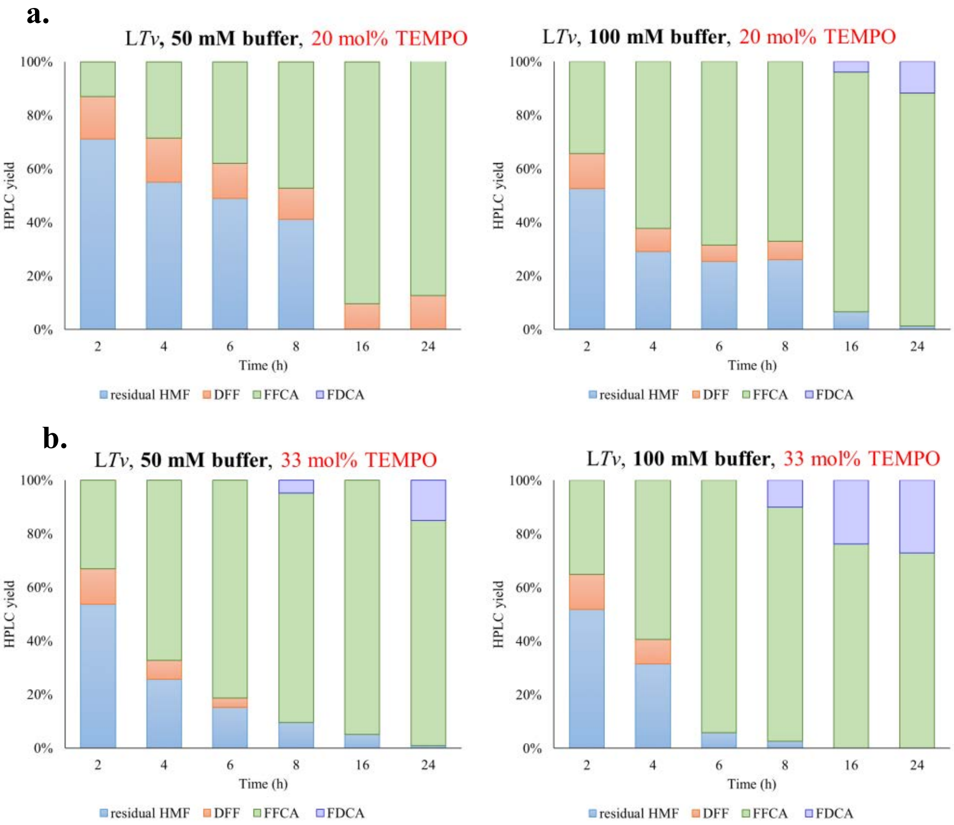

Figure 4.11. Conversion of HMF into the oxidized derivatives mediated by TEMPO in the presence of L*Tv* at 50 and 100 mM of citrate buffer concentration and TEMPO at 20 mol% (**a**) and 33 mol% (**b**).

An approximately 85% accumulation of FFCA was observed when both 20 and 33 mol% of TEMPO were used after 24 h. In the case of the former, 10% of residual DFF was still detected as a reaction intermediate, while with 33 mol% of TEMPO, FFCA underwent partial oxidation into FDCA (approximately 15%). This confirms the previously described accumulation of FDCA for this mediator system. Under these reaction conditions, after 16 h, the use of 33 mol% of TEMPO allowed for the highest FFCA accumulation, reaching close to 95%.

When 20 mol% of TEMPO was employed, HMF conversion reached 95% after 16 h, with roughly 87% of FFCA being produced. On the other hand, in presence of 33 mol% of TEMPO (as illustrated in Figure 4.11b), the reaction progressed at a faster rate. After 8 h, at 100 mM buffer concentration, the overall conversion of HMF had already reached 98%, and within just 6 h, under the same conditions, approximately 95% of FFCA accumulation had been quantified. Over the course of 16 to 24 h, the accumulation of FDCA became noticeable, highlighting the less specificity on the FFCA accumulation in L*Tv*-TEMPO system. An effective method for achieving very high FFCA yields with L*Tv* laccase (95%, 95 mM) was established using 33 mol% of TEMPO in a 50 mM citrate buffer at pH 5.0.

Instead, in case of POXA1b and POXC-mediated oxidations, the combination of an increased buffer strength and a higher mediator quantity resulted in a significant conversion improvement, enabling FFCA formation at 90% for POXA1b. However, under these optimized conditions, POXC could only achieve HMF conversion of approximately 60% after 24 h, accompanied by FFCA accumulation. Previously, we demonstrated that the stability of POXC decreased rapidly over time, with a measured half-life of 10 h. Consequently, conversions increased steadily up to 8 h and remained relatively constant in nearly all the examined systems (Figure 4.12).

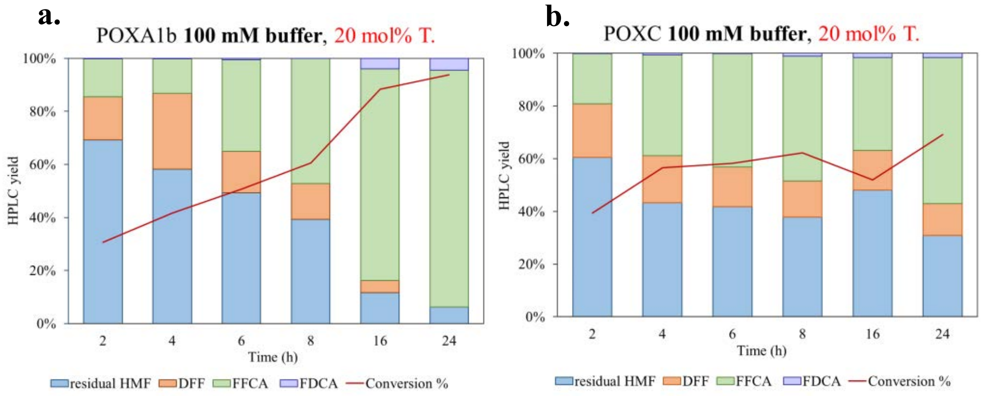

Figure 4.12. Conversion of HMF in the oxidative derivatives mediated by TEMPO in the presence of POXA1b (**a**) and POXC (**b**) under the optimal conditions.

In contrast, POXA1b exhibited remarkable stability, allowing the efficient TEMPO recycling throughout the observed reaction time, resulting in satisfactory levels of product accumulation when buffer strength was increased. Surprisingly, in the studied reaction conditions, TEMPO stability did not appear to be the limiting factor for HMF oxidation. This was evidenced by the increasing conversion values observed in all the systems catalyzed by POXA1b.

4.2.2.3. Influence of the laccase amount

The laccase amount was reduced by half to 29 U/mmol$_s$ in 100 mM buffer concentration, with the aim of studying the impact on the *P. ostreatus*-mediated oxidation of HMF. The reduction in enzyme quantity to 29 U/mmol$_s$ resulted in an overall decrease in HMF conversion for both systems, whether using 10 mol% (as shown in Figure 4.13a) or 20 mol% (as shown in Figure 4.13b) of TEMPO. This highlights that 58 U/mmol$_s$ is the necessary amount of *P. ostreatus* laccases for achieving effective HMF oxidation.

In conclusion, the entire reaction pattern reveals that both the amount of catalysts and the ionic strength of the buffer play crucial roles in HMF oxidation when using *P. ostreatus* laccases, resulting in the accumulation of

FFCA as the main reaction product. An insufficient quantity of TEMPO leads to reduced catalytic efficiency, primarily manifested by lower HMF conversion and greater DFF accumulation, albeit still falling short of satisfactory levels (not exceeding 17%). The conversion of HMF increased significantly, reaching 90% for POXA1b and 70% for POXC, when the amount of TEMPO was increased from 10 mol% to 20 mol%, and the buffer strength was raised to 100 mM after 24 h. This increase was mainly attributed to the enhanced interaction between TEMPO and DFF, as well as the system's ability to buffer the accumulation of acidic compounds. However, the yield of DFF decreased significantly with the gradual increase in FFCA production over the time, with the highest measured DFF yields of 20% (20 mM) occurring at 2–4 h in a 100 mM buffer strength and 20 mol% of TEMPO (resulting in 50–70 % HMF conversion in both systems).

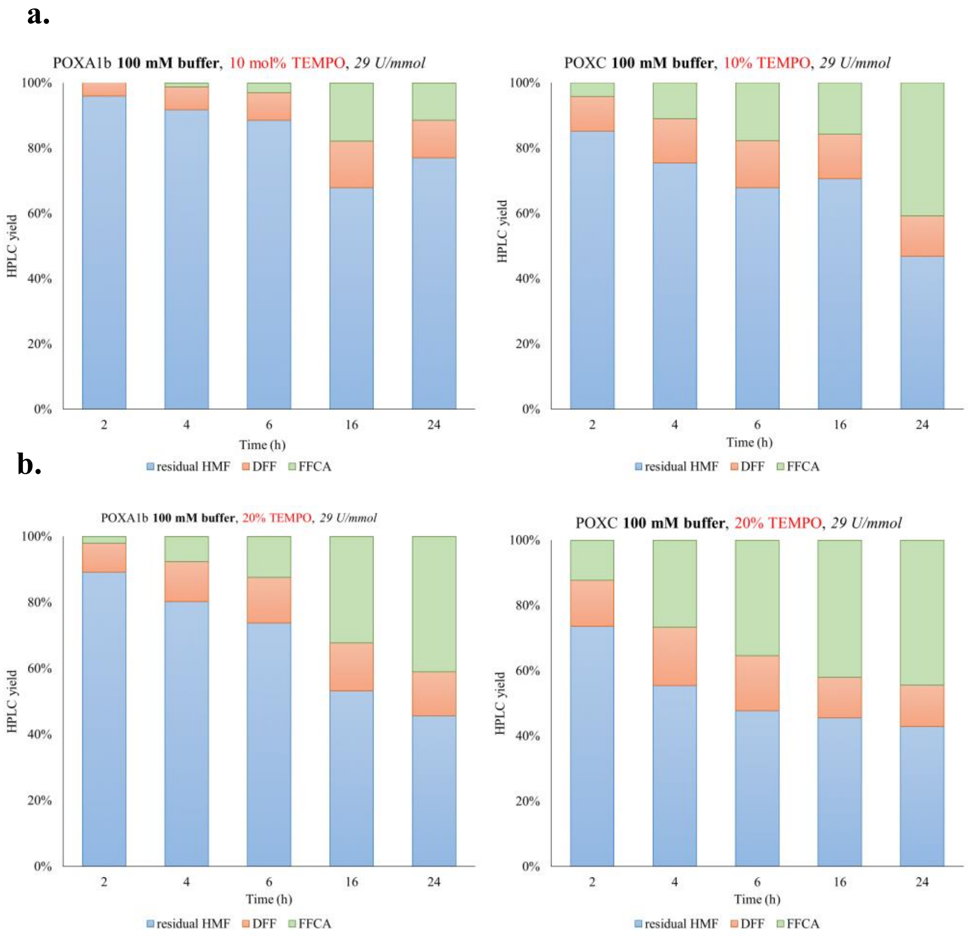

Figure 4.13. Conversion of HMF into DFF, FFCA, FDCA mediated by laccase-TEMPO system using POXA1b and POXC, at lower enzyme loadings (29 U/mmol$_s$) using TEMPO 10 mol% (**a**) and 20 mol% (**b**). Conversions were measured by RP-HPLC using calibration curves of the compounds.

Conversely, together with L*Tv*-TEMPO system, another efficient method for producing FFCA in high yields was established using the POXA1b laccase as mediator regenerating system, with less mediator (20 mol% TEMPO) in 100 mM citrate buffer at pH 5.5 (90%, 90 mM) (as shown in Figure 4.12a). In this case, FDCA was slightly observed, achieving a clearest reaction crude, in contrast with L*Tv*-mediated ones.

It is worth commenting that the choice of buffer preparation can also influence the FFCA yields of the system. Phosphate salts have been previously noted to be less conducive to DFF hydration, while acetate or citrate buffers, with their greater degree of aldehyde hydration, appear to buffer the system effectively, preventing significant pH changes in the reaction mixtures. This buffering action aids in the FFCA hydration and the rate-determining TEMPO oxidation of the system, resulting in the kinetic acceleration of alcohol and aldehyde oxidation.[445]

Furthermore, the oxidation of FFCA to FDCA in buffer systems has been shown to be extremely slow, likely due to the lower degree of hydration of FFCA in the citrate buffer at 100 mM and pH 5.5.[446] In conclusion, fine-tuning of the reaction conditions, such as adjusting the buffer pH and composition, appears to be the key to improving the activity and stability of the catalysts, ultimately enhancing HMF conversion.

4.2.2.4. Organic co-solvent addition

The next phase of the study involved exploring the impact of different co-solvents on the product distribution during the oxidation of HMF. Various solvents at a concentration of 10% v/v were tested, as shown in Figure 4.14. DMF was chosen as a water-soluble solvent because both enzymes exhibited good stability and activity in its presence. DCM (dichloromethane) and chloroform were considered due to the high solubility of DFF in these solvents, which promotes the oxidation process. Immiscible-water solvents were also selected because of their high boiling points, which could aid in the continuous extraction of the less hydrophilic compound, DFF, from the water system.

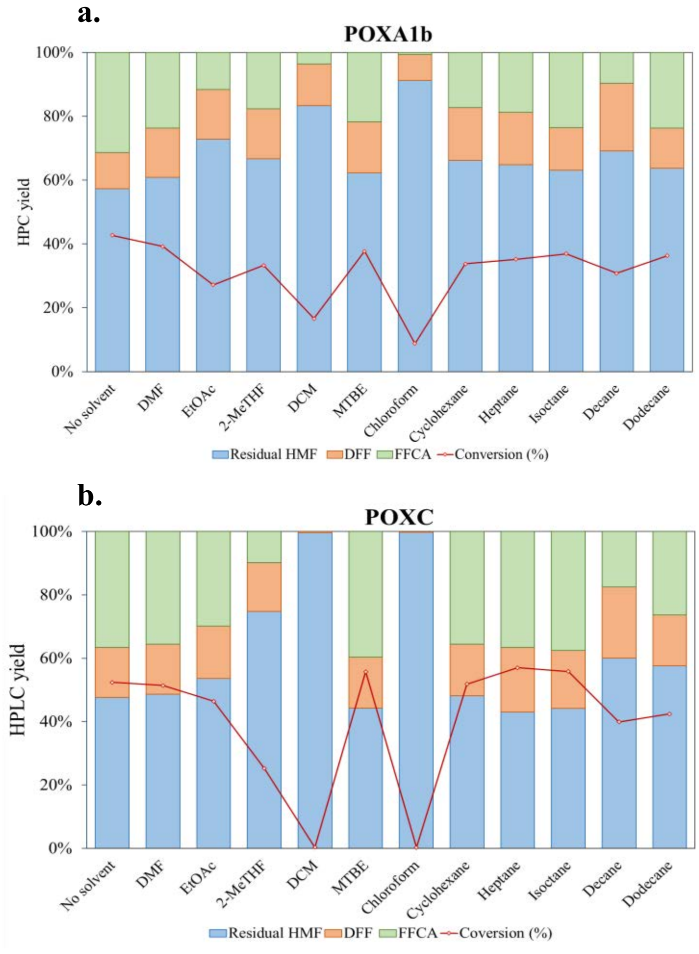

Figure 4.14. Conversion of HMF in the oxidative derivatives mediated by TEMPO in the presence of POXA1b (**a**) and POXC (**b**) with different co-solvents. Solvents were ordered according to their calculated logP value. The reaction conditions were the following: 100 mM of HMF, 10 mol% of TEMPO, 10% (v/v) organic co-solvent, 59 U/mmol$_s$ of laccase, O_2, 30 °C, magnetic stirring. For POXA1b (**a**) citrate buffer, 100 mM, pH 5.5; for POXC (**b**) KPi buffer, 100 mM, pH 6.5.

In the case of POXA1b-mediated oxidation (Figure 4.14a), the presence of co-solvents had a noticeable impact. Overall conversions were slightly lower compared to the buffer system. The conversion rates and product distribution remained relatively consistent when using 2-MeTHF, MTBE, cyclohexane, heptane, iso-octane, and dodecane. However, poor conversion were achieved, especially when DCM and chloroform were used, and the accumulation of DFF remained low at around 10%. The negative effect observed with these chlorinated solvents was even more significant in the case of the POXC-catalyzed reaction (Figure 4.14b). On the other hand, similar conversion values and product distribution were observed for the other solvents, except for 2-MeTHF. The maximum conversions achieved in both systems were only 40% and 50% for POXA1b and POXC, respectively.

Interestingly, at lower conversion rates, the processes were more selective in accumulating DFF. Nevertheless, the DFF yield did not exceed 20% in any case, with decane being the most favorable solvent in terms of DFF yield.

4.2.2.5. HMF protecting group strategy

In order to try to promote the accumulation of DFF applying *P. ostreatus*-TEMPO mediated oxidation of HMF, we employed a strategy involving the protection of the aldehyde group using butan-1-amine as a reactant. The aim was to utilize amine derivatives for safeguarding the aldehyde residue of HMF. This approach allowed for the selective oxidation of the alcohol portion, followed by a temporary safeguarding of the resulting aldehyde group (Scheme 4.10).

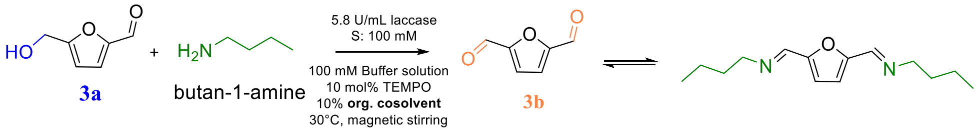

Scheme 4.10. Reversible protection of the aldehyde groups of HMF and DFF using butan-1-amine as protecting reagent.

First trials were conduced with two equivalents of this aliphatic amine. Furthermore, heptane was selected as a co-solvent in the reaction mixture with the goal of segregating the hydrophobic product from the buffer solution, thereby driving the entire equilibrium towards the desired reaction product (Table 4.2).

Table 4.2. Effect of the presence of butan-1-amine in the oxidation of HMF catalysed by laccases and TEMPO. Conversions (%) were measured by RP-HPLC after acidifying the reaction crude, through comparison with a standard curve based on the peak area.

Conditions	Residual HMF (%)	DFF, 3b (%)*	FFCA, 3c (%)*
POXC (pH 6.5)			
1	93	7	<1
2	100	<1	<1
3	91	8	1
4	8	10	4
5	84	10	6
6	78	11	11
POXA1b (pH 5.5)			
1	90	10	<1
2	99	1	<1

Entries 1: Butan-1-amine (2 equiv), heptane (10% v/v).
Entries 2: Incubation of HMF with amine (1 equiv), then oxidation with heptane (10% v/v).
Entry 3: Butan-1-amine (1 equiv), heptane (10% v/v), pH 7.5.
Entry 4: Butan-1-amine (1 equiv), MTBE (10% v/v), pH 7.5.
Entry 5: Butan-1-amine (2 equiv), heptane (10% v/v), pH 7.5.
Entry 6: Butan-1-amine (2 equiv), MTBE (10% v/v), pH 7.5.

Under their respective optimal working conditions (citrate buffer, pH 5.5 for POXA1b; KPi buffer pH 6 for POXC), both laccases were unable to efficiently catalyze the TEMPO regeneration in the new reaction system, resulting in HMF conversions of less than 10% (as indicated in Table 4.2, entry 1). The presence of free amine in the buffer was found to quench TEMPO, thus deactivating the recycling system. As a potential solution, HMF was pre-incubated with the amine and then introduced into the reaction system. However, this approach did not yield any measurable HMF conversion either (entry 2).

Examination of ^{1}H-NMR spectra of the protected substrate revealed the instability of the imine derivatives from HMF and DFF within the buffer system, even at elevated pH levels (up to 7.5), while co-presence of free HMF and DFF was maintained. In contrast, when the incubation reaction took place at higher pH levels (around 9–10), full imine HMF and DFF derivatives were detected. Consequently, it became evident that the protecting imine moiety was prone to hydrolysis in buffer solutions at pH levels compatible with enzymatic activity. This, in turn, hindered the TEMPO-mediated oxidation of HMF.

Attempts to improve the situation, such as increasing the pH to 7.5 and reducing the quantity of amine to 1 equivalent (entry 3), changing the solvent to MTBE using 1 equivalent of the protecting amine (entry 4), or using 2 equivalents of the amine reactant (entry 5), all resulted in HMF conversions lower than 20%. A comparison between the results reported in entries 1 and 2 confirmed that no differences were observed if the imine was pre-formed. It quickly hydrolyzed when added to the buffer solution, yielding even less favorable outcomes. There were slight improvements in conversions observed when MTBE replaced heptane (entry 6, compared to entry 5) in the presence of 2 equivalents of the amine reactant, possibly due to better solubilization of the formed DFF imine derivatives.

It is worth noting that Kim *et al.*, had previously employed a cyclic acetal protective group to favor the formation of FDCA from HMF using a cerium O_2-supported gold catalyst.[480] While this strategy had shown potential in influencing the oxidation product panel from HMF, the buffer reaction system applied in the current study for the same purpose did not yield reliable results under the optimal reaction conditions.

---

[480] M. Kim, Y. Su, A. Fukuoka, E. J. M. Hensen, K. Nakajima, *Angew. Chem. Int. Ed.* **2018**, *130*, 8367–8371.

4.2.3. Transamination of FFCA (3c) in AMFC (3g)

FFCA was identified as the primary accumulated product resulting from the oxidation of HMF by the tested LMSs. As a result, we delved into the thorough investigation of the single-step transamination of FFCA into AMFC (Scheme 4.11).

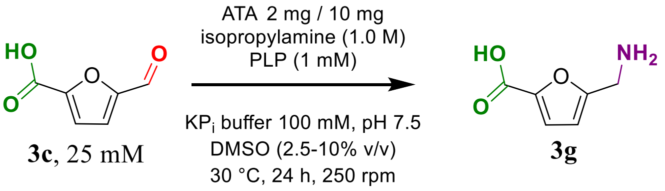

Scheme 4.11. FFCA (**3c**) transamination into AMFC (**3g**).

4.2.3.1. ATAs screening

A screening of ATAs was performed to identify the most efficient enzymes for catalyzing the amination of FFCA (**3b**) into AMFC (**3g**, Figure 4.15). These screening experiments validated the previously established reaction conditions, which involved the utilization of IPA as the amine donor at an initial concentration of 1 M. IPA was chosen due to its volatile nature, allowing the co-product acetone to be easily evaporated, thereby shifting the reaction equilibrium in the desired direction.

In our initial approach, we employed whole recombinant cells that overexpressed ATAs. The substrate concentration for this screening was set at 25 mM (in a 1 mL reaction volume), determining the conversion of **3c** into **3g** through RP-HPLC analysis, and the HPLC yield of the product was calculated by interpolating the area values using a previously prepared calibration curve.

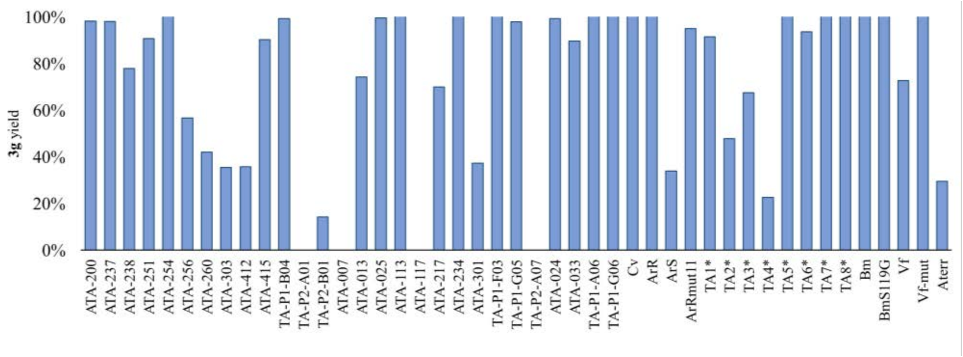

Figure 4.15. Conversion of **3c** into **3g** (%) calculated by HPLC RP-using calibration curve. For the origin of the enzymes refer to Table 3.5.

In contrast to DFF as a substrate, FFCA appeared to be more stable within the reaction system, as no mass loss was detected when the conversion was not quantitative. A total of 17 ATAs enabled us to achieve conversions exceeding 98%, with 8 of these being in-house overexpressed enzymes. These initial findings provided the necessary encouragement for us to continue our efforts in the amination of HMF for AMFC production.

4.2.3.2. Study of the reaction at higher substrate concentration

From the top-performing ATAs identified in the screening, eight were enzymes that we produced in-house. We proceeded to examine the performance of these ATAs using higher FFCA concentrations, extending the range up to 200 mM (Figure 4.16).

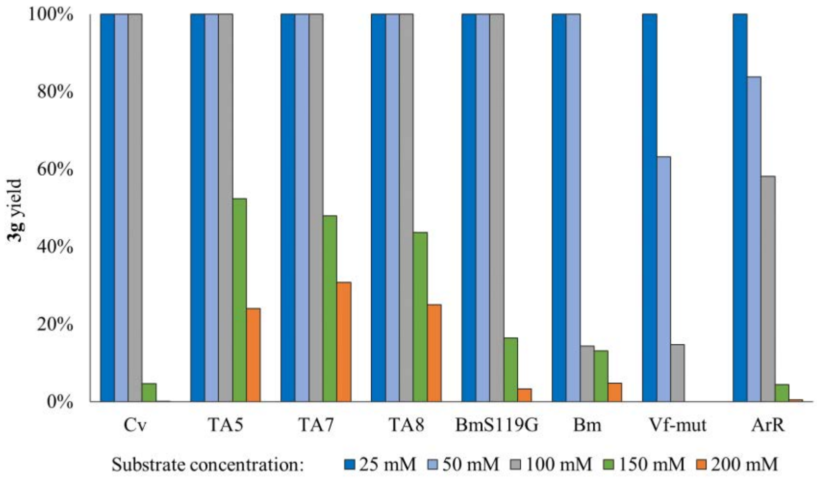

Figure 4.16. Transamination of FFCA (**3c**) into AMFC (**3g**) at increasing substrate concentrations (25–200 mM).

When the substrate concentration was increased from 25 to 50 mM in reactions catalyzed by Vf-mut-TA and ArR-TA, the HPLC-measured yields of AMFC significantly decreased to 60% and 80%, respectively. Bm-TA did not effectively catalyze FFCA amination even at a substrate concentration of 100 mM. On the other hand, TA5, TA7, TA8, and BmS119G-TA kept their performance until a substrate concentration of 150 mM, where they achieved approximately 50% AMFC accumulation. At 200 mM of substrate concentration, no enzymatic reaction yielded satisfactory conversion values.

Generally, DMSO was the chosen co-solvent in terms of solubility for such furan derivatives. DMSO concentration in the reaction system was adjusted to 5% v/v for 100 and 150 mM substrate concentrations, and 10% v/v for 200 mM substrate concentrations. It is important to note that as the substrate concentration increased while keeping the IPA amount constant in the reaction system, the equilibrium shift of the reaction could be affected. Starting with a 1:40 ratio of substrate to IPA (at 25 mM substrate concentration), this gradually shifted to an excess of 1:5 (at 200 mM substrate concentration).

Considering the planned cascade reaction conditions to be investigated (from hydroxy aldehyde HMF, **3a** to the amino acid AMFC, **3g**), a substrate concentration of 100 mM was selected as the target. At this concentration, Cv-TA, TA5, TA7, TA8, and BmS119G-TA efficiently catalyzed FFCA conversion into AMFC, achieving a yield of 99%.

4.2.3.3. Organic co-solvent influence

To scale up the transaminase reaction, either for combining it with LMS oxidation or other purposes, we sought to replace DMSO with alternative solvents. At this stage, we selected Cv-TA and the BmS119G-TA variant for further experiments in the presence of two alternative co-solvents for the reaction.

The choice of co-solvent for the FFCA transaminase reaction was influenced by the solubility of the substrate at higher concentrations. After several trials, it was found that FFCA exhibited high solubility in 2-MeTHF and MeCN. Consequently, the potential impact of these co-solvents on the reaction was investigated once again, this time with increasing substrate concentrations, reaching up to 200 mM. The conversion data in the presence of DMSO are also included in Figure 4.17 for comparison.

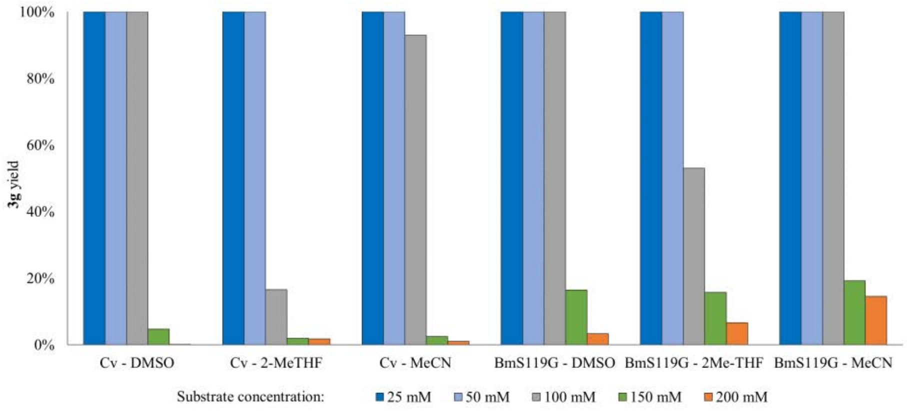

Figure 4.17. Conversion of FFCA (**3c**) into AMFC (**3g**) in presence of 2-MeTHF and MeCN as co-solvents of the reaction. The ATA-cosolvent conditions are indicated in the X-axis.

In contrast to DMSO, 2-MeTHF adversely affected the performance of both enzymes, even at a substrate concentration of 100 mM (where 5% of co-solvent was utilized). For Cv-TA, **3g** accumulation decreased by up to 17%, and for TA, it dropped by 50%. On the other hand, MeCN, at the same FFCA concentration, preserved the catalytic performance of both enzymes. No significant enhancements in **3g** synthesis were observed at substrate concentrations of 150 and 200 mM. In the presence of MeCN, Cv-TA achieved a 95% conversion to the amino acid, while BmS119S conversion at an initial substrate concentration of 100 mM was quantitative.

Hence, MeCN was chosen as the replacement for DMSO in the reaction system because of its lower boiling point that would simplify product isolation in scale-up experiments. Fortunately, our previous study demonstrated that MeCN did not affect the stability and activity of POXA1b in the TEMPO-mediated oxidative system for furfuryl alcohol, making both reaction steps compatible in terms of co-solvent use (see Section 3.2.1.6).

Lastly, the S119G variant transaminase from *B. megaterium* was selected for the scale-up of FFCA transamination and was subsequently employed in combination with the LMS oxidation step for the one-pot sequential synthesis of **3g** from HMF.

4.2.3.4. AMFC biosynthesis from FFCA at preparative scale

The upscaling of the POXA1b-TEMPO oxidation of HMF into FFCA, **3c** and the **3c** transamination using BmS119G into AMFC, **3g** were successfully performed with 100 mg of substrates in different reaction pots, and the products efficiently isolated. MeCN was used as the co-solvent in place of DMSO. HPLC analyses confirmed that both single-step reactions resulted in quantitative conversions. FFCA was isolated through liquid-liquid extraction using EtOAc as the solvent, while AMFC underwent prior derivatization with di-*tert*-butyl dicarbonate (Boc_2O). The amino-group protection strategy and reaction conditions are summarized in Scheme 4.12. Ultimately, both compounds were obtained at yields of 60% for FFCA (in the form of a brownish powder) and 50% for AMFC (Boc-AMFC, as yellow liquid, NMR spectra in Section 4.3.9).

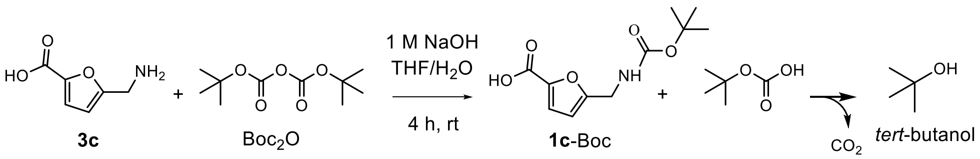

Scheme 4.12. Amino group protection with Boc_2O to derivatize AMFC.

4.2.4. One-pot sequential synthesis of AMFC from HMF at preparative scale

Only a few studies have reported the successful synthesis of FFCA (**3c**) and AMFC (**3g**) in sequential approaches. One of the most recent examples involved a hybrid chemo-catalytic oxidation and subsequent transamination of HMF, as revealed by Lancien and their colleagues.[421a] They outlined the oxidation of HMF into AMFC using a Pt/SiO_2 catalyst, which served as the substrate for the subsequent transamination step catalyzed by Cv-TA. In their study, **3g** was achieved with a final yield of 77%, although the rate-limiting step was the oxidation, which took 52 h to complete, resulting in quantitative HMF production with FDCA as the main by-product (21%).

In contrast, our methodology has already demonstrated the successful accumulation of **3c** in a reaction catalyzed by LMSs, achieving a conversion and selectivity of the reaction of 90%.

After performing both single reaction steps in large scale, cascade reaction that combined POXA1b and BmS119G-TA for the AMFC synthesis from HMF (100 mg), was established under the optimal conditions previously determined for both steps (Scheme 4.13). Due to the inherent incompatibility of the two reaction steps, the protocol was executed in a sequential manner, with the addition of the ATA-catalyzed reaction components immediately after the conclusion of the first oxidative step. It is worth noting that the direct addition of IPA led to a significant increase in the pH of the reaction. To address this, the phosphate salt of IPA was prepared and tested, resulting in a change in the buffer salts. The increase in pH proved to be sufficient to facilitate the ATA-catalyzed step at a suitable pH for the transaminase reaction.

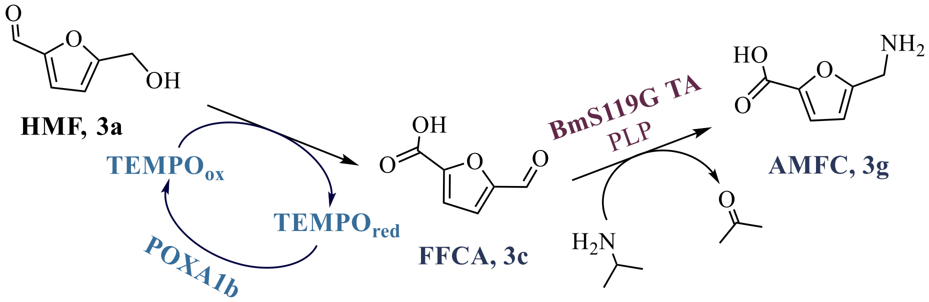

Scheme 4.13. One-pot sequential reaction for AMFC (**3g**) synthesis from HMF (**3a**). Reaction conditions: (**3a**) (100 mM, 100 mg), POXA1b laccase (58 U/mmol$_s$), oxygenated citrate buffer (100 mM, pH 5.5), MeCN (5% v/v), TEMPO (20 mol%), 30 °C, 24 h, magnetic stirring. ATA step: BmS119G-TA (70 mg DCW), KPi buffer (pH 7.0, 100 mM), MeCN (5% v/v), PLP (1 mM), $(IPA)_3PO_4$ (330 mM), 30 °C, 24 h and 250 rpm.

The performed cascade reaction yielded 93% of FFCA (**3c**) accumulation in the first oxidation step and 97% of the desired **3g** after the second transamination step, as determined by HPLC analysis. The reaction mixture was subsequently derivatized with Boc_2O, resulting in the Boc-derivatized AMFC. Due to difficulties encountered in extracting the compound from the aqueous phase when it was obtained from **3c** under preparative conditions, the product was isolated through continuous extraction over 8 h using CH_2Cl_2. Prior to this procedure, several extractions were carried out to remove potential by-products. **3g**-Boc was obtained as a yellow oil with a 67% isolated yield. To remove impurities observed in the ^{1}H-NMR, the compound was subjected to column chromatography using a minimal amount of silica, which marginally affected the final yield (resulting in a 63% final product yield). The NMR spectra were consistent with those obtained during the scale-up of the ATA-catalyzed step.

4.2.5. Environmental impact study of the preparative biosynthesis of 3g

The environmental impact of the sequential system for the synthesis of **3g** was again assessed using the *E*-factor concept. The assessment primarily examined how the reaction conditions, waste generation, and the work-up procedure impacted the overall environmental footprint. It was observed that the downstream process accounted for a significant 98% of the total environmental impact. Within this, the use of organic solvents during product extraction was the main contributor, making up more than 80% of this impact, with ethyl acetate accounting for the 71% and CH_2Cl_2 the 20% (as shown in Figure 4.18). When excluding the solvents, the *E*-factor for the cascade transformation was calculated to be 25.4, which aligns with furfuryl alcohol oxidative systems studied previously (see Section 3.2.5).

To enhance the environmental sustainability of the laccase/TEMPO-ATA cascade protocol, possible measures could involve the purification using alternative methods, excluding derivatization, and potentially increase product yield.

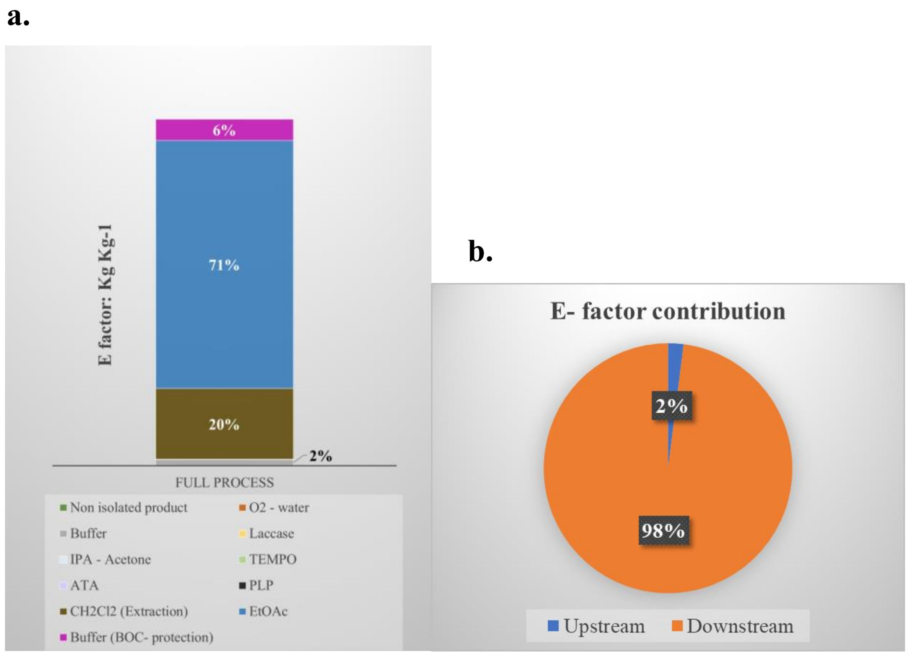

Figure 4.18. Contribution (%) to the *E*-factor (including solvents) for each element of the process (a) and for upstream and downstream (b) for the sequential oxidation and amination of **3a** into **3g**.

Experimental Section

4.3.1. General information

All chemicals were purchased from commercial sources, purchasing HMF, DFF, and BAMF from Sigma-Aldrich. Heterologously expressed Cv-TA, ArS-TA, ArR-TA, ArRmut11-TA, Vf-TA, Vf-mut-TA, and At-TA were donated by Wolfgang Kroutil (University of Graz, Austria), while heterologously expressed Bm-TA and BmS199G-TA by Prof. Nicholas J. Turner (The University of Manchester). Commercial ATAs were received from Codexis Inc.

Reverse phase HPLC (RP-HPLC) analyses were performed using an Agilent 1100 Series chromatograph equipped with a photodiode array detector, using a Mediterranea Sea C18 column from Teknokroma (18.5 µm x 250 mm x 4.6 mm) as stationary phase. For the monitorizatin of biotransformations, 10 µL of each sample were automatically injected.

NMR spectra were recorded on a Bruker AV300 MHz spectrometer including ^{1}H and ^{13}C. All chemical shifts (δ) are reported in parts per million (ppm) and referenced to the residual solvent signal (DMSO-d_6 or $CDCl_3$) as internal standard. Multiplicities of signals in the ^{1}H-NMR spectra are the following: s = singlet, d = doublet, t = triplet, q = quadruplet, p = quintet, hept = heptuplet, dt = doublet of triplets, td = triplet of doublets, m = multiplet.

4.3.2. General procedure for the transamination of DFF into BAMF

Reactions were performed on a total reaction volume of 1 mL in an Eppendorf vial, including DFF (**3b**, 25–200 mM), DMSO (2.5–5% v/v), PLP (1 mM), potassium phosphate buffer (pH 7.5, 100 mM) containing IPA (1 M), and the *E. coli* lyophilized cells heterologously expressing the corresponding ATA (10 mg) or a commercially available ATA (2 mg) from Codexis Inc. After incubation at 30 °C and 250 rpm for 24 h, samples were diluted with 500 µL of MeCN in order to solubilize all the compounds. Then, 20 or 25 µL of the crude sample were diluted in the HPLC mobile phase (MeCN/H_2O with TFA 0.01%, 85:15), according to the starting substrate concentration, filtered with a 45 μm micro-filter and injected in HPLC for the analysis.

4.3.3. LMS oxidation of HMF

In a test tube open to air, TEMPO (20 mol%, 2.52 mg) was added to a solution of the appropriate substrate (0.1 mM, 12.6 mg) in an oxygen-saturated buffer. The reaction mixture was magnetically stirred for a few minutes to dissolve all the reagents. At this point, the corresponding laccase was then added and the mixture was stirred for additional time at 30 °C. For HPLC analyses, aliquots of 20 μL were taken within the time, diluted with the eluting solvent (15% MeCN/TFA 0.01%) up to 1 mL, filtered with 45 μm micro-filters, transferred to an injection vial and injected at the RP-HPLC for the analysis. HPLC measurements were performed through comparison to a standard curve based on the peak area. To quench the reaction, 100 μL of 10% TFA (v/v) was added to the reaction as well as 0.5 mL of MeCN for allowing the possible complete solubilization of the less water-soluble compounds. The total amount of the compounds was summed up and used to calculate the complete conversions of the studied systems.

For HMF oxidation trials with organic cosolvent addition were attempted, 10% (v/v) of a determinate solvent was added to the reaction. Reactions with water miscible cosolvents were also quenched by adding 100 μL of 10% TFA (v/v) and 0.5 mL of MeCN for allowing the possible complete solubilization of the less water-soluble compounds. Aliquots of 25 μL were diluted with the eluting solvent up to 1 mL, filtered and transferred to an injection vial. RP-HPLC measurements were performed through comparison to a standard curve based on the peak area.

Reactions with water immiscible cosolvents with low boiling points were quenched by adding 100 μL of 10% TFA (v/v), left open to air under nitrogen flux for several minutes aiming the complete co-solvent evaporation and then diluted with 0.5 mL of MeCN. Aliquots (20–25 μL) of the crude were then taken for dilution in the HPLC eluent, filtered and injected in RP-

HPLC for the analysis through comparison to a standard curve based on the peak area.

Reactions with water immiscible cosolvents with high boiling points were centrifuged and the organic layer was removed and dried over Na_2SO_4. The aqueous fraction was extracted with CH_2Cl_2 (3 x 1 mL), and the combined prganic layers were mixed with the previous organic phase on Na_2SO_4 and completely evaporated. The residue was solubilized in 1 mL of MeCN, and 25 µL of this solution were diluted in 1 mL of the elution solvent, filtered and injected in HPLC for the analysis through comparison to a standard curve based on the peak area. The water phase was acidified with 100 µL of TFA 10%, and 25 µL were taken and diluted up to 1 mL with the eluting solvent. After filtration, a sample was injected in the HPLC for the conversion measurements through comparison to a standard curve based on the peak area. The total amount of the compounds was summed up and used to calculate the complete conversions of the studied systems.

4.3.4. Biocatalytic synthesis of FFCA at preparative scale

For the up-scaled LMS oxidation of HMF (**3a**) into FFCA (**3c**), 100 mg of HMF were subjected to the oxidative reaction following the same protocol described in Section 4.3.3. After 24 h of incubation, the reaction crude was first basified with an aqueous NaOH 10 M solution (until pH 11–12), and extracted with EtOAc (3 x 5 mL). Then, the resulting aqueous phase was acidified with an aqueous HCl 4 M solution (until pH 2), and extracted with EtOAc (5 x 25 mL). The organic phases were combined, dried over Na_2SO_4 and filtered. The product was obtained as a brownish powder and characterized by NMR without any additional purification.

4.3.5. General procedure for the transamination of FFCA into AMFC

In an Eppendorf vial, the corresponding aldehyde FFCA (**3c,** 25–200 mM) was dissolved in an adequate co-solvent (2.5–10%. v/v). KPi buffer (pH 7.5, 100 mM) containing PLP (1 mM), IPA (1.0 M) - for a final volume of 1 mL and the corresponding whole cell expressing ATA (10 mg) were added after 5 min of pre-incubation at 35 °C with gentle shaking. The reaction mixture was shaken at 30 °C and 250 rpm. Amination reaction was stopped by adding 100 µL of an aqueous NaOH 1 M solution and diluted with 0.5 µL of MeCN. A 15–25 µL of sample (lower volume for reactions with higher FFCA concentrations) was diluted in the HPLC mobile phase (15% MeCN/TFA 0.01%), filtered with 45 µm micro-filters and injected in RP-HPLC for determining the conversion through comparison to a standard curve based on the peak area of each compound.

4.3.6. Preparative scale reaction for AMFC synthesis: Product isolation

For the scaled-up transamination of HMF (**3c**) into AMFC (**3g**), the protocol for isolating the product was performed by adapting a work described in the literature.[477] The reaction was stopped with MeOH (7 mL), centrifuged for removing residual cells, and basified with NaOH pellets (for a final concentration of 1 M, 560 mg). The compound was derivatized with Boc_2O according to the following reported protocol: after quenching, the residual cells were removed by centrifugation (4000 rpm, 20 °C, 10 min). A sample of 20 µL of the supernatant was processed and injected into HPLC to measure conversion of FFCA into AMFC (95%). The solution was evaporated by removing methanol, the residual aqueous phase was basified with NaOH pellets (1 M final concentration, 550 mg) and about 8 mL of a THF:water 1:1 (v/v) mixture were added to the solution. Boc_2O (4 equiv, 624.2 mg) was added to this solution and the reaction was stirred at room temperature. Reaction progress was followed by TLC (10% EtOAc/MeOH) until residual substrate disappeared (approximately 4 h). THF was removed under reduced pressure and the residue diluted in water (20 mL).

Then, the reaction was basified by addition of an aqueous NaOH 10 M solution (1 mL, until pH 11–12) and extracted with EtOAc (2 x 20 mL), for removing residual reaction residues. The aqueous layer was acidified by addition of an aqueous HCl 6 M solution (2 mL, until pH 2) and extracted again with EtOAc (6 x 30 mL). The organic fractions were collected, dried over anhydrous Na_2SO_4, filtered, and evaporated under reduced pressure. The AMFC (**3g**) was collected as a yellow oil and its purity was confirmed by NMR analyses.

4.3.7. General procedure for the one-pot sequential protocol from HMF into AMFC

In a test tube open to air, TEMPO (20 mol%, 25 mg) was added to a solution of HMF (**3a**, 100 mM, 100 mg) in the proper oxygen-saturated buffer (8 mL, 100 mM citrate buffer pH 5.5). The reaction mixture was magnetically stirred for a few minutes to dissolve all the reagents, the POXA1b laccase (58 U/mmol$_S$) was then added, and the mixture was stirred for additional time at 30 °C. After the selected reaction time (24 h), PLP, and $(IPA)_3PO_4$ were added to the mixture containing FFCA as intermediate, leading to approximately 1 mM for PLP and 1 M for IPA in the 300 mM KPi buffer. The addition of this concentrated salt form of IPA to the reaction medium caused both the change of citrate buffer to phosphate, and an increase in the pH from an initial value of 5.5 to approximately 7. No further pH adjustment was done for the bio-transamination reaction systems. Finally, 70 mg of the whole cells expressing BmS119G were added. The tube was closed and the reaction mixture was vigorously shaken for 24 h at 30 °C and 250 rpm. After this time, the reaction was centrifuged for removing solid residual cell pellets at 4000 rpm, at room temperature (20 °C) for 5 min. Then, the solution was basified by addition of an aqueous NaOH 10 M solution (1 mL, until pH 11–12) and extracted with EtOAc (2 x 10 mL), for removing residual TEMPO and other possible by-products. Then, the reaction was acidified by addition of an aqueous HCl 6 M solution (2 mL, until pH 2) and extracted again with

EtOAc (2 x 10 mL) for removing residual FFCA (**3c**). The last fraction was analysed by NMR, confirming residues of DFF and **3c** from the first reaction step.

The solution was evaporated for removing solvent traces, and next derivatized with Boc_2O in the reported reaction conditions (see Section 4.3.6). **3g**-Boc was extracted from the water mixture with a continuous extraction apparatus (CH_2Cl_2, 70 mL). After 8 h, the organic phase was dried over anhydrous Na_2SO_4, filtered, and evaporated under reduced pressure. The **3g**-Boc was subjected to column chromatography starting with a mixture of 10% EtOAc/MeOH as eluent. After elution of impurities, 50% EtOAc/MeOH was used for **3g**-Boc recovery. The product was filtered to keep away silica gel, and solvent evaporated, isolating the compound as a yellow oil (115.5 mg, 63% isolated yield). The spectroscopical data were identical to the **3g**-Boc obtained from preparative scale amination of FFCA (**3c**) disclosed in Section 4.3.6.

4.3.8. Analytics

4.3.8.1. HPLC method for the separation of compounds 3a-g

HMF derivatives were analysed in Mediterranea Sea-C18 column (4.6 mm × 250 mm, 5 μm) by using a RP-HPLC equipped with a photodiode array detector. 10 μL of each sample was automatically injected. The reactions were stopped by adding 100 μL of TFA 10% or an aqueous 1 M NaOH solution, and diluted with 0.5 mL of 100% MeCN for allowing the complete solubilization of the compounds. According to the starting substrate amount, 15–25 μL of each sample were diluted in the HPLC solvent mixture: H_2O/MeCN (15:85 v/v) and filtered through 0.45 mm, 13 mm Nylon filters.

The gradient elution has been set up by automatically mixing MeCN 100% and water acidified with TFA (0.01% v/v). The optimized method led to 30 minutes of each run with the following gradients:

- 7 min, H_2O/MeCN (15:85 v/v);
- then up to 100% MeCN in 3 min;
- 5 min at 100% MeCN,
- up to H_2O/MeCN (15:85 v/v) in 3 min,
- finally 12 min at H_2O/MeCN (15:85 v/v).

Flow rate was set at 0.9 mL/min and column temperature at 30 °C. Biotransformations were monitorized at the three wavelengths were the maximum absorbances were observed (210, 245 and 280 nm). The selected wavelength and retention times of the compounds involved in the cascade amination of HMF are the depicted in Figure 4.19.

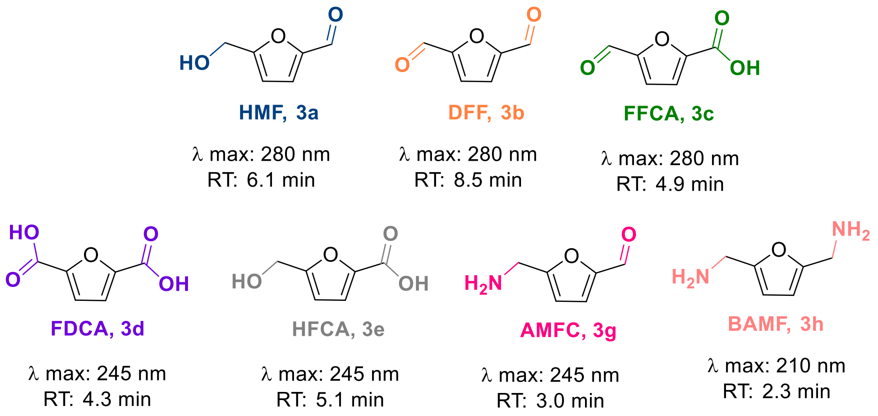
HMF, 3a
λ max: 280 nm
RT: 6.1 min
DFF, 3b
λ max: 280 nm
RT: 8.5 min
FFCA, 3c
λ max: 280 nm
RT: 4.9 min
FDCA, 3d
λ max: 245 nm
RT: 4.3 min
HFCA, 3e
λ max: 245 nm
RT: 5.1 min
AMFC, 3g
λ max: 245 nm
RT: 3.0 min
BAMF, 3h
λ max: 210 nm
RT: 2.3 min

Figure 4.19. Retention times of studied compounds for HPLC analyses.

Efforts for a better separation of FFCA and HFCA have failed: indeed, similar results are reported in other works despite the use of different HPLC methods and RP-HPLC columns.[427] Nonetheless, the slight shift together with a strong difference in the maximum absorbance wavelengths (280 nm and 245 nm, respectively) allowed to clearly recognize them in the reaction crude (confirmed also by mixing both the compounds).

4.3.8.2. Calibration curves for compounds 3a-g

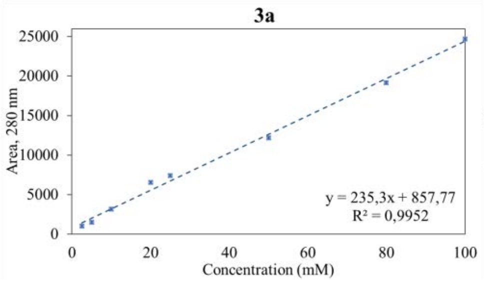

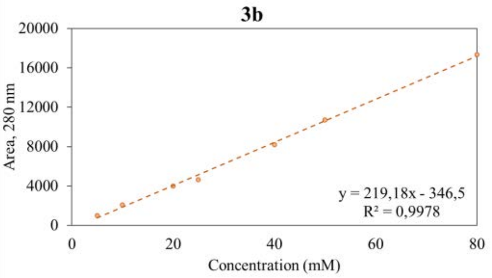

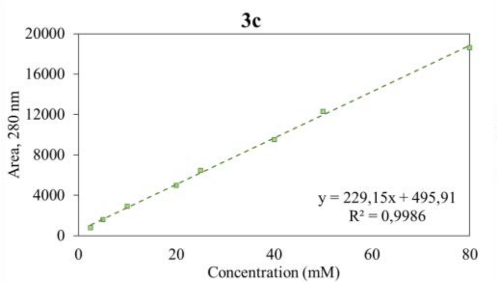

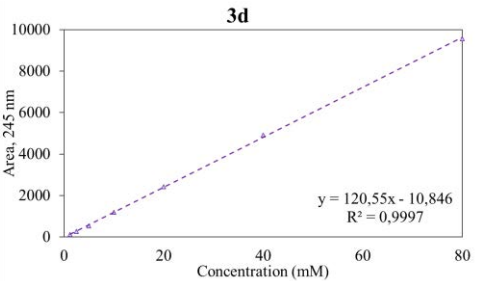

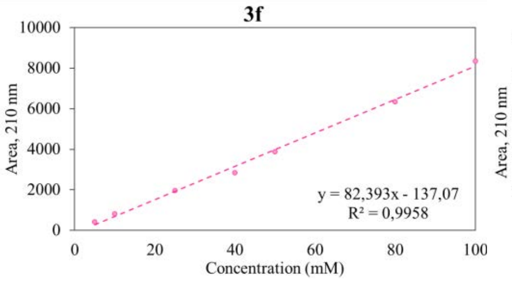

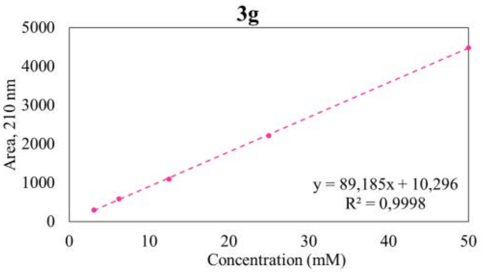

Due to the absence of HFCA (**3e**) in the reaction crude, no calibration curves have been performed for this compound.

4.3.9. Compounds characterization

(1*E*,1'*E*)-1,1'-(Furan-2,5-diyl)bis(*N*-isopropylmethanimine) (3h). Isolated from the blank reaction (without ATA) of **3b** in presence of IPA.

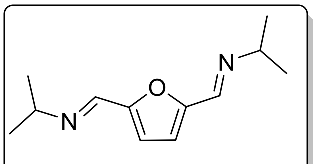

3h

Yellow oil (75%)

Molecular formula: $C_{12}H_{18}N_2O$

Molecular weight: 206.29 g/mol

^{1}H NMR (300 MHz, $CDCl_3$) δ 8.16 (s, 2H), 6.83 (s, 2H), 3.50 (hept, *J*=6.5 Hz, 2H), 1.24 (d, *J*=6.4 Hz, 12H).

^{13}C NMR (75 MHz, $CDCl_3$) δ 153.1 (2C), 147.8 (2CH), 114.1 (2CH), 62.0 (2CH), 24.1 ($4CH_3$).

(*E*)-(5-((Butylimino)methyl)furan-2-yl)methanol (1)

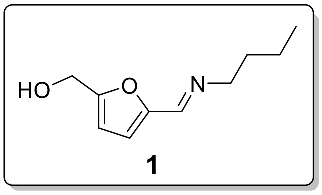

1

Brownish powder (92%)

Molecular formula: $C_{10}H_{15}NO_2$

Molecular weight: 181.24 g/mol

^{1}H-NMR (300 MHz, $CDCl_3$) δ 8.00 (s, 1H), 6.66 (d, J=3.3, 1H), 6.36 (d, J=3.3, 1H), 4.65 (s, 2H), 3.55 (t, J=7.1, 2H), 1.74–1.60 (m, 2H), 1.45–1.23 (m, 2H), 0.93 (t, J=7.3, 3H).

^{13}C-NMR (75 MHz, $CDCl_3$) δ 157.2 (CH), 150.8 (C), 149.6 (CH), 115.4 (CH), 109.1 (CH), 61.4 (CH_2), 57.2 (CH_2), 32.8 (CH_2), 20.4 (CH_2), 13.8 (CH_3).

(1*E*,1'*E*)-1,1'-(Furan-2,5-diyl)bis(*N*-butylmethanimine) (2)

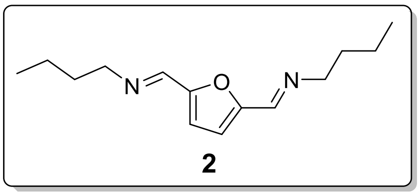

2

Red oil (95%)

Molecular formula: $C_{14}H_{22}N_2O$

Molecular weight: 234.34 g/mol

^{1}H-NMR (300 MHz, $CDCl_3$) δ 8.12 (d, J=1.3, 2H), 6.83 (s, 2H), 3.58 (td, J=7.0, 1.4, 4H), 1.66 (p, J=7.1, 4H), 1.33 (dt, J=14.6, 7.4, 4H), 0.91 (t, J=7.3, 6H).

^{13}C-NMR (75 MHz, $CDCl_3$) δ 153.0 (2CH), 149.9 (2C), 113.9 (2CH), 61.8 ($2CH_2$), 32.9 ($2CH_2$), 20.5 ($2CH_2$), 13.9 ($2CH_3$).

5-Formyl-2-furancarboxylic acid (FFCA, 3c)

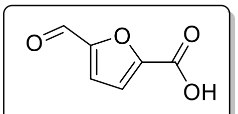

3c

Brownish powder (60%).

Molecular formula: $C_6H_4O_4$

Molecular weight: 140.09 g/mol

^{1}H-NMR (300 MHz, $CDCl_3$) δ 9.72 (s, 1H), 7.58 (d, J=3.7 Hz, 1H), 7.38 (d, J= 3.7 Hz, 1H).

^{13}C-NMR (75 MHz, $CDCl_3$) δ 180.4 (CH), 159.5 (C), 153.7 (C), 148.6 (C), 122.8 (CH), 119.0 (CH).

((*E*)-5-(((3,3-Dimethyl-2-oxobutyl)imino)methyl)furan-2-carboxylic acid (3f-Boc)

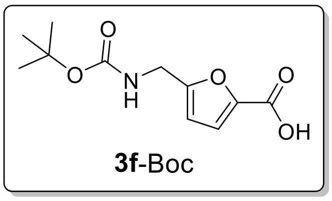

3f-Boc

Yellow oil (63%).

Molecular formula: $C_{11}H_{15}NO_5$

Molecular weight: 241.24 g/mol

^{1}H-NMR (300 MHz, $CDCl_3$) 7.39 (t, J= 5.9 Hz, 1H), 6.72 (d, J= 3.2 Hz, 1H), 6.15 (d, J= 3.0 Hz, 1H), 4.09 (d, J= 5.9 Hz, 2H), 1.37 (s, 9H).

^{13}C-NMR (75 MHz, $CDCl_3$) δ 163.3 (C), 155.6 (C), 153.5 (C), 151.0 (C), 113.5 (CH), 107.7 (CH), 78.2 (C), 37.3 (CH_2), 28.3 ($3CH_3$).

GENERAL CONCLUSIONS

As general conclusions drawn from this Doctoral Thesis, the in-depth exploration of the individual (chemo)enzymatic steps for the transformation of furan-based alcohols, specifically focusing on 5-hydroxymethylfurfural and furfuryl alcohol, were investigated. The ultimate goal was to combine an oxidation and a transamination using a laccase and an ATA in a one-pot sequential approach. The study encompassed both single-step reactions and their combination, with a comprehensive characterization of the resulting reaction products. Various strategies were also employed to expand the range of enzymes tested and enhance their functionalities.

In the first chapter, laccase mutagenesis was employed to understand how furan-based molecules interact with the enzyme's active site. Molecular docking and directed evolution experiments were conducted on POXA1b laccase, an efficient laccase from *P. ostreatus*. While no positive hits were found, this approach revealed that the primary obstacle to furan molecules oxidation was likely related to their redox potential, not due to steric factors. In the mutagenesis strategy, a robust colorimetric assay for detecting 5-hydroxymethylfurfural oxidation products, particularly 2,5-diformylfuran, was established. Using a cost-effective compound, 1,4-phenylenediamine, this assay proved very promising for high-throughput screening of redox biocatalysts for new or enhanced enzyme variants. Additionally, it effectively assessed the kinetic properties of different laccase-mediated HMF oxidations into DFF.

In the second chapter, we focused on broadening the range of laccases used. We expressed a laccase, Lacc12, in *P. pastoris* through recombinant techniques. We optimized the production medium and conditions to ensure the enzyme's activity. Our hypothesis was that the challenge in overexpressing this specific isoform of *P. ostreatus* laccase, typically produced during the fungal fruiting body growth process, stemmed from its instability at high temperatures and when expressed constitutively. Therefore, by lowering the fermentation temperature to 20°C and inducing enzymatic production with methanol, we facilitated the gradual accumulation of the active enzyme form. This proof-of-concept paved the way for further improvements and larger-scale laccase production.

In the third chapter, we expressed new amine transaminases and incorporated them into a panel of ATAs to convert furfural into valuable furfuryl amine under mild aqueous conditions, using an excess of IPA. Some of the overexpressed ATAs, such as Cv-TA, ArS-TA, ArRmut11-TA, and Vf-mut-TA, showed high conversion rates and selectivity, with Cv-TA achieving up to quantitative yield. In order to set-up a cascade for converting furfuryl alcohol into furfuryl amine, we optimized the initial oxidation step using three laccase-TEMPO systems (L*Tv*, POXC, and POXA1b). *P. ostreatus* laccases, exhibited remarkable selectivities in producing furfural, avoiding the formation of 2-furoic acid. Taking advantage of POXA1b's high stability over extended reaction times, we significantly reduced the mediator usage (down to 5 mol%). These TEMPO oxidative systems with *P. ostreatus* laccases tolerated various water-immiscible co-solvent mixtures at notable concentrations (up to 10% v/v), and effectively operated at 100 mM substrate concentration. The laccase-mediator systems were successfully applied in a one-pot, two-step cascade with Cv-TA, resulting in the efficient production of furfuryl amine from furfuryl alcohol.

In the fourth chapter, we investigated the production of BAMF and AMFC from DFF and HMF, respectively, via transamination. These reactions occurred alongside with the *in situ* formation of (poly)imines due to the presence of reactive carbonyl species and amines in the medium. The reversibility of the imine bonds allowed us to shift the equilibrium toward the desired amine product, particularly by adjusting parameters like pH. More acidic pH values improved productivity without compromising enzyme stability or activity. We also explored HMF oxidation by LMSs, examining factors like buffer concentration, mediator, and laccase quantity. FFCA was the main product, despite attempts to protect the aldehyde group of HMF or use biphasic systems to obtain DFF. Hence, FFCA was used as starting material for transamination, optimizing various conditions, including substrate concentration and co-solvent addition. In the presence of MeCN, BmS119G-TA efficiently converted FFCA up to 100 mM into AMFC. Thus, the POXA1b-mediated oxidation of HMF, followed by transamination of FFCA using BmS119G-TA, produced AMFC in a sequential manner, which was then isolated as a Boc-protected compound.

In summary, this Doctoral Thesis demonstrates the versatility of the combination of laccases and amine transaminases in a multienzymatic sequential approach for the production of furan derivatives which are valuable chemicals platforms to modern biorefineries. The optimization of these processes was carried out with the goal of aligning with the principles of sustainable chemistry. The objective was to produce high-value furan derivatives through environmentally friendly and efficient methods, with the intention of reducing the environmental impact of the transformations. Furthermore, the utilization of renewable feedstocks and the exploration and application of efficient catalysts in minimal quantities contribute to the broader sustainability objectives within the chemical industry.

CONCLUSIONES GENERALES

Como conclusiones generales de esta Tesis Doctoral, se han explorado en detalle los pasos individuales de varios procesos (quimio)enzimáticos para transformar alcoholes conteniendo anillos de furano, focalizándose especialmente en el 5-hidroximetilfurfural y el alcohol furfurílico. El objetivo final ha sido combinar una oxidación y una transaminación usando una lacasa y una ATA en un proceso secuencial en un solo recipiente. Este estudio se centró en la optimización de cada paso por separado y luego en la integración de ambos, caracterizando los productos de la reacción. Se han estudiado diferentes estrategias para expandir el panel de enzimas, así como para mejorar sus propiedades.

En el primer capítulo, se realizó un estudio sobre una lacasa para entender cómo las moléculas furánicas interaccionaban con el centro activo de la enzima. Así, se utilizaron técnicas de modelado y de evolución dirigida sobre la lacasa POXA1b de *P. ostreatus*. Aunque no se encontraron variantes con actividad sobre los sustratos de interés, estos estudios revelaron que el principal problema es el alto potencial redox de dichas moléculas para poder ser oxidadas, y no la imposibilidad de que entren en el centro activo. Además, se ha desarrollado un método colorimétrico robusto para detectar el 2,5-diformilfurano, producto proveniente de la oxidación del 5-hidroximetilfurfural. Usando un reactivo barato como la 1,4-fenilendiamina, este ensayo demostró ser una herramienta muy prometedora para el cribado a gran escala de enzimas redox para encontrar variantes nuevas o mejoradas. Además, se estudiaron las propiedades cinéticas de diferentes sistemas oxidativos con lacasas para transformar HMF en DFF.

En el segundo capítulo, se estudió expandir el número de lacasas empleadas. Se expresó una nueva lacasa, la Lacc12, en *P. pastoris* a través de técnicas de recombinación. Se optimizó el medio de producción, así como las condiciones para mejorar la actividad enzimática. Nuestra hipótesis fue que el problema para sobreexpresar esta isoforma de lacasa de *P. ostreatus*, producida durante el proceso de crecimiento del cuerpo fructífero del hongo, provenía de su inestabilidad a las altas temperaturas cuando se expresaba. Por lo tanto, disminuyendo la temperatura de inducción a 20°C e induciendo la producción enzimática con metanol, se facilitó la acumulación de la forma activa de esta enzima. Esta prueba de concepto abre las puertas para futuras mejoras para la producción de lacasas a mayor escala.

En el capítulo tercero, se expresaron nuevas amino transaminasas y se incorporaron al panel de ATAs para transformar furfural en furfuril amina, molécula de interés, en medio acuoso y bajo condiciones suaves, usando un exceso de IPA. Algunas de las ATAs sobreexpresadas, como la Cv-TA, ArS-TA, ArRmut11-TA, y Vf-mut-TA, mostraron altas conversiones y selectividades, siendo la Cv-TA la que dio lugar a un rendimiento cuantitativo de la amina. Para desarrollar el proceso en cascada desde el alcohol furfurílico a la furfuril amina, se optimizó también el proceso de oxidación inicial empleando tres sistemas distintos de lacasa con TEMPO (L*Tv*, POXC y POXA1b). Las lacasas de *P. ostreatus* exhibieron una selectividad excelente para dar lugar al furfural, evitándose la formación del ácido 2-furoico. Tomando ventaja de la gran estabilidad de la POXA1b a largos tiempos de reacción, se pudo reducir notablemente la carga del mediador químico (hasta un 5 mol%). Estos sistemas oxidativos con las lacasas de *P. ostreatus* demostraron tolerar varios disolventes inmiscibles con el agua hasta concentraciones notables (hasta un 10% v/v), operando a una concentración de sustrato de 100 mM. Posteriormente, se aplicaron en un proceso en un mismo recipiente y en dos etapas junto con la Cv-TA, para obtener de manera eficiente y selectiva la furfuril amina desde el alcohol furfurílico.

En el cuarto capítulo, se investigó la producción de BAMF y de AMFC desde DFF y HMF, respectivamente, mediante transaminación. Estas reacciones ocurrieron adicionalmente con la formación *in situ* de (poli)aminas debido a la presencia de grupos carbonílicos muy reactivos y de las aminas en el medio de reacción. La reversibilidad de los enlaces imínicos en medio acuosos nos permitió desplazar el equilibrio hacia la formación de las aminas, particularmente ajustando distintos parámetros como el pH. Así, pHs más ácidos mejoraron la productividad de estos procesos sin comprometer la estabilidad o actividad de las enzimas. También se exploró la oxidación del HMF utilizando diversos LMSs, examinando factores como la concentración de la reguladora, del mediador y la cantidad de la lacasa. Se obtuvo FFCA como producto principal, incluso cuando se intentó proteger el grupo aldehído del HMF o se emplearon medios bifásicos para mejorar la producción del DFF. Así, el FFCA se utilizó como material de partida para estudiar su transaminación, optimizando distintos parámetros, incluyendo la concentración del sustrato y la adición de cosolventes. En presencia de MeCN, la BmS119G-TA catalizó eficientemente la conversión del FFCA (hasta 100 mM) en AMFC. La combinación de la oxidación mediada por la POXA1b, seguida de la transaminación del intermedio FFCA empleando la BmS119G-TA, dio lugar a la formación de la AMFC de manera secuencial, que se aisló protegido con el grupo Boc.

En resumen, en esta Tesis Doctoral se ha demostrado la versatilidad de la combinación de lacasas y transaminasas en procesos secuenciales multienzimáticos para obtener derivados furánicos de interés que son plataformas químicas para las biorefinerías modernas. Se llevó a cabo la optimización de estos procesos con el fin de cumplir además con los principios de la química sostenible. Así, el objetivo has sido desarrollar métodos químicos medioambientalmente benignos y eficientes para producir los derivados de interés, con el fin de disminuir el impacto ambiental de dichas transformaciones. Además, la utilización de fuentes renovables y la exploración y aplicación de catalizadores eficientes para usarlos en cantidades mínimas, contribuyen a que la industria química pueda cumplir con objetivos más amplios de sostenibilidad.